

524
1998

ISSN — 0132 — 1447



BULLETIN

OF THE GEORGIAN ACADEMY
OF SCIENCES

საქართველოს
მეცნიერებათა აკადემიის

ბოაბა

157

№ 36
(T. 157 № 3)

№ 3

1998

The Journal is founded in 1940



BULLETIN

OF THE GEORGIAN ACADEMY OF SCIENCES

is a scientific journal, issued bimonthly in
Georgian and English languages

Editor-in-Chief

Academician **Albert N. Tavkheldidze**

Editorial Board

T. Andronikashvili,
T. Beridze (Deputy Editor-in-Chief),
G. Chogoshvili,
I. Gamkrelidze,
T. Gamkrelidze,
R. Gordeziani (Deputy Editor-in-Chief),
G. Gvelesiani,
I. Kiguradze (Deputy Editor-in-Chief),
T. Kopaleishvili,
G. Kvesitadze,
J. Lominadze,
R. Metreveli,
D. Muskhelishvili (Deputy Editor-in-Chief),
T. Oniani,
M. Salukvadze (Deputy Editor-in-Chief),
G. Tsitsishvili,
T. Urushadze,
M. Zaalishvili

Executive Manager - L. Gverdtsiteli

Editorial Office:

Georgian Academy of Sciences
52, Rustaveli Avenue,
Tbilisi, 380008,
Republic of Georgia

Telephone : +995 32 99.75.93

Fax : +995 32 99.88.23

E-mail : **BULLETIN@PRESID.ACNET.GE**

CONTENTS



MATHEMATICS

G. Oniani. On Upper and Lower Derivatives of Lebesgue Integral	357
N. Tsalugelashvili. The Construction of the Bases of Some Eight Step Cusp Form Spaces	359
M. Shubladze. On Finite Multiplicity of a Hypersurface Singularity	362
D. Gordeziani, N. Gordeziani, G. Avalishvili. Non-Local Boundary Value Problems for Some Partial Differential Equations	365
V. Baladze. On Spectral Coshape Theory	369

MATHEMATICAL PHYSICS

T. Chilachava. On the Asymptotic Method of Solution of One Class of Nonlinear Mixed Problems of Mathematical Physics	373
--	-----

CYBERNETICS

G. Tsuladze. Structuring Facilities in the Language "Ladis" for Designing Information Systems	378
Z. Kipshidze, G. Ananiashvili. Decision Making Informational Model for Ergative Systems	383
A. Gabelaia, V. Ivanenko. On the Use of Statistical Regularity Concept in Decision-Making	386

PHYSICS

V. Gersamia, M. Kvernadze, M. Mirianashvili, Sh. Mirianashvili, A. Mirtskhulava. The Investigation of Photoelectrical Characteristics of Silicon Semiconductor Structures by Dynamical Lattice Method	388
V. Kashia, P. Kervalishvili, I. Zhvania, Academician R. Salukvadze. Universal Method for Control of Heat Carrier Leakage from Various Contours ..	390
A. Gerasimov, G. Chiradze, N. Kutivadze, A. Bibilashvili, Z. Bokhochadze. Influence of Isotropisation of Chemical Bonds on Anisotropy of Photomechanical Effect	396
I. Loria. Diffraction of Electromagnetic Waves on the Periodic Thin Strip Lattice Located in Medium	400

ASTRONOMY

Corr. Member of the Academy R. Kiladze, T. Kvernadze, M. Gikoshvili. Observation of Saturn Rings in Abastumani in 1995	404
--	-----

ANALYTICAL CHEMISTRY

O. Manjgaladze, F. Broucek, N. Telia. Acid-Base Properties of Azo- and Oxiazo-Derivatives of Rodanine and their Application Ability in Chemical Analysis	407
--	-----



V.Eristavi, V.Ivanov, D.Eristavi, N.Kutsiava. Atom Absorption Methods of Determining Molybdenum in Sulfuric Acid	411
--	-----

GENERAL AND INORGANIC CHEMISTRY

I.Samadashvili, T.Macharadze. Synthesis of Mg-Zn Ferrites and their Properties	413
G. Khelashvili, R.I.Gigauri, M. Indjia, L. Gurgenshvili, R.D.Gigauri. Coordination Compounds of d-Metals Monothioarsenates with Pyridine	415

ORGANIC CHEMISTRY

D. Tsakadze, M. Gverdtsiteli. Algebraic Investigation of the Alkaloids from Plants of <i>Cocculus</i> Family	418
--	-----

PHYSICAL CHEMISTRY

M.Rukhadze, Academician V. Okujava, M. Sebiskveradze, M. Rogava, S. Tsagareli. Determination and Evaluation of Solvent Strength Parameter in Conventional Reversed-Phase, Ion-Pair and Micellar Chromatography	421
A.Nadiradze, K.Ukleba, Academician G.Gvelesiani, J.Baratashvili, D.Tsagareishvili, J.Omiadze. A New Method of the Calculation of Standard Enthalpy of Formation of Double Oxides	424
E.Kachibaya, Corr. Member of the Academy L.Japaridze, R.Akhvlediani, Sh.Japaridze, T.Paykidze, R.Imnadze. Synthesis and Structure of Spinel Type Lithium- Manganese Composition	428

CHEMICAL TECHNOLOGY

L. Baiadze, G. Gaprindashvili, O. Modebadze, J. Nakaidze, N. Papunashvili, Academician G. Tsintsadze. Investigation of Some Physico-Chemical Properties of High-Manganese Boron Oxide Glassy Semiconductors .	432
---	-----

ECONOMIC GEOGRAPHY

I.Iashvili. Contemporary Tendencies of Demographic Processes Development in Kutaisi City	436
--	-----

GEOLOGY

M. Tvalchrelidze. Geological History of the Sokhumi Peninsula in Late Pleistocene and Holocene	439
Sh. Keleprishvili. Stratigraphical Significance of the Early Cretaceous Belemnitida of Georgia	443

MACHINE BUILDING SCIENCE

T.Javakhishvili. Transfer Function of a Single Way Pendulum Rope Way Mechanical System	447
M.Shalamberidze. Self-regulation Coefficient of Welding Current	450

HYDRAULIC ENGINEERING

Academician Ts. Mirtskhoulava. On the Assessment of Erosion Processes Effect on the Social Tension in the Society	452
V.Nadirashvili. Estimation of Slope Reliability from the Point of View of Erosion Caused by Rain	456

HYDROLOGY

Sh.Kunchulia. The Influence of Hydrometeorologic Factors on the Economy of Commercial Sea Passages	459
--	-----

ELECTROTECHNICS

O. Labadze, M. Tsertsvadze, G. Kublashvili, P. Manjavidze. Mutual Inductance between Flat-Parallel Convex Contours Having Conjugate Pieces	462
--	-----

AUTOMATIC CONTROL AND COMPUTER ENGINEERING

A. Chaduneli, A. Kurtishvili, G. Cheishvili, I. Lomtadize. Digital Representation of a Continuous Process with a Wide Dynamic and Frequency Spectrum	466
--	-----

SOIL SCIENCE

R. Lortkipanidze. Agroindustrial Characteristics of the Main Types of Soils of Imereti Region	469
---	-----

BOTANY

M.Davidadze. Systematic Structure of the Adjarian Adventive Flora	473
---	-----

HUMAN AND ANIMAL PHYSIOLOGY

G. Todua. Electrophysiological Investigation of the Descending Connections of the Posterior and Anterior Sylvian gyri with the Amygdaloid Complex ...	476
N. Archivadze. Active Avoidance Reactions (AAR) Dynamics in Rats with Dorsal Hippocampus Bilateral Coagulation	479

BIOPHYSICS

E.Chikvaidze, I.Kirkashvili, A.Lebanidze. Electron Spin Resonance (ESR) of Copper Proteins and Some Model Systems	482
M. Melikishvili, G. Mikadze, L. Visochech, Academician M. Zaalishvili. Thermal Denaturation of Rabbit Gastric Muscle Tropomyosin	486
J.Gogorishvili, R.Sujashvili, Academician M.Zaalishvili. Some of the Physico-Chemical Properties of Proteins Extracted from the Kidney by 0.5M KCl Solution	489

BIOCHEMISTRY

- L. Shanshiashvili, Ch. Todadze, I. Chogovadze, N. Natsvlshvili, G. Lezhava, D. Mikeladze. The Influence of Toluene and Ethyl Alcohol on Opiate and Dopamine Receptor Activity in Rat Brain. 493
- G. Gigolashvili, T. Dalalishvili, Corr. Member of the Academy D. Jokhadze. Comparative Study of Some Varieties of Mulberry Trees (*Genera Morus*) by the Method of Isoelectric Focusing 497
- M. Jincharadze, G. Pruidze, N. Omiadze, N. Mchedlishvili. Effect of Tea-Leaf Peptides on the Monophenol Monooxygenase and Catechol Oxydase Activities. 500
- M. Gomarteli, T. Janelidze. Usage of Thermostable Xylanase Preparation Obtained from *Allescheria terrestris* for Plant Waste Hydrolysis 502

MICROBIOLOGY AND VIROLOGY

- N. Manvelidze, E. Adeishvili, E. Kvesitadze. Selection of Antibiotic-Producing Basidiomycetes 505

CYTOLOGY

- E. Tavdishvili, P. Chelidze, D. Dzidziguri, E. Cherkezia, Academician G. Tumanishvili. The Study of Interdependency between the Changes of RNA Synthesis Intensity and the Morphological Transformation of White Rat Hepatocyte Nucleoli in Postnatal Period of Development 508

EXPERIMENTAL MEDICINE

- M. Zimmermann, T. Ebanoidze. The Treatment of the Postextraction Syndrome with Taurolin® 511
- T. Shatilova, I. Oniani, M. Chikovani, Z. Zambakhidze. Organo-specific Stimulation as a Method of Treatment of the Pigmentary Dystrophy of the Retina 515
- L. Gogichaishvili, M. Chikhladze, N. Meskhishvili. Spring Palynospectra of Tbilisi and Dynamics of Allergic Diseases in Children in 1997 519

PHILOLOGY

- M. Badriashvili. The Metaphor of Torturer and Victim as the Basis of World Perception 523

HISTORY OF ART

- M. Andriadze. Terminology of Old Georgian Professional Music According to Old Tropologion 526

G. Oniani

On Upper and Lower Derivatives of Lebesgue Integral

Presented by Academician L. Zhizhiashvili, October 6, 1997.

ABSTRACT. In the paper the Guzman-Menarges' theorem about possible meanings of upper and lower derivatives of Lebesgue integral is generalized. Herewith it's shown that the established theorem does not extend on homothety invariant density bases formed of convex sets.

Key words: DIFFERENTIATION, BASIS, INTEGRAL.

1. A mapping B defined on \mathbb{R}^n is called a differentiation basis in \mathbb{R}^n , if for every $x \in \mathbb{R}^n$ $B(x)$ is a collection of bounded open subsets of \mathbb{R}^n containing x such that there is a sequence $\{R_k\} \subset B(x)$ with $\text{diam} R_k \rightarrow 0$ ($k \rightarrow \infty$).

For $f \in L(\mathbb{R}^n)$ numbers

$$\overline{D}_B(\int f, x) = \overline{\lim}_{\text{diam } R \rightarrow 0, R \in B(x)} \frac{1}{|R|} \int_R f \quad \text{and} \quad \underline{D}_B(\int f, x) = \underline{\lim}_{\text{diam } R \rightarrow 0, R \in B(x)} \frac{1}{|R|} \int_R f$$

are called respectively upper and lower derivatives of the integral of f at the point x . If the upper and lower derivatives are equal, then their common meaning is called a derivative of the integral of f at the point x and it is denoted by $D_B(\int f, x)$. The basis B is said to differentiate the integral of f , if for almost every x

$$D_B(\int f, x) = f(x).$$

A basis B is called a density basis, if it differentiate an integral of characteristic function of any measurable set. Denote by \overline{B} the collection $\bigcup_{x \in \mathbb{R}^n} B(x)$.

B is called a Buseman-Feller basis if for every $R \in \overline{B}$, we have that $R \in B(y)$ for every $y \in R$. We shall call a B homothety invariant if for every $x \in \mathbb{R}^n$, $R \in B(x)$ and a homothety H with the centre in x $H(R) \in B(x)$. We shall say that a basis B is formed of sets from a certain class K , if $\overline{B} \subset K$.

2. Let B be the basis in \mathbb{R}^2 , for which $B(x)$ ($x \in \mathbb{R}^2$) consists of all two-dimensional intervals containing x . Then by virtue of the known theorem of Besicovitch (see [1] or [2], ch. IV, §3) for every function $f \in L(\mathbb{R}^2)$ both of sets

$$\{x: f(x) < \overline{D}_B(\int f, x) < \infty\}, \tag{1}$$

$$\{x: -\infty < \underline{D}_B(\int f, x) < f(x)\} \tag{2}$$

have a measure equal to zero.

Guzman and Menarges (see [2], ch. IV, §3) established that the analogous result is

21211



true for any density and Buseman-Feller basis B , formed of convex sets having the centre of symmetry, which is homothety invariant.

We have established that in Guzman-Menarges' assertion the condition of central symmetry of B 's forming sets is unnecessary, in particular, it's just

Theorem 1. *Let B be a homothety invariant Buseman-Feller density basis in \mathbb{R}^n ($n \in \mathbb{N}$), formed of convex sets. Then for every $f \in L(\mathbb{R}^n)$ the sets (1) and (2) have a measure equal to zero.*

This theorem does not extend on homothety invariant density bases, formed of convex sets, in particular, it's just

Theorem 2. *There is a homothety invariant basis B , formed of two-dimensional intervals, for which there is a function $f \in L(\mathbb{R}^2)$, $f \geq 0$ such that*

$$f(x) < \bar{D}_B(\int f, x) < \infty$$

almost everywhere on \mathbb{R}^2 .

Tbilisi I. Javakhishvili State University

REFERENCES

1. A. S. Besicovitch. *Fund. Math.*, 25, 1935, 209-216.
2. M. de Guzman. *Differentiation of integrals in \mathbb{R}^n* . Lecture notes in Mathematics 481. Springer, 1975.



N. Tsalugelashvili

The Construction of the Bases of Some Eight Step Cusp Form Spaces

Presented by Corr. Member of the Academy Kh. Inassaridze, November 10, 1997

ABSTRACT. The modular properties of general theta-functions with characteristics are used to build the basis of the cusp form spaces corresponding to some diagonal eight step quadratic forms. It gives the opportunity of obtaining formulae for the number of representations of positive integers by these forms.

Key words: CUSP FORM SPACES, QUADRATIC FORMS.

Let $r(n; f_{(s,k)})$ denote a number of representations of a positive integer n by the eight step quadratic form

$$f_{(s,k)} = 2 \sum_{j=1}^k x_j^2 + \sum_{j=k+1}^s x_j^2 \quad (2 \mid s; s \geq 6; k = 1, \dots, s-1; k \equiv 1 \pmod{2}). \quad (1)$$

It is well known that $r(n; f_{(s,k)})$ can be expressed as follows: $r(n; f_{(s,k)}) = \rho(n; f_{(s,k)}) + \nu(n; f_{(s,k)})$, where $\rho(n; f_{(s,k)})$ is a singular series which is already fully studied and the formulae for its calculations are known ([1], Theorem 4). The latter equality can be expressed in terms of the theory of modular forms by stating that

$$\theta(\tau; f_{(s,k)}) = E(\tau; f_{(s,k)}) - X(\tau; f_{(s,k)}), \quad (2)$$

where $E(\tau; f_{(s,k)})$ is the Eisenstein series and $X(\tau; f_{(s,k)})$ is a cusp form of type

$$\left(-\frac{s}{2}; \Gamma_0(8), \nu_s(L)\right), \quad \text{where } \left(L = \begin{pmatrix} \alpha & \beta \\ \gamma & \delta \end{pmatrix} \in \Gamma_0(8)\right) \text{ is the corresponding multiplier system [1,2].}$$

To construct these functions we use the generalized thetafunctions with characteristics that were introduced by Vepkhvadze [1] as follows: Let g and h be the special vectors with

respect to the matrix $A = (a_{jk})$ of quadratic form $f = \frac{1}{2} \sum_{j,k=1}^s a_{jk} x_j x_k$ in s variables. Let N

be the step of f and $P_\nu = P_\nu(x)$ be the spherical function of order ν with respect to f . Then

$$\vartheta_{gn}(\tau; P_\nu, f) = \sum_{x=g \pmod{N}} (-1)^{\frac{h'A(x-g)}{N^2}} P_\nu(x) e^{\frac{\pi i x' A x}{N^2}}$$

Theorem 1. Assume, that

$$f_s = 2 \sum_{j=1}^{s-5} x_j^2 + x_{s-4}^2, \quad P_2 = x_{s-4}^2 - 2x_1^2,$$

$$h = \begin{pmatrix} 0 \\ \vdots \\ 0 \end{pmatrix}, \quad g^{(j)} = \begin{pmatrix} 4 \\ \vdots \\ 4 \\ 0 \\ \vdots \\ 0 \end{pmatrix} 2^j \quad \left(j = 1, 2, \dots, \frac{s}{2} - 3 \right), \quad g^{\left(\frac{s}{2}-2\right)} = \begin{pmatrix} 0 \\ 4 \\ \vdots \\ 4 \\ 0 \end{pmatrix} s - 6.$$

Then the functions

$$\mathcal{G}_{g^{(j)}, h}(\tau; P_2 f_s) \quad \left(j = 1, 2, \dots, \frac{s}{2} - 2 \right) \quad (3)$$

create the bases of the cusp form spaces of type $\left(-\frac{s}{2}; \Gamma_0(8), \nu_s(L) \right)$.

Proof. It is well known [2] that the dimension of $\left(-\frac{s}{2}; \Gamma_0(N), \nu_s(L) \right)$ cusp form spaces in case of $k \equiv 1 \pmod{2}$ is equal to $\frac{s}{2} - 2$. According to the theorem 1[1] the functions (3) belong to the cusp form space of type $\left(-\frac{s}{2}; \Gamma_0(8), \nu_s(L) \right)$. It is easy to check up that these functions are linear independent. This completes the proof.

Therefore by (2) there exist numbers $B_j^{(s,k)}$ such that

$$\mathcal{G}(\tau; f_{(s,k)}) = E(\tau; f_{(s,k)}) + \sum_{j=1}^{\frac{s}{2}-2} \beta_j^{(s,k)} \mathcal{G}_{g^{(j)}, h}(\tau; P_2 f_s).$$

It is easy to calculate the $B_j^{(s,k)}$ coefficients.

If we equalise the coefficients in both sides of this formula we will have the formulae for the number of representations of positive integer n by $f_{(s,k)}$:

$$r(n; f_{s,k}) = p(n; f_{(s,k)}) + \sum_{j=1}^{\frac{s}{2}-2} a_j^{(s,k)} \nu_j^{(s)}(n),$$

where $\rho(n; f_{(s,k)})$ is a singular series which is calculated as follows:
if $n = 2^\omega m$, $m \equiv 1 \pmod{2}$, $\omega \geq 0$, then

$$\rho(n; f_{(s,k)}) = \frac{\pi^{\frac{s}{2}} 2^{\frac{\omega s - 2\omega - k}{2}}}{\left(\frac{s-2}{2}\right)!} L^{-1}\left(\frac{s}{2}, (-1)^{\frac{s}{2}} \cdot 2\right) \chi_2^{(s,k)}(n) \sum_{d_1 d_2 = m} \left(\frac{(-1)^{\frac{s}{2}} \cdot 2}{d_1}\right) d_2^{\frac{s}{2}-1},$$

$$\chi_2^{(s,k)}(n) = \begin{cases} 1 + \frac{1}{2^{\left(\frac{s}{2}\right)(\omega+2) - \frac{k-1}{2}}}, & \text{if } \begin{cases} m \equiv 5 \text{ or } 7 \pmod{8}, s \equiv 6 \pmod{8} \\ \text{or } m \equiv 1 \text{ or } 7 \pmod{8}, s \equiv 0 \pmod{8} \\ \text{or } m \equiv 1 \text{ or } 3 \pmod{8}, s \equiv 2 \pmod{8} \\ \text{or } m \equiv 3 \text{ or } 5 \pmod{8}, s \equiv 4 \pmod{8}, \end{cases} \\ 1 - \frac{1}{2^{\left(\frac{s}{2}\right)(\omega+2) - \frac{k-1}{2}}}, & \text{if } \begin{cases} m \equiv 1 \text{ or } 3 \pmod{8}, s \equiv 6 \pmod{8} \\ m \equiv 3 \text{ or } 5 \pmod{8}, s \equiv 0 \pmod{8} \\ \text{or } m \equiv 5 \text{ or } 7 \pmod{8}, s \equiv 2 \pmod{8} \\ \text{or } m \equiv 1 \text{ or } 7 \pmod{8}, s \equiv 4 \pmod{8}, \end{cases} \end{cases}$$

the values of $L^{-1}\left(\frac{s}{2}, (-1)^{\frac{s}{2}} \cdot 2\right)$ are given in [3],

$$v_j^{(s)}(n) = \sum \left(2x_{s-4}^2 - x_1^2\right),$$

$$\sum_{e=1}^{2j} x_e^2 + 4 \sum_{e=2j+1}^{s-5} x_e^2 + 2x_{s-4}^2 = 2n$$

$$x_1 \equiv x_2 \equiv \dots \equiv x_{2j} \equiv 1 \pmod{2}$$

$$v_{\frac{s}{2}-2}^{(s)}(n) = \sum \left(x_{s-4}^2 - 2x_1^2\right),$$

$$4x_1^2 + \sum_{e=2}^{s-5} x_e^2 + 2x_{s-4}^2 = 2n,$$

$$x_2 \equiv x_3 \equiv \dots \equiv x_{s-5} \equiv 1 \pmod{2}$$

$$\alpha_j^{(s,k)} = 32\beta_j^{(s,k)} \left(j = 1, 2, \dots, \frac{s}{2} - 3\right), \quad \alpha_{\frac{s}{2}-2}^{(s,k)} = 64\beta_{\frac{s}{2}-2}^{(s,k)}$$

It must be pointed out that in the case of eight step quadratic forms only formulae for $s = 6$ and $s = 8$ are known (see, for example, [2]).

Tbilisi I. Javakhishvili State University

REFERENCES

1. T. Vepkhvadze. Georgian Mathematical Journal, 4, 1997, 385-400.
2. H. Peterson. Modulfunktionen und quadratische Formen, Springer-Verlay, Berlin, 1982, 307.
3. G. A. Lomadze. A. Razmadze Institute of Applied Mathematics Works, 19, 1949, 280-314.



M. Shubladze

On Finite Multiplicity of a Hypersurface Singularity

Presented by Corr. Member of the Academy N. Berikashvili, October 20, 1997.

ABSTRACT. For hypersurface singularity of type A_{k-1} the criterion of finite multiplicity is proved.

Key words: ISOLATED SINGULARITY, COMPLETE INTERSECTION, HOLOMORPHIC FUNCTION, TRANSVERSAL SINGULARITY.

Let Σ be a one-codimensional complete intersection with isolated singularity at $0 \in \mathbf{C}^{n+1}$, i. e. $\Sigma = (g(z) = 0)$, where $g: (\mathbf{C}^{n+1}, 0) \rightarrow (\mathbf{C}, 0)$ is isolated singularity. We consider $f: (\mathbf{C}^{n+1}, 0) \rightarrow (\mathbf{C}, 0)$ a holomorphic function germ with singular locus

$$\text{sing } f = \{z \in \mathbf{C}^{n+1}; \text{grad } f(z) = 0\} = \Sigma$$

The situation when Σ is a one-dimensional complete intersection was completely studied by D. Siersma [1].

Let O_{n+1} be the local ring of germs of holomorphic functions defined on $(\mathbf{C}^{n+1}, 0)$, i.e. $O_{n+1} = \{f, f: (\mathbf{C}^{n+1}, 0) \rightarrow (\mathbf{C}, 0)\}$. Let $I = (g)$ be ideal in O_{n+1} generated by isolated singularity $g: (\mathbf{C}^{n+1}, 0) \rightarrow (\mathbf{C}, 0)$. Then we have

Proposition. Holomorphic function f is singular on Σ if $f \in I^2$ [2].

In this case we can write $f = g^2 h$, with $h \in O_{n+1}$.

On I and I^2 there acts the subgroup D_Σ of D of local diffeomorphisms defined by:

$$D_\Sigma = \{\Phi \in D; \Phi^*(g) \in (g)\}.$$

Let $\tau_\Sigma(f)$ be the tangent space of the D_Σ -orbit and

$$J(f) = \left(\frac{\partial f}{\partial z_0}, \frac{\partial f}{\partial z_1}, \dots, \frac{\partial f}{\partial z_n} \right)$$

the Jacobian ideal of f , while z_0, z_1, \dots, z_n be the coordinates in $(\mathbf{C}^{n+1}, 0)$. Define I -codimension of f as follows

$$c_I(f) = \dim_{\mathbf{C}} I^2 / \tau_\Sigma(f)$$

Definition. A germ $f: (\mathbf{C}^{n+1}, 0) \rightarrow (\mathbf{C}, 0)$ is called of type $D(k, p)$, or $D(k, p)$ -singularity, if there exist some local coordinates

$$x_{ij} \ (1 \leq i \leq j \leq p), \ z_1, \dots, \ z_q, \ y_1, \dots, \ y_m$$

of $(\mathbf{C}^{n+1}, 0)$ such that

$$f(x, y, z) = \sum_{i \leq j \leq p} x_{ij} y_i y_j + \sum_{l=p+1}^m y_l^2$$

Remark. The singular locus of a $D(k, p)$ singularity is smooth and of dimension $1/2 p(p+1) + q$, while $n+1 = k+m$ [2]. $D(k, 0)$ - singularity is also called $A(k)$:

$$A(k) := D(k, 0): \sum_{l=1}^m y_l^2$$

We note also:

$$D(k, 1): x_1 y_1^2 + \sum_{l=1}^m y_l^2$$

In [1] and [3], the names D_∞ for a $D(1, 1)$ -singularity and A_∞ for a singularity of type $A(1) = D(1, 0)$, were used.

We can prove a result similar to [2,4].

Theorem 1. *Let $f \in I^2$. The following are equivalent*

- (i) $c_f(f) < +\infty$
- (ii) *The critical locus of f is Σ and the germ of f in every point of $\Sigma \setminus \{0\}$ is equivalent to a $D(k, p)$ - singularity, for a suitable p .*

Proof. To prove this theorem we define a sheaf of O_{n+1} - modules as follows:

$$\mathcal{F}(U) = I^2 / \tau_\Sigma(f),$$

where I^2 and $\tau_\Sigma(f)$ are considered as modules over the holomorphic functions on open set U . It is clear that F is coherent. We intend to use the fact: The sheaf \mathcal{F} is coherent if $\dim \Gamma(f) \leq \infty$.

(ii) \Rightarrow (i). For $z \in \mathbf{C}^{n+1} \setminus \Sigma$, f is regular at z and we have $\dim \mathcal{F}_z = 0$ since in this case $I^2 \cong O_z$. Let $z \in \Sigma \setminus \{0\}$ then f is of type $D(k, p)$ at z for some p , and we have $\dim \mathcal{F}_z = 0$ since $c_f(f)$ equals zero. It follows that \mathcal{F} is concentrated at 0, hence $c_f(f) < +\infty$.

(i) \Rightarrow (ii). Since $c_f(f) < +\infty$ we have that $\dim \mathcal{F}_z = 0$, for $z \neq 0$. Thus if $z \in \Sigma \setminus \{0\}$ we obtain that $\dim_{\mathbf{C}}(I^2 / \tau_\Sigma(f))_z = 0$, which means according to [2], that the germ of f at z of type $D(k, p)$ at z for some p .

When $z \in \mathbf{C}^{n+1} \setminus \Sigma$, we obtain that $\dim_{\mathbf{C}}(O_{n+1} / J(f))_z = 0$, which means that f is regular at z .

We would like to make this theorem more precise with respect to $D(k, p)$ -singularity on $\Sigma \setminus \{0\}$.

Let $f = g^2 h$, where $h: (\mathbf{C}^{n+1}, 0) \rightarrow (\mathbf{C}, 0)$ is isolated singularity. Consider the following ideal $I + (h) = (g, h)$. It is clear that it defines a complete intersection in $(\mathbf{C}^{n+1}, 0)$, and depends only on f . Let us denote by Δ the zero set of $I + (h)$:

$$\Delta = \nu(I + (h)).$$

The following are valid

Theorem 2. *Let $f \in I^2$, then the germ of f in every point of $\Sigma \setminus \Delta$ is equivalent to a A_∞ singularity (local formula x^2), and in every point of $\Delta \setminus \{0\}$ is equivalent to a c singularity (local formula $x^2 y_1$)*

Proof. Since $f \in I^2$ we have $f(z_0, z_1, \dots, z_n) = g^2 h$. If $z \in \Sigma \setminus \Delta$ let us consider a transformation from the group D_Σ :

$$x = g\sqrt{h}$$

$$y_1 = z_1$$

.....

$$y_n = z_n$$

whose Jacobian is equal to $g_{z_0}\sqrt{h} + g\left(\frac{1}{2}\sqrt{h}\right)h_{z_0} = g_{z_0}\sqrt{h}$ on $\Sigma\Delta$ since $g = 0$, where g_{z_0} and h_{z_0} are the derivatives of holomorphic functions g and h with respect to z_0 . The expression $g_{z_0}\sqrt{h}$ isn't equal to zero on $\Sigma\Delta$, since the function $h \neq 0$ and $g: (\mathbf{C}^{n+1}, 0) \rightarrow (\mathbf{C}, 0)$ has isolated singularity and we may renumber coordinates if needed, to achieve $g_{z_0} \neq 0$ on $\Sigma\Delta$.

This transformation reduces f to the form x^2 , i. e. in that points f has type A_∞ .

Now take $z \in \Delta \setminus \{0\}$, then consider the following transformation from group D_Σ .

$$x = g$$

$$y_1 = h$$

$$y_2 = z_2$$

.....

$$y_n = z_n$$

whose Jacobian has the form

$$\begin{vmatrix} g_{z_0} & g_{z_1} & g_{z_2} & \cdots & g_{z_n} \\ h_{z_0} & h_{z_1} & h_{z_2} & \cdots & h_{z_n} \\ 0 & 0 & 1 & \cdots & 0 \\ \cdots & \cdots & \cdots & \cdots & \cdots \\ 0 & 0 & 0 & \cdots & 1 \end{vmatrix}$$

which isn't zero, since Δ is complete intersection.

This transformation reduces f to the x^2y_1 , i. e. in that points f has type D_∞ .

Let us consider holomorphic function of $n + 1$ complex variables from I^k , i. e. $f = g^k h$, where g and h are isolated singularities at $(\mathbf{C}^{n+1}, 0)$. Such singularities we called in [5] hypersurface singularity of transversal type A_{k-1} . For those classes of singularity we can prove similarly to theorem 2:

Theorem 3. *Let $f \in I^k$. Then the germ of f in every point $\Sigma\Delta$ is equivalent to the germ of function x^k , and in every point of $\Delta \setminus \{0\}$ is equivalent to the germ of function $x^k y_1$ while z_0, z_1, \dots, z_n are the coordinates in $(\mathbf{C}^{n+1}, 0)$.*

Georgian Technical University

REFERENCES

1. D. Stiersma. Topology and its application, 27, 1987, 51-73.
2. G. R. Pellicaan. Hypersurfaces singularities and resolutions of Jacobi modules. Thesis, Rijksuniversitet Utrecht, 1985.
3. M. Shubladze. Bull. Georg. Acad. Sci., 128, 2, 1987, 241-244 (Russian).
4. A. Zakharia. A study about singularities with non-isolated critical locus, Thesis, Rijksuniversitet Utrecht, 1993.
5. M. Shubladze. Bull. Georg. Acad. Sci., 156, 3, 1997.

D. Gordeziani, N. Gordeziani, G. Avalishvili

Non-Local Boundary Value Problems for Some Partial Differential Equations

Presented by Academician T. Burchuladze, November 3, 1997

ABSTRACT. The results of investigation of non-local boundary value problems for some type of elliptic, parabolic and hyperbolic equations are presented. The non-local boundary value problems considered in this article comprise boundary conditions of the type of Bitsadze-Samarskii conditions or some versions of their generalization. In the case of rather wide class of elliptic and parabolic equations suggested iteration method allows not only to prove the existence and uniqueness of solution of the non-local problem, but also to construct an algorithm for numerical resolution. For some particular forms of hyperbolic equations a method of direct construction of solutions is given. The uniqueness for rather general type hyperbolic equations is proved using the properties of the solution on characteristics.

Key words: PDE, NON-LOCAL CONDITIONS, CHARACTERISTICS, ITERATION PROCEDURE.

Many works are devoted to non-local problems ([1-9] and a literature quoted). As is known [3,9] non-local conditions naturally arise while modelling various phenomena and processes. The iteration method suggested in [2] allows not only to prove existence of the solution of general type non-local problem for rather wide class of elliptic and parabolic equations, but also to construct an algorithm for numerical resolution of the problem. Right there the non-local problem from [2] was called Bitsadze-Samarskii problem. In some particular cases of hyperbolic equations initial-boundary value non-local problems are investigated by the method of direct construction of the solution. The uniqueness of the solution is proved using properties of solutions on characteristics.

We consider a bounded region $\Omega \subset \mathbb{R}^n$, $x = (x_1, \dots, x_n) \in \mathbb{R}^n$, Γ - boundary of Ω . Let $\Omega_i (i = 1, \dots, m)$ be regions with boundaries Γ_i , such that $\bar{\Omega} \supset \bar{\Omega}_1 \supset \dots \supset \bar{\Omega}_m$ and each of the following regions is placed strictly inside of proceeding one. Additionally Γ_i represents a diffeomorphical image of Γ , i.e. $x^{(i)} = I_i(x)$, $x^{(i)} \in \Gamma_i$, $x \in \Gamma$, $I_i(\cdot)$ -diffeomorphism, Γ, Γ_i -Lyapunov surfaces ($i = 1, \dots, m$).

Let L be uniformly elliptic operator of the type
$$L \equiv \sum_{i,k=1}^n a_{ik} \frac{\partial^2}{\partial x_i \partial x_k} + \sum_{i=1}^n b_i \frac{\partial}{\partial x_i} + c,$$

where $a_{ik}, b_i, c (c \leq 0)$ are prescribed functions.

Consider the non-local problem for elliptic equation

$$Lu(x) = f(x), \quad x \in \Omega, \quad (f(x) \text{ is the prescribed function}) \quad (1)$$

with non-local condition

$$u(x) = \sum_{i=1}^m q_i u(x^{(i)}) + \phi(x), \quad x \in \Gamma, \quad x^{(i)} \in \Gamma_i, \quad x^{(i)} = I_i(x), \quad (2)$$

where $\phi(x)$ is defined on Γ , $q_i = \text{const}$ are prescribed. We have to find a regular solution $u(x)$ of the equation (1) satisfying condition (2).

Assume, that the following conditions are true: $A_1 - a_{ik}, b_i, c, f, \Phi$ are such that there exists regular solution of Dirichlet problem for the equation (1), when $u|_{\Gamma} = \Phi(x); B_1$ - the principle of Hopf is in force.

Let us consider the following iteration procedure:

$$Lu^{(k)}(x) = f(x), \quad x \in \Omega, \quad u^{(k)}(x) = \sum_{i=1}^m q_i u^{(k-1)}(x^{(i)}) + \Phi(x), \quad k = 1, 2, \dots$$

$$u^{(0)}(x^{(i)}) = 0, \quad x \in \Gamma, \quad x^{(i)} \in \Gamma_i, \quad x^{(i)} = I_i(x), \quad (i = 1, \dots, m). \quad (3)$$

The following theorem is true.

Theorem 1. We assume that the conditions A_1 and B_1 are in force, $\left| \sum_{i=1}^m q_i \right| = q_0 = \text{const} < 1$, and additionally, either all $q_i \leq 0$, or $q_i > 0$. Then there exists unique regular solution $u(x)$ of the problem (1), (2) and $\max_{\Omega} |u(x) - u^{(k)}(x)| \leq cq_0^k, \quad \forall k \in \mathbb{N}$, $c = \text{const}$, which does not depend on $u(x)$ and $u^{(k)}(x)$.

Let us consider now the following problem: we are searching for a regular solution of the equation

$$\frac{\partial u}{\partial t} - Lu = f(x, t), \quad (x, t) \in Q_T = \Omega \times (0, T), \quad (4)$$

satisfying non-local and initial conditions

$$u(x, t) = \sum_{i=1}^m q_i u(x^{(i)}, t) + \phi(x, t), \quad (x, t) \in S_T = \Gamma \times [0, T], \quad (5)$$

$$x \in \Gamma, \quad x^{(i)} \in \Gamma_i, \quad x^{(i)} = I_i(x), \quad (i = 1, \dots, m), \quad u(x, 0) = u_0(x), \quad x \in \Omega, \quad (6)$$

where $f(x, t), \phi(x, t)$ are prescribed functions, $0 < T = \text{const} < \infty, a_{ik}, b_i, c$ coefficients depend on t , and between (5) and (6) compatibility condition takes place. In this case we consider the following iteration procedure:

$$\frac{\partial u^{(k)}}{\partial t} - Lu^{(k)} = f(x, t), \quad (x, t) \in Q_T,$$

$$u^{(k)}(x, t) = \sum_{i=1}^m q_i u^{(k-1)}(x^{(i)}, t) + \phi(x, t), \quad (x, t) \in S_T, \quad (7)$$

$$x \in \Gamma, x^{(i)} \in \Gamma_i, x^{(i)} = I_i(x), (i=1, \dots, m),$$

$$u^{(k)}(x, 0) = u_0(x), x \in \Omega, k = 1, 2, \dots,$$

$$u^{(0)}(x, t) = 0, (x, t) \in Q_T.$$

Assume, that the following two conditions are true: $A_2 - a_{ik}(x, t), b_i(x, t), c(x, t), f(x, t), \phi(x, t), u_0(x)$ are such functions, that there exists regular solution of the equation (4) with the initial condition (6) and condition of Dirichlet on $\Gamma u(x, t)|_{S_T} = \phi(x, t); B_2$ - the principle of maximum is in force.

The following theorem is true.

Theorem 2. We assume that conditions A_2, B_2 are in force, $\left| \sum_{i=1}^m q_i \right| = q_0 =$

$= \text{const} < 1$, and in addition, either all $q_i \leq 0$, or $q_i > 0$. Then there exists unique regular solution $u(x, t)$ of the problem (4)-(6) and

$$\max_{Q_T} |u(x, t) - u^{(k)}(x, t)| \leq cq_0^k, \quad \forall k \in \mathbb{N},$$

$c = \text{const} > 0$, does not depend on $u(x, t)$ and $u^{(k)}(x, t)$.

The proofs of the theorems 1 and 2 are based on the principle of Hopf, principle of maximum and analogue of the first theorem of Harnack for the equations (1) and (4). Let us consider now the non-local problem for hyperbolic equation

$$\frac{\partial^2 u}{\partial t^2} = \Delta u + c^2 u + f(x, t), \quad (x, t) \in Q_T \quad (8)$$

with non-local condition (5) and the following initial conditions

$$u(x, 0) = u_0(x), \quad u_t(x, 0) = u_1(x), \quad x \in \Omega, \quad (9)$$

where c is a real number, or imaginary, $u_0(x), u_1(x)$ are prescribed and between (5) and (9) compatibility conditions are in force.

Using the properties of solution of hyperbolic equation on characteristic cones here can be proved

Theorem 3. The problem (8), (6), (9) can not possess more than one regular solution.

In the particular case, when $n = 1, \Omega = (0, l), f(x, t) \equiv 0, u_0 \equiv 0, u_1 \equiv 0, c = 0$ and

$$u(0, t) = \omega_1(t), \quad u(l, t) = u(\xi, t) + \omega_2(t), \quad (10)$$

where $\xi \in (0, l), \omega_1(t), \omega_2(t)$ are prescribed, the solution can be constructed directly.



Under the above mentioned conditions and $c \neq 0$ we can search for the solution $u(x, t)$ in the following form

$$u(x, t) = \frac{\partial}{\partial x} \left\{ \int_0^{t-x} \varphi(\tau) I(c\sqrt{(t-\tau)^2 - x^2}) d\tau + \int_0^{t-x} \psi(\tau) I(c\sqrt{(t-\tau)^2 - (l-x)^2}) d\tau \right\},$$

where $I(z) = \sum_{s=0}^{\infty} \frac{1}{(s!)^2} \left(\frac{z}{2}\right)^{2s}$. We have to find functions $\varphi(\tau)$, $\psi(\tau)$, such that $\varphi(\tau) = \psi(\tau) = 0$, for $\tau \leq 0$. As $u(x, t)$ satisfies the condition (10), we get the Volterra type integral equations

$$-\varphi(t) + \psi(t-l) + \int_0^{t-l} \psi(\tau) \frac{c l I'(c\sqrt{(t-\tau)^2 - l^2})}{\sqrt{(t-\tau)^2 - l^2}} d\tau = \omega_1(t),$$

$$-\varphi(t-l) + \psi(t) - \int_0^{t-l} \varphi(\tau) \frac{c l I'(c\sqrt{(t-\tau)^2 - l^2})}{\sqrt{(t-\tau)^2 - l^2}} d\tau + \varphi(t-\xi) - \psi(t-l+\xi) +$$

$$+ \int_0^{t-\xi} \varphi(\tau) \frac{c \xi I'(c\sqrt{(t-\tau)^2 - \xi^2})}{\sqrt{(t-\tau)^2 - \xi^2}} d\tau - \int_0^{t-l+\xi} \psi(\tau) \frac{c(l-\xi) I'(c\sqrt{(t-\tau)^2 - (l-\xi)^2})}{\sqrt{(t-\tau)^2 - (l-\xi)^2}} d\tau = \omega_2(t),$$

where $I'(z) = \frac{d}{dz} I(z)$.

From these equations the functions φ and ψ can be constructed directly in succession by step $\tau_0 = \min(\xi, l-\xi)$ first on the interval $[0, \tau_0]$, then on $[\tau_0, 2\tau_0]$ and so on. Hence the following theorem can be proved.

Theorem 4. *If $n = 1$, $f \equiv 0$, $u_0 \equiv 0$, $u_1 \equiv 0$, $\omega_1(t)$, $\omega_2(t)$ are twice continuously differentiable, then there exists unique regular solution of the problem (8), (9), (10).*

Tbilisi I. Javakhishvili State University
I. Vekua Institute of Applied Mathematics

REFERENCES

1. A. V. Bitsadze, A. A. Samarskii. Dokl. AN SSSR, **185**, 4, 1969, 739-740 (Russian).
2. D. G. Gordeziani. Abstracts of reports of Inst. Appl. Math. Tbilisi State Univ., **2**, 1970, 38-40 (Russian).
3. D. G. Gordeziani, T. Z. Djioev. Bull. AN GSSR, **68**, 2, 1972, 289-292 (Russian).
4. D. G. Gordeziani. On methods of resolution for one class of non-local boundary value problems. Tbilisi University Press, Tbilisi, 1981 (Russian).
5. A. L. Skubachevskii. Mat. Sb., **117**, 4, 1982, 548-558 (Russian).
6. B. P. Paneyakh. Mat. Zam., **35**, 3, 1984, 425-433 (Russian).
7. V. A. Il'in, E. I. Moiseev. Mat. Mod., **2**, 8, 1990, 139-159 (Russian).
8. D. V. Kapanadze. Diff. Urovn., **23**, 3, 1987, 543-545. (Russian).
9. M. P. Sapagovas, R. I. Chegis. Diff. Urovn., **23**, 7, 1987, 1268-1274 (Russian).



V. Baladze
 On Spectral Coshape Theory

Presented by Academician G. Chogoshvili, November 20, 1997

ABSTRACT. In this paper the spectral coshape category having all objects of an arbitrary category for objects is constructed. The internal categorical description of coshape category is also given.

Key words: DIRECT SYSTEM, COEXPANSION, COSHAPE CATEGORY.

Introduction. The dual theory to the shape theory [1] is the coshape theory. The notion of coshape of space has been introduced by T. Porter [2] as a modification of homotopy type of space. The coshape theory as the shape theory is the spectral homotopy theory and meaningful extension of homotopy theory of given subcategory. An alternate coshape extensions of homotopy theory were constructed [3-4].

The purpose of this paper is to exhibit the notion of coshape for objects of arbitrary category K . First we develop the category $\text{dir}-K$ of direct systems of category K . Next we define general spectral coshape category $\text{CHS}_{(K,L)}$ for category K and its codence subcategory L . We also give internal categorical description of $\text{CHS}_{(K,L)}$.

Let K be an arbitrary category. Consider a category $d-K$ whose objects are direct systems $\underline{X} = (X_\alpha, p_{\alpha\alpha'}, A)$, where (A, \leq) is a directed set, X_α is object of K for every $\alpha \in A$ and $p_{\alpha\alpha'}$ is bonding morphism of X_α to $X_{\alpha'}$ for every $\alpha \leq \alpha'$. Moreover, $p_{\alpha\alpha} = 1_{X_\alpha}$ and $p_{\alpha'\alpha''} \cdot p_{\alpha\alpha'} = p_{\alpha\alpha''}$ for every $\alpha \leq \alpha' \leq \alpha''$. A morphism $(f_\alpha, \varphi) : \underline{X} \rightarrow \underline{Y} = (Y_\beta, q_{\beta\beta'}, B)$ of $d-K$, called a mapping of direct systems, consists of a function $\varphi : A \rightarrow B$ and of a collection of morphisms $f_\alpha : X_\alpha \rightarrow Y_{\varphi(\alpha), \alpha \in A}$ such that for $\alpha \leq \alpha'$ there is an index $\beta \geq \varphi(\alpha), \varphi(\alpha')$ with $q_{\varphi(\alpha)\beta} \cdot f_\alpha = q_{\varphi(\alpha')\beta} \cdot f_{\alpha'} \cdot p_{\alpha\alpha'}$. The identity mapping of direct system $(1_{X_\alpha}, 1_A) : \underline{X} \rightarrow \underline{X}$ is given by identity function $1_A : A \rightarrow A$ and identity morphisms $1_{X_\alpha} : X_\alpha \rightarrow X_\alpha$, $\alpha \in A$. The composition (h_α, ζ) of morphisms $(f_\alpha, \varphi) : \underline{X} \rightarrow \underline{Y}$ and $(g_\beta, \psi) : \underline{Y} \rightarrow \underline{Z} = (Z_\gamma, r_{\gamma\gamma'}, C)$ is defined in the usual manner. The mapping of direct systems $(h_\alpha, \zeta) : \underline{X} \rightarrow \underline{Z}$ consists of a function $\zeta = \psi \cdot \varphi$ and of a collection of morphisms $h_\alpha = g_{\varphi(\alpha)} \cdot f_\alpha : X_\alpha \rightarrow Z_{h(\alpha)}$. For every object $X \in K$ by (X) we denote direct system indexing by a singleton and having only one term X .

Two mappings of direct system $(f_\alpha, \varphi), (g_\alpha, \psi) : \underline{X} \rightarrow \underline{Y}$ are said to be equivalent, $(f_\alpha, \varphi) \sim (g_\alpha, \psi)$, if for every $\alpha \in A$ there is a $\beta \geq \varphi(\alpha), \psi(\alpha)$ such that $q_{\varphi(\alpha)\beta} \cdot f_\alpha = q_{\psi(\alpha)\beta} \cdot g_\alpha$. There is a quotient category $\text{dir}-K$, whose objects are of $d-K$ and morphisms are equivalence classes $\underline{f} = [(f_\alpha, \varphi)]$ of (f_α, φ) from $d-K$. The category $\text{dir}-K$ is dual to the category $\text{pro}-K$ [1]. Using the lemma 1 of ([1], ch. I. §1.2) we obtain

Lemma 1. Let $(f_\alpha, \varphi) : \underline{X} \rightarrow \underline{Y}$ be a morphism of category $\text{dir}-K$ and let A be a cofinite directed set. Then there exists a morphism $(g_\alpha, \psi) : \underline{X} \rightarrow \underline{Y}$ of category $d-K$ such that $\psi : A \rightarrow B$ is an increasing function, $g_\alpha \cdot p_{\alpha\alpha'} = q_{\psi(\alpha)\psi(\alpha')} \cdot g_{\alpha'}$ for every $\alpha \leq \alpha'$ and $\underline{f} = \underline{g}$.

2 12 11



Theorem 1. Let $\underline{X} = (X_\alpha, p_{\alpha\alpha'}, A)$ be an object of category dir-K . Then there exists a direct system $\underline{Y} = (Y_\beta, q_{\beta\beta'}, B)$ isomorphic to \underline{X} and indexed by a directed cofinite ordered set B , whose cardinality $|B| \leq |A|$. Moreover, each term Y_β and bonding morphism $q_{\beta\beta'}$ of \underline{Y} respectively are term and bonding morphism of \underline{X} .

Let $\underline{X} = (X_\alpha, p_{\alpha\alpha'}, A)$ and $\underline{Y} = (Y_\alpha, q_{\alpha\alpha'}, A)$ be direct systems of $d\text{-K}$. A morphism (f_α, φ) between \underline{X} and \underline{Y} is said special morphism if it satisfies the following conditions: $\varphi = 1$, and for every $\alpha \leq \alpha'$ $q_{\alpha\alpha'} f_\alpha = f_{\alpha'} p_{\alpha\alpha'}$.

Theorem 2. For every morphism $f: \underline{X} \rightarrow \underline{Y}$ of dir-K there exist direct systems \underline{X}' and \underline{Y}' indexed by cofinite directed ordered set N such that every term and bonding morphism of \underline{X}' (\underline{Y}') is also one in \underline{X} (\underline{Y}). Moreover, there exist isomorphisms $j: \underline{X}' \rightarrow \underline{X}$ and $i: \underline{Y}' \rightarrow \underline{Y}$ of dir-K and a special morphism $(f'_\alpha, 1_N): \underline{X}' \rightarrow \underline{Y}'$ of $d\text{-K}$ such that $j \circ f' = f \circ i$, $f' = [(f'_\alpha, 1_N)]$.

Theorem 3. A morphism of dir-K $f: \underline{X} = (X_\alpha, p_{\alpha\alpha'}, A) \rightarrow \underline{Y} = (Y_\alpha, q_{\alpha\alpha'}, A)$ given by a special morphism $(f_\alpha, 1_A): \underline{X} \rightarrow \underline{Y}$ is an isomorphism of dir-K iff every index $\alpha \in A$ admits an index $\alpha' \geq \alpha$ and a morphism $g_\alpha: Y_\alpha \rightarrow X_{\alpha'}$ of K such that $g_\alpha f_\alpha = p_{\alpha\alpha'}$ and $f_{\alpha'} \cdot g_\alpha = q_{\alpha\alpha'}$.

Let A be a category satisfying the following conditions:

- There is a small subcategory A' of A such that for every object $\alpha \in A$ there exist an object $\alpha' \in A'$ and morphism $u: \alpha \rightarrow \alpha'$.
- For every two objects $\alpha', \alpha'' \in A$ there exist an object $\alpha \in A'$ and morphisms $u': \alpha' \rightarrow \alpha$ and $u'': \alpha'' \rightarrow \alpha$.
- For every two morphisms $u', u'': \alpha \rightarrow \alpha'$ there exist an object α'' and a morphism $u'': \alpha' \rightarrow \alpha''$ such that $u \cdot u' = u \cdot u''$.

A generalized direct system in K is defined as covariant functor $\underline{X}: A \rightarrow K$ of category A to the category K . For every object $\alpha \in A$ we have an object $\underline{X}(\alpha) = X_\alpha$ and for every morphism $u: \alpha \rightarrow \alpha'$ of A we have bonding morphism $\underline{X}(u) = p_u: X_\alpha \rightarrow X_{\alpha'}$. A generalized direct system \underline{X} we denote by $\underline{X} = (X_\alpha, p_u, A)$.

In analogy of construction of category dir-K we can construct the category Dir-K , whose objects are generalized direct systems and whose morphisms are morphisms of generalized direct systems described in [4].

Theorem 4. Let \underline{X} be a generalized direct system of Dir-K . Then there exists isomorphic to \underline{X} in Dir-K a direct system \underline{Y} such that every term and bonding morphism of \underline{Y} respectively are term and bonding morphism of \underline{X} and the index set of \underline{Y} is a cofinite directed ordered set.

Let L be a full subcategory of K . We define a dual version of expansion ([1], ch. I, §2.1).

Let $X \in K$. A K -coexpansion of X is a morphism $p: \underline{X} = (X_\alpha, p_{\alpha\alpha'}, A) \rightarrow (X)$ in dir-K of direct system \underline{X} in the category K to direct system (X) with the condition:

For every direct system $\underline{Y} = (Y_\beta, q_{\beta\beta'}, B)$ in the subcategory L and every morphism $\underline{Y} \rightarrow (X)$ in dir-K there exists a unique morphism $f: \underline{Y} \rightarrow \underline{X}$ in dir-K such that $p \circ f =$

If \underline{X} and f respectively are object and morphism of dir-L then we say that p is a L -coexpansion of X .

Theorem 5. A morphism $p: X = (X_\alpha, P_{\alpha\alpha'}, A) \rightarrow (X)$ of direct system $X \in \text{dir-K}$ ($X \in \text{dir-L}$) to (X) is a K -coexpansion (L -coexpansion) iff the morphisms $p_\alpha: X_\alpha \rightarrow X$, $\alpha \in A$, satisfy the following conditions:

CE0) $p_{\alpha'} \cdot P_{\alpha\alpha'} = p_\alpha$ for every $\alpha \leq \alpha'$.

CE1) For every $P \in L$ and every morphism $g: P \rightarrow X$ from K there exist an index $\alpha \in A$ and morphism $f: P \rightarrow X_\alpha$ in K (in L) such that $g = p_\alpha \cdot f$.

CE2) For every morphisms $f, f': P \rightarrow X_\alpha$ in K (in L) satisfying the condition $p_\alpha \cdot f = p_\alpha \cdot f'$ there exists a bonding morphism $p_{\alpha\alpha'}: X_\alpha \rightarrow X_{\alpha'}$ such that $p_{\alpha\alpha'} \cdot f = p_{\alpha\alpha'} \cdot f'$.

Note that if $p: X \rightarrow (X)$ and $p': X' \rightarrow (X)$ are two L -coexpansions of object $X \in K$ then there is an isomorphism $i: X' \rightarrow X$ in the category dir-L .

A subcategory $L \subset K$ is called a codense subcategory of category K provided every object $X \in K$ admit a L -coexpansion.

Let X^L be the category whose objects are all morphisms $f: P \rightarrow X$, $P \in L$ and whose morphisms $u: f \rightarrow f': P' \rightarrow X$ are all morphisms $u: P \rightarrow P'$ in L such that $f = f' \cdot u$.

Theorem 6. A subcategory $L \subset K$ is codense subcategory of category K iff for every object $X \in K$ the category X^L satisfies conditions a), b) and c).

We define the coshape category for arbitrary category K and its full codense subcategory L . Let $p: X \rightarrow (X)$, $p': X' \rightarrow (X)$ and $q: Y \rightarrow (Y)$, $q': Y' \rightarrow (Y)$ are L -coexpansions of X and Y , respectively. Then there are isomorphisms $i: X' \rightarrow X$ and $j: Y' \rightarrow Y$. We say that morphisms $f: X \rightarrow Y$ and $f': X' \rightarrow Y'$ are equivalent if $f \cdot i = j \cdot f'$. The equivalence class of $f: X \rightarrow Y$ we denote by F and call a coshape morphism of X to Y . The composition $G \cdot F: X \rightarrow Z$ of coshape morphisms $F: X \rightarrow Y$ and $G: Y \rightarrow Z$ we can define as equivalence class of morphism $g \cdot i \cdot f$, where $f: X \rightarrow Y$ and $g: Y' \rightarrow Z$ respectively are representatives of F and G . Let I_X be equivalence class of morphism $I_X: X \rightarrow X$. It is clear that $I_Y \cdot F = F \cdot I_X = F$ and $H \cdot (G \cdot F) = (H \cdot G) \cdot F$ for every coshape morphisms $F: X \rightarrow Y$, $G: Y \rightarrow Z$ and $H: Z \rightarrow W$. We have obtained the coshape category $CSH_{(K,L)}$, whose objects are objects of category K and whose morphisms are coshape morphisms.

From theorem 5 follows that for every morphism $f: X \rightarrow Y$ of category K and for any L -coexpansions $p: X \rightarrow (X)$, $q: Y \rightarrow (Y)$ there exists a unique morphism $f: X \rightarrow Y$ in dir-L such that $f \cdot p = q \cdot f$. Let $CS(f)$ denote the equivalence class of f . If we put $CS(X) = X$ for every object $X \in K$ then we obtain a covariant functor $CS: K \rightarrow CSH_{(K,L)}$, called the coshape functor. For any $f: X \rightarrow Y$ morphism in dir-L there exists a unique coshape morphism $F: X \rightarrow Y$ such that $q \cdot f = F \cdot p$. If the objects X and Y are isomorphic in the coshape category $CSH_{(K,L)}$ than we say that they have some coshape and write $cs(X) = cs(Y)$.

Theorem 7. For every coshape morphism $F: P \rightarrow X$ of $P \in L$ to $X \in K$ there exists a unique morphism $f: P \rightarrow X$ in K such that $F = CS(f)$.

From theorem 7 follows that the category L and the full subcategory of $CSH_{(K,L)}$ restricted to objects of L are isomorphical.

Theorem 8. Let $Y \in K$ and $p: X \rightarrow (X)$ be a K -coexpansion of X . For every morphism $h: Y \rightarrow (Y)$ of $\text{dir-CSH}_{(K,L)}$ there exists a unique coshape morphism $F: X \rightarrow Y$ such that $h = F \cdot p$.

Let $F: X \rightarrow Y$ be a coshape morphism of $X \in K$ to $Y \in K$ and let $f: P \rightarrow X$ be a morphism of $P \in L$ to X . By theorem 7 the coshape morphism $F \cdot f: P \rightarrow Y$ is some morphism $g: P \rightarrow Y$ of category K . Then there is a function $F_p: K(P, X) \rightarrow K(P, Y)$ such that $F_p(f) = g = F \cdot f$. Let $v: P \rightarrow P'$, $P' \in L$ be a morphism and let $f': P' \rightarrow X$ be a morphism of category K such that



$$f' \cdot v = f$$

We have $g' \cdot v = F \cdot f' \cdot v = F \cdot f = g$. Consequently (1) implies

$$g' \cdot v = g \quad (2)$$

Let $F, F': X \rightarrow Y$ be two coshape morphisms such that $F_P = F'_P$, for every $P \in L$. Then $F = F'$. Let $G_P: K(P, X) \rightarrow K(P, Y)$ be a map such that (1) implies (2). Then there is a coshape morphism $F: X \rightarrow Y$ such that $G_P = F'_P$.

The composition $G \cdot F$ of coshape morphisms $F: X \rightarrow Y$ and $G: Y \rightarrow Z$ assigns to every morphism $f: P \rightarrow X$ the morphism $G \cdot F \cdot f: P \rightarrow Z$ so that

$$(GF)_P(f) = G_P(F_P(f)) \quad (3)$$

For identity coshape morphism $I_X: X \rightarrow X$ we have $(I_X)_P(f) = f$. Consequently a coshape morphism $F: X \rightarrow Y$ is a collection of functions $F_P: K(P, X) \rightarrow K(P, Y)$, $P \in L$, such that (1) implies (2). The identity coshape morphism $I_X: X \rightarrow X$ is defined by the identity functions $K(P, X) \rightarrow K(P, X)$, L and the composition is given by formula (3).

Let $K(-, X): L \rightarrow \text{Set}$ be the functor with assigns to each object $P \in L$ the set $K(P, X)$ and to morphism $v: P' \rightarrow P$ of L the function $v_X = K(v, X): K(P, X) \rightarrow K(P', X)$ given by formula:

$$v_X(f) = f' = f \cdot v, \quad f \in K(P, X).$$

For every coshape morphism $F: X \rightarrow Y$ we have defined functions $F_P: K(P, X) \rightarrow K(P, Y)$, $P \in L$, such that (1) implies (2) and $F_{P'} \cdot v_X = v_Y \cdot F_P$. Consequently F_P , $P \in L$, is a natural transformation of functor $K(-, X)$ to functor $K(-, Y)$.

Theorem 9. Let M be the category whose objects are the objects of category K and whose morphisms $X \rightarrow Y$ are the natural transformations $K(-, X) \rightarrow K(-, Y)$. The functor $A: \text{CSH}_{(K,L)} \rightarrow M$ which assigns to object $X \in \text{CSH}_{(K,L)}$ the same object X and to coshape morphism $F: X \rightarrow Y$ the natural transformation (F_P) , $P \in L$, is an isomorphism.

The homotopy category (HPol) of spaces having homotopy type of polyhedra (of compact polyhedra) is a codense subcategory of the homotopy category HTop of topological spaces.

The homotopy category (HPol_{*}) of pointed spaces having homotopy type of pointed polyhedra (of pointed compact polyhedra) is codense subcategory of the homotopy category HTop_{*} of pointed topological spaces.

Let $K = T$ be any category of topological spaces and homotopy classes of continuous maps and $L = T_0$ be a full codense subcategory of T . We have following theorem

Theorem 10. The functor $\Lambda: \text{CSH}_{(T, T_0)} \rightarrow M$ establishes the isomorphism between the spectral coshape category and the T_0 -coshape category of T . Porter [2].

Theorem 11. The spectral coshape category $\text{CSH}_{(\text{HTop}, \text{HCPol})}$ and the coshape category ${}^c\text{SH}$ [4] are isomorphical.

Tbilisi I. Javakhishvili State University

REFERENCES

1. S.Mardesic, J.Segal. Shape Theory. The Inverse System Approach. Amsterdam. New York. Oxford, 1982.
2. T.Porter. Proc. Royal Irish Acad. Sec., A 74, 1974.
3. Yu.Lisica. Proc. Intern. Conf. on Geom. Top., Warszawa, 1980.
4. V.H.Baladze. Coll. Math. Soc. J.Bolyai, 55, Topology, Pecs (Hungary), 1989.



T.Chilachava

On the Asymptotic Method of Solution of One Class of Nonlinear Mixed Problems of Mathematical Physics

Presented by Academician T.Burchuladze, February 5, 1998

ABSTRACT. This work proposes an asymptotic method of solution for a system of nonlinear nonhomogeneous equations of one class of mixed problems with an unknown external boundary in the domain. The system of equations describes an adiabatic spherical and symmetrical motion of a gravitating gas, while a moving shock or detonation wave (a spherical surface where the solution undergoes the first kind of discontinuity) is the external boundary of the domain.

Key words: ASYMPTOTIC METHOD, DETONATING WAVE, EXPLOSION, COLLAPSE.

The problem of a central explosion ($t_0 < 0$ is the instance of explosion) of a homogeneous gas sphere collapsing at zero pressure and followed by a thermonuclear detonation is discussed here.

The first two approximations for the motion law and the thermodynamic characteristics of the medium are calculated. The analysis of the solution shows that beginning from a certain instance a disseminating detonating wave begins to be brought to the centre.

1. Let us discuss the equations of the adiabatic spherical and symmetrical motion of a gas that are written in Lagrange's form:

$$\frac{\partial^2 u}{\partial t^2} + 4\pi u^2 \frac{\partial v}{\partial x} + \frac{kx}{u^2} = 0, \quad v = (\gamma - 1)f(x)w^\gamma, \\ w = \left[4\pi u^2 \frac{\partial u}{\partial x} \right]^{-1} \quad (1.1)$$

Here x is the $u(x, t)$ radius sphere mass, k the gravitation constant, γ the adiabatic indicator, $f(x)$ the function connected with the distribution of entropy by Lagrange's x coordinate.

The integral equation of the energy of the gas layer situated between the $x=0$ and $x=M(t)$ surfaces is as follows:

$$T + U + V = E + \int_{t_0}^t \left[\dot{M} \left(\frac{\dot{u}^2}{2} + \frac{v}{(\gamma - 1)w} - \frac{kM}{R} + Q \right) - 4\pi R^2 \dot{u}v \right] d\tau \quad (1.2) \\ T = \frac{1}{2} \int_0^M \dot{u}^2 dx, \quad U = \frac{1}{\gamma_2 - 1} \int_0^M \frac{v dx}{w}, \quad V = -k \int_0^M \frac{x dx}{u}, \quad \dot{u} \equiv \frac{\partial u}{\partial t}$$



Here T, U, V are the kinetic, inner and potential (gravitation) energies of the gas, Q is the energy excreted during the burning of a gas mass unit on the $x=M(t)$ surface, E - the explosion energy, $x=M(t)$ - the law of motion shock ($Q=0$) or detonation ($Q \neq 0$) wave with gas mass, $R=u(M(t), t)$ is the radius of a shock or detonation wave. 1,2 indices denote correspondingly the gas position in front and behind the wave.

If boundary conditions on the $x=M(t)$ discontinuity are solved with respect to parameters of the gas behind the wave we get the following:

$$w_2 = \frac{\gamma_2 + 1}{\gamma_2 - 1} w_1 \left[1 + \frac{1}{\gamma_2 - 1} \left(\frac{\gamma_2}{\gamma_1} \frac{a_1^2}{(\dot{R} - \dot{u}_1)^2} + 1 - g \right) \right]^{-1}, \quad a_1^2 = \frac{\gamma_1 v_1}{w_1} \quad (1.3)$$

$$v_2 = \frac{1}{\gamma_2 + 1} \left[v_1 + w_1 (\dot{R} - \dot{u}_1)^2 + w_1 (\dot{R} - \dot{u}_1)^2 g \right]$$

$$\dot{R} - \dot{u}_2 = \frac{\dot{R} - \dot{u}_1}{\gamma_2 + 1} \left[\gamma_2 + \frac{\gamma_2}{\gamma_1} \frac{a_1^2}{(\dot{R} - \dot{u}_1)^2} - g \right]$$

$$g = \left[\left(1 - \frac{\gamma_2}{\gamma_1} \frac{a_1^2}{(\dot{R} - \dot{u}_1)^2} \right)^2 + \frac{2(\gamma_2 + 1)(\gamma_1 - \gamma_2)a_1^2}{\gamma_1(\gamma_1 - 1)(\dot{R} - \dot{u}_1)^2} - \frac{2(\gamma_2^2 - 1)Q}{(\dot{R} - \dot{u}_1)^2} \right]^{\frac{1}{2}}$$

Besides, the continuity of Euler's and Lagrange's variables ought to be taken into account.

$$[u]_1^2 = 0, \quad [x]_1^2 = 0. \quad (1.4)$$

In fact, we get a mixed problem for the (1.1) system of nonlinear, nonhomogeneous equations where the $u(x, t)$, $v(x, t)$, $w(x, t)$ functions are unknown.

Initial conditions ($t=t_0$, phone) determine the initial state of a gas sphere and are the exact $u_1(x, t)$, $v_1(x, t)$, $w_1(x, t)$ solutions of the (1.1) system.

Thus, the mixed problem is considered in the Ω domain:

$$\Omega = \{t \in (t_0, t_*), x \in (0, M(t))\},$$

where t_0 is the moment of explosion, t_* the moment of time when the wave comes out on the surface of the body, or the moment of collapse.

Boundary conditions on the external unknown $x=M(t)$ boundary are like (1.3), (1.4), and

$$u(x, t) = 0 \quad \text{when} \quad x = 0$$

2. For the most of the gases $\varepsilon = \frac{\gamma_2 - 1}{\gamma_2 + 1}$ is a small parameter. Besides, it is included in (1.1) as a system of equations, in the (1.3) boundary conditions and in the (1.2) integral equation, whence the $R(t)$ law of wave motion is established.

Thus, the analysis of the system of equations and boundary conditions makes it clear that the solution can be sought for behind the wave with respect to the ε small parameter as a kind of several decompositions.



But the decomposition becomes irregular near the symmetry centre ($x=0$) [1-3]. In the solution regularization in this domain we use the method of consecutive approximation the essence of which is that the members of the ε series are maintained in the zero $w_0(x,t)$ approximation of the $w(x,t)$ expression. Then the first approximation for the medium motion and wave laws is found from the continuity equation $w = \frac{1}{4\pi u^2 u'}$, $u' = \frac{\partial u}{\partial x}$ by means of the boundary condition $u(0,t)=0$ and the zero approximation. The first approximations of the $v(x,t)$ and $w(x,t)$ functions will be found in the rest of the (1.1) system of equations.

The described method makes it possible to solve quite a wide range of the (1.1) equations system mixed problems. It is natural that the choice of decomposition depends on the initial state of the gas sphere (the exact solution before the wave) and on the energy of the explosion.

3. For example, let us discuss the problem of a central explosion ($t_0 < 0$ is the moment of explosion) followed by a thermonuclear detonation of a homogeneous gas sphere collapsing at zero pressure.

The exact solution of the (1.1) equations corresponding to the homogeneous parabolic compression (collapse) of dust (gas pressure $v=0$) is taken as initial data. Besides, the gravitation constant, the moment of explosion and the energy t_0, E are taken as basic dimension units:

$$u = \left[\frac{9x(1-\tau)^2}{2} \right]^{\frac{1}{3}}, \quad w = \frac{1}{6\pi(1-\tau)^2}, \quad v = 0, \quad \tau = 1 - \frac{t}{t_0} \quad (3.1)$$

We obtain a mixed problem in the Ω domain:

$$\Omega = \{ \tau \in (0, 1), x \in (0, M(\tau)) \},$$

where the system of equations is like (1.1), the energy integral equation- (1.2), the boundary conditions- (1.3), the initial conditions- (3.1).

Let us introduce a small parameter $\varepsilon = \frac{\gamma_2 - 1}{\gamma_2 + 1}$.

The analysis of the system of equations and the boundary conditions makes it clear that the solution can be sought behind the detonating wave as the following decomposition:

$$\begin{aligned} u &= R_0(\tau) + \varepsilon H(x, \tau) + \dots, \quad R(\tau) = R_0(\tau) + \varepsilon R_1(\tau) + \dots, \\ v &= v_0(x, \tau) + \varepsilon v_1(x, \tau) + \dots, \quad w = w_0(x, \tau)/\varepsilon + w_1(x, \tau) + \dots \end{aligned} \quad (3.2)$$

Including the (3.2) decomposition into the (1.1) system of equations, in the (1.2) integral equation and the (1.3) boundary conditions, we shall obtain the zero approximation of the problem solution using the regularization method.



$$v_0(x, t) = \frac{1}{6\pi(1-\tau)^2} \left(R'_0 + \frac{2R_0}{3(1-\tau)} \right)^2 + \frac{R''_0}{4\pi R_0^2} (M_0 - x) + \frac{1}{8\pi R_0^4} (M_0^2 - x^2), \quad (3.3)$$

$$w_0(x, \tau) = v_0'^2 \left\{ \left[6\pi(1-\tau)^2 \right]^{\frac{1-\gamma_2}{\gamma_2}} + \left(R'_0 + \frac{2R_0}{3(1-\tau)} \right)^{\frac{2}{\gamma_2}} \left[1 + \frac{2Q}{\left(R'_0 + \frac{2R_0}{3(1-\tau)} \right)^2} \right]^{-1} \right\}_{\tau=T_0(x)}$$

$$R_0(\tau) = \left[\frac{9M_0(1-\tau)^2}{2} \right]^{\frac{1}{3}} = \left(\frac{9}{2} \right)^{\frac{1}{3}} (1-\tau)^{\frac{15-\sqrt{17}}{24}} \left[1 - (1-\tau)^{\frac{\sqrt{17}}{3}} \right]^{\frac{1}{4}}$$

$$M_0(\tau) = (1-\tau)^{\frac{\sqrt{17}+1}{8}} \left[1 - (1-\tau)^{\frac{\sqrt{17}}{3}} \right]^{\frac{3}{4}}$$

Here $\tau = T_0(x)$ is the moment of time when the detonating wave passes the particle with Lagrange's x coordinate and is determined from the equation

$$x = (1-\tau)^{\frac{\sqrt{17}+1}{8}} \left[1 - (1-\tau)^{\frac{\sqrt{17}}{3}} \right]^{\frac{3}{4}}. \quad (3.4)$$

We shall obtain the following from the continuity equation in the next approximation:

$$\frac{4\pi u^3}{3} = \frac{4\pi R^3}{3} - \int_x^M \frac{\varepsilon dx}{w_0(x, \tau)}. \quad (3.5)$$

We shall use the boundary condition in the centre: $u=0$ when $x=0$, to establish the first approximation $R_1(\tau)$ of the detonation wave motion law. We shall obtain the following:

$$R^3 = \frac{3}{4\pi} \int_0^M \frac{\varepsilon dx}{w_0(x, \tau)}, \quad (3.6)$$

where

$$M(\tau) = \frac{2R^3}{9(1-\tau)^2}.$$

Thus, taking into account (3.5), (3.6) the medium motion law is determined by the formula:

$$\frac{4\pi}{3}u^3 = \int_0^x \frac{\varepsilon dx}{w_0(x, \tau)} \quad (3.7)$$

Using the motion law of the gas found behind the detonating wave (3.7) we shall calculate $v_1(x, \tau)$ and $w_1(x, \tau)$ from the (1.1) system of equations. The following asymptotics are easily obtained from (3.3):

$$R_0(\tau) \approx \left(\frac{9}{2}\right)^{\frac{1}{3}} \left(\frac{17}{9}\right)^{\frac{1}{8}} \tau^{\frac{1}{4}}, \quad \text{when } \tau \rightarrow 0_+$$

$$M_0(\tau) \approx \left(\frac{17}{9}\right)^{\frac{3}{8}} \tau^{\frac{3}{4}}, \quad \text{when } \tau \rightarrow 0_+$$

$$R_0(\tau) \approx \left(\frac{9}{2}\right)^{\frac{1}{3}} (1-\tau)^{\frac{15-\sqrt{17}}{24}}, \quad \text{when } \tau \rightarrow 1_-$$

$$M_0(\tau) \approx (1-\tau)^{\frac{\sqrt{17}+1}{8}}, \quad \text{when } \tau \rightarrow 1_-$$

The exact solution $R_0(\tau)$ of the detonating wave radius zero approximation makes it clear that from the τ_{cr} moment of time

$$\tau_{cr} = 1 - \left(\frac{15-\sqrt{17}}{15+\sqrt{17}}\right)^{\frac{3}{\sqrt{17}}}$$

The initially divergent detonation wave begins to drift to the centre and when $\tau = 1$ a collapse will take place.

Sukhumi Branch of I.Javakhishvili Tbilisi State
University

REFERENCES

1. *A.N.Golubyatnikov, T.I.Chilachava*. Dokl. Acad. Nauk SSSR, 273,4,1983,825-829(Russian).
2. *A.N.Golubyatnikov, T.I.Chilachava*. Izv. Akad. Nauk SSSR, M.Zh.G., 4,1986,187-191(Russian).
3. *T.I.Chilachava*. Izv. Akad. Nauk SSSR, M.Zh.G., 3,1988,179-184(Russian).

G. Tsuladze

Structuring Facilities in the Language "Ladis" for Designing Information Systems

Presented by Academician V. Chavchanidze, October 27, 1997

ABSTRACT. The language for aggregation and structurization of data in the information tasks is defined. Some operations of construction of complex data structures are considered. A corresponding example is also given.

Key words: PROGRAMMING, INFORMATION SYSTEM, DATA DECLARATION, DATA AGGREGATION, DESIGNING LANGUAGE.

The data structuring is one of the most important problems in designing of information systems. Much attention is paid to this problem in the field of developing the programming languages, and there are given different ways for defining and declaring complex data structures. For example in [1], there are proposed facilities for defining records including the description for collections of different types of data. To this end a structured type "Record" is introduced. However, in designing of information systems often main difficulties arise at the data defining stage.

In the present paper a gathering (assembling) approach for constructing complex and weakly expressed data is given using constructions defined in the language LADIS (Language for Designing of Information Systems). This paper contains a natural extension of the results given in [2-4].

Let $\{a\}$ be some finite set of signs such as letters, digits, delimiters, key abbreviations etc., which form LADIS language alphabet. Split the set $\{\alpha\}$ into certain subsets on the base of some semantic meaning: subsets of letters, Arabian digits, operation signs etc.; some of them may be split into farther subsets: e.g. the subset of operations may be divided on the subset of arithmetic operations and the subset of logical operations. Denote the subsets of $\{\alpha\}$ by $\{\alpha\}_i$ and the subsets of $\{\alpha\}_i$ by $\{\alpha\}_i^k$ ($i=1, \dots, m$) ($k=1, \dots, n$).

We now define the constructions of the first level for LADIS.

Let $\{a\}_t$ be the subset of the letters of a natural language. The construction WORD is given as follows: $\langle \text{word} \rangle ::= \langle \text{element of } \{\alpha\}_t \text{ subset} \rangle | \langle \text{word} \rangle \langle \text{element of } \{\alpha\}_t \text{ subset} \rangle$

Usually a word carries some semantic load (meaning). Formally word is any collection of letters. However, by semantic meaning a word may only belong to some set of any collections of letters of some natural language. In the LADIS language a word needs a semantic checking as well as syntactic. Let us denote by $\{S\}$ the set of all words and define operations over words. Let $S_\tau = \alpha_1 \alpha_2 \dots \alpha_k$ be some word in $\{\alpha\}_\tau$.

-Occurrence operation: designation OCCURRENCE.

Let $m_v = \alpha_j \alpha_w$ be some sequence of the subset $\{\alpha\}_k$. We will say that m_v occurs in S_τ if, beginning from some α_b , S_τ contains elements of α_k , which are in m_v , in the same

sequence as they are in m_v . The output is true if S_τ contains m_v , and false if it does not!

-Operation of calculation of the number of elements of $\{\alpha\}_k$ in the word S_τ : designation QUANTITY $\alpha_i S_\tau$.

This operation calculates the quantity of elements α_i in S_τ . The output is a natural number. The quantity of α_i in S_j word is called word length and is very important when organizing words in memory.

-Operation of tree structure formation: designation $TS S_\tau S_v$.

Let S_τ and S_v be two words. It is checked coincidence of elements forming these two words from left; farther checking on coincidence is stopped after finding different (non coinciding) elements. The same elements will be written only once and the rest part will be adjusted in two lines. For instance if there are two words "element" and "elephant", then the result of applying TS operation over them will be:

$$\begin{array}{r} \text{ment} \\ \text{elephant} \end{array}$$

This operation will be applied for formation of packed records by chain list representations and very important when organizing data in memory.

Let $\{\alpha\}_e$ be subset of Arabian digits. The construction NUMBER is given as follows:

$\langle \text{number} \rangle ::= \langle \text{unsigned number} \rangle | \langle \text{signed number} \rangle | \langle \text{combined number} \rangle |$
 $\langle \text{fractional number} \rangle$

$\langle \text{unsigned number} \rangle ::= \langle \text{element of } \{\alpha\}_e \text{ subset} \rangle | \langle \text{unsigned number} \rangle$
 $\langle \text{element of } \{\alpha\}_e \text{ subset} \rangle$

$\langle \text{signed number} \rangle ::= + \langle \text{unsigned number} \rangle | - \langle \text{unsigned number} \rangle$

$\langle \text{combined number} \rangle ::= \langle \text{unsigned number} \rangle / \langle \text{unsigned number} \rangle |$
 $\langle \text{unsigned number} \rangle - \langle \text{unsigned number} \rangle$

$\langle \text{fractional number} \rangle ::= \langle \text{unsigned number} \rangle . \langle \text{unsigned number} \rangle |$
 $\pm \langle \text{fractional number} \rangle$

Consider the union of subsets $\{\alpha\}_\tau \cup \{\alpha\}_e = \{\alpha\}_k$. Let's define identifier.

$\langle \text{identifier} \rangle ::= \langle \text{element of } \{\alpha\}_\tau \text{ subset} \rangle | \langle \text{identifier} \rangle$

$\langle \text{element of } \{\alpha\}_e \text{ subset} \rangle | \langle \text{identifier} \rangle \langle \text{element of } \{\alpha\}_\tau \text{ subset} \rangle$

Let us define conception LABEL.

$\langle \text{label} \rangle ::= \langle \text{identifier} \rangle$

This conception is used for labeling different elements, constructions and records; label is unique name and can not be used for labeling two different elements.

First level elements in LADIS language have their types: WORD and CHARACTER have type "char". NUMBER has types: "real", "integer" and "CNUM" (combined number). Identifier has the same type as the value, which name it represents. LABEL has type "char".

From the first level constructions were built constructions of second level of LADIS language.

Let S be set of all words, H -set of all numbers, I -set of all identifiers and L -set of all characters.

Let us define some constructions of second level and operations over them.

Consider $S \cup \{\alpha\}_p$, where $\{\alpha\}_p$ is subset of signs of punctuation and some separators

(space, dash, slash, etc.) and let's define SENTENCE.

< sentence > ::= < sentence term > { < sentence term > }

< sentence term > ::= < element of S set > | < sentence term > < element of { a }_p subset >

Sentence has the type CHAR (character) and is applied for passing some maintenance i.e. it has semantic load in natural language; each sentence is ending by ".".

Let Π be some set of sentences. Let us define operation of aggregation of more complex constructions and new sentence generation.

Operation of inserting word in a sentence-IW; has four modifications:

1. IW $\Pi_i S_j S_k$; where

Π_i -sentence, in which a word is inserted, S_j -the word, which is inserted, S_k -a word after which is inserted.

2. IW $\Pi_i S_j S_k$ PUNCT (+ ", " | - ":"); -means:

-In Π_i sentence after word S_k insert word S_j before S_j insert comma and after colon.

3. In the IW operation the quantity of inserting words may be several.

IW $\Pi_i S_j S_k S_r S_v \dots$

IW $\Pi_i S_j S_k$ PUNCT (+ ", " | - ":"); $S_r S_v$ PUNCT (- ";");...

4. Considering also mixed case.

IW $\Pi_i S_j S_k S_r S_v$ PUNCT (- ";");...

Punctuation sign standing before inserting word will not be replaced if we don't point its change.

The operation of adding one sentence to another sentence.

1. AS $\Pi_i \Pi_j$; add sentence Π_j to the sentence Π_i . New construction is beginning with Π_i and after "." (which is ending sign of Π_i) is written Π_j sentence.

The result will be labeled and constructions is considering as an indivisible text. Labels which are used for Π_i and Π_j won't be moved to new construction. In general the quantity of adding sentences may be any:

AS $\Pi_i \Pi_j \Pi_k \dots$;

It is obvious, that changing the sequence of sentences will lead to different results.

2. AS Π_i PS (N) Π_j ; add Π_j sentence to Π_i sentence and place between them N spaces. "PS" is "place spaces".

3. AS $\Pi_i \Pi_j$ PS (N) $\Pi_k \Pi_r \dots$; mixed case.

Let us define conception of key word.

< key word > ::= < word > | < key word > { | < key word > } < word >

Key words are defined for the indexing aggregated element TEXT.

Let's define the conception of aggregating complex construction-text record-TEXR.

< text record > ::= < text label > | < ttext > | < text record > < not text construction > |

< text record > < text > | < text record > END

< text label > ::= < header > | < division > | < paragraph > | < item >

< header > ::= < sentence > | < clause >

< clause > ::= < element of S set > | < element of I set > |

< clause > < element of S set > | < clause > < element of I set > |

< clause > < element of H set > | < clause > < element of L set >

< division > ::= DIVISION < element of H set > | < division > < sentence > |

< division > < clause >

<paragraph> ::= §<element of H set>|<paragraph><clause>|

<paragraph><sentence>

<item> ::= ITEM<element of H set>|<item><sentence>|<item><clause>

<non text construction> ::= <expression>|<clause>|<drawing>|<picture>

The essence of these constructions are obvious and we don't write here the formal definitions because of their bulky definitions. Text labels are sorted by the containing operation:

HEADER \supset DIVISION \supset PARAGRAPH \supset ITEM

A designer can use the text labels by his will e.g. pass any of them or enter new, pointing their sequence. Let's define facilities for aggregation documents having some graphical structure. Presented facilities are development of methods given in [2].

Analogous to [5] let's define the operation of followness between clauses. Let F set of clauses and f_i and f_j be elements of this set. Will say, that f_j directly follows f_i , if $i \neq j$, $i < j$ and there is no index k , which satisfies the $i < k < j$ condition and f_k directly follows f_i and f_j directly follows f_k .

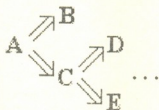
Let's assign the direct followness operation by \Rightarrow .

$f_i \Rightarrow f_j$, if $i < j$, $i \neq j$ and there is no such k , where $f_k \Rightarrow f_j$, $f_j \Rightarrow f_k$

Will say that f_j follows f_i , if there are indexes k, l, m, \dots , that $j < k < l < m < \dots < j$ and

$f_i \Rightarrow f_k \Rightarrow f_l \Rightarrow \dots \Rightarrow f_j$. Let's assign operation of followness by \rightarrow .

The direct followness operation is defining a graph which in knots has clauses:



<line record> ::= <number>|<word>|<clause>|<graph>|

<line record><delimiter><number>|

<line record><delimiter><word>|

<line record><delimiter><clause>|

<line record><delimiter><graph>

The type (sort) of delimiter is not fixed and can be defined by a designer in the division DELIMITERS. Over lines are defined unification, intersection and addition. Let A and B be the lines: $A \cup B$ forms a new line, which contains hole A line and only those elements of B , which are not in A . $A \cap B$ contains only the same elements from A and B . $A \text{ ADD } B$ is a new record, which contains whole A and B in the same sequence as they were in A and B . There are distinguished: specifier line, definition line, format line, pointer line and value line.

Line records which have the same definition and format are united in one record (array of line-records). Array of line-records may have TITLE. There are also entered conceptions of left (right) over title and under title inscriptions, left (right) corner labels.

It should be noticed, that in the definition of this kind of constructions there is entered a PROCESSING division, containing statements, which establishes relations between individual values.

For example:

DEFINITION STRUCTURE 'PH' DELIMITERS ' * ' RIGHT LABEL 'Table 9.15'
 TITLE 'calculation of rejection of appeal time from norm' SPECIFIER LINE (CLAUSE
 *KEYWORD*CLAUSE*GRAPH*GRAPH*KEYWORD*GRAPH)

DEFINITION LINE (№№ n/n*Title of goods*norm, days*I-st quarter (average stock
 of goods, hundred dollars*time of appeal, days)*II quarter (IDENTICAL I quarter) *re-
 jection in II quarter with I quarter*rejection by norms, days(I quarter*II quarter)).

POINTER LINE (A,B,C,1,2,3,4,5,6,7,8,9,10,11)

FORMAT LINE (2*9*3*3*3*4*5*3*3*4*5*6*6*6)

ARRAY LINE VALUE

(1*jam*170*46,0*21,0*0,233*197,42*...*-63,91*+27,42*-36,49)

(2*stewed fruit*230*40,0*18,0*0,200*200,0*,...)

LEFT LABEL 'Kutaisi <<signature>>'

PROCESSING

'3':='2':90; '4':='1':3';

'7':='6':90; '8':='5':7'; '9':='8':4'

'10':= etc.

END

In the statements of processing division for the names of variables instead of their numbers from the pointer line may be used names from the definition line.

Presented work is supported by GAS Grant №1.19

N. Muskhelishvili Institute of Computational Mathematics
 Georgian Academy of Sciences

REFERENCES

1. K. Jensen. N.Virt, Pascal. Moskva, 1982, 150 (Russian).
2. M. Tsuladze. Proc. Comput. Center of Academy of Sciences of Georgia SSR, XVIII:1, 1979 (Russian).
3. M. Tsuladze, A.N. Dolidze. Bull. Acad. Sci. Georg. SSR, 119, 3, 1985 (Russian).
4. M. Tsuladze. Proc. Comput. Center Acad. Sci. Georg. SSR, XVI:1, 1977 (Russian).
5. M. Tsuladze. V sb. : Nekotorye voprosy programirovaniya. 1965 (Russian).

Z. Kipshidze, G. Ananiashvili

Decision Making Informational Model for Ergative Systems

Presented by Academician V. Chavchanidze, July 31, 1997

ABSTRACT. Experts knowledge based on computing consultant-system construction problem is considered. Using correcting codes theory mathematical apparatus, control and decision making general informational model for the ergative systems is suggested.

Key words: DECISION MAKING, ERGATIVE SYSTEMS, CORRECTING CODE, ERROR CORRECTION, DECODING MATRIX, SYNDROM, KERNEL, RANK.

The computerization and informatization of the modern society and also the wide usage of ergative computing complexes in social, economic and other spheres make the problem of process management in the complex open-nonlinear systems very actual.

All this is closely connected with organisation of the banks of complex computing systems and the problem of decision making. So it's necessary to work out the general principle of the problem oriented computer-adviser construction and developing the general information model the main element of which is the decision making block.

The problem can be solved by using the correcting codes theory in two procedures considering objects in normal position and deviation.

In the first procedure we have the object's normal position recognition, on the second-organisation of the initial objects set by means of expert's knowledge in the limits of the problem region and decision making by the evaluation of information connected with new object.

Let's assume that "error" is such an effect on the object in the connection channel, that it changes objects normal position, i.e. the deviation from the "norm". Let's also assume that the position of the i -th object in the $V^{n,q}$ space is described by the vector of n -dimension

$$x_i = (x_{i1}, x_{i2}, \dots, x_{in}), \quad (j = \overline{1, n}),$$

where x_{ij} components belong to $\{0, 1, \dots, q-1\}$ set and $x_i \in V^{n,q}$ is the element of linear n -dimensional vector space on the $GF(q)$ finite field, $q > 0$ [1,2]. Let's assume that statistically informational system is described by the object positions' probabilities $P_0(x)$ and $P_e(\varepsilon/x)$ of which the $P_0(x)$ is the probability of the object appearance on the system's input, and $P_e(\varepsilon/x)$ - probability of the ε error's addition on the x vector

$$P(\varepsilon) = \sum_G P_0(x) P_e(\varepsilon/x),$$

where $\mathcal{C} \subset V^{n,q}$ is the code vectors' set, $P_e(\varepsilon)$ - error's frequency on the output of the disturbances' source. Then $P_{e_r}(\varepsilon/x) = P_e(\varepsilon)$, where $G \subset V^{n,q}$ is the code vector set. Finally



we'll have $P(\varepsilon) = P(\varepsilon)$.

Let's assume U is the set of all admissible deviations with positive probabilities, otherwise $U = V^{n,q}$, when U contains all n -dimensional space. Arranging $U \leq q^n$ ($u \in U$) vectors descending by their probabilities

$$P(\varepsilon^1) \geq P(\varepsilon^2) \geq \dots \geq P(\varepsilon^N)$$

some of which could be equal.

As $P(U) = \sum_{\varepsilon \in U} P(\varepsilon) = 1$, for any $\sigma < 1$ there exists minimal number $k(\sigma)$ that one and

only one $P(U_{k(\sigma)}) \sum_{v=1}^{k(\sigma)} P(\varepsilon^v) \geq \sigma$.

For $U_{k(\sigma)}$ error-set there is constructed the correcting code with $(n \times r)$ dimensional decoding H matrix. By this the system's education stage finished: $V^{n,q}$ space is factorized by nonintersected classes for G kernel of H matrix. From the decoding matrix we receive its orthogonal coding L matrix, by which the initial vectors' coding is realised in $m = (n - r)$ dimensional G kernel of H . Distorted (error) vectors exist in adjacent classes and form the set of the objects deviated from the norm. If $a_v = x_i + \varepsilon_v$ - is the v -th vector corresponding to the distorted object, where $x_i \in G$ ($i = \overline{0, q^m - 1}$), and H is the checking $(n \times r)$ matrix, and the result of multiplication

$$a_v H = (x_i + \varepsilon_v) H = s_v \quad (v = \overline{1, k(\sigma)})$$

will be univocal r -component compressed pattern of a_v , where r is the H matrix rank. At the same time the r -length sequence $s_v \in S$ called "syndrome" can be used as an address (number) of the systems memory cell in which information on ε_v error is recorded. This is the knowledge of a a_v vector deviated from the normal position as a result of ε_v disturbance effect. It fixes all deviations because in the system's memory to every ε_v is assigned the one-valued address s_v , syndrom [3]. Hence the determination of deviation and error correction are performed as precisely as the experts knowledge is complete on v -th address. Because the experts' knowledge is evristical, it may be insufficient for decision making and might be necessary to make it more precise: in our case via dialogue with open type system in interactive regime. At the same time the dialogue is realized in accordance with questions stored at v address. Therefore if the distorted vector, that is not found in adjacent classes, appears at system input $\varepsilon_\sigma \notin U_{k(\sigma)}$ the answer will be wrong. The system will not be able to recognize and when 2 or more distored vectors occur at one address in the class the so-called "collisions" will take place. To avoid such situations it is necessary forecast it: one must construct such code structure which will correct not only the fixed deviations, but can also detect "unknown" ones. At multiple repetition of the mentioned cases the filling of initial set of disturbances with new deviations, and consequently with a new knowledge is accomplished. A new code and H matrix will be constructed for correction of filled $\varepsilon_v \in U_{k(\sigma)}$ ($v = \overline{1, k(\sigma)}$) set of disturbances.

One should take into consideration the situation when adjacent classes are left not containing the fixed deviations. When the distorted vector appears in the mentioned class, a corresponding new knowledge about this deviation should be recorded there. In this case the education of system does not require the construction of a new code. In such case the coding is considered in terms of pattern recognition problem, as the positions of the recognizable objects are not structured preliminarily in code subspace. The solution of the mentioned problem is possible by using the natural informational redundancy characteristic of the objects in coding process [4].

There exists a class of problems, where the expert is able to restore the normal image according to main components (information symbols) representing the object position, which may not have initial image. In this case the coding of localized normal informational symbol sequences is executed in systematic code by coding matrix recorded in computer memory. Then if we connect the redundant symbols (checking part) obtained in such method to already existed informational part relevant object we obtain distorted code vector n -dimensional sequence, representing the recognizable object in code structure. As the number of recognizable objects is small, the number of vectors in code space can be much more, than it is necessary for presenting the positions of the given objects. Thus from the code set such vectors are selected, which exactly correspond to the code structure of the recognizable objects positions and at the decision making the error is excluded. In such a case it is reasonable to use the general method of linear code synthesis [2]. At the same time such problems are frequently considered, where normal position of the objects is characterized by one, e. g. zero vector from the coding set. Then all the other positions deviated from the normal represent probable deviations and on their basis by using definite checking matrix the problem will be solved by direct addressing method. The decision making will be made by realization of identification scheme.

Institute of Cybernetics

Institute of Computational Mathematics

Georgian Academy of Sciences

REFERENCES

1. U. Peterson, E. Weldon. Kody, ispravlyayushchie oshibki. Moskva, 1976, 23-52 (Russian).
2. R. R. Varshamov. Izv. AN SSSR (Tekhnicheskaja kibernetika). 4, 1964, 53-58 (Russian).
3. G. G. Ananiashvili. Slovenska Akademia, Vied, 7, 6, 1988, 531-541
4. J. G. Savtchenko. Sistemy avtomaticheskogo upravlenija. (Problemy obespechenija nadezhnosti). Kiev, 1971, 49-55 (Russian).

A. Gabelaia, V. Ivanenko

On the Use of Statistical Regularity Concept in Decision-Making

Presented by Academician V. Chichinadze, September 15, 1997

ABSTRACT. The examples of statistically stable and unstable realizations of unknown parameter are given. The application of statistical regularity concept in decision making is shown.

Key words: DECISION MAKING, STATISTICAL REGULARITY.

In decision making within uncertainty it is very important to have the information about possible behavior of an unknown parameter. This information, together within our choice, determines the results of our decision. If the certain sequence of realization of the parameter is known, then it is natural to try to obtain the necessary information using this sequence. In this situation we may have one of the following cases:

1. The sequence of realization of parameter is regular (non-random);
2. The sequence of realization of parameter is stochastic (i. e. the parameter has some distribution);
3. The sequence of realization of parameter is non-stochastic or it is random in a broad sense phenomena [1] (i. e. the parameter has not the distribution function).

The last case is called statistically unstable [2].

Let us consider the simplest case, when the unknown parameter θ can take only two possible values ("0" and "1"), i. e. when the set of possible values of parameter has form $\Theta = \{0, 1\}$. Now let us study the behavior of the frequency of this values, when the number of realization grows infinitely.

Example 1. (Regular (deterministic) case). Let the realization of parameter $\theta = (\theta_1, \theta_2, \dots)$ has the form: 0, 1, 0, 1, 0, 1, 0, 1, 0, 1, ...

Build now the dynamic $P_n(\{0\})$, ($n \in N$), where $P_n(\{0\})$ denotes the frequency of zero value into n -realization, where N denotes set of natural numbers.

In this case we have 1, 1/2, 2/3, 1/2, 3/5, 1/2, 4/7, 1/2, 5/9, 1/2, ...

Hence, in this case $\lim_{n \rightarrow \infty} P_n(\{0\}) = 1/2$, moreover $P_n(\{0\}) \geq 1/2$, for any $n \in N$.

Besides this, in this case, from the relation $P_n(\{1\}) = 1 - P_n(\{0\})$ we have

$\lim_{n \rightarrow \infty} P_n(\{1\}) = 1/2$ and $P_n(\{1\}) \leq 1/2$, for any $n \in N$.

Consequently, in the case of regular (non-stochastic) sequence of realization, the limit point of this sequence is simultaneously the extreme point.

Example 2. ($P_n(\{0\}) = 1/2$, stochastic case).

Let the realization of θ parameter has the form 0,1,0,0,1,1,0,1,0,0, 1, 1, 1, 0, ...

The dynamics of frequency $\{P_n(\{0\}), n \in N\}$ in this case, has the form 1, 1/2, 2/3, 3/4, 3/5, 1/2, 4/7, 1/2, 5/9, 1/2, 5/11, 5/12, 5/13, 3/7, ...

In this case we have $\lim_{n \rightarrow \infty} P_n(\{0\}) = \lim_{n \rightarrow \infty} P_n(\{1\}) = 1/2$.

Example 3. (Non-stochastic case).

Let us consider the following realization of parameter [3]

0, 1, 0, 1, 0, 0, 1, 1, 0, 0, 0, 0, 1, 1, 1, 1, 0, 0, 0, 0, 0, 0, 0, 0, 1, 1, 1, 1, 1, 1, 1, 1, ...

The dynamics of frequency $\{P_n(\{0\})\}$, in this case has the form 1, 1/2, 2/3, 1/2, 3/5, 2/3, 5/6, 3/5, 7/11, 2/3, 5/13, 3/7, 7/15, 1/2, ...

It's easy to show [3], that this sequence of realization is not statistically stable, i.e. $P_n(\{0\})$ has no limit when $n \rightarrow \infty$. Moreover the set of limit points of sequence $P_n(\{0\})$, in this case, is $\{\alpha_i: 1/2 \leq \alpha_i \leq 2/3, \text{ where } \alpha_i \text{ is rational number}\}$.

Hence, this sequence of realization θ , can be characterized by following statistical regularity (i. e. family of distributions of values) $P(\bar{\theta}) = \{P_1(\cdot), P_2(\cdot), \dots\}$, where $P_i(\cdot)$

denotes the distribution $P_i(\cdot) = \begin{Bmatrix} \{0\} & \{1\} \\ \alpha_i & 1-\alpha_i \end{Bmatrix}, (i \in N)$

α_i - rational number, such that $1/2 \leq \alpha_i \leq 2/3$.

To illustrate the application of statistical regularity concept, consider the decision making problem with loss function $L(\theta, u)$, where L is a bounded real function on the set $\Theta \times U$. (Here $L(\theta, u)$ determines the loss corresponding to the choice u , when the unknown parameters value is θ).

Assume that the realization of parameter θ , is characterized by statistical regularity $P(\bar{\theta})$, described above. Following [2], in this case we may evaluate our decisions by the optimality criterion

$$K(u) = \sup_{1/2 \leq \alpha_i \leq 2/3} [L(0, u) \cdot \alpha_i + L(1, u) \cdot (1 - \alpha_i)] = \sup_{1/2 \leq \alpha_i \leq 2/3} \{[L(0, u) - L(1, u)] \cdot \alpha_i + L(1, u)\},$$

$$\text{from where } K(u) = \begin{cases} [L(0, u) - L(1, u)] \cdot 2/3 + L(1, u), & \text{if } L(0, u) \geq L(1, u) \\ [L(0, u) - L(1, u)] \cdot 1/2 + L(1, u), & \text{if } L(0, u) \leq L(1, u). \end{cases}$$

$$\text{Equivalently } K(u) = \begin{cases} 2/3L(0, u) + 1/3L(1, u), & \text{if } L(0, u) \geq L(1, u) \\ 1/2[L(0, u) + L(1, u)], & \text{if } L(0, u) \leq L(1, u). \end{cases}$$

Now the decision making problem reduced to the problem

$$K(u) \rightarrow \inf, u \in U.$$

What is transformable to following two mathematical programming problems

$L(0, u) - L(1, u) \rightarrow \inf$, subject to $L(0, u) \geq L(1, u)$, $u \in U$, and $L(0, u) + L(1, u) \rightarrow \inf$, subject to $L(0, u) \leq L(1, u)$, $u \in U$.

REFERENCES

1. A. N. Kolmogorov. Teoria veroiatnosti i matematicheskaja statistica. M., 1986, 467-471 (Russian).
2. V. I. Ivanenko, V. A. Labkovskij. Problema neopredelennosti v zadachakh prinyatiya reshenij. Kiev, 1990 (Russian).
3. V. I. Ivanenko, I. V. Zorych. Paper for the Workshop on the Dynamics and Control. Rio de Janeiro, 1996.

V. Gersamia, M. Kvernadze, M. Mirianashvili, Sh.Mirianashvili, A.Mirtskhulava

The Investigation of Photoelectrical Characteristics of Silicon Semiconductor Structures by Dynamical Lattice Method

Presented by Academician N. Amaglobeli, June 27, 1997.

ABSTRACT. By dynamical lattice method based on the phenomenon of light diffraction on light-induced periodical structure (lattice) from non-balanced charge carriers the photoelectrical characteristics of semiconductor structures has been investigated on the basis of monocrystal silicon. It has been shown that the dynamical method sensibly expresses the quality of plate surface treatment through effective lives of non-balanced charge because of difference of surface recombination rates.

Key words: DYNAMICAL LATTICE METHOD, DEFECT-ADMIXTURE.

New methods of active laser spectroscopy allow us to study the electrical properties of semiconductor materials [1] by the dynamics of non-balanced processes.

The purpose of this work is the investigation of photoelectrical characteristics of semiconductor silicon structures by the method based on the phenomenon of light diffraction on the light-induced periodical structure from the non-balanced charge carriers.

Physical essence of dynamical lattice method supposes the defect-admixture system state reflection in electrophysical parameters of silicon and through their connection with optical characteristics in diffraction effectiveness η , which is connected with the modulation concentration change of non-balanced charge carrier $\Delta N = N_{\max} - N_{\min}$ by ratio:

$$\eta_1 = (\Phi/2)^2 = \left[\frac{\pi}{2\lambda_1} \int_0^d \Delta n dz \right]^2 = \left\{ \frac{\pi}{2\lambda_1} n_{eh} \left[\int_0^d (N_{\max} - N_{\min}) dz \right] \right\}^2$$

In its turn modulation concentration is stipulated by generation, recombination and diffusion processes of non-balanced charge carriers:

$$\Delta N(t) = \alpha_2 I_{02} \int_0^t e^{-\alpha_2 z} dz \int_0^t f(t-\xi) e^{-\xi(\frac{1}{\tau})} d\xi$$

In these formulae: Φ is phase running of the wave at wave length λ_1 by passing the lattice; Δn is magnitude of light-induced refraction index $\Delta n = n_{eh} \times \Delta N$, where n_{eh} is modulation factor of refraction index by single $e-h$ couple; $f(t)$ is time form of laser impulse; τ , is decay time of dynamical lattice; d is the thickness of the sample.

The induction of dynamical lattice on the plate surface and their synchronous sounding (for these purposes the second and the first laser harmonics were used) have been carried out on the experimental plant containing solid impulse laser (impulse duration

3 ms), laser radiation detectors, measuring system of collection and treatment of dates on computer.

In these experiments the excitation level I_{O_2} at wave length $\lambda_2 = 0.53$ mkm (absorption factor $\alpha_2 = 8 \times 10^3$ cm⁻¹) and I_{O_1} at wave length $\lambda_1 = 1.06$ mkm. Intensities of passed I_T and diffracted in first degree of bunch diffraction I_1 at wave length λ_1 have been recorded.

The samples represent the monocrystal silicon plates ($\Phi = 76$ mm) grown by Chokhralsky method in direction $\langle 100 \rangle$, alloyed by phosphorus (n -type) and boron (p -type). For structure formation (n - n and n - p transitions) the method of ion alloyage was used. The ion implantation P^+ and B^+ has been carried out on the plant "vesuvius-3M": $E_{P^+} = 10$ keV, $D_{P^+}(\text{dose}) = (1 \div 4) \times 10^{15}$ cm⁻²; $E_{B^+} = 10$ keV, $D_{B^+} = (10^{-1} \div 4) \times 10^{15}$ cm⁻². Besides, for the formation of isotype n - n^+ and p - p^+ transitions, all plates on the back side were implanted by ions P and B with energy 60 keV and dose 4×10^{15} cm⁻².

The ion implantation for dose, usually used for making photoelectrical semiconductors, leads to the whole amorphisation of surface layer with thickness ~ 0.2 mkm. The removal of radiation damages in implanted area is reached by the corresponding annealing through epitaxial recrystallization of amorphous layer on the lower nondamaged crystal structure.

On the experiment at the given constant (with accuracy $\pm 5\%$) excitation level I_{O_2} capacity $T = I_T I_{O_1}$ and diffraction effectiveness $\eta = I_1 I_T$ of the investigated plates, averaged according the results of 10 and more measurements were calculated.

The experiments with ion-implanted Si [2] showed, that the decrease of diffraction effectiveness is stipulated by the imperfectness degree of crystal lattice, which may be described qualitatively through the effective life and quantitatively through the value of diffraction effectiveness. For the initial plates the ratio of diffraction effectiveness of frontal (working) and back sides is 3:1 for n and 2:1 for p . After the implantation this ratio as well as the value of diffraction signal appreciably decreases for both n and p -Si, but the thermal annealing of radiation defects restores both the perfectness of the crystal structure and the initial values of η . However, for n -Si apparently more whole admixture activation takes place and the diffraction signal decreases till its initial value and more, which may be connected with restoration by annealing of more perfect structure than the initial one [3]. This effect is more expressed for the surface of comparatively low quality surface. It must be noted, that dynamical lattice method in this case expresses the properties of surface area with thickness of ~ 2 mkm, i.e an implanted area and adjoining defective area. Clear correlation between η and T was also observed.

Thus, the quality of made structure may be estimated by ratio of diffraction effectiveness of working and back sides and corresponding meanings of these values for the initial plates. In p -Si the initial parameters of layers aren't restored for the structures. This may be possibly explained by incomplete annealing of defects at their high concentration.

Tbilisi I. Javakishvili State University

REFERENCES

1. J. Vaitkus, K. Jarashjunas, E. Ganbas. IEEE, J. Quant. Electron, QE-22, 8, 1986, 1298-1305.
2. N. T. Kvasov, V. Butkus, et al. Theses of reports of International Conference Vilnius, 1983, 81-82 (Russian).
3. N. T. Kvasov, et al. Physics and Techniques of Semiconductors, 22, 5, 1988, 806-810 (Russian).

V. Kashia, P. Kervalishvili, I. Zhvania, Academician R. Salukvadze

Universal Method for Control of Heat Carrier Leakage from Various Contours

Presented November 3, 1997

ABSTRACT. In the article the need for the elaboration express methods for the monitoring leak-proofness of the electric power generation and heat transfer systems in every kind of power units is substantiated. It is shown that one of the most promising directions in the leak-proofness control for the electric power generation and heat transfer contours of power units is the creation of a universal method of leakage monitoring.

The block-diagram of an electronic system based on personal computer enabling the registration with high precision of the starting moments of leakage of a working medium out of a circulation contour is represented.

Based on the electronic systems there may be developed automated remote control systems for the monitoring of the welding seams leak-proofness along fuel (oil, gas, mazot) pipelines, which would be capable and instantly registrate the starting moments of fuel leakage out of the pipelines, and also indicate the places where they occur and switch on alarm and protection systems.

Key words: MULTILAYER SENSORS, POWER UNIT, ALKALI METAL, PSEUDOCAPACITOR, CAPACITANCE, EXTERNAL METALLIC ELECTRODE, MULTILAYER EXTERNAL ELECTRODE, WORKING MEDIUM, DIELECTRICAL PERMITTIVITY, TITANIUM, TANTALUM, TITANIUM OXIDE, TANTALUM OXIDE, GERMANIUM.

The electric power generation, transformation, and heat transfer systems of every modern power unit contain, without exception, the circulation contours for the alkali metals, their eutectics or other working media (water, water vapor, oil, gas). Disorders in tightness of such contours lead to uncontrollable changes in the parameters of the units, which end up in their break down and local ecological pollution [1]. Accidents like that on power units could be avoided, if the very starting moments of leakage of a medium out of a circulation contour were detected in time.

These problems are very urgent [2-4] and being studied intensively [5-8].

The available leak-proofness control methods for the circulation contours can be divided into two groups. The first group contains the direct methods for detection of a working medium, leaked out of the system, the second one consists of methods for the registration of the secondary effects caused by working medium leakage. The methods of the first type are of less interest, since they are used in vacuum and practically only in sodium containing systems, where owing to the ample quantity of sodium, even its con-

siderable leak does not lead to the significant changes in the parameters of the units. The same is true in the cases of turbo-generators.

The situation is completely different, when the leakage of a sodium containing eutectic into the atmosphere takes place. Since sodium and other components of eutectic possess different kinetic-thermodynamic properties, they leave the system at different rates; this leads to the nonuniform changes in contour components and, consequently, uncontrollable changes in the working temperatures of an eutectic.

One of the most developed directions in the leak-proofness control in the power unit contours containing alkali metals is the creation of solid sensors [4,5]. The operation principles of sensors like that are based on changes in electro-physical properties of their sensitive elements as a result of their contact with alkali metal atoms. Nowadays, from technological and constructional points of view, semiconductor, carbon-graphite and, especially, multilayer sensors of alkali metals [8] are best developed. In general even the best alkali metal sensors (multilayer system metal-insulator-germanium) are not able to detect those working mediums, which do not interact with the active layer of germanium. Besides, mechanical contacts are unreliable, and special low resistance multilayer contacts are too expensive. Generally, solid sensors of every type show inertness towards one or another kind of working medium. That makes impossible the use of a single type sensors for detecting the leakage of any kind of working medium.

The problem of registering starting moments of leakage of any working medium can be successfully solved if we manage to check continuously the condition of the environment adjacent to the controlled surface (those are, first of all, welding seams and their adjacent areas in the texture of a contour) and not the condition of a sensor itself, as it is the case in other methods.

To realize the method, it is necessary to place an electrically insulated thin external metal electrode, repeating the checked space configuration, at the checked surface as close as possible. As a result a flat or cylinder type pseudocapacitor is formed, in which the checked surface serves as one of the plates of the capacitor and the outer metal electrode - as the other one.

The capacitance of any kind of capacitor depends only on geometrical sizes of its plates, their shape, gap between them and dielectrical permittivity of a medium filling it. In case of leakage of working medium, its components appear in the gap of ϵ pseudocapacitor; this leads to the changes in dielectrical permittivity of the medium, and consequently, in the capacity of a pseudocapacitor.

Thus, if at the moment of leakage we manage to measure with high precision the change in the capacity of a pseudocapacitor, the relative value of which can be calculated by equation

$$\frac{\Delta C}{C} = \frac{\Delta \epsilon}{\epsilon}, \quad (1)$$

then we shall be able to register easily the moment of a working medium leakage out of any contours.

The capacity of a pseudo-capacitor can be measured with various methods: using amperemeter and voltmeter, by direct measurement, by comparison (bridge method) or resonance method.



From the methods for the precise measurements of small capacities the resonance method is the best. The contour contains an electric voltmeter connected parallelly with the pseudocapacitor and a high frequency generator. The frequency of the high frequency generator is changed until a certain frequency resonance is reached, which is indicated by maximum reading of the electronic voltmeter. Total capacitance is calculated by the equation :

$$C_0 = \frac{1}{(2\pi f_0)^2} L_0, \quad (2)$$

where f_0 is a resonance frequency, and L_0 - natural inductivity of the high frequency generator coil.

The total capacity of the circuit is the sum of capacitances of the pseudocapacitor, the coil itself and the construction.

The most precise scheme for the measuring low capacitance is that of developed in the research institute "Optica" based on PC and which is designated for the study of liquid turbulence problems by measuring electronic quantities without any influence on turbulent flux of liquid even at microscopic level. The range of this system is 10-500 pF, and the precision - 1.0 pF.

The same scheme served as the base for an electronic system model, which enables the measurement of pseudocapacitor's capacity with high precision. A block-diagram of the model is represented in Fig.1. It consists of a pseudocapacitor, termocouple, signal converter, parallel-software port and computer.

One plate of the pseudocapacitor is formed by surface of the pipeline (2), the other one by multilayer external electrode, consisting of metallic base layer (1), dielectric (3) and active sorbent (4). In pipeline (2) semimetal eutectic or gaseous working medium is flowing. On the surface of the inner plate of pseudocapacitor two thermoresistors (5), measuring temperature at the upper and lower borders of the pseudocapacitor are placed. The value of the capacitor's capacitance, converted into voltage in the signal converter (6), together with thermoresistors readings go into multichannel commutator (7), which is connected with analogue-digital converter (8). After that the coded information goes to the parallel-software port (9), which regulates counting modes of incoming data and sends obtained results into PC (10). Channel commutator receives signals from measuring devices and sends received data to analogue-digital converter. The commutator has 8 input channels (6 for the thermoresistor signals, 1 for capacitance converter signals and 1 for photoresistor signals). The regulation of the work and order of the input channels is carried out from parallel-software port by establishing channel addresses.

The softwares specially developed for this system provide the processing and visualization of the information entering into PC.

The measurable quantity, characterizing the state of the space between pseudocapacitor's plates is capacity, which according to (1) is a function of dielectrical permittivity $C=f(\epsilon)$. Dielectrical permittivity between the plates of pseudocapacitor (checked surface - external electrode) changes only in case of leakage of the atoms of the heat transfer from the controlled system. Therefore the measuring of the capacitance of the pseudocapacitor and the registration of the changes in time of its values enables the determination of the

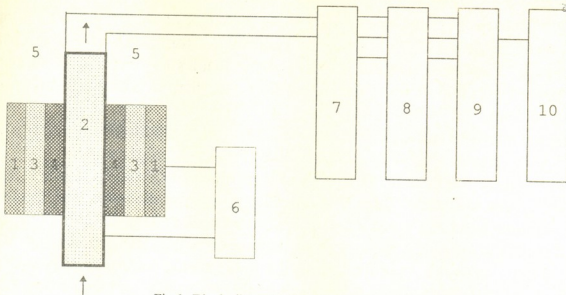


Fig. 1. Block-diagram of the electronic system

moment of the working medium atoms leakage from the system. The precision of measurement is 0.5 pF , and the range - $1\text{-}800 \text{ pF}$.

The electronic system of measurement and the methods of information processing, in contrast with resonance methods of capacitance measurements, do not require a high frequency generator. So, the capacitance of the pseudocapacitor itself and not the total capacity of the capacitor, coil and assembly scheme is measured. In the case of necessity, as a high frequency generator, PC may be used.

Electronic system and methods make it possible to perform the registration of characteristic parameters of the process in a completely automated mode (i.e. to automate an experiment). This, in its turn, makes it possible to make complete automation of the control systems of the circulation contours of power units and ensure practically immediate switching on of the alarm and protection systems in case of the leakage of the working medium from the contour under control. Measurements are made in an idle operation mode and are not dangerous for the electrical system even in the case of contacts between the plates of a pseudocapacitor.

In the universal method of detection the leakage of a heat carrier agent from the contours of different functions, developed by us, the use of multilayer external electrode makes it possible not only to register the moment of leakage, but also to utilize leaked substance in case it reacts with the active layer of the external electrode. As investigations showed, in the cases of liquid metal contours of nuclei power facilities, when as a heat carrier or working medium sodium and its eutectic alloys with other alkali metals are used, the best substance for the sensitive layer of the external electrode is germanium [8,9], and the most efficient external electrode is a thin film system tantalum (or titanium) - tantalum (or titanium) oxide - germanium.

In this case the most practical procedure is a creation of a dielectrical layer of tantalum or titanium in the process of anode oxidation of tantalum or titanium surface, and then placing a germanium layer over the oxide surface. It is obvious, that a pseudocapacitor - checked surface - multilayer external electrode will be formed with a high nominal capacity, which is due to the high values of dielectrical permittivity of tantalum and titanium oxides (20 and 80 accordingly), as well as to the possibility of obtaining very thin



layers of dielectrics. For the measuring of the thickness of an insulator layer optical interference methods are used, and for the obtaining of thin layers of germanium the three electrode ion-plasma method is used, which enables the creation of tantalum or titanium oxide layers and then a germanium layer over them in a single process, without damaging vacuum.

Using the above technological procedures there were produced multilayer external electrodes with circular (Fig. 2.a) and band like (Fig.2.b) configurations.

In the first case the metallic base layer of a multilayer external electrode is made of approximately one millimeter thick titanium disc of a given diameter, and in the other case of a tantalum band of a given lengths, 15-20 mm wide and 0.2-0.3 mm thick. On the lower surface of the metallic base layer of an external electrode, by use of the spot welding method, metallic leads are fixed for connecting to electronic control system, and on the upper surface of it there are deposited subsequently corresponding metal oxide and germanium layers. A band type external electrode forms an elastic system, which is mounted on the surface under control repeating its shape and, in case of alkali metal leakage, making its utilization.

At present under the grant financed by Eurocouncil under the aegis of the International Scientific Technological Center, the work for obtaining analytical equations describing the leakage process, polarization of components of leaking working medium, diffusion-intercalation of various impurity atoms and ions in the nonhomogeneous dielectric is being carried out.

The development of adequate algorithms and software products will enable us to create a physical model of working medium leakage out of any contour and a completely automated system for the monitoring leak-proofness of the contours.

Based on the above mentioned electronic systems there may be developed automated remote control systems for the monitoring the leak-proofness of welding seams along fuel (oil, gas, mazot) pipelines, which would not only register, practically instantly, the start-

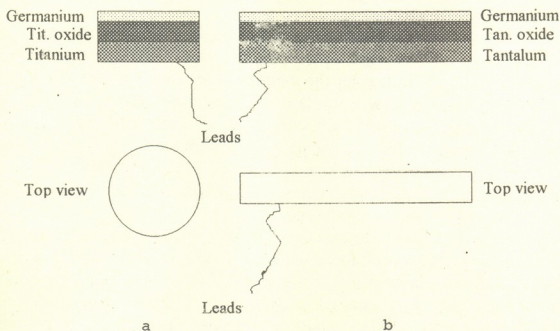


Fig. 2. Multilayer external electrodes of different configurations

ing moments of fuel leakage out of pipelines, but also indicate the places where they occur and switch on alarm and protection systems. It is not difficult to anticipate the economic advantage of the use of systems like that for the companies engaged in extracting and transporting fuels and ecological advantage to avoid ecological catastrophes for the countries through the territories of which fuel is being transported.

This work was supported by International Science and Technology Center (ISTC) Grant G-25.

Sokhumi Institute of Physics and Technology

REFERENCES

1. *V.M. Borishanskiy, S.S. Kutateladze, I.I. Novikov, O.S. Fedinskiy.* Zhidkometallicheskie teplonositeli. M., 1976, 328.
2. *V. Kashia, P. Kervalishvili, R. Salukvadze.* Bull. Georg. Acad. Sci., **153**, 2, 1996, 227.
3. *G.F. Arakelov, P.L. Bistrov, V.D. Judizkiy et al.* Trudy Raschetno-Kosmicheskoi korporazii "Energia", XII, 3, 1995, 220 (Russian).
4. *V. Kashia et al.* Georgian Simp. for Project Development and Conversion. May 15-18, 1995 Tbilisi, 96.
5. *V. Kashia, P. Kervalishvili.* III Nexuspan Workshop on Microsystems in Environmental Monitoring, M., 1996, 4.
6. *V. Kashia, P. Kervalishvili, R. Salukvadze, Z. Salukvadze.* Bull. Georg. Acad. Sci., **155**, 2, 1997, 194.
7. *V. Kashia, P. Kervalishvili.* III Nexuspan Workshop on Microsystems in Environmental Monitoring, M., 1996, 10.
8. *V. Kashia.* KEY INTERFACE. Tbilisi, 1, 1997, 17.

A. Gerasimov, G. Chiradze, N. Kutivadze, A. Bibilashvili, Z. Bokhochadze

Influence of Isotropisation of Chemical Bonds on Anisotropy of Photomechanical Effect

Presented by Corr. Member of the Academy T. Sanadze, November 20, 1997

ABSTRACT. The anisotropy of photomechanical effect (PME) is experimentally studied on monocrystalline Si, illuminated by photons of various spectral composition. It is shown, that nonequilibrium charge carriers arising under influence of light, promote change of atoms positions not only owing to weakening of chemical bond strength, but also as a result of decrease of chemical bond anisotropy, that causes change of microhardness (MH) anisotropy.

Key words: MICROHARDNESS, PHOTOMECHANICAL EFFECT.

Photomechanical effect (PME) or change of microhardness (MH) of substance in a process of its lighting [1] takes place, when displacement of a certain part of the substance is facilitated under influence of indenter. This is caused by increase of atoms mobility in the substance. Since MH anisotropy in covalent crystals is determined by anisotropy spatial orientation of rigidly directed sp^3 hybrid bonds, or electronic structure [2], therefore change of MH anisotropy in covalent crystals should be a change of spatial orientation of hybrid sp^3 orbitals.

The purpose of this work was to determine the influence of isotropisation of chemical bonds on atoms position change on a basis of comparative study of MH anisotropy in monocrystalline Si. MH anisotropy was studied in darkness and under the irradiation by light of two various spectral composition. Specifically, by photons $h\nu > E_g$ and $h\nu < E_g$ (where $h\nu$ is the energy of photons and ΔE_g is the width of Si forbidden zone). We have studied (100) surface of monocrystalline n-type Si without dislocations, with specific resistance $\rho \sim 200$ ohm.cm. Measurements of MH in darkness and in lighting, preparation of sample surface was made according to the methods, described in [3].

As it is known [2], due to Si crystallographic symmetry the dependence of MH values on angle has one and same form within intervals of angles 0-90, 90-180, 180-270 and 270-360 between the long diagonal of Knoop indenter and chosen crystallographic direction. Respectively, MH values for the plane (100) are equal for all directions $\langle 100 \rangle$ and $\langle 110 \rangle$. On the surface (100) the direction $\langle 100 \rangle$ has more hardness, than the direction $\langle 110 \rangle$, hence MH values change periodically from minimum to maximum (Fig. 1, curve 1). It is clear, that anisotropy must be caused by orientation of an indenter in respect of the directed sp^3 chemical bonds. Let us consider this question in detail.

In Fig. 2 the two-dimensional analogue of configuration of atoms and directions of chemical bonds on the surface Si (100) is given (the Figure corresponds to the non-reconstructed and non-relaxed surface [4]. As much as indentation depth contains large number of atomic layers, the influence of the layer may be neglected. In reality chemical bonds, do not locate on the surface, but form a certain angle with the surface (Fig.3). As it

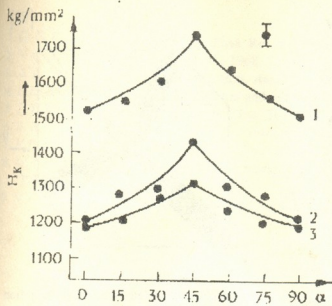


Fig. 1 The dependence of MH on Si(100) surface on the angle of diagonal of Knoop pyramid with $\langle 100 \rangle$ direction darkness (1) and under lighting (2, 3) load 25 gr (2- by photons with energy $h\nu < \Delta E_g$ 3- by photons with energy $h\nu > \Delta E_g$).

is seen from the Fig. 2, when long diagonal of Knoop pyramid is perpendicular to the projection of chemical bond and parallel on the Si (100) surface, the value of MH is minimum (a), and when the same diagonal of Knoop pyramid makes 45° angle with the projection of chemical bond on the surface (100), then MH value is maximum (b). If we take into consideration that for covalent crystals (of Si and Ge type) normal elasticity modulus is maximum, when a force is directed along to rigid covalent bonds [5], then it is obvious, that in a case of maximum MH value spatial orientation of sp^3 hybridized orbitals in respect to the stress, induced by indenter on the crystal surface, the greater part of chemical bonds undergo compression, than in the case, when MH value is minimum. It is also obvious, that

in the case of minimum value of MH the direction of stress, caused by indenter, makes definite angles with directions of covalent bonds, that causes a tensile deformation, that more greatly weakens chemical bonds, than in the previous case.

The investigations have shown anisotropy of MH on the given crystallographic surface to be dependent on the spectral composition of light (Fig. 1, curves 2, 3).

To explain the phenomenon we shall consider, what decreases MH under influence of light. As it was shown in [6] PME is caused by arising of antibonding quasiparticles free electrons and holes (AQP). They change spatial directivity of electron clouds and decrease bonding energy of these atoms, near which they occur in their chaotic motion. It promotes facilitation of change of atoms positions. Thus, change of mutual mobility of atoms is caused by change of interaction and spatial directivity (anisotropy) of electron clouds of electrons, participating in chemical bond, that in general manifests itself in PME.

The curve 2 in Fig. 1 corresponds to the case, when crystal surface was lighted by photons with energy $h\nu < \Delta E_g$ and the curve 3 – to the case of photons with energy $h\nu > \Delta E_g$. Comparison of the curves with the initial one shows, that crystal directions on the surface

Table 1

$\{(H_d - H_l)/H_d\}$ % - relative change of MH (where H_d and H_l are the values of MH in darkness and under lighting, respectively). $H_{\langle 100 \rangle} / H_{\langle 110 \rangle}$ - grade of anisotropy (ratio of maximum and minimum values of MH on the given plane) in two different cases: $h\nu > \Delta E_g$ and $h\nu < \Delta E_g$.

Spectral ingredients of radiation	$\frac{H_d - H_l}{H_d}$ % for the direction $\langle 100 \rangle$	Quality of anisotropy $H_{\langle 100 \rangle} / H_{\langle 110 \rangle}$
$h\nu > \Delta E_g$	25	1.1
$h\nu < \Delta E_g$	18	1.17

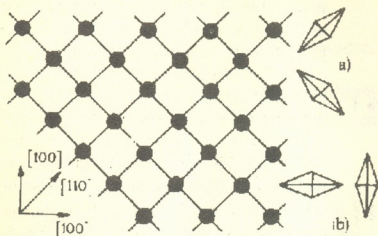


Fig. 2 The configuration of atoms and projections of chemical bonds on (100) surface of monocrystalline Si and two different locations of indenter, corresponding to minimum (a) and maximum (b) values.

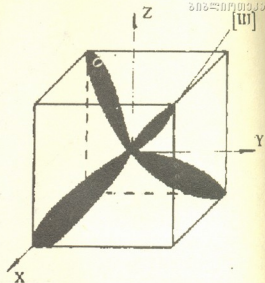


Fig. 3 The spatial (tetrahedral) configuration of hybridized sp^3 orbitals.

change their MH values differently under the influence of light with different spectral composition. For the direction $\langle 100 \rangle$, corresponding to high MH (45° in Fig. 1), the value of PME under the influence of light with energy $h\nu > \Delta E_g$ is higher, than in the case of $h\nu < \Delta E_g$. The curve 3 in Fig. 1 is more smooth, than the curve 2. It is well seen from the data in the Table 1. Proceeding from the experimental results the crystal illuminated by photons $h\nu > \Delta E_g$ is more isotropic, than the crystal illuminated by light $h\nu < \Delta E_g$. As it is known [7], formation of indentation has elastic-plastic character and during formation of indentation under an indenter the imperfect structure is formed that contains various defects (point defects, dislocations etc. [8]). Because imperfect area has not crystalline structure, causing MH anisotropy, therefore MH anisotropy should be caused by the surrounding defectless crystalline area. Indeed, the photons with energy $h\nu < \Delta E_g$ are absorbed only in the damaged area of indentation, and surrounding area is transparent for this light. But, since the damaged area is isotropic, the anisotropy does not change. Therefore anisotropy, stimulated by this light, is almost the same, as in darkness.

In the case of photons $h\nu > \Delta E_g$, AQP are generated in defectless area, surrounding this indentation, because, according with [9], absorption of photons with energy $h\nu > \Delta E_g$ in the defect area is smaller, than in the defectless area. AQP decrease binding force between atoms and also a share of rigidly directed in space p states at the expense of increase of a share of isotropic s states.

As it was noted above, compression of chemical bonds corresponds to the case of max MH. Therefore a small change of rigidity of chemical bonds (isotropisation) will cause comparatively more decrease of maximum value of MH, than of MH, corresponding to minimum value of MH when chemical bonds are weakened as a result of tensile and bending deformation. Proceeding from this, a difference between maxima of curves 2, 3 (Fig. 1) should be caused by partial isotropisation of rigidly directed covalent bonds in defectless area, around an indentation, or so-called "smoothing".

REFERENCES

1. G. C. Kyczycki, R. H. Hochman. *Phys. Rev.* v. 108, 1957;
2. V. K. Grigorovich. *Sclerometry*, M., 1968, 71.
3. A. B. Gerasimov, G. D. Chiradze. *Bull. Acad. Sci. Georg.* **142**, 1, 1991, 61.
4. F. Bekhishteg, R. Engerlinc. *Surfaces' and interfaces of Semiconductors*. M., 1990, 488.
5. T. T. Wortman, R. A. Svans. *J. Appl. Phys.* **36**, 1, 1965.
6. A. B. Gerasimov, Z. V. Dgibuti, G. D. Chiradze. *Bull. Acad. Sci. Georg.* **142**, 1, 1991, 53.
7. V. P. Alokhin, A. P. Ternovski. In conf. *The new feature in microhardness lesi*. M. 1974, 29.
8. M. I. Valkovskaia et al. *Pleability and fragility of the semiconductors during the microhardness*. Kishinev, 1984, 100.
9. N. C. Basov, V. I. Panteleev. *Science and mankind*, 1989, 198.

I. Loria

Diffraction of Electromagnetic Waves on the Periodic Thin Strip Lattice Located in Medium

Presented by Corr. Member of the Academy T. Sanadze, December 25, 1997

ABSTRACT. By strict mathematical approximation and using a method of iteration there has been solved a task of diffraction on flat electromagnetic wave on the lattice formed on thin infinitely long, completely conductive strips located in a matter medium. Analytical expression for the diffraction spectrum of scattered field was obtained.

Key words: ELECTROMAGNETIC WAVES, DIFFRACTION, THIN STRIP LATTICE, FOURIER COEFFICIENTS.

Let us assume S is a flat surface which divides free space from a matter medium where on the depth of level l_1 an infinitely long and completely admitting lattice formed of extremely thin strips is embedded. Lattice orientation in the XOY plane can be observed in Fig. 1.

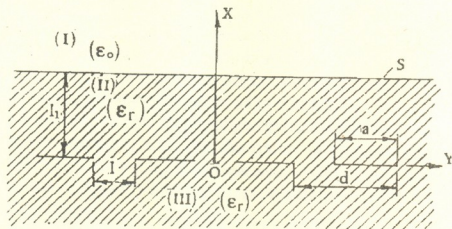


Fig. 1. The periodic lattice formed of thin strips is located in dielectrical medium.

Let us assume that from the area I E -polarized wave falls on the medium II:

$$E_z = e^{ik(x-l)}, \quad (1)$$

where $k = 2\pi/\lambda$, λ is a wave length in free space.

Our problem is to determine a scattered field in both media, the field being formed due to diffraction of primary field on the given system.

Scattered field in free space can be expressed as follows:

$$E_{z1} = e^{ik(x-l)} + \sum_{m=-\infty}^{\infty} R_m e^{ig_m y - ih_m(x-l)}, \quad (2)$$

where $g_m = 2\pi m/d$, $h_m = \sqrt{k^2 - g_m^2}$, R_m are the unknown constants of diffraction spectrum.

In the matter medium

$$E_{z2} = \sum_{m=-\infty}^{\infty} \left(A_m e^{ih'_m x} + B_m e^{-ih'_m x} \right) e^{ig_m y} \quad (0 \leq x \leq l, -\infty < y < \infty), \quad (3)$$

$$E_{z3} = \sum_{m=-\infty}^{\infty} C_m e^{ig_m y + ih'_m x} \quad (x \leq 0, -\infty < y < \infty), \quad (4)$$

where A, B, C are the unknown constants, $h'_m = \sqrt{k^2 \epsilon_r - g_m^2}$.

Our main goal is to determine the field factors. For this reason it is necessary to use the limiting conditions, which lead us to the dual system of functional equations:

$$\sum_{m=-\infty}^{\infty} C_m H_m e^{ig_m y} = 1, \quad \left(-\frac{l}{2} \leq y \leq \frac{l}{2} \right) \quad (\text{on clearance}),$$

$$\sum_{m=-\infty}^{\infty} C_m e^{ig_m y} = 0, \quad \left(\frac{l}{2} \leq y \leq \frac{l}{2} + a \right) \quad (\text{on a strip}),$$

where

$$H_m = 2h_m^* q_m / \sigma_m f(kl), \quad h_m^* = h'_m / h_0,$$

$$\sigma_m = (1 - \gamma_m) e^{-ih'_m l} + (1 + \gamma_m) e^{ih'_m l}, \quad (5)$$

$$f(kl) = -(1 - \gamma_0) e^{-ih'_0 l} + \frac{1}{2} (1 + \gamma_0) \frac{\bar{\sigma}_0}{\sigma} e^{ih'_0 l},$$

$$\bar{\sigma}_0 = (1 + \gamma_0) e^{-ih'_0 l} + (1 - \gamma_0) e^{ih'_0 l},$$

When a specific case is considered, when $\epsilon_r \rightarrow 1$ and $l \rightarrow 0$, the system (5) takes the form:

$$\sum_{m=-\infty}^{\infty} h_m^* C_m e^{ig_m y} = 1 \quad \left(-\frac{l}{2} \leq y \leq \frac{l}{2} \right) \quad (\text{on clearance}),$$

$$\sum_{m=-\infty}^{\infty} C_m e^{ig_m y} = 0 \quad \left(\frac{l}{2} \leq y \leq \frac{l}{2} + a \right) \quad (\text{on a strip}). \quad (6)$$



The system corresponds to a lattice located in free space. Analytical solution of the system (6) is possible only in case when the strip width is equal to the clearance width; A method used is the factorization one [1].

Strict numerical solution of the system (6) is given in [2,3]. In [2] the problem is reduced to the Riman-Hilbert task. Solution of the task showed that the c_m constants satisfy the system of linear inhomogenous infinite algebraic equations of II type. Their numerical solution is possible by using the computer reduction method. It must be noted that matrix elements of the algebraic system have rather a complex structure; therefore high values of reduction factor are to be used.

A method applied for the investigation of the system (6) is a modification of the method applied in [4].

Solution of the system can be found in the following way:

$$C_m = \frac{1}{m} \sum_{s=0}^{\infty} X_s I_{2s+1}(m\alpha) \quad (7)$$

where x_s are solutions of the system of infinite algebraic equations of II type:

$$X_n + \frac{\alpha}{\pi} \sum_{s=0}^{\infty} X_s k_{sn} = -\frac{iD\alpha}{2} \delta_{n0}, \quad (8)$$

where

$$\alpha = \pi l / d, \quad D = d / \lambda,$$

$$k_{sn} = \frac{\pi}{\alpha} (2n+1) \left\{ \frac{i\alpha^2}{2} D \delta_{s0} \delta_{n0} + 2 \sum_{m=1}^{\infty} \frac{\varepsilon_m}{m} I_{2s+1}(m\alpha) I_{2n+1}(m\alpha) \right\}.$$

Matrix elements k_{sn} quickly eliminate with increasing of indices. Therefore the reduction constants can be limited by low values.

The results of numeric calculations are in good agreement with those given in ref. [2].

For the solution of dual system (5) may be used as it is proposed in [4]. For the X_s constants we receive the system of infinite algebraic equations of II types

$$X_n + \frac{\alpha}{\pi} \sum_{s=0}^{\infty} X_s T_{sn} = -\frac{i\alpha D}{2} f(kl) \delta_{n0}, \quad (9)$$

where

$$T_{sn} = \frac{\pi}{\alpha} H_0^*(2n+1) \left\{ \frac{i\alpha^2}{4} D \delta_{s0} \delta_{n0} + 2 \sum_{m=i}^{\infty} \frac{X_m}{m^2} I_{2s+1}(m\alpha) I_{2n+1}(m\alpha) \right\} +$$

$$+ \frac{\pi}{\alpha} (2n+1) \left\{ \frac{i\alpha^2}{4} D \delta_{s0} \delta_{n0} + 2 \sum_{m=i}^{\infty} \frac{\varepsilon_m}{m} I_{2s+1}(m\alpha) I_{2n+1}(m\alpha) \right\},$$

$$H_m^* = h_m^* \left(\frac{2q_m}{\sigma_m} - 1 \right) / f(kl).$$

For the low values of α , the system (9) can be solved by iteration method and if we limit it by first approximation $X_n \approx -\frac{i\alpha D}{2} \delta_{n0} f(kl)$, then according to the (6) there will be received approximate values of sought for constants of the diffraction spectrum:

$$C_m \approx -\frac{i\alpha D}{2} \frac{I_1(m\alpha)}{m} f(kl) (m = 0, \pm 1, \pm 2, \dots). \quad (10)$$

The constants A_m , B_m and R_m can be determined with suitable relationships.

Georgian Technical University

REFERENCES

1. *L. A. Vainshtain. Theoria difraktsii i metod faktorizatsii. M., 1966 (Russian).*
2. *Z. S. Agranovich, V. L. Marchenko, V. P. Mestopolov. TPh., XXXII, 4, 1962 (Russian).*
3. *V. V. Malin. Radiotekhnika i elektronika, 8, 2, 1963, 211. (Russian).*
4. *G. Sh. Kevanishvili, Z. I. Sikmashvili, O. P. Tsagareishvili. Soobshchenia AN GSSR, 79, 1, 1975, 93. (Russian).*

Corr: Member of the Academy R.Kiladze, T.Kvernadze, M.Gikoshvili

Observation of Saturn Rings in Abastumani in 1995

Presented October 6, 1997

ABSTRACT. During the Earth transition through the plane of Saturn's rings in 1995 the observations of this phenomenon were fulfilled in Abastumani Astrophysical Observatory. The moment of one of these observations exactly coincides with the transition moment. The thickness of rings was estimated in 12 points. Their preliminary values vary in the bounds of 3-6 km.

Key words: SATURN RINGS, THICKNESS.

One of the most significant parameters of Saturn rings is their thickness. The first objective estimations of this parameter were performed in 1966 during the Earth transition through the plane of Saturn rings by Kiladze and Focas and Dollfus using the method of photographic photometry. They determined the thickness as 1.42 [1,2] and 2.8 km [3].

During 1980 transition the observations using electronographic camera were led to the result 1.4 km [4,5].

The last measurements of the thickness were carried out by "Voyager-2" in 1981 during its flight towards Saturn. The variation of brightness of star δ Sco during its eclipse by the rings was used to estimate the thickness which appeared to be equal to 0.15 km.

During 1995 transition the CCD observations were carried out at the Abastumani Astrophysical Observatory using primary focus (16m) of 125cm Ritchie-Chretien telescope. The CCD used were SBIG ST-6 Camera with 375x242 area and 23x27 mkm pixel. The scale was about 0.3 arc sec/pixel. The typical exposures of Saturn were 10-60 sec. using standard B filter. Two stars with UBV electrophotometry of about 10 and 7 mag were observed for rings' flux calibration and the mean rms error of photometry appeared to be 0.007 mag.

Twelve successful nights were used from July 20 till August 27 with 10 or even 20 individual frames of Saturn.

The most important night was at August 10/11 when it happened to be the exact moment of transition through the plane of Saturn rings.

The most significant problem for determination of rings brightness is a subtraction of background. The mean backgrounds for individual points of rings were calculated, using the scans along the corresponding concentric isophotal curves with identical parameters as for image of Saturn limb itself. Photometry of the rings were performed for both sides of Saturn and for C, B, A and F rings which correspond to the following distances from Saturn centre: 84.000-145.000 km.

Preliminary reduction of observational data led to the following results:

1. The exact moment of the Earth's transition through Saturn rings plane appeared to be $01^{\text{h}}:03^{\text{m}} \pm 10^{\text{m}}$ of Universal Time at August 11, 1995. The CCD frame of Saturn rings at this moment is shown in Figure:

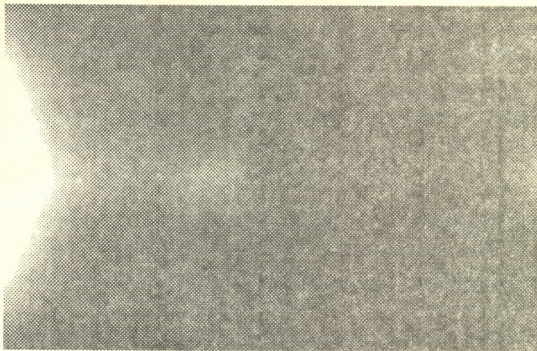


Fig. The CCD frame of Saturn rings at the moment of transition.
 Grabbed at 01:02:54 (UT) of August 11, 1995. Exposure - 60 sec.

2. According to distance from the planet ring thickness varies in such a way: 4 km (C ring), 6 km (B ring), 4 km (A ring) and 3 km (F ring) with rms error of about ± 0.5 km (Table);
3. If we omit the observations of August 10/11 then the extrapolated value of thickness equals 1-3 km, which corresponds to the earlier estimations (Table);
4. The new estimations of Saturn ring thickness contradict with well-known "plane-parallel" model of Bobrov [6].

In Table following data are given: distance from Saturn's centre (in arcsec and km), an apparent equivalent thickness of rings for both (east and west) sides and extrapolated thickness (if we omit observations of August 10/11).

Table

Thickness of Saturn Rings

Distance		Thickness		Extrapolated thickness	
Arc sec	10^3 km	East	West	East	West
13.2	84	3.6	4.2	1.5	0.5
14.1	90	5.8	5.1	2.4	0.8
15.0	95	6.1	5.5	2.7	1.4
15.8	101	6.6	6.1	3.1	1.6
16.7	106	6.1	6.1	3.0	2.3
17.6	112	6.1	5.9	2.5	2.4
18.4	117	5.5	5.9	2.3	2.4
19.3	123	4.7	5.4	2.1	2.1
20.2	128	4.8	5.4	2.4	2.4
21.0	134	4.7	5.1	2.6	3.3
21.9	139	3.9	4.9	2.3	3.5
22.8	145	2.3	3.5	2.2	3.0



This work was supported by the Grant of Academy of Sciences of Georgia at 1997. Authors wish to express special thanks to the EAS and especially to Dr. Richard West for donation of the SBIG ST-6 CCD Camera to the Abastumani Astrophysical Observatory.

Abastumani Astrophysical Observatory
Georgian Academy of Sciences

REFERENCES

1. *R.I. Kiladze*. *Astron. Tsirkular AN SSSR*, **439**, 1967, 1 (Russian).
2. *R.I. Kiladze*. *Abastumni Astrophys. Obs. Biul.*, **37**, 1969, 151-164 (Georgian).
3. *J.H. Focas, A. Dollfus*. *Astron. & Aph.*, **2**, 3, 1969, 251-265.
4. *A. Brahic, B. Sicardy*. *Nature*, **289**, 5797, 1981, 447-450.
5. *B. Sicardy et al.* *Astron. & Aph.*, **108**, 2, 1982, 296-305.
6. *M.S. Bobrov*. *Kol'tsa Saturna*, Nauka : M., 1970, 118 (Russian).



O. Manjgaladze, F. Broucek, N. Telia

Acid-Base Properties of Azo- and Oxiazo-Derivatives of Rodanine and their Application Ability in Chemical Analysis

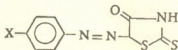
Presented by Academician G. Tsintsadze, September 8, 1997

ABSTRACT. It was established that azo- and oxiazo-derivatives of rodanine are perspective reagents for analytical chemistry and photometry.

Key words: RODAZOLE, SULPHORODAZOLE, CHLORORODAZOLE, PHOTOMETRY.

The states and properties of some azo- and oxiazo-derivatives of rodanine were studied spectrophotometrically in diluted solutions. Taking into account the acidity of medium, forms of their existence and the fitness of these first-synthesized compounds for forming intensively coloured compounds were established. Among oxiazorodazoles the complexes of rodazole and chlororodazole with copper (II) and nickel (II) are differed.

Heterocyclic azocompounds. The peculiarity of rodanine azocompounds [1-4] is that at the same time they contain three atoms with strong donor properties: oxygen, nitrogen and sulphur. The presence of imino- and carbonyl groups makes the properties of these compounds peculiar. Most of them are yellow or red crystalline compounds. They are badly-soluble in water and well-soluble in organic solvents; in solutions they undergo tautomeric transformations.



MBAR (X=CH₃); SBAR (X=SO₃H)

Methylbenzoazorodanine (MBAR) and sulphobenzoazorodanine (SBAR) are correspondingly amorphous yellow and crystalline compounds. They are well-soluble in ethanol, acetone, dimethylformamide and acetic acid.

The absorption electron spectra were studied in different acidity of the medium. As we can see in Fig. 1, in acid medium in the interval of pH 1-3, the maximum of absorption of SBAR solution is equal to 420 nm. In this condition the compound is presented in neutral form and hypochromic effect was observed (Table 1).

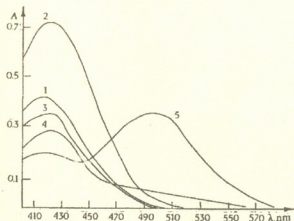


Fig. 1. The absorption spectra of solutions of SBAR at different intervals of pH: 1-1.0; 2-3.0; 3-7.0; 4-9.0; 5-12.5 (C_L=1.9×10⁻⁴M, I=1cm).

Acid-base properties of azoderivatives of rodanine

N	pH (Acidity)	The form of ligand	Colour	λ_{nm}	The effect of absorption
SBAR					
1	1-3	H_2L^0	yellow	420	hyperchromic *
2	3-7	HL^-	"----"	420	hypochromic **
3	7-10	L^{2-}	yel-orange	430	-----
4	>10	taut.	red-orange	500	batochromic
MBAR					
1	$5\text{NH}_2\text{SO}_4$	H_2L^+	red-violet	510	-----
2	1-4	HL^0	yellow	430	hyperchromic *
3	4-10	L^-	"----"	430	hypochromic **
4	>10	taut.	red-violet	510	batochromic

*Hyperchromic shift: $A = 0.4-0.7$ (for SBAR) and $A = 0.5-1.0$ (for MBAR).

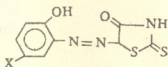
** Hypochromic shift: $A = 0.7-0.4$ (for SBAR) and $A = 1.0-0.4$ (for MBAR).

In the interval of pH 3-7 the maximum of absorption of solution was not changed and because of dissociation of sulpho-group, hyperchromic effect was observed. In neutral and weak-alkaline medium (pH 7-10) the optical density of solution was unchanged and hypochromic effect can be explained by dissociation of imino-group of rodanine cycle. The intensity of solution colour changes slightly.

At pH 12.5 colour changes sharply and from yellow-orange transforms into red-orange (500 nm). Slight batochromic effect is caused by tautomeric transformation of organic compounds ($\Delta\lambda = 80$ nm).

Nearly analogous results were established for MBAR. The acidity of medium effects on the colour of solution. At pH 1-4 hypochromic effect was observed, which can be explained by deprotonation of organic reagents and the domination of their neutral form in this interval of acidity. At pH 1-4 the hyperchromic effect is connected with dissociation of imino-group of rodanine cycle of organic reagent (Table 1).

Heterocyclic oxiazocompounds. For investigating acid-base properties of oxiazorodanines [5-7] the absorption electron spectra of coloured solutions were studied at different acidities.



Rodazole (X=H); sulphorodazole (X=SO₃H); chlororodazole (X=Cl).

The example of sulphoazorodazole indicates that in acid solution (pH 1.0-3.0) organic reagents present in molecular states and slight hyperchromic effect ($\lambda_{\text{max}} = 420$) was established. In the interval of pH 3.0-7.0 the maxima of coloured solutions were not changed, but the appearance of orange colour indicates the dissociation of imino-group and formation of double-charged anionic forms of organic reagents.

In weak-alkaline medium (pH 7.0-10.0) hypochromic effect takes place which is

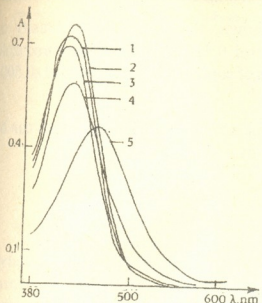


Fig.2. The absorption spectra of sulphorodazole solutions at different interval of pH: 1-1.0; 2-3.2; 3-7.0; 4-9.2; 5-12.5; ($C_L = 2 \times 10^{-3} M$, $l = 1 cm$).

connected with the formation of additional anionic form as the result of dissociation of hydroxyl-group.

From pH 12.5 organic reagents sharply change their colour and become red ($\lambda_{max} = 460 nm$). Simultaneously bathochromic shift of absorption band takes place ($\Delta\lambda = 40 nm$). It is connected with tautomeric transformation of organic reagents.

Tautomeric transformations take place in concentrated solutions of sulphuric acid and the colour changes from yellow to red. In strong acid medium protonation processes takes place (for sulphorodazole such form can be manifested as H_4L^+). In weak-acid solutions neutral particles dominate (H_3L^0). In neutral medium both sulpho- and iminogroups are dissociated and red-orange ionic forms (HL^{2-}) appear in solution. In weak-

alkaline solution hydroxyl group of benzene ring also dissociates and the colour becomes red (L^{3-}). Finally tautomeric transformation takes place and the colour of solution sharply changes.

With application of organic reagents the qualitative study of inorganic ions were carried out (Table 2). It was obtained, that many ions of d-metals form with rodanine oxiazo derivatives coloured intercomplex compounds, which can be used in chemical analysis. Many of these complexes are soluble in the system of water-organic medium and form orange (for example: zinc, iron and nickel - with rodazole) and red (copper and nickel - with chlororodazole). The ions of iron with chlororodazole and ions of mercury with both oxiazoderivatives form hardly-soluble sediments.

Table 2

Qualitative reactions on cations of d-metals with participation of oxiazo derivatives of rodanine ($1 \cdot 10^{-5} M$ metal, $5 \cdot 10^{-5} M$ organic reagent)

N	M	pH	λ_{nm}	$A \cdot 10^3$	Rodazole ($l = 2cm$)			Chlororodazole ($l = 3cm$)		
					pH	λ_{nm}	$A \cdot 10^3$	pH	λ_{nm}	$A \cdot 10^3$
1	Copper (II)	8.15	490	700	7.05	540	700			
2	Zink(II)	8.15	490	240	8.20	490	250			
3	Cadmium (II)	7.15	490	115	8.20	490	160			
4	Mercury (II)	-	-	-	-	-	-			
5	Aluminium (III)	7.15	490	360	7.05	490	440			
6	Lead (II)	7.15	490	130	7.05	490	355			
7	Manganese (II)	7.15	490	150	3.00	490	160			
8	Iron (III)	8.15	490	430	-	-	-			
9	Cobalt (II)	7.15	490	360	5.00	490	450			
10	Nickel (II)	6.50	500	500	7.20	490	460			
	"----"	8.15	490	440	7.50	510	520			



Spectrophotometrical investigations have shown, that the optical density of intracomplex compounds of rodazole changes in interval 0.115 - 0.700; for chlororodazole - 0.250 - 0.700. The maximal values have complexes of copper (0.700) and nickel (0.500 - 0.520)

Thus, according to our investigations, heterocyclic azo- and oxiazocompounds can be considered as effective reagents in qualitative analysis and in photometry.

Tbilisi I. Javakhishvili State University
Georgian Technical University

REFERENCES

1. N. Telia, O. Manjgaladze, D. Chichua. *Izv. AN Gruzii, Ser. Khim.* **17**, 2, 1991, 98 (Russian).
2. O. Manjgaladze, N. Telia, N. Basargan, D. Chichua. *Bull. Acad. Sci. Geog.*, **142**, 1, 1991, 65 (Russian).
3. O. Manjgaladze, N. Basargin, N. Telia, D. Chichua. *Koordin. khimya*, **12**, 9, 1992, 992 (Russian).
4. N. Telia, O. Manjgaladze, E. Kakabadze, Yu. Rozovski. *Izv. AN Gruzii, Ser. Khim.* **19**, 1, 1992, 12 (Russian).
5. Kh. Bochorishvili, N. Telia, O. Manjgaladze, L. Gvelesiani, N. Rosovski. *Ibid*, **18**, 4, 1992, 252 (Russian).
6. Kh. Bochorishvili, O. Manjgaladze et al. *Bull. Acad. Sci. Geog.*, **146**, 3, 1992, 550 (Russian).
7. O. Manjgaladze, L. Gvelesiani, N. Telia, N. Basargin. *Ibid.*, **152**, 4, 1995, 730 (Russian).



V.Eristavi, V.Ivanov, D.Eristavi, N.Kutsiava

Atom Absorption Method of Determining Molybdenum in Sulfuric Acid

Presented by Academician T.Andronikashvili, May 11, 1995

ABSTRACT. Atom absorption spectrophotometric method of determining molybdenum in sulfuric acid has been developed using it in technological processes of producing hydroxyl-amino sulfate in Rustavi Industrial Amalgamation "Azote". The essence of the method is to determine the value of selective absorption of emission of resonance lines by the atoms of the analyzing element by means of atom absorption spectrophotometer "Saturn".

Key words: MOLIBDENUM DETERMINATION IN SULFURIC ACID, ATOM ABSORPTION SPECTROSCOPY.

Peculiarities of technological processes in Rustavi Industrial Amalgamation "Azote" producing hydroxyl aminosulphate require to determine molybdenum in sulfuric acid because if its concentration exceeds 0.1 mg/kg, there occurs accelerated aging of platinum catalyst and platinum gets out of order.

Atom absorption spectrophotometry method has been used for determination of molybdenum in sulfuric acid. Recently this method is considered to be most effective to define metals in fluidal phase [1,2]. It is based on determining the value of selective absorption of emission of resonance lines by the atoms of the analyzing element using the samples preliminary chemically treated.

Preparation of the samples for analysis: 200 ml of concentrated sulfuric acid was placed in quartz vessel to be evaporated to dryness over the sand bath (on the surface of the dried mass a trace of sulfuric acid anhydride should be observed). A bit warm precipitant was drenched with distilled water and after 15 min the whole amount was transferred to the 100 ml measuring flask filled up to the mark. After that it was regulated to the solution of pH2.2-0.4 value and transferred to the separatory funnel, where 10 ml of extracting solution (0.75 g of oxyquinoline dissolved in 100 ml of methyl isobutylketone) was added to. It was allowed to stand in water for a minute and then was shaken violently for 15 min. After division in two phases the organic phase was removed and sprayed immediately through acetylene azote oxide flame. Organic phase can be stored for conservation in a well-stoppered glass vessel.

Analysis. Standard solution of molybdenum with weight concentration of 1 mg/ml was prepared to make up the calibre diagram. On this purpose 1.8403 g of ammonium molybdate $(\text{NH}_4)_6\text{Mo}_7\text{O}_{24}\cdot 4\text{H}_2\text{O}$ was dissolved in distilled water diluting it up to 1 l in the measuring flask. Out of it 10 ml of solution was transferred to the 100 ml measuring flask filling it up to the mark by adding the distilled water. Solution obtained was used to



prepare comparative solutions with concentration of 0.5 mkg/ml, 1 mkg/ml, 2 mkg/ml, 3 mkg/ml transferring 0.5 ml, 1.0 ml, 2.0 ml, 5.0 ml of corresponding adequates to the 100 ml measuring flask filling it up to the mark. Solutions obtained by distilled water were transferred to the separatory funnel, where by means of above mentioned method molybdenum oxyquinoline was separated (extracted) by methyl isobutyl ketone. Molybdenum atoms were atomized in acetylen-azote oxide flame and the value of absorption of emission of resonance lines (extinction) by the molybdenum atoms was detected. By means of atom absorption spectrophotometer "Saturn" the calibre diagram of "metal concentration (extinction)" was made up, according to which molybdenum concentration in the analyzing solution can be detected. Conditions of molybdenum concentration determination in analyzing and comparative solutions are given in the Table.

Table

Analytical line nm	Monochromate hole, nm	Spectro-filter	Acetylen charges, dm ³ /g	Nitrous acid charges dm ³ /g	Kind of the lamp	Current of the lamp, mA
313.3	0.2	1	370	560	ΛT-2	20

Molybdenum mass share in sulfuric acid can be calculated by the formula:

$$\%C = \frac{A \cdot V_1 \cdot 100}{10^6 \cdot V_2}$$

where C is the mass share in sulfuric acid, %; A is molybdenum concentration in the analyzing sample, mg/l; V_1 is the volume of analyzing solution of sulfuric acid obtained by preparing the sample, ml; V_2 is the volume of sulfuric acid solution taken for the analysis, ml.

Metrologic testing of the methods in the result of thirtyfold measuring revealed that total relative error of the data equals $\pm 7.63\%$ [3,4].

Georgian Technical University

REFERENCES

1. U.Slavin. Atomno-absorbtsionnaia spektroskopiya. L., 1971, 340. (Russian)
2. V.Prais. Analiticheskaia atomno-absorbtsionnaia spektroskopiya. M., 1976, 355. (Russian)
3. Metodika po normirovaniyu metrologicheskikh kharakteristik, graduirovke i otsenke tochnosti rezultatov izmereniya. M., 1978, 137-177. (Russian)
4. GOST 8, 207-76. Pryamye izmereniya s mnogokratnymi nablyudenyami. Metody obrabotki rezultatov nablyudeniya. (Russian)



I.Samadashvili, T.Macharadze

Synthesis of Mg-Zn Ferrites and their Properties

Presented by Academician G.Tsintsadze, December 22, 1997

ABSTRACT. Complex Mg-Zn ferrites were obtained by the ceramic method. Chemical and X-ray analysis were performed. Stoichiometry was found to be fairly well sustained and all the types had spinel structure. A linear dependence was noted between the elementary cell constant and composition.

Key words: FERRITES, SPINEL STRUCTURE.

Magnesium ferrite is considered to be interesting from magnetic and crystallographic points of view. More improved compounds are obtained in solid solution series of MgZn mixed ferrites. The paper reports on preliminary results of study of Mg-Zn ferrites obtained by ceramic method for calorimetric study.

As initial substance there were taken Fe_2O_3 of "УДА" type, ZnO and MgO. Compositions of mixed ferrites were estimated according to general formula $\text{Mg}_{1-x}\text{Zn}_x\text{Fe}_2\text{O}_3$ where $x=0; 0.2; 0.4; 0.6; 0.8$;

To obtain the samples with dense ceramic structure the synthesis of polycrystal ferrites should be carried out as far as possible at high temperature. At the same time volatility of zinc is to be taken into account (ZnO is reduced up to Zn, which is volatilized at 970°C) [1]. For final roasting of samples we chose 900°C and oxygen zone. Roasting time is 30h. As it is known gradual cooling contributes to such distribution of ions in lattice which corresponds to room temperature [2]. After roasting the samples were cooled for 5 h at 500°C together with the furnace. Beneath 500°C distribution velocity of particles equals 0.

The purity of obtained ferrites and completeness of feritization process was examined by chemical and roentgenographic analysis. The analysis was carried out at the laboratory of physical and chemical methods of the Institute of Inorganic Chemistry and Electrochemistry. Ferrites were dissolved in diluted salt acid by heating. Ferrous was determined by permanganate method. After removing Fe zinc was determined by trilonmetric method, magnium was determined by weighing method, as magnesium phosphate by means of precipitation.

Roentgenographic analysis was carried out by Debais method with simultaneous determination of ferrites monophase and lattice parameters. Roentgenograms have been done on DRON-3M apparatus by Cu filtering radiation, with U-25cV and J-20mA regime.

Unlike other ferrites, magnium monoferrite as spinel structural system monophase substance doesn't exist. Spinel structural system $\text{MgO}\cdot\text{Fe}_2\text{O}_3$ is characterized by lack of oxygen, i. e. has more quantity of Mg^{2+} ions compared to equimolar composition. Otherwise certain quantity of MgO should be dissolved in magnesium ferrite for crystallization by spinel structure. The formula of substance corresponding to magnesium monoferrite is given as [3]



Data of chemical and roentgenographic analysis

Composition	Mg %		Fe %		Zn %		Lattice parameters Å
	Analit.	Theoret.	Analit.	Theoret.	Analit.	Theoret.	
MgFe ₂ O ₄	12.06	12.15	58.21	55.85			8.386
Mg _{0.8} Zn _{0.2} Fe ₂ O ₄	9.00	9.34	56.55	53.64	6.80	6.28	8.399
Mg _{0.6} Zn _{0.4} Fe ₂ O ₄	6.85	6.74	54.80	51.61	11.80	12.08	8.410
Mg _{0.4} Zn _{0.6} Fe ₂ O ₄	4.37	4.33	51.56	49.72	17.40	17.46	8.412
Mg _{0.2} Zn _{0.8} Fe ₂ O ₄	2.16	2.09	47.05	47.97	25.20	22.46	8.425

We can suppose that compared to stoichiometry, excessive Mg ions are located in crystal lattice nodes and internodes [1]. It is known that in most cases the lattice constant of mixed ferrites is determined with satisfactory accuracy by linear interpolation of ferrites lattice constants (Vegardt's additivity law). In our case the ending is magnesium ferrite and zinc ferrite. Their lattice constants are correspondingly 8.38 (for monoferrite obtained oxygen zone) and 8.43 [4,5]. Lattice parameters of Mg-Zn ferrites are located on the connecting line of these two values i.e. Vegard's law is observed.

Thermogravimetric analysis of samples was carried out on derivatograph Q1500D of PAULIK, PAULIK, ERDEY system. Maximum temperature of heating was 1000°C, velocity 10°/min. Each sample was placed in ceramic tube; standard was α -Al₂O₃ (corundum). Mass was approximately 600g. The effects characteristic to oxides which compose ferrite are not marked on the thermograms i.e. the examined samples, ferrites, are completely uniform compounds.

R.Agladze Institute of Inorganic Chemistry and
 Electrochemistry
 Georgian Academy of Sciences

REFERENCES

- 1.L.I.Rabkin. S.A.Soskin. B.M. Epshtein. Ferity. M., 1968 (Russian).
- 2.Yu.D.Tretiakov. Termodinamika feritov. M., 1967 (Russian).
- 3.V.V.Bardich. Magnitnye elementy tzifrovikh vychislitelnykh mashin. M., 1967 (Russian).
- 4.V.A.Petrusheva, V.B.Balekhov et al. Neorganicheskaia Khimia, 19, 11, 1974, 3, 25-3127 (Russian).
- 5.S.R.Sawant, R.Nepatil. J.Mater. Sci., 16, 12, 1981, 3496-3499.



G. Khelashvili, R.I.Gigauri, M. Indjia, L. Gurgenishvili, R.D.Gigauri

Coordination Compounds of d-Metals Monothioarsenates with Pyridine

Presented by Corr.Member of the Academy J. Japaridze, July 10, 1997

ABSTRACT. Monothioarsenates pyridinates of d-metals of composition $[MPy]_3(AsO_3S)_2$, where $M=Ni, Co, Zn, Cd, Hg$ in hydrochemical conditions were synthesized. Their composition and constitution by chemical analysis, IR-spectroscopy, and X-ray crystal determination were studied.

Key words: MONOTHIOARSENATES PYRIDINATE, IR SPECTRA.

Following the earlier work [1] on the production and investigation of the metals monothioarsenates, the recent study examines the establishment of conditions of synthesis of d-metals coordination compound with pyridine. Silver(I) and mercury(II) nitrates, cobalt(II) and nickel(II) chlorides, cadmium and zinc acetate as initial substances were used; from arsenic contained compound – sodium monothioarsenate, which was obtained by the interaction of sulfur with sodium arsenite [2]. Pyridine was used as a ligand.

Production of d-metals pyridinates occurs in two ways: 1) by interaction of fresh made d-metals monothioarsenates with pyridine at room temperature. Pyridinates of nickel and cobalt monothioarsenates were obtained in the same way 2) by interchangeable reaction: by interaction of pyridinates of transition metals with sodium monothioarsenate.

The synthesized products are insoluble in water and alcohol. They are insoluble in alkalis as well (except zinc salt), but elaborated by acids, they reform by producing arsenic pentasulphide, e.g.



IR spectroscopy and X-ray crystal determination have presented the composition and structure of the mentioned compounds, as well as elementary analysis. In the IR spectra of all compounds there appeared band for AsO_3S^{3-} ion-valency in the region 420 and 880 cm^{-1} [3]. Except that, as known [3], by the coordination of free ligand with central atom value of valency vibration ν increase by 8-30 cm^{-1} . For the $\nu(C=N)$ band of free ligand appears at the 1580 cm^{-1} [4] and in the synthesized products the same band appeared at the 1610 cm^{-1} region. This fact indicates the presence of coordination pyridine in the mentioned samples.

In contrast to other complexes cobalt pyridinate precipitates with water of crystallization. The IR spectra of the latter shows, except for bands noted above, bands at 1630, 3180, 3290 and 3400 cm^{-1} region, that indicates the presence of water molecules [5]. To determine the place of the water molecules is a subject of separate research. Though, it could be mentioned in advance that it's doubtful that H_2O is in cation in the form of aquacomplex, because in such a case coordinating number of cobalt(II) may equal to 5, which is most rare.



Table 1

Experimental X-ray diffraction parameters of pyridinates of monothioarsenates of mercury(II) and nickel(II)

[HgPy ₄] ₃ (AsO ₃ S) ₂			[NiPy _{6,3}] ₃ (AsO ₃ S) ₂		
<i>I/I</i> ₀	<i>d</i> , Å	hkl	<i>I/I</i> ₀	<i>d</i> , Å	hkl
100	7.86	110	90	8.04	110
85	7.38	101	100	7.82	020
100	6.56	020	10	6.096	001
30	5.54	120; 002; 021	10	5.817	200
20	5.06	200; 012	10	5.452	101
17	4.282	022	25	4.731	220; 130
17	3.997	220	10	4.382	122
50	3.360	300; 230	20	4.183	202
30	3.196	023	25	3.867	300
68	3.070	123	15	3.708	310; 221
70	2.978	320	20	3.427	320
80	2.880	302	35	3.273	302
50	2.755	004; 240	20	3.132	050
30	2.637	050	10	3.053	002; 150
25	2.495	303	20	2.885	400
50	2.439	313	30	2.800	043; 303
15	2.240	005	15	2.684	420
10	2.103	314	15	2.600	060; 402
17	1.869	070	10	2.564	430; 222
15	1.796	451	25	2.500	421
20	1.784	026	10	2.178	052
20	1.740	271	10	1.993	540; 103
10	1.684	600	10	1.914	203
10	1.656	611	10	1.860	550; 223
15	1.595	612	10	1.830	512
			15	1.774	143
			10	1.730	560
			10	1.698	053
			10	1.642	462
orthorhombic crystal system			orthorhombic crystal system		
a=10.10 Å b=13.13 Å c=11.10 Å			a=11.60 Å b=15.64 Å c=6.10 Å		

As it was expected *A* it from the synthesized products, X-ray gram of silver(I), zinc, cadmium and cobalt(II) salts show diffusion character because of metastable state of products structure, which on the other hand, is due to high dispersion of mentioned products. As regards pyridinates of mercury(II) and nickel(II) monothioarsenates, X-ray diffraction parameters of which are given in Table 1, they crystallize in an orthorhombic crystal system.

The other monothioarsenate pyridinates were obtained in the same way. Charge of starting materials and yield of synthesized products is given in Table 2 and results of chemical analyses are shown in Table 3.

Table 2
Charge of starting materials and yield of synthesized products

Charge of starting materials						Yield, %			
Na ₃ AsO ₃ S·12H ₂ O		MX ₂ ·YH ₂ O							
g	mole	M	X	Y	g	mole	g	mole	%
6.0	0.0136	Co	Cl	6	5.2	0.0222	6.7	0.0051	75.4
3.0	0.0068	Ni	Cl	6	2.6	0.0111	8.8	0.0046	78.8
3.0	0.0068	Ag	NO ₃	-	3.7	0.0218	6.7	0.0070	97.6
3.0	0.0068	Zn	CH ₃ COO	2	2.4	0.0109	5.1	0.0034	95.8
3.0	0.0068	Cd	CH ₃ COO	2	2.9	0.0126	5.9	0.0040	96.8
3.0	0.0068	Hg	NO ₃	1	3.7	0.0114	6.9	0.0037	98.2

Table 3
Results of chemical analysis

Observed, %				Compound	Calculated, %			
As	N	M	S		As	N	M	S
11.40	9.52	13.44	5.00	Co ₃ (AsO ₃ S) ₂ ·9Py·6H ₂ O	11.49	9.65	13.53	4.90
8.04	9.11	13.53	3.07	[NiPy ₆] ₃ (AsO ₃ S) ₂	7.85	9.27	13.20	3.35
8.17	34.23	9.03	3.40	[AgPy ₂] ₃ AsO ₃ S	7.86	33.99	8.81	3.36
10.76	13.77	11.76	4.48	[ZnPy ₄] ₃ (AsO ₃ S) ₂	10.32	13.42	11.56	4.40
9.76	20.83	10.81	3.89	[CdPy ₄] ₃ (AsO ₃ S) ₂	9.41	21.08	10.54	4.01
8.12	32.57	9.24	3.67	[HgPy ₄] ₃ (AsO ₃ S) ₂	8.06	32.35	9.03	3.44

Tbilisi I. Javakhishvili State University

R. Agladze Institute of Inorganic Chemistry and Electrochemistry
Georgian Academy of Sciences

REFERENCES

1. R.D. Gigauri *et al.* Avtorskoe svidetelstvo1611869 USSR// B.Iz. 45, 1990, 124 (Russian).
2. Rukovodstvo po neorgan sintezu. Pod red. Brauera. 2. M., 1985, 627 (Russian).
3. K. Nakamoto. Infrazrasnye spektry neorganicheskikh i koordinatsionnykh soedinenii. M., 1966, 411 (Russian).
4. L. Bellami. Infrazrasnye spektry kompleksnykh molekul. M., 1963, 590 (Russian).
5. V.A. Kopilevich *et al.* J. Inorg. Chem. 37, 11, 1992, 2485-2489 (Russian).
5. შრომები, ტ. 157, №3, 1998



D. Tsakadze, M. Gverdtsiteli

Algebraic Investigation of the Alkaloids from Plants of *Cocculus* Family

Presented by Corr. Member of the Academy D. Ugrekhelidze, October 3, 1997

ABSTRACT. The alkaloids from plant of *cocculus* family - coculine, coculidine and coclaphine were studied by modernized ANB-matrices (quazi- $\tilde{A}NB$). Diagonal elements of quazi- $\tilde{A}NB$ -matrices represent atomic number of chemical elements (or molecular fragments), whereas nondiagonal ones – multiplicities of chemical bonds.

Key words: COCULINE, COCULIDINE, COCLAPHINE, $\tilde{A}NB$ MATRICES.

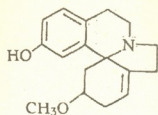
Contiguity matrices of molecular graphs and their various modifications are widely used in algebraic chemistry [1-2]. One type of such matrices are ANB-matrices; their diagonal elements represent atomic numbers of chemical elements, whereas nondiagonal elements – the multiplicity of chemical bonds [3]. For arbitrary XYV molecule ANB matrix has a form:

$$\begin{matrix} & \begin{matrix} 1 & 2 & 3 \\ X & Y & V \end{matrix} \\ \begin{matrix} Z_X & \Delta_{XY} & \Delta_{XV} \\ \Delta_{XY} & Z_Y & \Delta_{YV} \\ \Delta_{XV} & \Delta_{YV} & Z_V \end{matrix} & \parallel & \end{matrix} \quad (1)$$

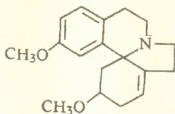
where, Z_X, Z_Y, Z_V are atomic numbers of X, Y, V chemical elements; $\Delta_{XY}, \Delta_{XV}, \Delta_{YV}$ represent multiplicities of chemical bonds between X and Y, X and V, Y and V.

The range of ANB-matrix is equal to the sum of atoms in molecule. The decimal logarithm of the determinant of ANB-matrix is topologic index [4] effectively used for constructing correlation "structure - properties" for molecules and their transformations. Calculations of the determinants of ANB-matrices for large molecules are very labour-consuming. We have elaborated simple model, which reproduces the specific character of system and at the same time is less labour-consuming. Whithin the limits of this model some unchangeable fragments of molecule are considered as pseudo-atoms. Such matrices are called quazi- $\tilde{A}NB$ -matrices [5].

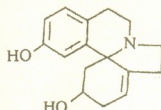
Let's consider the principles of construction of correlation equation "structure - properties" on the basis of quazi- $\tilde{A}NB$ -matrices for three alkaloids from plants of *cocculus* family: coculine, coculidine and coclaphine. The formulae of these alkaloids are:



Coculine



Coculidine



Coclaphine

(2)

All three molecules can be modeled by system:

$$R - O - A - O - R', \quad (3)$$

where: for coculine $R=H$, $R'=CH_3$; coculidine $R = R' = CH_3$; coclaphine $R = R' = H$; A - represents the molecule without OR and OR' groups. Corresponding quasi- $\tilde{A}N$ -matrix has a form:

$$\left\| \begin{array}{ccccc} Z_R & 1 & 0 & 0 & 0 \\ 1 & 8 & 1 & 0 & 0 \\ 0 & 1 & Z_A & 1 & 0 \\ 0 & 0 & 1 & 8 & 1 \\ 0 & 0 & 0 & 1 & Z_{R'} \end{array} \right\| \quad (4)$$

where

$$Z_R = \sum Z_r \quad (5)$$

$$Z_A = \sum Z_a \quad (6)$$

$$Z_{R'} = \sum Z_{r'} \quad (7)$$

Determinant (4) can be calculated as:

$$\Delta_{\tilde{A}NB} = 64 \cdot Z_R Z_A Z_{R'} - 8 \cdot Z_R Z_A - 16 \cdot Z_R Z_{R'} - 8 \cdot Z_A Z_{R'} + Z_R + Z_A + Z_{R'} \quad (8)$$

After calculation of determinants (4) for each compound correlation equation

$$W = a \lg \left(\frac{\Delta_{\tilde{A}NB}}{\Delta_{\tilde{A}NB}} \right) + b \quad (9)$$

can be constructed, where W is a concrete physico-chemical property (enthalpy, entropy, Gibbs thermodynamic potential, boiling point, melting point and etc); a and b are constants. (9) can be constructed on computer using special program [5].

The efficiency of correlation equation (9) for concrete case can be estimated according to the value of correlation coefficient r [3]. Finally, if the results are satisfactory, we can suppose that equation (9) expresses the correlation "structure - properties" for alkaloids of the mentioned type. In such a case we can interpolate and extrapolate the physico-chemical properties of such alkaloids with different R and R' within the limits of this approach.

REFERENCES

1. *P. R. Rouvray*. Chemical Application of Topology and Graph Theory. Ed. A. T. Balaban. Amsterdam, 1983.
2. *G. Gamziani*. Matematikuri kimiis rcheuli tavebi. Tbilisi, 1990 (Georgian).
3. *M. Gverdtsiteli et al.* The Contiguity Matrices of Molecular Graphs and their Modifications. Tbilisi, 1996.
4. *G. Gamziani et al.* Zogi ram topologiuri indeksebis shesakheb. Tbilisi, 1995 (Georgian).
5. *N. B. Kobakhidze, M. G. Gverdtsiteli et al.* Correlation "Structure - properties" in Algebraic Chemistry. Tbilisi, 1997.
6. *D. Tsakadze, M. Sturua et al.* Bull. Georg. Acad. Sci., **155**, 3, 1997.



M.Rukhadze, Academician V. Okujava, M. Sebiskveradze, M. Rogava, S. Tsagareli

Determination and Evaluation of Solvent Strength Parameter in Conventional Reversed-Phase, Ion-Pair and Micellar Chromatography

Presented July 31, 1997

ABSTRACT. The influence of organic modifiers additives on the retention of barbiturates in reversed-phase, ion-pair and micellar chromatography have been studied. The values of solvent strength (S) parameters in the range of linear dependence between retention and organic modifier content were determined. The fluctuation of S parameter with increase of molecular mass of investigated compounds is negligible in the presence of micellar aggregates.

Key words: REVERSED-PHASE LC, ION-PAIR MICELLAR CHROMATOGRAPHY, SOLVENT STRENGTH PARAMETER.

Ion-pair and micellar liquid chromatography (IPC and MLC) possess an evident advantage in comparison with traditional reversed-phase liquid chromatography (RPLC) when separation of ionic compounds, as well as simultaneous separation of ionic and non-ionic compounds is necessary to be realized [1,2]. The content of organic modifier is one of principal factors, which influences the solvent strength and selectivity in the given systems. The retention in RPLC as function of mobile phase composition with sufficiently precision is described with quadratic equation in the wide range of variation of organic modifier content. Within the most pertinent values of capacity factor k' ($1 \div 10$) for the binary and pseudobinary mixtures the retention quite satisfactorily may be circumscribed by linear equation:

$$\lg k' = \lg k'_w - S\Phi_{\text{org}} \quad (1)$$

where Φ_{org} is volume fraction of organic modifier in the waterorganic mobile phase, k'_w is extrapolated capacity factor when $\Phi_{\text{org}} = 0$, i.e. the retention in a purely aqueous mobile phase, S is solvent strength parameter, which reflects the extent of solvation of solutes by organic solvents and determines slope of $\lg k' - \Phi_{\text{org}}$ dependence. S must be independent from sample, i.e. S-coefficient must be a constant value for the given stationary phase and for the given binary or pseudobinary mobile phase. As is shown from the experimental data, in the RP-HPLC the increase of S with the rise of solutes molecular mass is observed [3]. The equation (1) may be used for the ion-pair and micellar systems [4,5]: In the IPC the variation of S is analogous to that of in the conventional RPLC [4]. It should be noted, that the dependence of retention from Φ_{org} is insufficiently investigated in IPC, where a great number of influencing factors has inhibited the study of mentioned relationship. The fluctuations of S parameter become negligible in the presence of micellar aggregates, which may be explained as a result of sample localization in nonhomogeneous micellar medium, where different compounds occupy different locations with different polarities in the micelle [5-9]. The goals of the present work were: the investigation of organic modifiers influence



on the retention of barbiturates in RPLC, IPC and MLC; estimation of fluctuations of solvent strength S - parameter in the given systems; study of dependence of S -parameter from retention of investigated compounds in pure water; exploration of relationship between selectivity (α) and organic modifier content in RPLC, IPC and MLC. As test solutes the group of barbiturates was selected, which are widely used for the medical purposes: barbital (BR), phenobarbital (PB), hexamidine (HD), benzobamyl (BB), nembutal (NB), barbamyl (BM), thiopental (TP), hexenal (HX), benzonal (BZ), halonal (HL).

Table

Solvent strength S -parameters values in different chromatographic systems

Compound	Mobile phase			
	Ethanol:0.05M NaH ₂ PO ₄ 30:70, 40:60, 50:50 pH 3	Acetonitrile:0.05M NaH ₂ PO ₄ 30:70, 40:60, 50:50 pH 3	Acetonitrile:0.05M NaH ₂ PO ₄ 30:70, 40:60, 50:50 modified with 4 mM SDS pH 3	100 mM SDS:pentanol:heptanol 98:1.5:0.5, 96:3:1, 94:4.5:1.5 pH 3
barbital (BR)	1.6	2.1	0.9	4.4
phenobarbital (PB)	2.5	3.6	1.3	4.6
hexamidine (HD)	2.1	3.0	1.4	4.9
benzobamyl (BB)	2.2	4.0	1.4	3.8
nembutal (NB)	3.4	3.8	2.5	4.0
barbamyl (BM)	2.1	3.8	2.1	4.3
thiopental (TP)	1.6	3.8	2.2	3.1
hexenal (HX)	2.4	4.0	2.2	4.8
benzonal (BZ)	5.5	5.0	4.5	3.8
halonal (HL)	5.7	5.1	4.5	4.5

The experiments were performed on a "Milichrom ("Nauchpribor", Oriol, Russia) microcolumn high-performance liquid chromatograph equipped with a UV absorption variable wavelength (190÷360 nm) detector and syringe type pump. The column used was a Separon-C₁₈ (Lachema, Brno, Czechoslovakia) column (62x2 mm, i.d.) with particle size 5 μ m. The mobile phases in conventional RP mode were prepared on the basis of mixture: a) acetonitrile+0.05 M NaH₂PO₄; b) ethanol + 0.05 M NaH₂PO₄ with the ratio 30:70, 40:60, 50:50. In ion-pair system the above mentioned mobile phases were modified with sodium dodecylsulfate (SDS) in amount 4 mM. For the micellar systems solution 100 mM SDS was used, which was modified by mixture pentanol-heptanol with ratio 98:1.5:0.5; 96:3:1; 94:4.5:1.5. The mobile phase pH was adjusted to 3 with phosphoric acid. The flow rate of eluent was 50 μ l/min. Analyses were carried out at

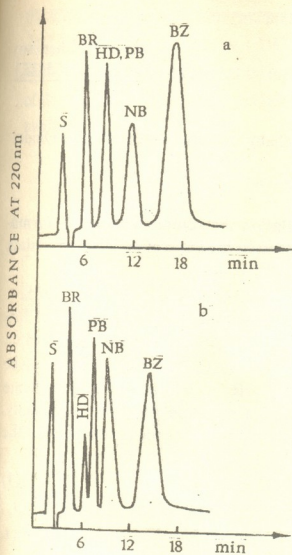


Fig. Chromatogram of mixture of barbiturates in MLC. Mobile phase: 0,1 M SDS - 0,05 M NaH_2PO_4 , modified with mixture of pentanol-heptanol a) 96:3:1, b) 94:4,5:1.5, S - solvent peak

ambient temperature. An UV detector was operated at 220 nm. All solutes were dissolved in ethanol.

The values of S-parameter, calculated with graphical method (slope of relationship $\lg k' - \Phi_{\text{org}}$) are presented in Table which shows that in RPLC and IPC solvent strength parameter varies within wider range than in MLC i. e. the tendency of S-parameter increase is most appreciable in RPLC and IPC than in MLC. The negligible variations of S-parameter with increase of molecular mass of solutes presumably is stipulated by localization of solute molecules in micellar environment, which reduces the size factor of molecules. The nonhomogeneous nature of micelles creates such surroundings, where different compounds are under the influence of different microenvironment polarities. The interaction between solutes and micelle may be realized by both solubilization and surface adsorption. The other mechanisms of interaction are also possible, e.g. formation of solute-surfactant coassembly etc.

The relationships between S and k'_w in all three systems (RPLC, IPC and MLC) are investigated. In the RPLC and IPC the linear relationship is observed, therefore the increase of organic modifier content deteriorates selectivity. In the MLC between S and k'_w the linear relationship is not revealed, rather an increase of k'_w results in sparing decrease of S-parameter, which may be explained so: micelles influence

on the function of organic modifiers, which in its turn are responsible for the value of solvent strength parameters. Thereby, in micellar systems an increase of organic modifier content often improves selectivity of hardly separable compounds (Fig.).

Tbilisi I.Javakhishvili State University

REFERENCES

1. B. A. Bidlingmeyer. *J. Chromatogr. Sci.*, **18**, 2, 1980, 525.
2. D. W. Armstrong. *Sep. Purif. Methods*, **14**, 2, 1988, 213.
3. J. W. Dolan, J. R. Gant, L. R. Snyder. *J. Chromatogr.*, **165**, 1, 1979, 31.
4. A. S. Kord, M. G. Khaledi. *Anal. Chem.*, **64**, 17, 1992, 1901.
5. M. G. Khaledi, E. Peuler, Ngeh-Ngwainbi. *Anal. Chem.*, **59**, 23, 1987, 2738.
6. M. G. Khaledi, J. K. Strasters, A. H. Rodgers, E. D. Breyer. *Anal. Chem.*, **62**, 2, 1990, 130.
7. A. S. Kord, M. G. Khaledi. *Anal. Chem.*, **64**, 17, 1992, 1894.
8. A. S. Kord, M. G. Khaledi. *J. Chromatogr.* **631**, 1993, 125.
9. M. L. Marina, M. A. Garcia. *J. Liq. Chromatogr.*, **17**, 95, 1994, 957.



A.Nadiradze, K.Ukleba, Academician G.Gvelesiani, J.Baratashvili, D.Tsagareishvili,
 J.Omiadze

A New Method of the Calculation of Standard Enthalpy of Formation of Double Oxides

Presented September 15, 1997

ABSTRACT. The new equation for calculation the standard enthalpy formation of double oxides from simple oxides was derived on the basis of experimental data of ΔH°_{298} for various classes of double oxides and PC program.

Key words: STANDARD ENTHALPY OF FORMATION, DOUBLE OXIDES.

The present work offers a new method of estimating standard enthalpy of formation of double oxides out of simple oxides on the experimental data on function ΔH°_{298} for different classes of these compounds. The investigated double oxide can be presented by the following general formula $xA_nO_m \cdot yB_pO_q$, where A and B indicate oxide formation elements, while x, y, n, m, p and q are stoichiometric coefficients. Then we choose triads of double oxides in the way that provides the proceeding of the following reaction:



Hence, the desired triad of double oxides will be $tE_\alpha O_\beta \cdot zD_kO_e$, $xA_nO_m \cdot zD_kO_e$, $tE_\alpha O_\beta \cdot yB_pO_q$, where, like the first compound, E and D are oxide forming elements, while t, z, k, e, α and β - stoichiometric coefficients.

For reaction (1) changing of crystal lattice energy of reagents may be the following:

$$\Delta E = E(xA_nO_m \cdot yB_pO_q) + E(tE_\alpha O_\beta \cdot zD_kO_e) - E(xA_nO_m \cdot zD_kO_e) - E(tE_\alpha O_\beta \cdot yB_pO_q) \quad (2)$$

The crystal lattice energy of each double oxide can be estimated from the following expressions:

$$E(xA_nO_m \cdot yB_pO_q) = E(xA_nO_m) + E(yB_pO_q) - \Delta H^\circ_{298}(xA_nO_m \cdot yB_pO_q) \quad (3),$$

$$E(tE_\alpha O_\beta \cdot zD_kO_e) = E(tE_\alpha O_\beta) + E(zD_kO_e) - \Delta H^\circ_{298}(tE_\alpha O_\beta \cdot zD_kO_e) \quad (4),$$

$$E(xA_nO_m \cdot zD_kO_e) = E(xA_nO_m) + E(zD_kO_e) - \Delta H^\circ_{298}(xA_nO_m \cdot zD_kO_e) \quad (5),$$

$$E(tE_\alpha O_\beta \cdot yB_pO_q) = E(tE_\alpha O_\beta) + E(yB_pO_q) - \Delta H^\circ_{298}(tE_\alpha O_\beta \cdot yB_pO_q) \quad (6),$$

where $E(xA_nO_m)$, $E(yB_pO_q)$, $E(tE_\alpha O_\beta)$ and $E(zD_kO_e)$ are the crystal lattice energies of simple oxides. If we insert expressions (3-6) into (2), and using the approximations $\Delta E=0$, we'll get equation for the calculation of ΔH°_{298} of the given double oxide:

$$\Delta H^\circ_{298}(xA_nO_m \cdot yB_pO_q) = \Delta H^\circ_{298}(xA_nO_m \cdot zD_kO_e) + \Delta H^\circ_{298}(tE_\alpha O_\beta \cdot yB_pO_q) - \Delta H^\circ_{298}(tE_\alpha O_\beta \cdot zD_kO_e) \quad (7)$$

In order to rise the precision of calculation it would be more expedient to determine ΔH°_{298} of the given double oxide by means of different variants using various triads of double oxides for which the experimental data of their ΔH°_{298} are known. At the same time

the mean value of the results of calculation of ΔH°_{298} should be given. Let us write down $\Delta H^{\circ}_{298} = \sum(\Delta H^{\circ}_{298})_i / r$, where $(\Delta H^{\circ}_{298})_i$ is the value of standard enthalpy of formation calculated while using i- variant, and r is the number of variants. The results of ΔH°_{298} of double oxide SrO·TiO₂ calculation are given in Table 1, according to the described method.

Table 1

The ΔH°_{298} calculated scheme for double oxide SrO·TiO₂

according to the equation (7) The triads of double oxides						SrO·TiO ₂ - ΔH°_{298} kcal/mol calc. from eq.(7)
tE _a O _p ZD _k O _e	- ΔH°_{298} kcal/mol	xA _n O _m ZD _k O _e	- ΔH°_{298} kcal/mol	tE _a O _p yB _p O _q	- ΔH°_{298} kcal/mol	
MgO·SiO ₂	8.7	SrO·SiO ₂	30.9	MgO·TiO ₂	6.4	28.6
CaO·SiO ₂	21.3	SrO·SiO ₂	30.9	CaO·TiO ₂	19.3	28.9
FeO·SiO ₂	4.6	SrO·SiO ₂	30.9	FeO·TiO ₂	6.4	32.7
2FeO·SiO ₂	8.9	SrO·SiO ₂	30.9	2FeO·TiO ₂	10.0	32.0
BaO·SiO ₂	37.7	SrO·SiO ₂	30.9	BaO·TiO ₂	38.7	31.9
Li ₂ O·ZrO ₂	14.8	SrO·ZrO ₂	17.3	Li ₂ O·TiO ₂	30.2	32.7
CaO·ZrO ₂	7.4	SrO·ZrO ₂	17.3	CaO·TiO ₂	19.3	29.2
CaO·MoO ₃	39.9	SrO·MoO ₃	54.0	CaO·TiO ₂	19.3	33.4
BaO·MoO ₃	56.9	SrO·MoO ₃	54.0	BaO·TiO ₂	38.7	35.6
Li ₂ O·MoO ₃	42.5	SrO·MoO ₃	54.0	Li ₂ O·TiO ₂	30.2	41.7

$$-(\Delta H^{\circ}_{298})_{av} = 32.7$$

$$-(\Delta H^{\circ}_{298})_{exp} = 32.5$$

To facilitate the choice of double oxide triads and subsequently their calculation it is reasonable to use computer. For this purpose we created the bank [1,2] of experimental data of standard enthalpy of formation of double oxides (Table 2), which was put into computer. At the same time we worked out the appropriate program for computer proceeding from the equation (7). In Table 2 for investigated compounds with experimental data the calculated values of ΔH°_{298} according to this program are given. In the same Table we inserted also values of δ to register the difference between the calculated and experimental data of ΔH°_{298} . The values of δ are calculated on one g. atom of given compound.

As indicated in Table 2 average divergence between experimental values of ΔH°_{298} and calculated by means of equation (7) for the considered double oxides makes $\pm 0,7$ kcal/mol, which is quite satisfactory for the accomplishment of thermodynamic calcula-

The correlation of experimental and estimated values according to the equation (7) for ΔH_{298}° double oxides

Compound	$-\Delta H_{298}^{\circ}$ kcal/mol exper.	$-\Delta H_{298}^{\circ}$ kcal/mol calc.	δ kcal/mol calc.-exper.	Compound	$-\Delta H_{298}^{\circ}$ kcal/mol exper.	$-\Delta H_{298}^{\circ}$ kcal/mol calc.	δ kcal/mol calc.- exper.
CaOMoO ₃	39.9	34.1	+1.0	Sm ₂ O ₃ .WO ₃	39.1	26.6	+1.4
SrOMoO ₃	54.0	44.9	+1.5	Sm ₂ O ₃ .2WO ₃	44.2	50.7	-0.5
BaOMoO ₃	56.9	48.3	+1.4	Sm ₂ O ₃ .3WO ₃	46.1	55.9	-0.6
Li ₂ O.MoO ₃	42.5	45.5	-0.4	FeOSiO ₂	4.6	9.4	-0.8
Li ₂ O.2MoO ₃	44.7	60.1	-1.4	2FeOSiO ₂	8.9	12.9	-0.6
Na ₂ O.2MoO ₃	81.3	65.9	+1.4	2CoO.SiO ₂	5.3	8.2	-0.4
ZnO.WO ₃	8.5	17.7	-1.5	2MnO.SiO ₂	11.8	11.0	+0.1
CdO.WO ₃	18.0	14.6	+0.6	MgO.SiO ₂	8.7	12.1	-0.7
NiO.WO ₃	10.7	15.7	-0.8	CaO.SiO ₂	21.3	23.6	-0.5
MnO.WO ₃	18.2	19.4	-0.2	2CaO.SiO ₂	32.4	32.5	0
CaO.WO ₃	38.8	31.0	+1.3	3CaO.SiO ₂	27.3	37.4	-1.1
SnO.WO ₃	48.3	46.7	+0.3	SrO.SiO ₂	30.9	35.8	-1.0
MnO.Fe ₂ O ₃	4.8	8.1	-0.5	2SrO.SiO ₂	49.7	39.5	-1.4
MgO.Fe ₂ O ₃	9.2	4.8	+0.6	BaO.SiO ₂	37.7	39.2	-0.3
CaO.Fe ₂ O ₃	14.4	19.9	-0.8	Li ₂ O.SiO ₂	33.3	30.5	+0.5
BaO.Fe ₂ O ₃	26.4	32.4	-0.8	ZnO.Fe ₂ O ₃	2.2	8.8	-0.9
ZnO.Al ₂ O ₃	9.8	6.4	+0.5	NiO.Fe ₂ O ₃	1.1	4.6	-0.5
MnO.Al ₂ O ₃	9.0	8.3	+0.1	Na ₂ O.2SiO ₂	56.7	59.3	-0.3
CaO.Al ₂ O ₃	12.8	17.6	-0.7	Li ₂ O.2SiO ₂	33.6	35.4	-0.2
Li ₂ O.Al ₂ O ₃	25.3	19.1	-0.8	Na ₂ O.SiO ₂	56.8	54.6	+0.4
Na ₂ O.Al ₂ O ₃	42.3	48.6	-0.8	MgO.GeO ₂	4.3	12.0	-1.5
MgO.Al ₂ O ₃	5.6	8.2	-0.4	2MgO.GeO ₂	9.8	2.7	+1.0
U ₂ O ₃ .3WO ₃	39.5	55.1	-0.9	CaO.GeO ₂	19.1	15.9	+0.6
La ₂ O ₃ .2WO ₃	64.2	57.7	+0.5	3CaO.GeO ₂	29.3	23.0	+0.7
LaO ₃ .3WO ₃	69.7	57.8	+0.7	2BaO.GeO ₂	43.9	53.4	-1.4
CoO.TiO ₂	6.6	9.0	-0.5	CaO.ZrO ₂	7.4	9.4	-0.4
FeO.TiO ₂	6.4	3.6	+0.6	SrOHfO ₂	19.4	21.7	-0.5
2FeO.TiO ₂	10.0	8.1	+0.3	BaOHfO ₂	31.4	24.3	+1.4
NiO.TiO ₂	4.4	8.8	-0.9	Li ₂ O.ZrO ₂	14.8	17.1	-0.4
MnO.TiO ₂	7.1	11.7	-0.9	SrO.ZrO ₂	17.3	19.8	-0.5
2MnO.TiO ₂	8.5	11.6	0.4	Li ₂ O.HfO ₂	15.4	20.4	-0.8
MgO.TiO ₂	6.4	9.9	-0.7	ZnO.Cr ₂ O ₃	14.1	9.3	+0.7
MgO.2TiO ₂	4.5	15.7	-1.4	CdO.Cr ₂ O ₃	9.1	11.0	-0.3
2MgO.TiO ₂	14.1	14.1	-1.4	MgO.Cr ₂ O ₃	10.8	7.0	+0.5
CaO.TiO ₂	19.3	22.1	-0.6	Na ₂ O.Cr ₂ O ₃	48.4	53.2	-0.6
3CaO.2TiO ₂	37.5	26.3	+0.9	FeOMoO ₃	12.5	20.8	-1.4
SrOTiO ₂	32.5	32.7	0	Ho ₂ O ₃ .WO ₃	28.7	28.7	0
2SrOTiO ₂	37.8	47.3	-1.4	Dy ₂ O ₃ .WO ₃	24.9	37.9	-1.4
BaOTiO ₂	38.7	34.3	-0.9	Dy ₂ O ₃ .3WO ₃	51.4	38.5	+0.8
Li ₂ O.TiO ₂	30.2	28.9	+0.2	Ho ₂ O ₃ .3WO ₃	44.9	44.8	0
BaO.ZrO ₂	28.6	23.1	+1.1				

tions. Consequently the precision of calculation (Δ) of the function ΔH_{298}° of double oxide under consideration can be estimated by combination $\Delta = \pm 0,7[x(n+m)+y(p+q)]$ kcal/mol.

F.Tavadze Institute of Metallurgy
Georgian Academy of Sciences

REFERENCES

1. A.Nadiradze et al. Izv. AN Gruzii, ser. Khimia, 1990, 16, 4, 277 (Russian).
2. Termicheskie konstanty veshstv (Pod. Red. V.P.Glushko).vip.4-10, m VINITI, 1972-1981 (Russian).



E.Kachibaya, Corr. Member of the Academy L.Japaridze, R.Akhvlediani, Sh.Japaridze,
 T.Paykidze, R.Imnadze

Synthesis and Structure of Spinel Type Lithium- Manganese Composition

Presented July 14, 1997

ABSTRACT. Solid state interaction reaction of MnO_2 and Li_2CO_3 in the temperature range $20-1000^\circ C$ has been investigated. It has been found that phase composition of synthesis products depends on molar ratio of Mn:Li in source charge. Formation of pure-phase cubic spinel $LiMn_2O_4$ takes place when Mn:Li = 2:1 and synthesis temperature is $850^\circ C$. By regulation of acidic treatment of $LiMn_2O_4$ it is possible to obtain a series of spinel type structure composition as $Li_xMn_2O_4$, $0 < x < 1$.

Key words : MANGANESE DIOXIDE, LITHIUM-MANGANESE, CUBIC SPINEL.

To study the synthesis possibilities of lithium-manganese spinels perspective to use as cathode materials in lithium accumulators, the solid state phase interaction reactions of manganese oxide with lithium compounds were investigated. As reagent sources electrolytic manganese dioxide [EMD] and reagent grade Mn_2O_3 and Li_2CO_3 have been used.

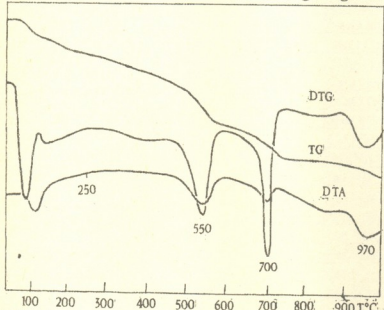
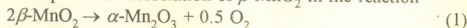


Fig.1 Derivatogram of $LiMn_2O_4$ received in the result of source charge thermotreatment (Mn:Li = 2:1) at $850^\circ C$.

Synthesis was carried out in different temperatures on air with intermediate samples cooling and grinding. Synthesis products were identified by X-ray, thermal, atomic-absorption and other analytical techniques [1,2]. Solid-state phase reactions of manganese oxides and lithium salts interaction in the temperature range $20-1000^\circ C$ were investigated. As a result of reactions compounds were obtained, phase composition and crystallographic parameters of which were determined by molar ratio between manganese and lithium in the source

charge (Table 1). X-ray diagrams of synthesis products are distinguished by character of main interplanar distances distribution (d); this fact reflects the appearance of one or another variety of lithium-manganese compositions. The appearance of pure-phase cubic spinel - $LiMn_2O_4$ takes place, when molar ratio Mn:Li=2:1. At a derivatogram of charge, composed from $\gamma-MnO_2$ (EMD) and Li_2CO_3 mix when Mn:Li= 2:1, in low temperature

range (up to 200°C) the effects corresponding to a loss of water by γ -MnO₂ modification and its transformation into β -MnO₂ modification are fixed (Fig.1.). Endothermic effect with a maximum at 550°C corresponds to dissociation of β -MnO₂ in the reaction



In the same temperature range in parallel with dissociation of MnO₂ melting and dissociation of Li₂CO₃ take place. X-ray phase analysis of products of charge burning in the temperature range 400-1000°C has confirmed that the interaction of manganese dioxide and lithium carbonate is possible already at $T > 500^\circ\text{C}$ (Table 1). Formation of pure-phase cubic spinel without Mn₂O₃ or Li₂CO₃ admixtures takes place only at 850°C. The last endothermic effect fixed at 970°C is the result of thermal decomposition of LiMn₂O₄ spinel. By further cooling the product of decomposition is once more oxidized by air oxygen into spinel.

Table 1

Phase composition and crystallographic parameters of products of solid-state phase interactions of MnO₂ and Li₂CO₃ depending on molar ratio Mn:Li in source and the burning temperature (the time of burning ~3h)

Mn:Li ratio in source charge	Burning T°C	Phase composition of product	Phase ratio, %	Lattice parameters, Å		System	Annotation
				a	c		
Mn:Li=1:1	550	Li ₂ MnO ₃ Li Mn ₂ O ₄	52.6 47.4	8.46 8.16	9.48	tetragonal cubic	Admixtures: Li ₂ CO ₃ and MnO ₂
	700	Li ₂ MnO ₃ Li Mn ₂ O ₄	55.5 44.5	8.48 8.22	9.47	tetragonal cubic	Admixtures: Li ₂ CO ₃ and MnO ₂
	850	Li ₂ MnO ₃ Li Mn ₂ O ₄	58.6 41.4	8.46 8.21	9.48	tetragonal cubic	No additional phases
	1000	Li ₂ MnO ₃ Li Mn ₂ O ₄	58.6 41.4	8.48 8.21	9.50	tetragonal cubic	diffuse X-ray diagram
Mn:Li=1:2	800	Li ₂ MnO ₃	~10			tetragonal	Mixture of MnO ₂ and Li ₂ CO ₃ ; low degree of crystallization
	850	Li ₂ MnO ₃		8.51	9.41	tetragonal	pure phase
	1000	Li ₂ MnO ₃		8.51	9.40	tetragonal	pure phase
Mn:Li=2:1	500	Li Mn ₂ O ₄ Li ₂ MnO ₃	~40	8.14		cubic tetragonal	parameters of Li ₂ MnO ₃ are not determined
	700	LiMn ₂ O ₄		8.23		cubic	Admixture Mn ₂ O ₃
	800	LiMn ₂ O ₄		8.23		cubic	insignificant admixture Mn ₂ O ₃
	850	LiMn ₂ O ₄		8.23		cubic	pure phase
Mn:Li=5:1	600	Li Mn ₂ O ₄		8.16		cubic	Admixtures: large amount of Mn ₂ O ₃ , insignificant of Li ₂ MnO ₃
	700	LiMn ₂ O ₄		8.20		cubic	large amount of Mn ₂ O ₃
	800	LiMn ₂ O ₄		8.19		cubic	large amount of Mn ₃ O ₄



When molar ratio in source charge Mn:Li = 2:1 the main structural motive of synthesized samples is face-centered cubic structure; when Mn:Li=1:2 phase of Li_2MnO_3 is formed (ASTM, 18-737) [2]. By data (ASTM, 27-1252) Li_2MnO_3 is characterized by monoclinic system. But for Li_2MnO_3 (ASTM, 18-737) no hkl values are given, and respectively there are no data about systems. By our calculations the product obtained, when Mn:Li=1:2, is Li_2MnO_3 (ASTM 18-737) and has tetragonal structure (Table 2). Using the charge, where molar ratio Mn:Li=1:1, two phase are obtained: tetragonal- Li_2MnO_3 and cubic- LiMn_2O_4 . In this case approximate quantitative calculation testifies to a presence of both these phases in the product in equal quantities (Table 1, p.5). Spinel LiMn_2O_4 as the product of lithium corporation into the manganese oxides and the possibility of lithium leaching from its structure was first presented in [3]. We have confirmed possibility of LiMn_2O_4 transformation with the removal of nearly all lithium into pure $\lambda\text{-MnO}_2$ with retaining spinel; structure (Table 3, samp. 6 and 7). Maximum removal of lithium from LiMn_2O_4 has been observed when 3N HCl, 4N HNO_3 and 15% H_2SO_4 solutions with pH 1.2-1.3 are used. Comparison of X-ray diagrams of $\lambda\text{-MnO}_2$ samples

Table 2

Diffractive characteristics of synthesized samples of LiMn_2O_4 and Li_2MnO_3 in comparison with ASTM data

Li_2MnO_3			Li_2MnO_3			LiMn_2O_4			LiMn_2O_4		
ASTM, 18-737			product			ASTM, 18-736			product		
I/I ₀	d, Å	hkl	I/I ₀	d, Å	hkl	I/I ₀	d, Å	hkl	I/I ₀	d, Å	hkl
45	4.79		100	4.74	002	100	4.72	111	100	4.67	111
35	4.23		20	4.23	200	-	-	-			
35	4.12		12	4.09	102	-	-	-			
20	3.66		10	3.42	112	-	-	-			
10	3.16		10	3.23	003	-	-	-			
5	2.72		20	2.675	301	-	-	-			
-	-		-	-	-	90	2.47	311	90	2.462	311
45	2.42		40	2.417	004;302	-	--				
-	-		-	-	-	5	2.37	222	10	2.36	222
-	-		-	-	-	100	2.05	400	100	2.04	400
100	2.02		90	2.020	124;133	-	-	-			
10	1.86		10	1.859	224;241	10	1.88	331	15	1.88	331
5	1.82		5	1.820	115;304	-	-	-			
5	1.70		5	1.698	340	-	-	-			
5	1.61		10	1.600	225	-	-	-			
40	1.57		20	1.566	250;106	50	1.58	333;511	30	1.57	333;511
5	1.53					-	-	-			
50	1.44					90	1.45	440	50	1.44	440
55	1.42					-	-	-	-	-	-
40	1.36					30	1.39	531	15	1.38	531
			Tetragonal system a = 8.46Å c = 9.67Å			cubic system face-centered a = 8.24Å			cubic system a = 8.162Å		



and X-ray LiMn_2O_4 samples diagram have shown some displacement of the main diffractive peaks towards more low values. The series of compounds placed between LiMn_2O_4 and $\lambda\text{-MnO}_2$ (Table 3), is obtained by regulation of conditions of acidic treatment of LiMn_2O_4 . These compounds can be represented by general formula $\text{Li}_x\text{Mn}_2\text{O}_4$, where $0 < x < 1$. The assumption was made that in such compounds the lattice vacancies, in which the lithium ions could incorporate, are capable to provide in or out the lithium ions easily, taking place respectively by charging -discharging of lithium accumulator without destroying its structure.

Table 3

Diffractive characteristics of $\text{Li}_x\text{Mn}_2\text{O}_4$ type compounds ($0 < x < 1$), obtained in the result of LiMn_2O_4 acidic treatment

Specimen N1 (initial LiMn_2O_4)		Specimen N2 $\text{Li}_{0.48}\text{Mn}_2\text{O}_4$		Specimen N3 $\text{Li}_{0.34}\text{Mn}_2\text{O}_4$		Specimen N4 $\text{Li}_{0.10}\text{Mn}_2\text{O}_4$		Specimen N5 ($\text{Li}_{0.05}\text{Mn}_2\text{O}_4$) $\lambda\text{-MnO}_2$		Specimen N6 ($\text{Li}_{0.03}\text{Mn}_2\text{O}_4$) $\lambda\text{-MnO}_2$	
d, Å	I/I ₀	d, Å	I/I ₀	d, Å	I/I ₀	d, Å	I/I ₀	d, Å	I/I ₀	d, Å	I/I ₀
4.790	100	4.72	100	4.72	100	4.70	100	4.670	100	4.670	100
2.495	70	2.42	90	2.42	70	2.43	80	2.423	90	2.427	80
2.380	20	2.32	20	2.31	20	2.34	20	2.321	15	2.315	15
2.062	100	2.01	100	2.015	100	2.011	100	2.010	100	2.013	100
1.895	20	1.845	20	1.845	20	1.848	20	1.841	20	1.841	20
1.585	40	1.546	30	1.547	30	1.549	30	1.545	40	1.544	30
1.456	70	1.419	55	1.423	50	1.421	50	1.419	60	1.417	50
1.391	20	1.359	25	1.361	20	1.361	20	1.361	90	1.350	25
1.250	5	1.225	5	1.226	5	1.220	5			1.220	5
2.240	5	1.212	5	1.210	5	1.210	5			1.210	5
		1.162	15			1.160	10				
a = 8.24Å		a = 8.04Å		a = 8.04Å		a = 8.05Å		a = 8.04Å		a = 8.02Å	

R. Agladze Institute of Inorganic Chemistry and
Electrochemistry
Georgian Academy of Sciences

REFERENCES

1. X-ray diffraction data cards ASTM, 1977.
2. F. Paulik, I. Paulik, L. Erdey. *Talanta Review*, **13**, 1966, 1405.
3. J. C. Hunter. *J. Solid State Chem.*, **39**, 1981, 142.



L. Baiadze, G. Gaprindashvili, O. Modebadze, J. Nakaidze, N. Papunashvili,
 Academician G. Tsintsadze

Investigation of Some Physico-Chemical Properties of High-Manganese Boron Oxide Glassy Semiconductors

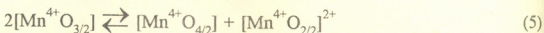
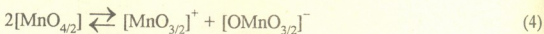
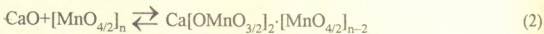
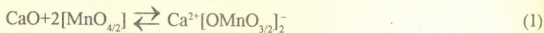
Presented August 4, 1997

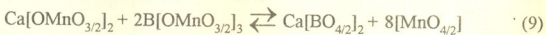
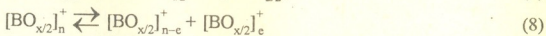
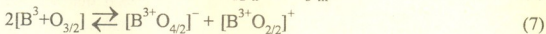
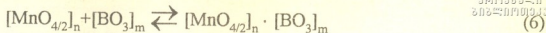
ABSTRACT. The intermediate reactions in the melt of glass during synthesis of high-manganese boron oxide glassy semiconductors (OGS) have been investigated. These reactions make possible to establish the technological cycle for melting of the glass with predetermined electrophysical parameters. We have shown that the stability of electrophysical parameters of OGS with composition of $2\text{CaO} \cdot 3\text{B}_2\text{O}_3 \cdot 2\text{MnO} \cdot 2\text{MnO}_2$ depends on the coordinational environment of cations (B^{3+} , Mn^{2+} , Mn^{4+} , Ca^{2+}). On the basis of such glasses the switching electronic elements having stable threshold voltage can be produced.

Key words: GLASS, SWITCHING and MEMORY ELEMENT.

Georgia possesses one of the richest manganese ores in the world. It has been experimentally established that boron and boron-silicate glasses consisting of 40-50 mass% different valency manganese oxides (mainly MnO and MnO_2) have electrical conductivity and are able to be switched from the high to the low resistance state [1]. On the basis of these glasses it is possible to produce the switching and memory electronic devices. Due to the manganese polyvalency, it is difficult to preserve manganese in the predetermined valency and coordinational state and therefore to synthesize manganese oxide glassy semiconductors (OGS) having stable electrophysical properties. Analogously to the other glasses [2], many intermediate reactions take place during melting of starting materials in the $\text{CaO}-\text{B}_2\text{O}_3-\text{MnO}-\text{MnO}_2$ system and it is necessary to develop satisfactory technological cycle which can be applied to synthesize manganese OGS with predetermined properties.

For example, during the melting of glass with composition $2\text{CaO} \cdot 3\text{B}_2\text{O}_3 \cdot 2\text{MnO} \cdot 2\text{MnO}_2$ the following intermediate reactions could take place:





As seen from these reactions, the complicated processes are proceeded in the melt and as a result the integration (1,2,3,6), differentiation (4,5,6,7,8,9) of ingredients of glass, change in coordinational environment (3,4,5,7,9), formation of some complexes and other processes could take place. Due to these processes the network of glass could be weakened or strengthened.

From the point of view of switching mechanism the most favourable conditions should be formed when coordinational number of Mn^{2+} is equal to 6 (octahedral environment) and that of Mn^{4+} is equal to 4 (tetrahedral environment). Network of glass must be weakened by Ca^{2+} in order to make possible the formation of conductive crystalline channel in the bulk of glass when threshold voltage is applied. From the point of view of the same mechanism, part of B^{3+} should form the triangles with anions (coordinational number is equal to 3) and the other part of B^{3+} should be located in the tetrahedral environment in order to make possible the transition of two oxygen anions to the Mn^{4+} (when $[\text{Mn}^{4+}\text{O}_4]$ passed in $[\text{Mn}^{4+}\text{O}_6]$ by means of passage of $[\text{BO}_4]$ to the $[\text{BO}_3]$).

The existence of undistorted polyhedra or cationic groups with distorted but strongly determined coordinational environment could not be identified in the glasses. Therefore, theoretical estimations could be fulfilled only with certain approximation.

On the other hand, if we do not assume the existence of certain coordinational groups in the glass then it could be impossible to establish the reasons of existence of OGS with high electronic conductivity and switching ability.

Above mentioned ideas were confirmed experimentally. It was established that synthesis of high-manganese OGS (electronic conductivity $\sigma = 10^{-9} - 10^{-11} \text{ ohm}^{-1} \text{ cm}^{-1}$) is possible under certain technological conditions when predetermined value of $\text{Mn}^{2+}:\text{Mn}^{4+}$ ratio can be ensured $\text{Mn}^{2+}:\text{Mn}^{4+} = 0.5-1$. The compositions of these glasses are shown in Table 1.

Area of glass-formation in the $\text{CaO}\cdot\text{MnO}\cdot\text{B}_2\text{O}_3$ system is sufficiently wide and has been investigated in [3]. The lack of investigation [3] is that manganese was introduced in the samples only in MnO form although the authors confirm the existence of MnO_2 in the glass.

Table 1

Molecular formula of the glass	Oxides Content, mass%			
	CaO	B_2O_3	MnO	MnO_2
$2\text{CaO}\cdot 3\text{B}_2\text{O}_3\cdot 2\text{MnO}\cdot 2\text{MnO}_2$	17.64	32.63	22.21	27.52
$\text{CaO}\cdot 1.49\text{B}_2\text{O}_3\cdot 0.99\text{MnO}\cdot 1.37\text{MnO}_2$	16.04	29.66	20.19	34.11
$\text{CaO}\cdot 5.55\text{B}_2\text{O}_3\cdot 4.34\text{MnO}\cdot 5.40\text{MnO}_2$	4.58	31.65	25.22	38.55
$\text{CaO}\cdot 5.55\text{B}_2\text{O}_3\cdot 3.154\text{MnO}\cdot 6.05\text{MnO}_2$	4.36	30.18	23.26	42.20
$\text{CaO}\cdot 5.58\text{B}_2\text{O}_3\cdot 5.23\text{MnO}\cdot 6.15\text{MnO}_2$	4.16	28.77	27.47	39.60

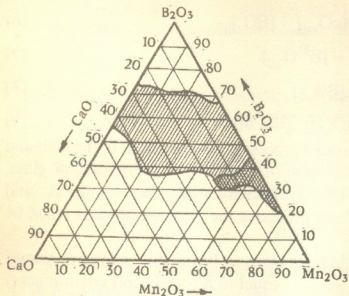


Fig. 1. Glass formation area in the $\text{CaO-B}_2\text{O}_3\text{-Mn}_2\text{O}_3$ system

Experimental investigations

showed that when MnO_2 is added to the starting material (in the above mentioned proportion), then area of glass-formation is significantly enlarged. Area of glass-formation in the $\text{CaO-Mn}_2\text{O}_3\text{-B}_2\text{O}_3$ system is shown in Fig. 1. Joint content of MnO and MnO_2 is given by Mn_2O_3 . Data from [3] for the $\text{CaO-MnO-B}_2\text{O}_3$ system and results of the present study are indicated by dashed and solid lines, respectively.

Properties of OGS (see Table 1) and switching elements (those are produced on the basis of OGS) are presented in Table 2.

Table 2

Properties of the glass and switching element	Sample No				
	1	2	3	4	5
Melting temperature $t_m, ^\circ\text{C}$	1350	1360	1370	1400	1380
Melting duration T_m, h	2.5	2.62	2.7	2.8	2.6
Annealing temperature, $t_a, ^\circ\text{C}$	630	650	670	680	650
Temperature of thermal processing, $t_{th}, ^\circ\text{C}$	610	630	650	660	630
Electric conductivity, $\sigma, \text{ohm}^{-1}\cdot\text{cm}^{-1}$	10^{-10}	$0.5\cdot 10^{-10}$	$5\cdot 10^{-9}$	$0.3\cdot 10^{-9}$	$0.4\cdot 10^{-9}$
Threshold switching voltage, V_{sw}, V	100	90	80	90	70
Distance between electrodes of nickel's element, $l, \mu\text{m}$	30	35	40	35	50
Switching time, t_{sw}, sec	10^{-7}	$5\cdot 10^{-7}$	$3\cdot 10^{-7}$	$9\cdot 10^{-8}$	$7\cdot 10^{-8}$

Fig. 2 shows a possible structural fragment of glass with the composition of $2\text{CaO}\cdot 3\text{B}_2\text{O}_3\cdot 2\text{MnO}\cdot 2\text{MnO}_2$.

Typical volt-ampere characteristic of boron-manganese OGS is given in Fig. 3. This characteristic is S-like and shows that when voltage is less than the threshold one, then current increases proportionally to the voltage (according to Ohm's law). Ohm's law is broken when voltage approaches to the threshold magnitude ($\sim 10^4 \text{ V}\cdot\text{cm}$) and current increases exponentially. When the threshold voltage is reached then current increases during $10^{-6}\text{-}10^{-8}$ sec in jump-like manner (resistance decreases in the same manner).

If the most part of manganese cations will pass to the tetrahedral environment and take part in weaving of network as glass-former, then according to the evaluations and despite the high content of manganese oxides (more than 60 mass%, Table 1), inverted glasses will be transformed to the so-called normal glasses.

Thus, it has been demonstrated by the present experimental work that on the basis of high-manganese boron OGS it is possible to produce the electronic elements of switching and memory devices. Electrodes of glassy switching element are separated from each

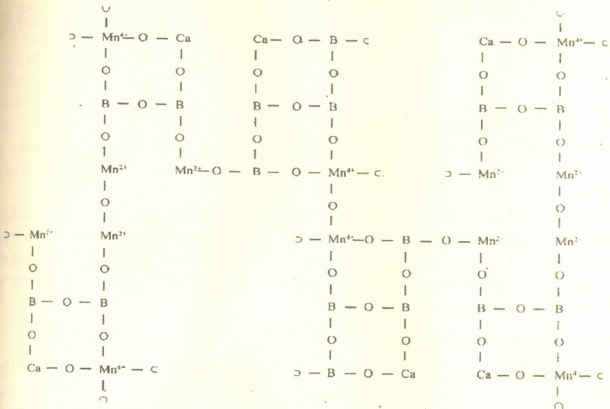


Fig. 2. Possible structural fragment of boron-manganese OGS with the composition of $2CaO \cdot 3B_2O_3 \cdot 2MnO \cdot 2MnO_2$

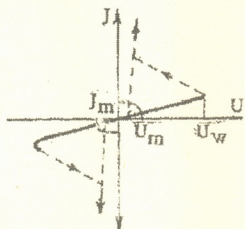


Fig. 3. Typical volt-ampere characteristic of boron-manganese OGS

other by the distance $\sim 50-100 \mu m$. Threshold switching voltage is equal to 80-100V, while the switching time from the high to the low resistance state is $10^{-5}-10^{-8}$ sec.

This work was financially supported by the Georgian Academy of Sciences.

Institute of Cybernetics
Georgian Academy of Sciences

REFERENCES

1. L. Baiadze, O. Modebadze et al. Proc. Georgian Technical University, N8 (405). Tbilisi, 1993, 67-74. (Georgian).
 2. M. M. Shultz. Fizika i khimya stekla, 10, 2, 1984, 129-138 (Russian).
 3. M. G. Kuznetsov. Avtoreferat diss. Leningrad, 1972 (Russian).

I.Iashvili

Contemporary Tendencies of Demographic Processes Development in Kutaisi City

Presented by Academician G.Svanidze, February 2, 1998

ABSTRACT. A study of demographic processes in Kutaisi city in the nineties has demonstrated a decrease of population caused on the one hand by hard political and economic situation and on the other hand by a decrease of birth and increase of death among the population being employed. Inappropriate demographic policy in Kutaisi is regarded as national crisis.

Key words: BIRTH RATE, DEATH RATE, POPULATION.

Demographic processes in Kutaisi city are characterised by strong mobility caused by its social and economic position. The dynamics of Kutaisi population for 1985-1996 was studied. Four stages were defined in this period: 1) rapid increase of population in 1985-1989; 2) comparatively insignificant increase; 3) population decrease in 1992-1994; 4) slow increase from 1994 up to 1996 (Fig. 1). In the decade under consideration Kutaisi population reaches its maximum (240000 men) in 1992. From 90s birth rate significantly decreases. Thus if in 1987 coefficient of birth rate made 21‰, in 1995 its index was not more than 14.3‰. While making demographic analysis during political and economic cataclysms as well as war periods sharp decrease of birth rate is usually marked.

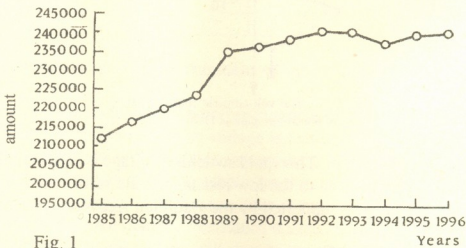


Fig. 1

One of the main reasons of this process is the absence of hope in future. Of no less importance is ignorance of solid and concrete social guarantees from the Government (i.e. maternity leaves, real financial support for newborns and so on), which really had sense in previous decades.

At present young families face such significant problems as: specialised employment, decrease of real income. Young families have difficulties in feeding and clothing of their children. The compensations given by the state are insufficient and do not keep

up with the inflation rate. Strong immigration processes also encouraged the decrease of birth rate. Negative influence on growth of Kutaisi population has rapid death rate (Fig. 2). Common coefficient of death rate has been increased from 6.8‰ up to 9.6‰. In the studied period this index was several times repeated and preserved. In the majority of cases death was caused by unnatural reasons and the Civil war, i. e. who appeared socially insecure. A decrease of real incomes, depreciation of material support given by the Government, worsening of health status, low-calorie food and even starvation greatly increased death rate.

Besides, since 1990 the mortality was also caused by the other factors. The amount of the dead was significantly increased in the result of accidents and trauma. In the course of

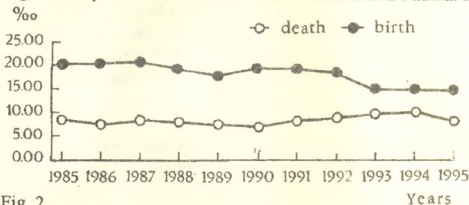


Fig. 2

five years from 1990 including 1994 the mortality has grown in 41.1%. According to the obtained medical statistical data the tendency to the decrease of many diseases is marked, which in our opinion doesn't create a real picture, because existed economic hardships in the last seven years makes it difficult to receive medical treatment at the clinic. People have to cure at home deprived of qualified treatment. Tuberculosis among children is progressing and its treatment in home conditions is practically impossible. The mortality among new-borns is the indicator of socio-economic development. The dynamics of death rate among new-borns in Kutaisi since 1986 reveals the tendency to decrease. From 1991 this index decreases (Fig. 3), otherwise the increase of new-borns is accompanied with increase of death rate and vice versa. Two main socio-economic reasons of mortality among new-borns are impoverish of population and worsening of medical service. Therefore the stronger the society, the less problems are. Our society always paid much attention to the treatment and care of children. The statistics evidenced that even in conditions of birth rate decrease, this positive tendency is preserved. In our opinion just high level of medical service creates favourable conditions for newborns diagnosis in Tbilisi. (Fig. 3). Birth rate and natural growth coefficients here are lower and death rate coefficients are higher as compared to Kutaisi.

For the last seven years in Kutaisi natural growth coefficient decreases. Average indices of the eighties decreased from 13‰ up to 4.7‰ in 1994.

B.S.Khorev singles out three types of reproduction [1]: 1) high birth rate, high death rate; 2) low birth rate, low death rate; 3) comparatively high birth rate. He also states about the fourth type of reproduction which was formed in Russia in 90s i.e. too low birth rate and too high death rate. It is a unique case when in peace period death rate exceeds birth rate.

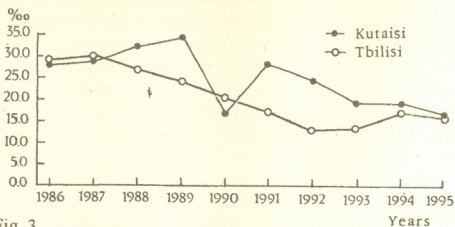


Fig. 3

Despite the fact that the process of depopulation has not yet been started, according to contemporary demographic parameters Kutaisi city can be referred to the fourth type. On the basis of obtained data we can make the following conclusions:

1. Hard political, economic and social situation in Kutaisi in nineties significantly reduce the birth rate.

2. One of the main features of the worsening of demographic situation is the increase of death rate. The analysis of statistical data testifies to the rapid approximation of the senility boundary. It happens not through average life duration as it is in developed countries (i.e. senility "from above"), but by the decrease of birth rate (i.e. senility "from beneath") and high death rate of capable population.

3. The decrease of birth rate and increase of death rate first of all causes the decrease of natural growth. In Kutaisi death rate increased (in 90-94 by 41.1%); it goes beyond birth rate (for the same period birth rate decreased in 32%).

4. The problem of new-borns mortality is still very actual. Despite the fact that along with the decrease of birth rate the mortality among new-borns decrease in future, new-borns life preservation is of great importance.

5. Demographic policy in Georgia at present is not on appropriate level. It should be aimed at stimulation of birth-rate.

Kutaisi State University

REFERENCES

1. *B.S.Khorev*. Proceedings of Russian Geographical Society. **127**, 2, 1995, 50 (Russian).

M. Tvalchrelidze

Geological History of the Sokhumi Peninsula in Late Pleistocene and Holocene

Presented by Academician I. Gamkrelidze, August 14, 1997

ABSTRACT. Forming of the Sokhumi peninsula started in the Lower Holocene, at the terminative stage of the transgression of the Black Sea New Euxinic basin and at the end of the Upper Holocene it gained its recent form. Glacio-eustatic transgression of the Black Sea and world ocean, volumes of alluvions delivered by rivers into the coastal line and litho and morphodynamics of the coast-line are of determinative role in its formation.

Key words: EUSTATIC, TRANSGRESSION, ALLUVION, PLEISTOCENE, HOLOCENE.

In Late Pleistocene, 18-19 thousand years ago, during the last maximal stage of Würmian glaciacion the Black Sea level subsided at the altitude of minus 90-100 m at absolute mark. If we take into account that 32-24 thousand years ago the world Ocean and accordingly the Black Sea levels had been close to the recent one [1], then rate of the Black Sea lowering during this period was no less than 1.4 cm per year.

Alongside with the beginning of regression of the Black Sea New Euxinic sedimentary basin river erosion basis also relatively lowered causing channel erosion processes. Morphology of paleogorges - high indices of longitudinal and transverse profiles, points to the intensity of these processes. From the drill-holes (Fig. 1) on the Sokhumi peninsula and its adjacent territory it is obvious that during the maximal regression of the Black Sea New-Euxinic sedimentary basin overdeepened rivergorges existed. They were worked out mainly in Neogene and partially in Paleogen terrigene sediments. In particular between drill-holes 50 and 93, drill-holes 93 and 41, and between drill-holes 41 and 120. Continuation of above mentioned gorges deep in the land is fixed between drill-holes 71 and 65, 65 and 36, and 36 and 120. According to available actual data, during the maximal regression the coastline was about 2.5 km westwards from the recent one. Maximal depth of paleogorges on the Sokhumi peninsula is fixed near the recent coast; in drill-hole 48. Here it attains - 78.5 m (in the text the depth of drill-holes is considered relative to the recent sea-level). Inclination angles of floors of paleogorges are featured by rather high indices. The distance between drill-holes 65 and 49 is 1250 m, difference in the depths between these two points of the paleogorge bottom is up to 40 m. Width of paleogeorges near the recent coast varied within 2.5-3.7 km. Alluvial sediments preserved fragmentarily are fixed on the bottom of paleogorges, they are unconformably bedded on Paleogene and Neogene sediments.

During the regressive phase relief and deposits of the drained shelf part underwent significant change conditioned mainly by hydrogene (wave) and subaerial processes.

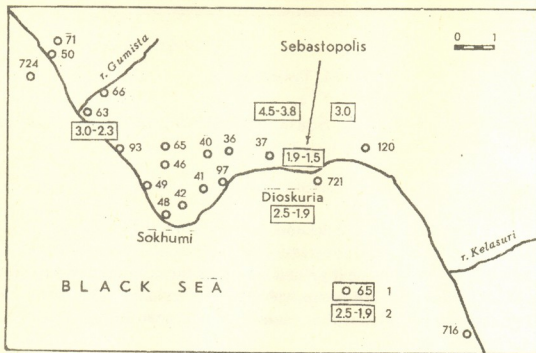


Fig. 1. Drill-hole number, 2. archeological monument and its age (thousand years).

Balance of the material delivered by rivers into the coastal line are of great importance in transformation of the shelf relief.

Simultaneous to the lowering of the sea level in lower zones of the nival belt took place intense erosion of river gorges.

This process gave rise to the delivery of considerable amount of terrigene, coarse grained material into the paleoshelf area where their natural selection by waves took place aeuloritic-pelitic fractions were taken to the continental slope and farther.

Age of marine fauna shells obtained on the shelf from drill-hole 724 within the interval of -46.6-47.1 m is (C^{14})-10895 \pm 100 year (ТБ<-370) and within the interval of -41.2-41.6 m in drill-hole 721 the coarse-grained alluvial deposits of continental genesis are substituted by a peat layer of 9310 \pm 80 year age (ТБ-346). If we take into account the character of sediments (sandy clays), where remains of dated fossil fauna occur, and turf-forming conditions at the Black Seaside, then we can assume that in the mentioned time span (10895-9310 years) the sea level varied within -35-42 m. This point of view is evidenced with the alluvial coarse grained sediments from drill-hole 716 at -24.5 m and deeper.

From the above it follows that around the opening of the Holocene (10 000 years ago) the Black Sea level appeared to be about -38-42 m, i.e. after the glaciacion was over the sea level increased on 60 m. Average rate of the sea level rise was 0.9 cm per year. High rate of the Black Sea transgression before the beginning of the Holocene caused intensification of hydrodynamic processes. On one hand it was due to significant extension of the sea aquatoria. From sedimentological structures of drill-holes existing on the shelf and in the Sokhumi area and from absolute ages of different horizons (levels) it's obvious, that high rate of the sea transgression was accompanied by dislocation of coastal line towards the depth of the land (eastwards). It was due to scanty (comparative to the transgression rates), volumes of alluvium delivered into the coastal line by rivers. Otherwise, alongside with the sea level rise, elevation of topographic surface of the seaside would have taken

place and the sea couldn't cut deep into the land.

Due to the mentioned process since the beginning of the Black Sea transgression the coast-line had intensely moved to the east. Before the beginning of the Holocene the sea envaded almost all the territory of the Sokhumi peninsula (drillholes 63, 49, 48, 42, 41, 97, 37, 120, 36, 40, 46).

In the beginning of the Holocene high rate of the sea transgression was still preserved, that's why the area covered by the sea had extended. In drill-holes 50.65 and 66 marine sedimentation is also vivid. From the lowermost Holocene and to the Upper Holocene inclusive it was going on uninterruptedly in drill-holes 50, 63, 49, 48, 42, 41, 97, 37, 120, 36, 40, 46, 65 and 66.

High rates of marine transgression before the Holocene and at the very beginning of Holocene significantly reduced further (average 0.2 cm per year) and it was of pulsate character (low range transgressive and regressive phases of against the general background of the Holocene transgression). This process is vividly reflected in the coastal zone in drill-hole 93. Here in vertical section of the Holocene sediments resting unconformably on the Neogene ones is well established alternation of marine and continental facies that correspond to transgressive and regressive phases of the sea.

Due to lowering of transgression rate at the end of the Lower Holocene started the process of development of the Sokhumi peninsula. Age of turfs overlying the lower Holocene marine sediments in drill-hole 36 is 6425 ± 60 y (ТБ<-352). In drill-holes 41, 37, 120 and 40 since that time continuous continental sedimentation took place. But in drill-holes 50, 63, 49, 42, 97, 36, 46, 65 and 66 again occured already mentioned marine sedimentation, which was substituted by continental sedimentation only at the end of the Upper Holocene.

From the above it follows that in Late Pleistocene and Holocene morphology of the coastline sharply differed from the recent one. Dynamics of the coastline was different as well. Alluvial material delivered by rivers was almost completely carried out of the limits of the territory under study due to dynamic processes, which occured in the coast-line i.e. the greatest part of the alluvium didn't participate in the coast-line forming processes it moved through paleogorges (canyons of erosive genesis) towards the deep part of the sea taking part in shelf-forming processes.

Volumes of river alluvions in the second half of Holocene not only compensated the low rate of the transgression, but from that period also began advancing (westwards) of the land and forming of peninsula. Due to abundant terrigene material shelf gained its balance, and all the terrigene material was spent on the formation of the rear of shelf and the coast-line. Gradually changed the morphology of the coast-line as well which was conditioned by the coast dynamics mainly and volumes of alluvions. Gumista and Kelasuri river alluvions were directed along the coast opposite to each other and this abundant beach-forming material was used on formation of Sokhumi peninsula.

Alongside with the drill-hole data on evolution processes of Sokhumi peninsula a very interesting additional information was obtained from the existing results of researches of archeological monuments. Deep into Sokhumi peninsula, between drill-holes 37 and 120 (Fig. 1) age of archeological monuments is correspondingly 4.5-3.0 and 3.0-2.3 thousand years, and near the drill-hole 93 the town of Sebastopolis existed 1.9-1.5 thousand



years ago. As for t. Dioskuria it was functioning 2.5-1.9 thousand years ago. In the coastline of that period its fragments are preserved at 5-6 m from the sea level. The town had been built during the Phanagorian regressive phase and after the Nimphean transgressive phase [2] it was covered by the sea. The last transgressive phase (Nimphean) gave rise to forming of Sokhumi peninsula in a final form. According to absolute ages of marine fauna and turf present at different levels of one and the same drill-holes existing on the shelf, rate of sedimentation varies for different centuries of Holocene. Rate of sedimentation within the 10895-3335 years interval is 5.1 mm per year. Maximal sedimentation is observed within the 7495-7040 years interval and is 11 mm per year. Since the end of the Lower Holocene rate of marine sedimentation considerably lowered and for the last 6540 years up to now it doesn't exceed 1 mm per year.

A. Janelidze Geological Institute
Georgian Academy of Sciences

REFERENCES

1. A. I. Ionin, V. S. Medvedev, Y. A. Pavlidis. Problems of Quaternary History of Shelf. M., 1982 (Russian).
2. M. V. Tvalchrelidze. Bul. Georg. Acad. Sci., **153**, 1, 1996, 57-60.

Sh. Keleptrishvili

Stratigraphical Significance of the Early Cretaceous Belemnitida of Georgia

Presented by Academician I. Gamkrelidze, July 7, 1997

ABSTRACT. The Lower Cretaceous sediments of Georgia are well characterized by belemnites. The scheme of division of inclusive sediments is given on the basis of the development stages of these organisms.

Key words: BELEMNITE, EARLY CRETACEOUS.

The belemnites play an important role in the complex of Early Cretaceous fauna of Georgia [1-15]. However, they are distributed unevenly in the sections. Barremian-Albian sections are characterized more completely. The belemnites are not found in Berriasian sediments.

The belemnites are extremely rare in Valanginian deposits. Only single findings are discovered here: *Curtohibolites orbignyus* (Duval-Jouve), *Conobelus conicus* (Blainville), *C. extingtorius* (Raspail), *Duvalia lata lata* (Blainville), *Pseudobelus bipartitus* (Blainville), *Hibolites prodromus* Schwetzoff. These forms are well known within the Mediterranean region and they are characterized by a rather wide range of the stratigraphical extension - from Berriasian up to Hauterivian. However, a part of species particularly: *Pseudobelus bipartitus*, *Conobelus conicus*, *C. extingtorius* occur in Georgia only in the Valanginian.

Hauterivian sediments are also poor in belemnites, particularly their lower substage. Some authors indicate to *Curtohibolites orbignyus* (Duval-Jouve), *Hibolites prodromus* Schwetzoff, *Duvalia binervia* (Raspail), *Pseudoduvalia polygonalis* (Blainville) from this level. Due to wide vertical extension of the above-mentioned species, this complex unfortunately does not allow to identify the Early Hauterivian age of the inclusive layers. The sediments of Upper Hauterivian are rich by rostrums of belemnites, which with the rare exception are connected with the upper zone of the upper Hauterivian - *Pseudothurmannia mortilleti*. The belemnites: *Hibolites longior* Schwetzoff, *H. inae* Eristavi, *H. jaculoides* Swinnerton, *Duvalia binervia* (Raspail), *D. lata lata* (Blainville), *Oxityeuthis jasikkovi* (Lahusen) are found in the upper zone of Upper Hauterivian in the sections of Georgia.

Barremian sediments are better characterized by belemnites, than Hauterivian one. The representatives of genus: *Mesohibolites* Stolley appeared for the first time in the lower Barremian. Early Barremian complex of belemnites are presented by the following species: *Mesohibolites gagricus* (Schwetzoff), *M. abchasiensis* Krimholz, *M. trastikensis* Stoyanova-Vergilova, *M. garshini* Stoyanova-Vergilova, *Hibolites subfusiformis* (Raspail), *H. jaculoides* Swinnerton, *H. pistilliformis* (Blainville), *Pseudoduvalia gagrica* (Schwetzoff), *P. pontica* (Schwetzoff). The rich complex of following belemnites occurs in upper Barremian: *Mesohibolites gladiiformis* (Uhlig), *M. varians* (Schwetzoff), *M. platyurus* (Duval-Jouve), *M. uhligi uhligi* (Schwetzoff), *M. uhligi georgicus* Nazarishvili,



Stratigraphical subdivision of Lower Cretaceous sediments of Georgia by belemnites

Stage	Substage	Zones and Layers (Kotetishvili, 1985), (Kakabadze, 1987)	Index belemnites
Albian	Upper	Stoliczkaia dispar, Mortonicea rostratum	Parahibolites pseudoduvalia
		L.w. Aucellina gryphaeoides	
		Hysterocheras orbigny, Mortonicea inflatum	
		L.w. Actinoceramus sulcatus	
	Middle	Oxytropidoceras roissyanum	Neohibolites minimum
		Hoplites dentatus	
Lower	Douvilleiceras mammilatum	Neohibolites minor	
	Leymeriella tardefurcata		
Aptian	Upper	Hypracanthoplites jacobi	Neohibolites wollemanni
		Acanthoplites nolani	Mesohibolites brevis
		Colombiceras tobleri	Mesohibolites moderatus
	Middle	Epicheloniceras subnodocostatum	Neohibolites aptiensis
		Dufrenoya furcata	Neohibolites clava clava
		Deshayesites deshayesi	
Lower	Deshayesites weissi, Procheloniceras albrechtiaustriac	Hibolites bzibiensis, Neohibolites ewaldi	
Barremian	Upper	Horizon Pseudocrioceras waagenoides	Mesohibolites longus longus
		Colchidites securiformis	
		Imerites giraudi	
		Hemihoplites feaudianus	
		Heinzia matura	
	Ancyloceras vandeheckii		
	Lower	Holcodiscus caillaudianus	Mezohibolites gagricus, Mesohibolites trastikensis
		Pulchellia compressissima	
Spitidiscus hugii			
Hauterivian	Upper	Pseudothurmania mortilleti	Hibolites jaculoides, Hibolites longior
		Speetonicerias subinversum	-----
	Lower	Crioceratites nolani	-----
		Lyticoceras ambligionium	-----
Valanginian	Upper	Neocomites noemiensis	Pseudobelus bipartitus
	Lower	Thurmanniceras thurmanni	
Barriasian	U.	Negreliceras negreli	-----
	M.	Berriasella subrichteri	-----
	L.		

Note: Division of Lower Barremian is given by I. Kvantaliani and L. Sakhelashvili (8) and the Upper Barremian - by M. Kakabadze and E. Kotetishvili (6).

M. longus longus (Schwetzoff), *M. longus bulgaricus* Stoyanova-Vergilova, *M. minaret* (Raspail), *M. fallauxi* (Uhlig), *M. beskidensis* (Uhlig), *Hibolites subfusiformis* (Raspail), *H. jaculum* (Phillips), *H. inae* Eristavi, *Mucrohibolites schaoriensis* (Hetchinashvili), *Duvalia grasiana* (Duval-Jouve).

Aptian sediments are in abundance presented by belemnites, though many species: *Mesohibolites beskidensis*, *M. fallauxi*, *M. minaret*, *M. uhligi uhligi*, *M. uhligi georgicus*, *Duvalia grasiana* and others, wide spread in Upper Barremian, are also extended in lower Aptian. This circumstances make it difficult to draw a distinct boundary between Barremian and Aptian stages by belemnites. At the beginning of Aptian stages *Neohibolites* and *Parahibolites* were found. The following complex of belemnites occurs in lower Aptian of Georgia: *Mesohibolites beskidensis* (Uhlig), *M. fallauxi* (Uhlig), *M. minaret* (Raspail), *M. minareticus* Krimholz, *M. kalamus* Stoyanova-Vergilova, *M. renngarteni renngarteni* Krimholz, *M. renngarteni caucasicus* Nazarishvili, *M. nalcikensis* Krimholz, *M. uhligi uhligi* (Schwetzoff), *M. uhligi georgicus* Nazarishvili, *Neohibolites ewaldi* (Strombeck), *N. clava clava* Stolley, *N. clava tudarica* Ali-zade, *N. clava colchica* Nazarishvili, *N. montanus* Ali-zade, *N. azerbaijanensis* Ali-zade, *Hibolites inguriensis* Rouchadze, *H. bzbiensis* Rouchadze, *H. horeshaensis* Rouchadze, *Duvalia grasiana* (Duval-Jouve). There is the following complex in the Middle Aptian: *Mesohibolites moderatus* (Schwetzoff), *M. ekimbontchevi* Stoyanova-Vergilova, *M. elegans* (Schwetzoff), *M. elegantoides* Stoyanova-Vergilova, *M. notus* Mishunina, *Mucrohibolites issiae* Nazarishvili, *Mucr. krimholzi* Nazarishvili, *Neohibolites aptiensis* (Killian), *N. inflexus inflexus* Stolley, *N. inflexus angelanica* Ali-zade and these species: *Mesohibolites brevis* (Schwetzoff), *Mucrohibolites krimholzi* Nazarishvili, *Neohibolites wollemanni* Stolley, *N. strombecki* (Müller), *N. kabanovi* Nazarishvili, *N. subminor* Stolley are in the Upper Aptian.

It is comparatively easy to define the boundary between Aptian and Albian sections, because the complex found in Albian is very different from Aptian one. Almost no species of Aptian stage passes to Albian. The Lower Albian is presented by the following complex of belemnites: *Neohibolites minor* Stolley, *N. andrussovi* Natzkiy, *N. lickovi* Natzkiy, *N. schvetzovi* Natzkiy, *N. alboaptiensis* Natzkiy, *N. bajaranasi* Natzkiy. The Middle Albian is characterized by this complex: *Neohibolites minimus* (Lister), *N. pinguis* Stolley, *N. attenuatus* (Sowerby), *N. spiniformis* Krimholz, *N. stylioides* Renngarten and the Upper Albian is presented by the following complex of belemnites: *Neohibolites subtilis* Krimholz, *N. stylioides* Renngarten, *N. ultimus* (d'Orbigny), *Parahibolites pseudoduvalia* (Sinzow).

Summarizing all the aforementioned facts based on a detailed study of lower Cretaceous sections in Georgia, gathering paleontological material and also rich literature sources [1-15], allow us to specify the stratigraphical meaning of the single genus and species of belemnites and to offer a new scheme of biostratigraphical division of lower Cretaceous sediments by belemnites (Table 1).

Georgian Technical University

REFERENCES

1. *M. Eristavi, I Hetchinashvili*. Bull. Acad. Sci. Georgian SSR, XII, 8, 1951, 487-492 (Georgian).
2. *M. Eristavi*. Geol. Inst. Acad. Sci. Georgian SSR, monogr. n. 6, Tbilisi, 1955, 224 (Russian).



3. *M. Eristavi*. Lower Cretaceous of the Caucasus and Crimea. Monografii, 10, 1960, 148 (Russian).
4. *I. Hetchinashvili*. Bull. of State Mus. of Georgia, Tbilisi, v. XV-A, 1952, 63-118 (Georgian).
5. *M. Kakabadze*. 3rd Inter. Cretaceous Symposium, Tubingen, 1987, 551-560.
6. *M. Kakabadze, E. Kotetishvili*. Mem. Descr. Carta Geol. d'Itali, 1995, 103-108.
7. *I. Kvantaliani, T. Nazarishvili*. Trudy Geol. inst. Acad. Nauk Gruzii, nov. Ser., 47, 1975, 132-153 (Russian).
8. *I. Kvantaliani, L. Sakhelashvili*. Geologica Carpatica, 47, 5, 1996, 285-288.
9. *E. Kotetishvili*. Trudy Geol. Inst. Acad. Nauk Gruzii, nov. ser., 25, 1970, 116 (Russian).
10. *E. Kotetishvili*. Trudy Geol. Inst. Acad. Nauk Gruzii, nov. ser., 91, 1986, 160 (Russian).
11. *G. Krimholz*. Monograph. Paleontol. USSR, t. 67, Moscow, 1939, 54 (Russian).
12. *T. Nazarishvili*. Trudy Geol. Inst. Acad. Nauk Gruzii, nov. ser., 40, 1973, 120 (Russian).
13. *I. Rouchadze*. Bull. du Musee de Georgie, Tbilisi, VI, 1930, 125-138.
14. *I. Rouchadze*. Bull. Geol. Inst. of Georgia, 3, 2, 1938, 129-138 (Georgian).
15. *M. Schwetsoff*. Annuaire geol. miner. de la Russie, M., t. XV, pl. II-V, 1913, 43-74.

T.Javakhishvili

Transfer Function of a Single Way Pendulum Rope Way Mechanical System

Presented by Corr. Member of the Academy K.Betaneli, October 30, 1997

ABSTRACT. Longitudinal oscillations of rope way draught rope are considered on the basis of wave equations. Lumped masses on it are examined using δ function. Transfer functions of the system are proposed for the case when perturbation acts upon the driving pulley or the car.

Key words: DRAUGHT ROPE, OBJECT WITH DISTRIBUTED PARAMETERS, LONGITUDINAL OSCILLATIONS.

Mechanical system of rope way contains ropes of great length, their effect on system dynamics exceeds the effect of other elastic ties [1-3]. The study of oscillations arising in dynamic conditions is of versatile interest; one of them is the problem of automatic control system design when its structure and parameters should be chosen with consideration of draught rope elastic deformation and mechanical oscillations. On the stage of design it is necessary to use comparatively simple methods of satisfactory accuracy which do not need complex computer calculations and enable to estimate the effect of different parameters on system dynamics.

As it is known, the boundary problem of longitudinal oscillations of ring structure visco-elastic rope, when m_i masses lumped in separate l_i points of rope are considered using δ function, is expressed as:

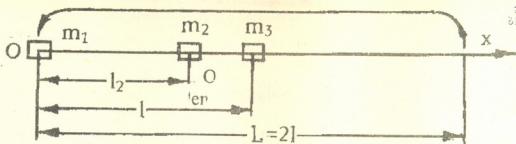
$$q(x) \frac{\partial^2 u}{\partial t^2} - EF \left(1 + \mu \frac{\partial}{\partial t} \right) \frac{\partial^2 u}{\partial x^2} = f(x, t);$$

$$u(x, 0) = u_0(x); \quad u(0, t) = u(L, t);$$

$$\frac{\partial u(x, 0)}{\partial t} = u_1(x); \quad \frac{\partial u(0, t)}{\partial x} = \frac{\partial u(L, t)}{\partial x}; \quad (1)$$

$$q(x) = q + \sum_{i=1}^n m_i \delta(x - l_i),$$

where $u(x, t)$ is rope point motion for x coordinate in time moment t ; $u_0(x)$, $u_1(x)$ are the displacement of rope section x and the displacement velocity in $t=0$ moment; μ is viscosity parameter; $E=const$ is sagged rope elasticity module; F is rope cross-section area; $q=const$ is linear density of rope; $f(x, t)$ is external action; $l=0, 5L$ is length of span and n is the quantity of masses.



If we assume that oscillation dumping is mainly realized with electric part of automated drive, in case of application of functional transformation method the standardized transfer function of the system is determined [4] as:

$$\tilde{W}(x, \xi, \tilde{p}) = \Phi(x - \xi, \tilde{p}) - \tilde{p}^2 \sum_{i=1}^n \eta_i \tilde{W}(l_i, \xi, \tilde{p}) \Phi(x - l_i, \tilde{p}), \quad (2)$$

$\tilde{p} = pa^{-1}$; $\tilde{W} = a^2 W$ standardization conditions;

$$\eta_i = \frac{m_i}{q} \quad \Phi(z, \tilde{p}) = \frac{ch \left[\tilde{p} \left(\frac{L}{2} - |z| \right) \right]}{2 \tilde{p} sh \frac{\tilde{p} L}{2}}, \quad -L \leq z \leq L,$$

$a = \sqrt{\frac{EF}{q}}$ is longitudinal wave propagation velocity in rope; $x = \xi$ is coordinate of perturbation action area.

Let's make the following assumptions: the carrier rope, draught rope tightening load and draught rope transverse oscillations do not affect the considered process; the car has one degree of freedom.

Let's consider one way rope (Fig.) when three masses m_1 , m_2 and m_3 are located on the draught rope; electromagnetic moment of the drive is applied on mass m_1 . Thus, $l_1 = 0$, $l_3 = l$, $\xi = 0$.

From (2) we derive the following system of equations for calculation of $\tilde{W}(l_i, 0, \tilde{p})$ values

$$\begin{aligned} a_{11} \tilde{W}(0, 0, \tilde{p}) + a_{12} \tilde{W}(l_2, 0, \tilde{p}) + a_{13} \tilde{W}(l, 0, \tilde{p}) &= \Phi(0, \tilde{p}); \\ a_{21} \tilde{W}(0, 0, \tilde{p}) + a_{22} \tilde{W}(l_2, 0, \tilde{p}) + a_{23} \tilde{W}(l, 0, \tilde{p}) &= \Phi(l_2, \tilde{p}); \\ a_{31} \tilde{W}(0, 0, \tilde{p}) + a_{32} \tilde{W}(l_2, 0, \tilde{p}) + a_{33} \tilde{W}(l, 0, \tilde{p}) &= \Phi(l, \tilde{p}); \end{aligned} \quad (3)$$

where $a_{ii} = 1 + \tilde{p}^2 \eta_i \Phi(0, \tilde{p})$; $a_{ij} = \tilde{p}^2 \eta_j \Phi(l_i - l_j, \tilde{p})$;

After solution of (3), if we take into account the standardization conditions, then make restandardization $\bar{p} = pL(2a)^{-1}$, $\mu_i = \eta_i L^{-1}$ and go to transfer functions expressed according to velocity, we shall have

$$\bar{W}(0, 0, \bar{p}) = k[\text{sh}^2 \bar{p} \text{ch} \bar{p} + \bar{p}(\mu_2 \bar{A} + \mu_3 \bar{B}) \text{sh} \bar{p} + \mu_2 \mu_3 \bar{p}^2 \bar{E}] \bar{D}^{-1}(\bar{p});$$

$$\bar{W}(l_2, 0, \bar{p}) = k \text{sh}^2 \bar{p} (\text{ch} \lambda \bar{p} + \mu_3 \bar{p} \text{sh} \lambda \bar{p}) \bar{D}^{-1}(\bar{p});$$

$$\bar{W}(l, 0, \bar{p}) = k \text{sh} \bar{p} \{ \text{sh} \bar{p} + \mu_2 \bar{p} \text{sh} \lambda \bar{p} \text{sh}(1 - \lambda) \bar{p} \} \bar{D}^{-1}(\bar{p}),$$

where $\lambda = 1 - 2l_2 L^{-1}$;

$$\bar{D}(\bar{p}) = \text{sh}^3 \bar{p} + (\mu_1 + \mu_2 + \mu_3) \bar{p} \text{sh}^2 \bar{p} \text{ch} \bar{p} + \bar{p}^2 (\mu_1 \mu_2 \bar{A} + \mu_1 \mu_3 \bar{B} + \mu_2 \mu_3 \bar{C}) \text{sh} \bar{p} + \mu_1 \mu_2 \mu_3 \bar{p}^3 \bar{E};$$

$$\bar{A} = \text{ch}^2 \bar{p} - \text{ch}^2 \lambda \bar{p}; \quad \bar{B} = \text{sh}^2 \bar{p}; \quad \bar{C} = \text{ch}^2 \bar{p} - \text{ch}^2(1 - \lambda) \bar{p};$$

$$\bar{E} = \text{ch} \bar{p} [\text{sh}^2 \bar{p} - \text{ch}^2 \lambda \bar{p} - \text{ch}^2(1 - \lambda) \bar{p} + 2 \text{ch} \lambda \bar{p} \text{ch}(1 - \lambda) \bar{p}];$$

$k = (2a)^{-1}$ is a constant coefficient.

Practically the case when perturbation acts on mass m_2 is also interesting. In this case, analogous to the above considered we obtain:

$$\bar{W}(0, l_2, \bar{p}) = k \text{sh} \bar{p} \{ \text{sh} \bar{p} \text{ch} \lambda \bar{p} + \mu_3 \bar{p} [\text{ch} \bar{p} \text{ch} \lambda \bar{p} - \text{ch}(1 - \lambda) \bar{p}] \} \bar{D}^{-1}(\bar{p});$$

$$\bar{W}(l_2, l_2, \bar{p}) = k [\text{sh}^2 \bar{p} \text{ch} \bar{p} + \bar{p} (\mu_1 \bar{A} + \mu_3 \bar{C}) \text{sh} \bar{p} + \mu_1 \mu_3 \bar{p}^2 \bar{E}] \bar{D}^{-1}(\bar{p}); \quad (5)$$

$$\bar{W}(l, l_2, \bar{p}) = k \text{sh} \bar{p} \{ \text{sh} \bar{p} \text{ch}(1 - \lambda) \bar{p} + \mu_1 \bar{p} [\text{ch} \bar{p} \text{ch}(1 - \lambda) \bar{p} - \text{ch} \lambda \bar{p}] \} \bar{D}^{-1}(\bar{p});$$

Transmission functions (4) and (5) enable to research the effect of the parameters of the object with distributed parameters on natural oscillation frequency spectrum. The effect of a and L parameters is derived from expression $\bar{\omega} = \omega L (2a)^{-1}$, while that of λ and μ_i parameters is determined on the basis of characteristic equation.

In particular case, when $\lambda = 0; 1$, (4) and (5) are considerably simplified and make possible to investigate the process of starting and braking of rope way and two way rope way as well, if we'll do the corresponding redistribution of masses and assume those masses m_1 and m_3 and the nearby cars have the same velocities.

On the stage of analysis and synthesis of the control system of rope way electronic drive, on approximation by finite dimension model, transfer function of the element with distributed parameters, a good result is obtained when hyperbolic functions are expressed through chain fractions and transfer function is expended into elemental fractions.

Georgian Technical University

REFERENCES

1. D. Pataraiia. Calculations and design of rope systems on example of aerial ways. Tbilisi, 1991, 102. (Russian).
2. T. Richter. Schwingungsverhalten von Einseilumlaufbahnen beim Anfahren und Bremsen. Zurich, ETH, 1989, 156.
3. O. Zweifel. Schwingungerscheinungen bei Seilbahnen Inbesondere Reibschwingungen an Stutzen. Zurich, 1971, 89.
4. N. Kiselev, V. Myadzel, L. Rassudov. Electric drives with distributed parameters. Leningrad, 1985, 220. (Russian).

M. Shalamberidze

Self-regulation Coefficient of Welding Current

Presented by Academician R. Adamia, December 31, 1997

ABSTRACT. The effect of a machine impedance and a welding zone resistance on the spot welding joint strength is considered. Self-regulation coefficient of welding current is introduced.

Key words: SELF-REGULATION COEFFICIENT, WELDING CURRENT.

The current self-regulation process for spot welding joint is well studied in literature [1,2]. It is regarded as helping factor for levelling of welded surfaces while washing and covering it with liquid steel layer. As to the contact spot welding the change of welding current correspondingly to the change of contact impedance is meant under self-regulation.

Experimentally it is proved that complete impedance of machine contact welding influences on welding active power. By increasing of active impedance the active power increases and it reaches its maximum in case of active and reactive impedances equilibrium. During such ratio of active and complete impedances the process of welding joint melting is stable. It is noted that the stability of the process is conditioned by optimal conditions of current [1].

The following experiment reveals the influence of reactive impedance of spot welding machine on welding strength. By putting the inductive rings in the contour of spot welding machine of MT-1214 type we change the reactive impedance of machine, which influences both the size of welding current and its strength (Fig. 1, curve 1). Then while putting the inductive ring into the contour the unchangeable value of welding current was reached by regulation of welding transformer, primary resistance. In spite of constant current by increase of circuit number welding strength was changed (Fig. 1, curve 2).

On the basis of critical analysis of joint welding and current self-regulation processes, and above mentioned experimental research, the hypothesis was formed that while contact spot welding before the formation of liquid nuclei and joint welding the self-regulation process of current occur according to one and the same scheme, which is as follows: in welding zone before current conductivity, under the action of compressive force welded surfaces come into contact by microreliefs; during current conductivity they melt; under the action of compressive force they approximate to each other; new pairs of microreliefs come into contact, then they also

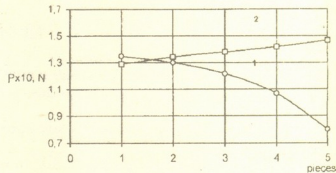


Fig. 1. Effect of inductive impedance on strength: 1) welding current is changing; 2) welding current is constant.

Academician Ts. Mirtskhoulava

On the Assessment of Erosion Processes Effect on the Social Tension in the Society

Presented October 2, 1997

ABSTRACT. The possibilities and perspectives of use of the modern theory of reliability for assessment of a quality of the environment condition, ecosystems, including erosion processes are described. Some aspects of the assessment of erosion processes effect on the social tension in the society are presented.

Key words: EROSION, SOCIETY, ENVIRONMENTAL THEORY OF RELIABILITY.

Soil protection from erosion takes the first place among the most acute problems of today. On a national scale it is not less important than the power problems. Considering the global scales and importance of the negative after-effects of soil erosion and comparing the damages related to this "gentle crisis" with the losses caused by reservoirs crude reclamation and power structures being the point at issue the lasts seem to be lesser of two evils. Unfortunately a damage caused by the erosion does not decrease and in a lot of regions even increases. This fact is related to the necessity to maintain and quite often to intensify a farm produce. This need, especially in market conditions, forces farmers to risk and to involve more and more erosionally dangerous lands into crop rotation.

Observation and analysis of negative after-effects of erosion show, that this disease of soil is accompanied by such grave results as: fail in productivity, decrease of reliability of farm produce, worsening of conditions in soil cultivating and operating, deterioration of safety of agricultural mechanisms, destruction of vegetational cover, silting and pollution of rivers and reservoirs, breakdown of territories by the thick net of gullies.

Migration of people from villages to town is related to the soil erosion and drop in fertility. It is established that the intensity of this migration directly depends on intensification of soil wash-out.

These negative after-effects of erosion lead to overall increase of social-psychological tension in the regions subjected to erosion processes. So far change (worsening) of social conditions of people is not taken into account sufficiently well in assessing of damages caused by the erosion. It is obvious that these problems need to be considered more seriously.

The aim of this paper is to substantiate a necessity of account of damages caused by erosion processes to the social sphere, to work out some methodical approach for assessment of influence of erosion processes on a change of social condition of society and to use the results obtained for solution some typical problems arising in designing soil protection measures.

Specific character of the problem stated is that its solution calls for combination of the modern possibilities of the erosion science with the reliability theory of ecological systems. Meanwhile the level of development of the erosion science and close fields of sciences makes it possible to come to proper mathematical description within which some concrete additions can be formed.

The most important stage in solution of the problem stated is formation of analytical expression for assessment of danger of social conditions worsening through other parametres, to find a criterion of quantitative analysis of observation data.

As the problem under investigation has a lot of criteria, when properties of system are characterized by many indices assessed by various units of measurement quite often differing from each other with their importance and contradictions, then a choice of complex criterion or index expressing the properties of system to a greater degree and having certain physical sense seems to be the most important. The best among them is to assess a degree of risk danger.

At the same time in order to choose measures aimed at a decrease of soil losses and economical, ecological and social changes related to them first of all it is necessary to work out methodology to compare versions of soil protection measures. One of the most serious problems we have while comparing is to find some comparable indicators, the sense of which in different versions of measures isn't the same.

Analysis of different indices which can be used in solution of the problem shows, that many of them have a little information in comparison with the assessment of this condition by the method of risk of danger. Assessment of risk means scientific analysis of its genesis, including exposure, determination of sources and factors of risk zones of their potential effects, definition of danger degree in some concrete situation [1]. "Risk" often means "probability of human and material losses or failures". Risk, sometimes may not be concreted with the human and material losses of failures, then the following expression is used for risk assessment:

$$\text{risk} \left[\frac{\text{after - effects}}{\text{time}} \right] = \left[\frac{\text{frequency event}}{\text{time limit}} \right] \times \text{value} \left[\frac{\text{after - effects}}{\text{event}} \right]$$

It is obvious, that assessment, analysis of risk will allow to find a way of minimization of risk at the prescribed limitations, to work out algorithm of priorities of activity for reasonable, safe technologies in soil developing and at the same time to get a minimal danger for people.

It follows from the above mentioned that it is very important to take into account disturbances of social stability caused by the erosion processes in the region under consideration in choice of version of soil protection measures. It should be noted, that contribution of this process to a worsening of social conditions is important enough to be disregarded.

In these conditions in order to determine a methodology of assessment of social risk it is very important to use possibilities and techniques of general theory of reliability and theory of reliability and safety of ecological system worked out by the author [2-6].

Risk and "reliability" - recently more often used for assessment of operating conditions of systems and different objects (considered as a failure free operation) are intercon-

nected with the function relation [4]

$$R(t) = 1 - P(t), \quad (1)$$

$R(t)$ - a function being an addition of reliability $P(t)$ to an unit is accepted as a function of risk. It is reasonable to use the function (1) for description of any dangers for people, material and moral damages including dangers caused by the soil erosion. The expression (1) allows to measure a risk qualitatively and thereby makes it possible to assess its perception by people.

The disturbance of social conditions as a rule does not occur by a simple scheme, but as a result of a combined effect of unfavourable factors of risk. Then a total value of dangers of after-effects of erosion processes can be simply assessed by a definition of a general risk stipulated by various processes of the soil erosion. In general an expression to assess a total risk under influence of different factors is presented as follows:

$$P[D_\eta] = \sum P[D_\eta / S_\beta] \cdot P[S_\beta], \quad (2)$$

where $P[D_\eta]$ is a probability of occurrence D_η ; D_η is an occurrence showing that a system is in η -condition; S_β means, that observed erosion effect (intensity of soil wash-out) characterized by the level β , $P[D_\eta / S_\beta]$ shows a probability that system's state will be D_η on condition of erosion effect S_β . Intensity of erosion, depth of soil wash-out and other characteristics of erosion can be expressed through S_β .

Let's remind, that conditional probability $P[D_\eta / S_\beta]$ is a probability of appearance of occurrence D_η on condition, that occurrence S_β has already occurred. This probability is determined as $P[D_\eta / S_\beta]$ - a relative part of causes leading to the occurrences D_η , among a group of factors leading to occurrence S_β .

Solution of the concrete problems requires to calculate a number of all the observations in which the accounted characteristics proved to be above tolerable limits, i.e. are dangerous $-n_D$. Then a probability of appearance of danger -risk P_D can be calculated by the following expression

$$P_D = \frac{n_D}{n_s} \quad (3)$$

Knowing a probability of appearance of danger $P_{(D)}$ a risk related to a danger D can be determined. A danger D is stipulated by exceeding of values of erosion intensity I_0 under consideration of a threshold of tolerable intensive erosion (normative threshold) I_p .

$$P(I_0 > I_p) = P(I_0 > I_p / D \cdot P_D), \quad (4)$$

where $P(I_0 > I_p)$ is a conditional probability of appearance of danger related to exceeding.

Probability $P(I_0 > I_p)$ may be determined with the help of known incontinuous distributions made with the use of observation data and tolerable limit of disturbance (change). These necessary data can be obtained on the basis of observations at the analogous objects where antierosion soil protection have been used.

Using expression (1) and (4) to assess a level of danger under the influence for example of two factors, we have an expression for assessment of total risk [7]

$$P_{(1,2)} = 1 - [1 - P(I_{01} > I_{p1})] \cdot [1 - P(I_{02} > I_{p2})],$$

(5)

where I_{01} and I_{02} are tolerable values for 1 and 2 factors of risk respectively.

Monte-Carlo method and Butstrep-method can be used in case of insufficient amount of investigations. When it is impossible to determine a total risk for lack of quantitative data of parameters of probabilities, presented in equation (5) then a risk may be assessed with the help of experimental estimation including the "Delphi" method with account of their characteristics [7,8].

The approach stated permits to choose the best way to minimize soil losses and disturbances of social stability. This methodology makes it possible to base a necessity of certain material expenditures which might be recompensed at the expence of decrease of social tension. The proposed methodological approach for determination the erosion process effects on the social condition of the society, unlike verbal and quantitative assessment, will allow to calculate indices of risk degree qualitatively at the various stages of soil development, taking into account the use of different soil-protection measures. In conclusion it should be noted, that this methodological approach of risk assessment can be used not only to assess effect of erosion processes on the social tension, but to assess negative effects, caused by any different processes, as there are no specific limitations in solving this problem.

Institute of Water Management and Engineering
Ecology
Georgian Academy of Sciences

REFERENCES

1. *Ts. Mirtskhoulava*. Ecologicheskije narusheniya, predskazanie riska narusheniya, mery po snizheniyu opasnosti. Tbilisi, 1993.
2. *V. Bolotin*. Statisticheskie metody v stroitelnoi mekhanike. M., 1965 (Russian).
3. *B. Gnedenko, Y. Belyaev, A. Solovyev*. Matematicheskie metody v teorii nadezhnosti. M., 1965 (Russian).
4. *K. Kapur, L. Lamberson*. Nadezhnost i proektirovanie sistem. M., 1980 (Russian).
5. *Ts. Mirtskhoulava*. Basic Physic and Mechanics of Channel Erosion. Tbilisi, 1989, 256.
6. *Ts. Mirtskhoulava*. Nadezhnost gidromeliorativnykh sooruzheneii. M., 1974 (Russian).
7. *Ts. Mirtskhoulava*. Reliability of Hydro-Reclamation Installations. A. A. Balkema/Rotterdam, 1987, 300.
8. *Ts. Mirtskhoulava*. Stochastic Estimation of Small Rivers' Ecological Stability Disturbances. 6th IAHR International Symposium on Stochastic Hydraulics. Taipei, Taiwan, China (Taipei). 1992, 15-23.



V.Nadirashvili

Estimation of Slope Reliability from the Point of View of Erosion Caused by Rain

Presented by Academician Ts.Mirtskhoulava, November 18, 1997

ABSTRACT. The method of estimation of slope stability in soil erosion is suggested with account of basic factors causing erosion and the danger of ravine formation on the slope.

Key words: EROSION, SOIL PROTECTION, RELIABILITY.

While developing theoretical models of erosion in most cases it is admitted that the velocity of the flow formed by rainfall is constant across the slope and the motion of the run-off across the slope is considered to be turbulent. However, experimental studies show that after filling all the hollows the rainfall forms a run-off which doesn't move uniformly. It consists of single streams and flows with different charges and velocities [1,2]. Quick cross-sections of the streams increase in the direction of motion. Their number on the slope is chaotic. Therefore in erosion forecasting equation the coefficient, which takes into account correction of difference between the accepted model and the natural one, should comprise all possible values of the factors defining the erosion and envisage their probability as well. General methodology of solution of hydraulic and erosion problems developed by Academician Ts.Mirtskhoulava [3], the determinate formulae of estimation of hydraulic parameters of slope run-off [1,4] and the theory of fall-out of the random functions permit to solve the problem [5].

If we assume that ground surface across the axis z (z is directed in parallel with the water separator according to the inclination of the x slope) is a slow variable, differentiable random function $f(z)$, which is approximated in the form of parabola in the area of its maximum and is subjected to the normal distributing law, then for high level fall-outs the maximum of the random function determines one positive fall-out and the distribution density of quick cross-sections of the streams formed on the slope by the rain can be written in the following way:

$$P(S) = \left(\frac{0.03}{S}\right)^{\frac{1}{3}} \left(\frac{\sqrt{i \cdot (\alpha^2 + \beta^2)}}{n_0 \sigma_0 I X}\right)^{0.5} \exp \left\{ \left(\frac{S}{3}\right)^{\frac{2}{3}} \left(\frac{\sqrt{i \cdot (\alpha^2 + \beta^2)}}{n_0 \sigma_0 I X}\right)^{0.5} \right\}, \quad (1)$$

where I is an average intensity of rainfalls (m/sec); n_0 is the coefficient of Manning; σ_0 is the coefficient of run-off; x the distance to the waterseparator (m); i the inclination of the ground surface; α , β are the parameters of correlation function

$R(b) = e^{-\omega b} \left(\cos \beta b + \frac{\alpha}{\beta} \sin \beta b \right)$ of ground surface irregularity.

Taking into account the above given dependence the probability of its unfailling work on the slope in the process of erosion can be written in the following way

$$P(S_0) = 1 - \exp \left\{ \left(\frac{S_0}{3} \right)^{\frac{2}{3}} \left(\frac{\sqrt{i \cdot (\alpha^2 + \beta^2)}}{n_0 \sigma_0 I X} \right)^{0.5} \right\}, \quad S_0 > 0, \quad (2)$$

where S_0 is such value of a quick cross-section of the stream on x distance, when only a permissible amount of ground surface is washed away.

Let's use the erosion forecasting formula [1] at t time interval to estimate this value

$$H = 0.0000064 \cdot \omega \cdot d \cdot \left(\frac{V_{\Delta X}^2}{V_{\Delta 0}^2} - 1 \right) \cdot t, \quad (3)$$

where H is the thickness of the soil wash-out; ω is an average value of the flow pulsation frequency (per sec); d is the size of the particle torn off the bottom (0.003-0.005m); t is the rain duration (sec); $V_{\Delta X}$ is the velocity of the flow on the bottom in x distance, which can be calculated by the formula $V_{\Delta X} = \Delta^{0.17} \sqrt{y \cdot i} / n_0$, m/sec; $V_{\Delta 0}$ is the limited velocity of the flow (nonerosive) on the bottom (m/sec); y is the depth of the flow, $y \approx \sqrt{S}$, (m); S is the quick cross-section of the flow (m^2). Taking into account equation (3) we get

$$S_0 = \left(\frac{V_{\Delta 0} \cdot n_0 \cdot \sqrt{BH_0 + 1}}{\Delta^{0.17} \sqrt{i}} \right)^4, \quad B = \frac{156250}{\omega \cdot d \cdot t}, \quad (4)$$

where $\Delta = 0.7d$ is the height of roughness of the flow bottom (m); H_0 is the permissible depth of erosion of the flow bottom (m).

If we introduce (4) into (2) we can estimate the probability that on the slope with certain parameters the rain of a given intensity won't cause erosion of the soil such that at any part of the slope it exceeds the permissible value H_0 , i.e. the slope reliability in the process of erosion

$$R_{H_0} = 1 - \exp \left(- \sqrt{\frac{V_{\Delta 0}^{5.4} \cdot (BH_0 + 1)^{2.7} \cdot n_0^{4.4} \cdot \sqrt{\alpha^2 + \beta^2}}{2.25 \cdot i^{0.8} \cdot d \cdot \sigma_0 \cdot I \cdot X}} \right). \quad (5)$$

Let's compare the values calculated by the formula (5) to the experimental data. Let's assume that the width of the slope $z = 10000/x$ m; the volume of the soil wash-out on the slope by one flow is $H^2 \cdot X/2$, (m^3); number of flows on the slope is $v_0 z$. Taking into account the volumetric mass of the ground γ (t/m^3) the permissible value of the erosion per

hectare can be calculated by the formula $q_0 = 5 \cdot 10^3 \gamma H_0^2 v_0$, (t/ha). An average permissible value of the erosion depth on the bottom of the flow $H_0 = 0.014 \sqrt{q_0 / \gamma v_0}$, (m).

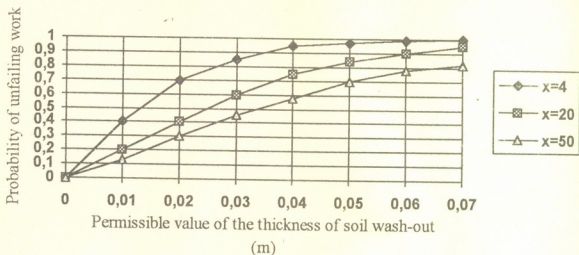


Fig. Probability of the unfailing work of the slope in the process of erosion caused by rain.

The diagram shows (Fig.) reliability of the cultivated slope calculated by equation (5) for the following parameters: the correlation function coefficients of ground roughness $\alpha=13.4$; $\beta=17.6$ per meter; rain intensity $I=1/60000$ m/sec; $n_0=0.12$; $\sigma_0=0.12$; $i=0.25$; $\nu=3.5$; $x=4$ m; $t=3600$ sec. According to the experimental data the value of the erosion on the slope with such parameters is $q=2.5$ t/ha [1,2], and as shown in the diagram the thickness of the soil wash-out varies from 0 to 7cm with appropriate probability.

It should be noted that an average index of slope erosion may not exceed the permissible value but at some parts of the slope the flow can form such deep gully which can't be smoothed by ordinary cultivation of the ground and ravine formation may begin. For example according to the given experimental data the ground is cultivated at 25 cm depth. If we add the depth of erosion to it, then at some parts of the slope the lowering of the mark of the ground surface will exceed 30 cm.

On the basis of the results obtained we can conclude that while developing the methods of experimental studying and forecasting the reliability of soil with respect to erosion it is reasonable to take into account an average index of solid run-off per hectare as well as the formation of flows after rain due to the unevenness of the slope, their number, gully formation and development, which is possible by the use of the formula (5).

Institute of Water Management and Engineering Ecology
Georgian Academy of Sciences

REFERENCES

1. Ts.E.Mirtskhoulava. Inzhenernye metody rascheta i prognoza vodnoi erozii. Moskva, 1970, 240..
2. M.S.Kuznetsov, G.P.Glazunov. Eroziya i okhrana pochv. Moskva, 1996, 330.
3. Ts.E.Mirtskhoulava. In: vopr. teorii i praktiki nadezhn. gidromel. sistem i sooruzhenii. Tbilisi, 1989, 112-129.
4. V.S.Nadirashvili. In: inzhenernye metody prognoza i borby s eroziiei pochv. Tbilisi, 1987, 85-89.
5. V.I.Tikhonov. Vybrosov sluchainykh protsessov. Moskva, 1970, 392.

Sh.Kunchulia

The Influence of Hydrometeorologic Factors on the Economy of Commercial Sea Passages

Presented by Academician G. Svanidze, May 5, 1998

ABSTRACT. Economic benefit of the sea passage greatly depends on hydrometeorological factors. Simplified expression to calculate the total of aero and hydrodynamic resistance of the ship in unfavourable weather is suggested. To evaluate the economy of the commercial passage of the ship the expression profitable for sea practice is offered.

Key words: COMMERCIAL PASSAGE, ECONOMY, HYDROMETEOROLOGY.

Oversea transportation charges depend on the economy of commercial passages (E) and the latter depends on the time duration (T) of the passage. Time (T) in its turn depends on several factors. Hydrometeorological factors (HMF) are one of the main factors, which influence on the rate and safety of the ship. Such hydrometeorological elements as wind, visibility, air temperature, precipitation and oceanographic elements as storm, current, water density, ice phenomena must be foreseen for successful commercial passage.

The speed (V_0) of the ship in still water depends on the rest (V) (the area of rest screw wing) of the propeller and on the total resistance of both water and air (ΣR). This dependence can be expressed by the equality:

$$V(V_0) = \Sigma R(V_0) \quad (1)$$

The aero and hydrodynamic stability of the ship depends on the ship's crossing area (S) with an angle formed under the influence of wind, current and storm against the direction of the ship. The area (S) is minimum when the wind, current and storm come along with the ship direction and it is maximum when they are against it. The aero and hydrodynamic resistance of the ship can be calculated by the following formula: [1]

$$R = C \frac{\rho V^2}{2} S, \quad (2)$$

where C is the coefficient of frontal resistance, ρ is the mass factor of air or water ($\text{kg} \cdot \text{sec}^2/\text{m}^4$) ($\rho = 102$ for water and 0.152 for air); V is the rate of wind or current (m/sec); S is the area crossed by the ship (m^2).

The speed of the ship is also kept behind by the orbital movement of water particles in the wave. The stronger the storm is the stronger the water particles orbital movement is. Taking into account this condition, the height of the inside water part of the commercial ship ($H \leq 10\text{m}$) and frontal resistance coefficient ($c = 0.4$) the formula (2) takes more simple and practical form



$$\Sigma R = 0.08V_w^2 S_1 + 33.6 \left(V_{current} + \frac{\pi h}{\tau} \right) S_2, \quad (3)$$

where ΣR is the total resistance of wind, current and storm (kg); S_1 and S_2 are the areas of crossing in the middle by the underwater and above-water parts of the ship (m) with wind and current along the course angle; V is an average rate of the current in the upper 10m layer of the sea (m/sec); h and τ are average height and period of the biggest waves.

Unfit hydrometeorological conditions are significantly holding the ship and sometimes the crew is to change the course, increase the distance (L) and cover it at small speed. In this case the shipping charges and probability of shipwreck increase greatly and the passage effectiveness decreases.

When TRACECA, the so-called "Silk Way" transportation corridor of the South Caucasus starts functioning within 200 miles of economic zone of Georgia and with the increase of oil transit the ignorance of HMF influence on safety and economy of the passages will cause the growth of loss. Therefore the individual and total influence of meteorological and oceanographic elements should be studied first of all and possible sea passages with minimum influence of HMF should be planned.

Thus the goal of the investigation can be formulated as follows: to define the influence of HMF on the effectiveness of economic passage and to create a mathematical formula which can be used in navigation practice.

The economy of commercial passage mainly depends on time duration T_p , therefore its correlation can be made according to the specific discharges in T_i time, which can be expressed in the following way [2]:

$$E = [(KL+S) - (K_h L + S_h)] P_h, \quad (4)$$

where P_h is the load capacity of the ship (T/mile) in the most profitable passage; K , K_h are specific investments (T/mile) in free and profitable passages respectively; S , S_h are the net cost of shipping in free and profitable passages (10T/mile); L is the investment coefficient which is about 0.12; K , S_h and P_h can be calculated by the formula:

$$K = \frac{CT}{T_E DV}; \quad S_h = S_x t + S_t m; \quad P_h = \frac{T_E DK_3}{T}, \quad (5)$$

where C is the shipbuilding costs; S_x , S are the ship and crew maintenance charges while sailing and mooring; T_E is the ship exploitation per day; D is the net shipping capacity (T); K_3 is loading area coefficient; T , t , t_m is the time while sailing and mooring during economic passage ($T = t + t_m$).

After a certain change and simplification with account of navigation practice the economy of the passage can be calculated by the following formula:

$$E = \frac{(0.12C + T_E S_x) \Delta T}{T}, \quad (6)$$

where ΔT is the time difference (T) while being in bad hydrometeorologic conditions and in the profitable passages.

To choose the economic or the most effective passage HMF forecast information and formula (3) must be used [3]. The more exact information is the more economic passage is.

The exact hydrometeorologic forecast will give the economic effect. This will considerably exceed the charges spent on the hydrometeorologic service within the economic zone of Georgia. It is especially important in urgent cases when operative hydrometeorologic service helps us to avoid shipwreck (especially of tanker) and crew victims. Practical measures and calculations for many years done in conditions of different HMF and in different seasons of the year confirm this point [2-4]. This information is corrected and supplemented with special calculations for the Black Sea (Table).

Table

The loss of time (ΔT_n) due to storm and current during the most economic passage

The season and the power of the storm	Height of the wave h(m)	Rate of the current V (knot)	Time duration of the economic passage (T_h)		ΔT (h)
			in fine weather	in conditions of storm current	
weak	2.5	0.2	1.0	11.5	1.5
strong	4.0	0.5	13.0	15.0	2.0
spring-summer	2.0	0.2	5.0	9.0	4.0
autumn-winter	4.0	0.5	4.0	8.0	4.0

The variability of ΔT values in different conditions of HMF clearly shows that time duration of the commercial passage increases by 1.5-4.0 h when storm current is against the direction of ship. In this case shipping charges within the exploitation of the whole commercial float will increase.

Soon in the navigation sector of TRACECA and Supsa Terminal the hydrometeorologic service which will have a good network of meteorological and oceanographic shore stations, autonomous buoy systems, drifting buoys and weather forecasting ship will start functioning. The versatile information obtained by such network will be processed in the information centre and will be rapidly delivered to the ships in the form of recommendations, prognoses and facsimile informations, according to which the most economic course can be planned to perform the passage with great economic effect.

Such service will guarantee the increase of stable ecological monitoring effectiveness of a commercial passage by 10-15%. It will essentially exclude the shipwreck and its grave consequences which might be caused by the ignorance of hydrometeorologic factors.

Batumi State Marine Academy

REFERENCES

1. G.S.Metreveli. Bull.Georgian Acad. Sci., 84, 33, 1976 (Georgian).
2. V.V.Dremlyug. Effektivnost plavanya sudov pri neodnorodnykh gidrometeorologicheskikh usloviyakh. M., 1977 (Russian).
3. Rukovodstvo po gidrologicheskim rabotam v okeanakh i moryakh, 1977 (Russian).
4. Sh.Kunchulia. J. Metsniereba da teknika, N2, 1998 (Georgian).

O. Labadze, M. Tsertsvadze, G. Kublashvili, P. Manjavidze

Mutual Inductance between Flat-Parallel Convex Contours Having Conjugate Pieces

Presented by Academician M. Salukvadze, September 15, 1997

ABSTRACT. The effect of the angular displacement on the mutual inductance between flat-parallel convex contours having conjugate pieces is considered. Appropriate characteristics are obtained on computer.

Key words: SENSING ELEMENT, MUTUAL INDUCTANCE, FLAT-PARALLEL, CONVEX CONTOURS.

Determination of mutual inductance between inductive contours is the theoretical basis to design sensing elements constructed on the base of the changing of mutual inductance [1].

Let's solve mentioned electrotechnical problem for the sensing elements with two flat-parallel convex contours having conjugate pieces and establish the relation among mutual inductance (M), axially symmetric displacement (d) and angular displacement about symmetry axis (α) (Fig. 1). Topology of contours corresponds to the curve that consists of two semi-circumferences with equal radii (R), centers of which are located at any distance (a) from each other and parallel straight lines joining the ends of these semi-circumferences.

Each of contours may be resolved into pieces (1, 2, 3, 4 and 5, 6, 7, 8 pieces). Since the resultant mutual inductance will be the sum of sixteen components (principle of superposition [2]). In view of the fact that these components are equal in value in pairs because of their symmetric location, resultant M will be

$$M = (M_{15} + M_{16} + M_{17} + M_{18} + M_{25} + M_{26} + M_{27} + M_{28}) ,$$

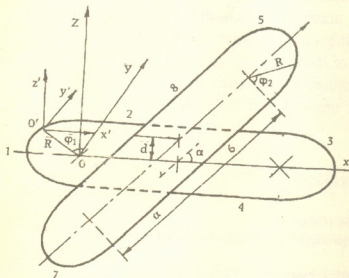


Fig. 1 Displaced flat-parallel convex contours having conjugate pieces.

where $M_{15}, M_{16}, M_{17}, M_{18}, M_{25}, M_{26}, M_{27}$ and M_{28} are mutual inductance components between corresponding pieces of contours. In order to determine these components the double integral formula known in theoretical electrotechnics may be used [2]. Just as in series transactions, dedicated to the problems of mutual inductance [1], $\cos\theta$ and D may be determined on the basis of coordinate method. Consequently Cartesian systems $XOYZ$ and $X'O'Y'Z'$ are constructed. After appropriate conversions the following expressions is derived:

$$M_{15} = \frac{\mu_0 R^3}{4\pi} \times$$

$$\times \int_0^\pi \int_0^\pi \frac{\operatorname{tg} \varphi_2 \cos(\varphi_2 - \varphi_1 + \alpha) (R^2 \operatorname{tg}^2 \varphi_2 + d^2)^{-1/2} d\varphi_1 d\varphi_2}{\sqrt{d^2 + \left(\frac{a}{2} + \frac{a}{2} \cos \alpha + R \sin(\varphi_2 + \alpha) + R \sin \varphi_1\right)^2 + \left(R \cos \varphi_1 - \frac{a}{2} \sin \alpha + R \cos(\varphi_2 + \alpha)\right)^2}};$$

$$M_{16} = \frac{\mu_0 R}{4\pi} \times$$

$$\times \int_0^\pi \int_0^\alpha \frac{\cos(\alpha - \varphi_1) d\varphi_1 dt}{\sqrt{d^2 + \left(\frac{a}{2} + R/\sin \alpha + \left(\frac{a}{2} - R \operatorname{ctg} \alpha - t\right) \cos \alpha + R \sin \varphi_1\right)^2 + \left(R \cos \varphi_1 - \left(\frac{a}{2} - R \operatorname{ctg} \alpha - t\right) \sin \alpha\right)^2}};$$

$$M_{17} = \frac{\mu_0 R^3}{4\pi} \times$$

$$\times \int_0^\pi \int_0^\pi \frac{\operatorname{tg} \varphi_2 \cos(\varphi_1 - \varphi_2 - \alpha) (R^2 \operatorname{tg}^2 \varphi_2 + d^2)^{-1/2} d\varphi_1 d\varphi_2}{\sqrt{d^2 + \left(\frac{a}{2} - \frac{a}{2} \cos \alpha - R \sin(\varphi_2 + \alpha) + R \sin \varphi_1\right)^2 + \left(R \cos \varphi_1 + \frac{a}{2} \sin \alpha - R \cos(\varphi_2 + \alpha)\right)^2}};$$

$$M_{18} = \frac{\mu_0 R}{4\pi} \times$$

$$\times \int_0^\pi \int_0^\alpha \frac{\cos(\alpha - \varphi_1) d\varphi_1 dt}{\sqrt{d^2 + \left(\frac{a}{2} - R/\sin \alpha + \left(\frac{a}{2} - t - R \operatorname{ctg} \alpha\right) \cos \alpha + R \sin \varphi_1\right)^2 + \left(R \cos \varphi_1 - \left(\frac{a}{2} - t + R \operatorname{ctg} \alpha\right) \sin \alpha\right)^2}};$$

$$M_{25} = -\frac{\mu_0 R}{4\pi} \int_0^\pi \int_0^\alpha \frac{\cos(\alpha + \varphi_2) d\varphi_2 dt}{\sqrt{d^2 + \left(t - \frac{a}{2} - \frac{a}{2} \cos \alpha + R \sin(\alpha + \varphi_2)\right)^2 + \left(R - \frac{a}{2} \cos \alpha + R \cos(\alpha + \varphi_2)\right)^2}};$$

$$M_{27} = -\frac{\mu_0 R}{4\pi} \int_0^\pi \int_0^\alpha \frac{\cos(\alpha + \varphi_2) d\varphi_2 dt}{\sqrt{d^2 + \left(t - \frac{a}{2} + \frac{a}{2} \cos \alpha + R \sin(\alpha + \varphi_2)\right)^2 + \left(R + \frac{a}{2} \sin \alpha + R \cos(\alpha + \varphi_2)\right)^2}}.$$

Notice, that the integrals for M_{15} and M_{17} are convergent, since the functions under integrals are discontinuous at the point $\varphi_2 = 90^\circ$. Because of this integral for this point determined in its own right has been added to the integrals for the ranges $\varphi_2 = 0 \div 89^\circ$ and $\varphi_2 = 91^\circ \div 180^\circ$. Such integral value because its calculating is realized with numerical methods. The components M_{16} , M_{18} , M_{27} and M_{28} have been also calculated in their own rights at the point $\alpha = 0^\circ$ for the same reason:

$$M_{15} = -\frac{\mu_0 R^3}{4\pi} \left(\int_{\varphi_1=0^\circ}^{180^\circ} \int_{\varphi_2=0^\circ}^{89^\circ} \frac{\operatorname{tg} \varphi_2 \cos(\varphi_2 - \varphi_1 + \alpha) d\varphi_1 d\varphi_2}{D_1 \sqrt{R^2 \operatorname{tg}^2 \varphi_2 + d^2}} + \right.$$



$$+ \int_{\varphi_1=0^\circ}^{180^\circ} \int_{\varphi_2=91^\circ}^{180^\circ} \frac{\operatorname{tg} \varphi_2 \cos(\varphi_2 - \varphi_1 + \alpha) d\varphi_1 d\varphi_2}{D_1 \sqrt{R^2 \operatorname{tg}^2 \varphi_2 + d^2}} + \frac{\mu_0 R^2}{4\pi} \int_{\varphi_1=0^\circ}^{180^\circ} \frac{\sin(\varphi_1 + \alpha) d\varphi_1}{D_2},$$

where

$$D_1 = \sqrt{d^2 + \left(\frac{a}{2} + \frac{a}{2} \cos \alpha + R \sin(\varphi_2 + \alpha) + R \sin \varphi_1\right)^2 + \left(R \cos \varphi_1 - \frac{a}{2} \sin \alpha + R \cos(\varphi_2 + \alpha)\right)^2};$$

$$D_2 = \sqrt{d^2 + \left(\frac{a}{2} + \frac{a}{2} \cos \alpha + R \cos \alpha + R \sin \varphi_1\right)^2 + \left(R \cos \varphi_1 - \frac{a}{2} \sin \alpha + R \sin \alpha\right)^2}.$$

$$M_{17} = \frac{\mu_0 R^3}{4\pi} + \left(\int_{\varphi_1=0^\circ}^{180^\circ} \int_{\varphi_2=0^\circ}^{89^\circ} \frac{\operatorname{tg} \varphi_2 \cos(\varphi_1 - \varphi_2 - \alpha) d\varphi_1 d\varphi_2}{D_1 \sqrt{R^2 \operatorname{tg}^2 \varphi_2 + d^2}} + \right. \\ \left. + \int_{\varphi_1=0^\circ}^{180^\circ} \int_{\varphi_2=91^\circ}^{180^\circ} \frac{\operatorname{tg} \varphi_2 \cos(\varphi_2 - \varphi_1 - \alpha) d\varphi_1 d\varphi_2}{D_1 \sqrt{R^2 \operatorname{tg}^2 \varphi_2 + d^2}} \right) - \frac{\mu_0 R^2}{4\pi} \int_{\varphi_1=0^\circ}^{180^\circ} \frac{\sin(\varphi_1 + \alpha) d\varphi_1}{D_2},$$

where

$$D_1 = \sqrt{d^2 + \left(\frac{a}{2} - \frac{a}{2} \cos \alpha - R \sin(\varphi_2 + \alpha) + R \sin \varphi_1\right)^2 + \left(R \cos \varphi_1 + \frac{a}{2} \sin \alpha - R \cos(\varphi_2 + \alpha)\right)^2};$$

$$D_2 = \sqrt{d^2 + \left(\frac{a}{2} - \frac{a}{2} \cos \alpha - R \cos \alpha + R \sin \varphi_1\right)^2 + \left(R \cos \varphi_1 + \frac{a}{2} \sin \alpha + R \sin \alpha\right)^2}.$$

$$M_{15}(0^0) = \frac{\mu_0 R}{4\pi} \int_{\varphi_1=0}^{\pi} \int_{t=0}^a \frac{\cos \varphi_1 d\varphi_1 dt}{\sqrt{d^2 + (t - a - R \sin \varphi_1)^2 + (R \cos \varphi_1 + R)^2}};$$

$$M_{18}(0^0) = \frac{\mu_0 R}{4\pi} \int_{\varphi_1=0}^{\pi} \int_{t=0}^a \frac{\cos \varphi_1 d\varphi_1 dt}{\sqrt{d^2 + (t - a - R \sin \varphi_1)^2 + (R \cos \varphi_1 - R)^2}}.$$

In order to determine components M_{26} and M_{28} the formula for mutual inductance between two linear contours has been used [2]. Their expressions after corresponding conversions are given below:

$$M_{26} = \frac{\mu_0}{2\pi} \cos \alpha \left[\left(2R \operatorname{ctg} \alpha + \frac{2R}{\sin \alpha} - a \right) \operatorname{Arth} \frac{a}{c+e} - \left(a + 2R \operatorname{ctg} \alpha + \frac{2R}{\sin \alpha} \right) \operatorname{Arth} \frac{a}{b+e} + \frac{dL}{\sin \alpha} \right];$$

$$M_{28} = \frac{\mu_0}{2\pi} \cos \alpha \left[\left(2R \operatorname{ctg} \alpha - \frac{2R}{\sin \alpha} - a \right) \operatorname{Arth} \frac{a}{h+n} - \left(a + 2R \operatorname{ctg} \alpha - \frac{2R}{\sin \alpha} \right) \operatorname{Arth} \frac{a}{g+n} + \frac{d}{\sin \alpha} N \right];$$

where $b^2 = 4(a/2 + R \operatorname{ctg} \alpha + R/\sin \alpha)^2 \sin^2(\alpha/2) + d^2$; $c^2 = 4(R \operatorname{ctg} \alpha + R/\sin \alpha - a/2)^2 \sin^2(\alpha/2) + d^2$;

$$e^2 = a^2 \cos^2(\alpha/2) + 4(R \operatorname{ctg} \alpha + R/\sin \alpha)^2 \sin^2(\alpha/2) + d^2;$$

$$L = \operatorname{arctg} \left(\frac{a + 2R \operatorname{ctg} \alpha + 2R/\sin \alpha + b}{d} \operatorname{tg}(\alpha/2) \right) +$$

$$+ \operatorname{arctg} \left(\frac{2R \operatorname{ctg} \alpha + 2R/\sin \alpha - a + c}{d} \operatorname{tg}(\alpha/2) \right) -$$

$$- 2 \operatorname{arctg} \left(\frac{2R \operatorname{ctg} \alpha + 2R/\sin \alpha + e}{d} \operatorname{tg}(\alpha/2) \right);$$

$$g^2 = 4(a/2 + R \operatorname{ctg} \alpha - R/\sin \alpha)^2 \sin^2(\alpha/2) + d^2;$$

$$h^2 = 4(R \operatorname{ctg} \alpha - R/\sin \alpha - a/2)^2 \sin^2(\alpha/2) + d^2;$$

$$n^2 = a^2 \cos^2(\alpha/2) + 4(R \operatorname{ctg} \alpha - R/\sin \alpha)^2 \sin^2(\alpha/2) + d^2;$$

$$N = \operatorname{arctg} \left(\frac{a + 2R \operatorname{ctg} \alpha - 2R/\sin \alpha + g}{d} \operatorname{tg}(\alpha/2) \right) +$$

$$+ \operatorname{arctg} \left(\frac{2R \operatorname{ctg} \alpha - 2R/\sin \alpha - a + h}{d} \operatorname{tg}(\alpha/2) \right) - 2 \operatorname{arctg} \left(\frac{2R \operatorname{ctg} \alpha - 2R/\sin \alpha + n}{d} \operatorname{tg}(\alpha/2) \right);$$

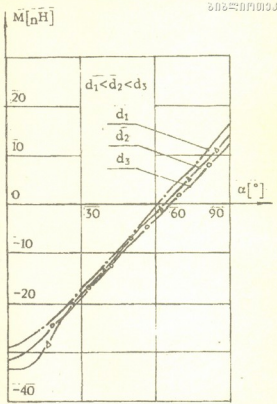


Fig.2 Diagrams for mutual inductance $M = f(\alpha)$.

On the basis of the above expressions and using the numerical method, resultant mutual inductance values have been calculated on computer for the angle range $\alpha = 0 \div 90^\circ$ and the following parameters $R = 5 \cdot 10^{-3}$ m, $a = 2 \cdot 10^{-2}$ m, $d_1 = 3 \cdot 10^{-3}$ m, $d_2 = 5 \cdot 10^{-3}$ m, $d_3 = 7 \cdot 10^{-3}$ m. In the Fig. 2 corresponding diagrams are shown. The diagrams they have monotonically increasing and sign-changing character. Obtained characteristics represent output characteristics for the interinductive transposition sensing element.

Institute of Control Systems
Georgian Academy of Sciences

REFERENCES

1. M. Tsertsvadze. In: Transactions of the Georgian Technical University, N2 (395), 1993 (Georgian).
2. P. Kalantarov, L. Tseitlin. Raschet induktivnostei. L., 1970 (Russian).

A. Chaduneli, A. Kurtishvili, G. Cheishvili, I. Lomtadze

Digital Representation of a Continuous Process with a Wide Dynamic and Frequency Spectrum

Presented by Academician M. Salukvadze, August 14, 1997

ABSTRACT. A principle and technical solution of transformation in a digital form of a continuous process with a wide dynamic range and frequency spectrum in the case of an analog-digital restricted efficiency transformer is given. The principle has been worked out particularly at processing seismic data.

Key words: TRANSFORMING RESOLVER, DIGITAL REPRESENTATION, CONTINUES PROCESS, SEISMIC DATE, FREQUENCY, SPECTRUM.

A message or information which is defined and expressed in certain material form, can be continuous or discrete. Respectively, there exist different forms of its recording, transmission and processing. A physical variable that transfers a continuous message can take any value in a certain interval, and it can change its value at any instant. In other words, a finite length continuous message represents infinitely values of the characteristics of the current process, while a feature of a discrete message is a fixed collection of certain elements or sequences of elements that form at discrete moments. Here of importance is the fact that a collection of elements is finite, rather than the physical nature of elements. This is the main difference between continuous and discrete message.

A device realising a link with the object and containing an analog-digital transformer represents the main conforming assembly between the experiment and the computer. It provides us with an information about the object of a discrete form representing values of a continuous process at fixed points of the time or space. In this way we replace infinite data chain by a numerical collection of a discrete form. This discretization procedure causes an error which sometimes is so large that its subsequent correction by high accuracy computations seems to be impossible.

The value of an error made in the process of recording of experimental information is determined by the analog-digital transformer's speed and accuracy, i.e. by its order (number of digits). Their increase is related with certain technical and economical problems. In particular, according to an assess that can be found in bibliography, each additional digit after 11-12 digits doubles the cost of a device. That's why the construction and production of high accuracy and low cost analog-digital and digital-analog transformers represent one of major problems of the computer technique.

Informaiton gained from many experiments is given in the form of a continuous process. In particular, such a continuous process is the seismic waves spread from the epicenter of an earthquake. On the basis of the criterion of setting the first appearance of seismic oscillations one is able to process automatically the kinematic information. The

kinematic information concerning seismic waves of various phases, recorded and buffered, subsequently is used to find the hypocenters of the main push as well as to figure out the seismic focus of the earthquake.

We give a principle and technical solution of transformation in a digital form of a continuous process with a wide dynamical and frequency spectrum in the case of an analog-digital restricted efficiency transformer.

The functioning circuit of the information recording and transforming resolver is given in Fig.

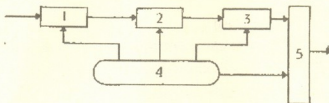


Fig.

The main nodes of the resolver are as follows: 1. Scale amplifying node. 2. Analog key node. 3. Analog-digital transformer. 4. Control node. 5. Accumulator.

The resolver works in a waiting mode. It starts after arrival of the first perturbation signal. From the trunk switch evenphase seismo-signals are sent to the input of the resolver, the amplitude of the signals being ranged from 20MkV to 10 V during the seismic activity period. While the analog-digital transformer, which is constructed on the base of the integral circuit $\Phi 7077M/1$, should be fed by certain voltage within the interval ± 1.022 which subsequently is transformed into corresponding binary code.

We have worked out a conforming node built on the base of operational amplifiers and analog-action keys. The extension of transformation limits is implemented by a scale amplifier with fixing the amplification level. There are selected four trunks with the amplification coefficients $k_1 \div k_4$. By selecting a scale amplifier and a state of an analog key the controlling node fixes an amplification coefficient that corresponds to given measurement limits. Choosing the amplification between the above four ones is going on automatically from the controlling node which at the same time works out the order of the necessary number of digits. Respectively we widen the dynamic limits of an analog-signal which reduces the relative measurement error. The analog key node contains also comparator with infinitely large amplification coefficient. If an input signal exceeds the limits of the above range, on the output there will be recorded the logical zero or one.

The existence in amplification trunks of independent scale amplifiers permits using of simultaneous parallel access. The latter increases the discreteness and correspondingly widens the frequency range.

The accumulator consists of acceptance register, where a transformed word forms in a binary code; operational storage unit where the first push is recorded and high capacity storage unit that accumulates the whole active seismic information. This node may be a part of a computer while the system operates in a real time.

On the acceptance register at each transformation step a twelve-digit binary code is recorded; 9-digit mantissa with its sign comes from the analog-digit transformer, and 2-order digits from the controlling node.



In the late eighties the Engineering Lab. of Georgian Academy of Sciences in collaboration with Moscow Earth Physics Institute have elaborated and released in a few samples an automatically controlled system for observing seismic processes. The system represents a complex of technical and programmed means for receiving, measuring, recording and real time processing of a wide class seismic and geophysical processes with a wide dynamic and frequency range.

In 1987-1988 the system has been successfully tested in joint USSR-USA experiments on nuclear-test checking in Semipalatinsk and Nevada firing grounds..

N.Muskhelishvili Institute of Computational
Mathematics
Georgian Academy of Sciences



R. Lortkipanidze

Agroindustrial Characteristics of the Main Types of Soils of Imereti Region

Presented by Corr. Member of the Academy T. Urushadze, January 26, 1998

ABSTRACT. The characters and compositions of mountain meadow, brownforest, rendzina-carbonate, red, yellow, yellow-podzolic (subtropical-podzolic) and the meadow alluvial soils are investigated according to the agricultural development program of the region. Agroindustrial characteristics of the soils and measures for increasing of the soils productivity are given.

Key words: AGROINDUSTRIAL GROUP, SOILS, MECHANICAL COMPOSITION, GLEI.

By geomorphologic division Imereti is located in the north-eastern part of humid subtropical area of West Georgia [1-3]. Vegetable cover of the region is characterized by strict vertical zonality.

In the low Imereti the Kolkheti lowland mainly consists of the forth strata; The rest area consists of the sandstones of Urassic period, glei slates and glei statums, also of the crystal matrix - granite and crystal slates, charts and urging lime-stones, which are the common creative rocks of these soils [6].

The complex relief, climate and geomorphologic conditions, variety of vegetable cover and human influence have stimulated the diversity of the soil cover. The mountain-meadow, brownforest, red, yellow, yellow-podzolic (subtropical-podzolic), yellow-podzolic glei (podzolic glei), meadow alluvial types of soils are spread in this region [4,5].

Imereti soils (Table), according to their natural potential fertility, hydro-physical characteristics, proper transportation of agricultural crops and other factors are divided in 8 agro-industrial groups.

In the first agro-industrial group there are united the soils with big and average stoutness, non-washed out and weakly washed out, weakly rich of stones yellow, red, rendzina-carbonate and brownforest types of soils, which are cultivated by annual and perennial agricultural crops: tea, grape, fruit, etc. The soils are characterized by relatively good hydro-physical and air conditions, high consistence of watertight aggregates, high level of general porosity and low weight by volume, which defines the good harvest of agricultural crops.

The soils do not need the special agro-technical and agro-meliorative measures to be carried out. In order to maintain and increase their fertility it is necessary to conduct agrotechnical actions in time and in a qualitative manner.

Except the primary cultivation, the sideration and timely introduction of organic and

Characteristics of the studied soils

cut #	Depth, sm	Higr. water	pH	Humus %	CaCO ₃	mg. equiv/on 100 g soil						<0.001	<0.01	
						Ca	Mg	H	Sum	% from the sum				
										Ca	Mg			H
A Alluvial														
50	0-20	4,40	5,0	2,8	not determ.	9,01	3,23	not determ.	12,24	74	26	-	9	36
	30-40	4,29	4,9	1,8	~	6,96	1,96	~	8,82	78	22	-	8	33
	60-70	3,98	5,0	1,1	~	13,81	1,17	~	14,98	92	8	-	11	38
	85-95	4,48	5,0	0,4	~	19,60	4,41	~	24,01	18	18	-	9	33
Yellow podzolic glei														
42	0-20	4,12	5,2	3,1	~	10,20	2,06	1,45	14,51	70	20	1	12	54
	30-40	6,00	5,2	1,7	~	8,32	2,45	1,35	12,12	69	20	11	36	60
	58-68	7,14	5,4	0,4	~	4,08	3,86	8,97	16,91	24	23	53	35	71
	100-110	7,22	5,0	0,4	~	13,06	3,86	9,85	26,77	11	14	75	15	71
Yellow podzolic														
109	0-16	1,52	6,2	3,12	~	12,06	1,43	3,63	17,12	70	8	22	18	43
	25-35	1,69	5,8	1,12	~	12,07	0,82	3,02	15,91	76	5	19	36	63
	45-55	1,71	6,2	1,00	~	12,06	0,81	3,02	15,89	76	5	19	35	64
	79-89	1,98	6,2	0,53	~	16,58	3,45	0,39	20,42	81	17	2	25	68
Yellow														
22	0-15	14,12	4,5	4,45	~	10,59	4,53	4,96	20,08	53	22	25	23	44
	18-28	4,20	4,6	2,09	~	10,37	2,58	4,03	16,98	61	15	24	25	59
	45-55	2,63	4,6	1,39	~	21,21	5,77	0,34	27,32	78	21	1	37	64
	60-70	-	4,8	-	~	22,23	2,46	0,12	24,81	90	9	1	44	60
Red														
70	0-20	5,30	4,7	9,59	~	4,66	1,62	4,19	10,47	44	15	41	17	59
	30-40	5,86	4,6	3,65	~	3,64	1,21	3,03	7,88	46	15	39	18	57
	46-56	7,50	4,9	2,96	~	3,64	2,81	2,07	8,52	43	33	24	29	51
	60-70	6,90	4,9	0,76	~	3,23	2,81	2,98	9,02	36	31	33	28	47
Rendzina-carbonate														
155	0-19	4,21	7,8	3,52	4,0	41,58	4,67	not determ.	46,25	90	10	-	27	63
	30-40	4,84	8,0	1,54	15,0	43,71	4,24	-	47,95	91	9	-	37	64
	56-66	6,01	8,2	-	17,4	45,80	3,89	-	49,69	92	8	-	32	62
Brown-forest														
39	0-17	4,45	5,6	5,87	not determ.	11,57	2,12	1,06	15,55	74	14	12	27	62
	25-35	4,08	5,6	3,09	~	10,81	2,57	2,51	15,89	68	16	16	39	71
	70-80	5,05	5,8	-	~	11,78	2,74	2,13	16,05	70	17	13	38	73
Mountain-meadow														
44	0-10	5,91	5,6	1,08	~	22,41	1,24	not determ.	23,65	95	5	-	14	38
	16-26	5,64	5,8	0,34	~	21,16	1,65	"	22,81	93	7	-	13	33

mineral fertilizers is of great importance.

To protect the soils' fertility anti-erosion preventive measures should be carried out.

In the second agro-industrial group there are united meadow alluvial and yellow-podzolic soils on which annual and perennial agricultural crops and natural plants are mainly cultivated. The soils are developed in conditions of lowland relief, are characterized by relatively high fertility and satisfactory hydro and physical conditions. Agricul-

tural crops and namely soil of teaplantations must be ploughed or cultivated, regularly make deeply friabilitated in order to create good conditions for water and air movement.

Sideration, applying of organic and mineral fertilizers (with nitrogen, phosphorus and potassium) and ploughing of soil give good results.

In the areas occupied by plants meliorative measures must be taken in order to remove surface waters.

The third agroindustrial group consists of weakly and completely washed out, weakly and average rocky mountain-meadow, brownforest, rendzina, yellow and red types of soils located on the slopes of different inclinations cultivated by both agricultural crops and forest, shruberry and pastures. In pasture land the processes of soil washing due to water erosion are clearly reflected, the turf stratum is destroyed and the profile of the soil is reduced.

Agricultural technical works are necessary to be carried out efficiently in the areas assimilated by agricultural crops. Soil must be cultivated across the inclinations. Organic and mineral fertilizers must be applied in accordance with agrochemical cartograms. Sideration gives good result.

In the fourth agroindustrial group there are weakly and average rocky, meadow alluvial and podzolic-yellow types of soils occupied by annual and perennial agricultural crops. Part of the soil is covered by vegetation. Less fertile soils are characterized by dissatisfied hydro-physical patterns.

To increase fertility and improve hydro-physical conditions stones must be removed, organic and mineral fertilizers must be introduced into spots assimilated by agricultural crops, and irrigation should be carried out in drought period.

The fifth agroindustrial group unites superfluous humid and glei meadow-alluvial, podzolic-yellow and podzolic -yellow glei types of soils that are spread in weakly drained lowlands of meadow and upper river terraces in mezo and micro relief conditions. In these soils presence of gleing and surplus humidity with different levels of depths are noticed.

The gleing stratum exists mainly on 60-100 cm. of depth. Soils are assimilated mainly by annual and perennial agricultural crops.

In the lower Imereti region which is located in new areas of Kolkhety irrigative measures should be carried out.

The cycle cultivation must be carried out during 3-5 years. This would mean frequent and deep cultivation, applying of organic and mineral fertilizers by overdoses, sowing siderites in the soil.

After the proper irrigation and cultivation it is important for these soils to be occupied by laurel, pheachoa, subtropical persimmon and volatile oil crops.

In the sixth agroindustrial group there are united heavily and at average washed-out brownforest, yellow, and rendzina soils that are located in slopes of high inclinataion. Some part of these soils is assimilated by annual agricultural crops and the rest part is occupied by thin forest, shruberry and pastures of poor quality. The soils are quite subjected to erosion. In order to maintain and recover their fertility the complex anti-erozion measures should be taken. On the slopes the soils should be ploughed periodically and cultivated across them.

Floral composition of the pastures must be improved and implanted by strong perennial herbs.



In order to regulate surface waters the water repellent, water collective channels and flower beds connected with the local hydro-graphic net should be arranged. Canyons, abysses and banks of rivers should be fortified.

The seventh agroindustrial group unites rocky and highly rocky soils located in upper terraces of the river bank, in lower relief and are composed of old alluvial boulders.

Extension of fertility of the soils is mainly connected with removal of stones from the plot, enrichment of soils by organic substances and application of mineral fertilizers. Sideration gives good result. In drought period irrigation should be conducted.

The eighth agroindustrial group is represented by canyons, rocky placers, stony rivers and bared rocks. Soils should be covered with forests and if it's possible the banks of rivers and abysses should be fortified.

Presented agroindustrial grouping of soils is good background for correct accounting of lands and quality of soil resources, optimal movement of crops and finally, improvement of agroindustrial production.

State Agrarian University of Georgia

REFERENCES

1. *N Ketskhoveli*. Sakartvelos mtsenareuli sapari. Tbilisi, 1960 (Georgian).
2. *M. Kordzaia*. Sakartvelos hava. Tbilisi, 1961 (Georgian).
3. *L. Maruashvili*. Sakartvelos pizikuri geograpia, nats.II, Tbilisi, 1970 (Georgian).
4. *M. Sabashvili*. Sakartvelos sssr niadagebi. Tbilisi, 1965 (Georgian).
5. *T. Urushadze*. Sakartvelos dziritadi niadagebi. Tbilisi, 1997 (Georgian).
6. *A. N. Djavakhishvili*. Geomorfologicheskie rajoni Gruzinskoi SSR. Moskwa, 1947 (Russian).

M.Davitadze

Systematic Structure of the Adjarian Adventive Flora

Presented by Corr. Member of the Academy G. Nakhutsrishvili, October 29, 1997

ABSTRACT. In the present letter systematic structure of the Adjarian adventive flora is proposed. Intensive process of antropogenic transformation of the Adjarian flora takes place during the last decades.

Key words: ADVENTIVE FLORA, EPHEMEROPHYTES

At present 439 adventive species have been registered in the Adjarian flora which makes 23% (1900 species) of general floristic variety in this region. Among them 79 species are ephemerophytes. Despite the fact that the existence of adventive ephemerophytes is unstable in local flora, we take them into account while analyzing systematic structure of Adjarian flora. The cases of extinct adventive ephemerophytes reappearance have been marked here and there [1].

The species of Adjarian adventive flora belong to 4 divisions and 2 classes (Table 1). Higher sporiferous plants are represented by 2 families (*Psilotaceae* and *Polypodiaceae*), 6 genera and 6 species, barseeds by 2 families, 2 genera and 2 species, and hidden seeds by 52 families, 252 genera and 421 species.

Table 1

Classification of the Adjarian adventive flora
 in large taxonomic units

Division, class	Amount		
	Family	Genus	Species
<i>Psilotophyta</i>	1	1	1
<i>Pteridiophyta</i>	1	5	5
<i>Pinophyta</i>	2	2	2
<i>Magnoliophyta</i>	59	252	431
<i>Magnoliopsida</i>	46	191	329
<i>Liliopsida</i>	13	61	102

The Adjarian adventive flora is characterized by a number of specific features. First of all it is the existence of higher sporiferous plants. From the Baltic Sea coast up to Kolkhida higher sporiferous plants are not found in the adventive flora of any region [2-5].

Up to now they have not been identified for Kolkhida either [6-8]. In Adjarian flora we have found *Psilotum nudum*, *Onoclea sensibilis*, *Dryopteris atrata*, *Cyrtomium falcata*,

Adiantum cuneatum and *Pteris vitata*.

Thus, Southern Kolkhida - (Adjara) represents a kind of refugium for higher spores of southern origin in the Caucasus.

Southern (subtropical) families of Adjarian adventive flora, except higher sporiferous, are as follows: *Taxodiaceae*, *Lauraceae*, *Lardisabalaceae*, *Hydrangiaceae*, *Simaroubaceae*, *Bignoniaceae*, *Saururaceae* and *Commelinaceae*. Representatives of the American families with nearly cosmopolitan areal such as *Phytolacaceae*, *Chenopodiaceae* and *Amaranthaceae* are also met here.

Dicotyledonous prevail in the Adjarian adventive flora (329 species) whereas the quantity of monocotyledonous is comparatively small (Table 1).

Similar ratio is characteristic to the adventive flora of regions with continental climate [9]. High percentage of taxonomic units of high rank is also specific for the Adjarian adventive flora. Thus, in Adjarian flora out of 138 families 14 i.e. 10.1% of total flora families are adventive. In floras of different regions of temperate zone such phenomena is rare. Out of 725 genera of the Adjarian flora 163 are adventive i.e. 22.4% of total flora genera (Table 2).

Table 2

The distribution of the Adjarian adventive species in taxonomic units

Families			Genera			Species		
Total No in Adjarian flora	Among them adventive	No of adventive families, %	Total No in Adjarian flora	Among them adventive	Total No of adventive genera, %	Total No in Adjarian flora	Among them adventive	No of adventive species, %
138	14	10.1	725	161	22.4	1900	439	23.1

Table 3

Taxonomic composition of basic families of the Adjarian adventive flora

Family	Genera	No of species	Total number of adventive species, %
<i>Poaceae</i>	41	74	16.8
<i>Asteraceae</i>	43	66	15.0
<i>Fabaceae</i>	19	38	8.6
<i>Brassicaceae</i>	22	31	7.0
<i>Apiaceae</i>	13	18	4.1
<i>Lamiaceae</i>	10	13	2.9
<i>Polygonaceae</i>	3	13	2.9
<i>Euphorbiaceae</i>	5	12	2.7
<i>Solanaceae</i>	4	12	2.7
<i>Caprifoliaceae</i>	8	10	2.5
<i>Cyperaceae</i>	5	9	2.3

The genus *Amaranthus* is represented by 9 species, *Chenopodium* by 6, *Hydrocotyle*, *Erigeron*, *Hordeum* and *Setaria* by 3-3 species; 11 genera by 2-2 species, the rest by one species. The majority of adventive (296 species, 67,4% of general flora) belong to 11 families. There are *Psilotaceae*, *Lauraceae*, *Rosaceae*, *Saxifragaceae*, *Fabaceae*, *Caprifoliaceae*, *Hypericaceae*, *Phytolacaceae*, *Iridaceae*, *Orchidaceae* and *Araceae*. Other families are represented by one or two species (Table 3).

The existence of enumerated species of the families has not been revealed in neighbouring regions of Kolkhida such as Crimea or Azerbaijan [10,11]. Such species have not been registered in other parts of Kolkhida [7,8].

The majority of the Adjaria adventive flora belong to five families: *Poaceae*, *Asteraceae*, *Fabaceae*, *Brassicaceae* and *Apiaceae* (Table 3). This regularity is common for temperate zone [12].

In the forties the share of adventive species in the Adjarian flora comprised only 7% [13]. Beginning from the fifties the Adjarian floristic variety enriched by 16%. Such a high percent of adventive species is characteristic for floras of Far East and some other regions [14-16].

In last 10 years many obstacles limiting plant migration have been removed. As a result the process of anthropogenic transformation of the Adjarian flora has been strengthened.

Batumi Botanical Gardens
Georgian Academy of Sciences

REFERENCES

1. A.A.Dmitrieva. Opredeletel rastenii Adjarii. Tbilisi, v.I-II, 1990, 328 (Russian)
2. A.A.Lyakovichyus, Z.M.Gudzinskaya, V.P.Motekaytite. Problemi izucheniya adventivnoi flory USSR, M., 1989, 22-25 (Russian)
3. A.N.Puziryiev. Candidate thesis (Russian).
4. E.N.Kondratyuk, V.P.Tarabrin, R.I.Burda. Problemi izucheniya adventivnoi flory USSR, M., 1989, 66-69 (Russian).
5. S.K.Kozhevnikova, N.N.Rubtsov. The works of Nikitskiy State Botanical Garden, 54, 1971, 23-54.
6. V.S.Yabrova-Kolokovskaya. Adventivnaya flora Abkhazii. Tbilisi, 1977, 62 (Russian).
7. M.T.Mazurenko, A.P.Khokhrakov. Newsletter. MOIP, Moscow, 1972, 128-138.
8. D.G.Kiknadze. Bull. Georgian Acad. Sci., 144, 2, Tbilisi, 1991, 301-304 (Georgian).
9. E.V.Lukina. Problemi izucheniya adventivnoi flory USSR, M., 1989, 42-45 (Russian).
10. V.N.Golubev, I.V.Golubeva. Ibidem, 72-75.
11. N.A.Mamedov. Ibidem, 81-84.
12. A.I.Tolmachyov. Introduction into Plant Geography. L., 1974, 243.
13. A.A.Grossgeim. Analiz flory Kavkaza. Baku, 1936, 557 (Russian).
14. E.I.Iager. Biol. Rdsch., 15, 1977, 287-300.
15. S.S.Kharkevich. Problemi izucheniya adventivnoi flory USSR, M., 1989, 88-92 (Russian).
16. S.D.Shotgauer. Ibidem, 89-101.

G. Todua

Electrophysiological Investigation of the Descending Connections of the Posterior and Anterior Sylvian Gyri with the Amygdaloid Complex

Presented by Corr. Member of the Academy V. Mosidze, July 17, 1997

ABSTRACT. Studies have been made on the distribution of the evoked potentials in amygdala during stimulation of the posterior and anterior sylvian gyri in acute experiments on cats under nembutal anesthesia. Potentials with the largest amplitude arise in basolateral part of the amygdaloid complex and central nucleus. Evoked potentials in cortical and medial nuclei sharply differ from those, registered in basolateral amygdala. Responses with the shortest latency (4.6-10ms) were registered in dorsal part of lateral nucleus. This fact is accounted for by the existence of direct corticofugal pathways.

Key words: AMYGDALOID COMPLEX, POSTERIOR SYLVIAN GIRUS, EVOKED POTENTIAL, AMPLITUDE, LATENCY.

Amygdaloid complex is involved in realisation of many aspects of behavioral reactions, differing from each other in character [1-4]. For better understanding of its polyfunctionality and integrative role it is important to investigate its connections with neocortical areas – higher integrative structures.

The aim of this study was to examine descending connections of the insular region homologous areas – posterior and anterior sylvian gyri with the amygdaloid complexes in cats.

Data were obtained from 9 adult cats, anesthetized with nembutal, given intraperitoneally. Bipolar silver ball stimulating electrodes were applied to the exposed pial surfaces. Single pulses of 0.5-1.0 ms duration were given from a stimulator. The range of stimulating potentials varied from 4 to 9 volts. Evoked potentials of amygdaloid complex with monopolar stainless-steel electrodes were recorded. Standard techniques for amplifying and recording were employed.

Evoked potentials of different latency were registered in amygdaloid complex following the single cortical stimulation. The shape and latency of potentials were found to depend both on stimulation and recording points. Stimulation of the posterior sylvian gyrus was most effective.

Stimulation of the posterior sylvian gyrus evoked responses in an extensive area of the amygdaloid complex. In all experiments, in all areas of amygdala the response was initially negative. The most prominent responses were recorded from the basolateral part and essentially from the lateral nucleus. The examples of responses in basolateral part of amygdala in frontal plane 11.5 of the atlas of Jasper and Ajmone-Marsan [5] are shown in Fig. 1A.

The typical evoked potential in *n. lateralis* consisted of initial negative wave at relatively brief latency, with a duration of 18-26 ms, followed by positive-negative deviation and later components which were variable even within a given experiment. The maximum amplitude of initially negative wave was $190\mu\text{V}$ and more. The latencies of evoked responses range from 4.6 up to 18 ms. The typical high amplitude response was seen only in dorsal part of lateral nucleus. The character of the response is altered when recording electrode is placed. In central part of *nucleus lateralis* evoked potentials were of less amplitude and their latencies were longer by 5-7 ms than those of potentials registered in dorsal part. At more ventral levels longer latency responses (14-18ms) could be evoked.

Study of distribution of evoked potentials in the rostro-caudal plane shows, that responses with minimal latencies were recorded from *A* 11 to 10.5. More anteriorly or posteriorly from lateral nucleus the medium amplitude responses were obtained.

Stimulation of the posterior sylvian gyrus evoked responses in basal nucleus, similar to those in the lateral nucleus. A medium amplitude response was obtained from the magnocellular part of the basal nucleus, as frontal plane *A* 11-11.5, whereas the parvocellular part gave a small or inconstant response. The latencies of responses registered in *n. basalis* ranged from 14 to 24 ms.

Responses to posterior sylvian gyrus stimulation were also recorded from the corticomedial part of amygdala (Fig. 1, B). In *n. centralis* single shock stimulation of the posterior sylvian gyrus gave a response with latency of 13-16 ms and amplitude $230\mu\text{V}$. Evoked potentials in medial and cortical nuclei sharply differ from those, registered in basolateral part. They showed the most inconspicuous biphasic response. Most responses

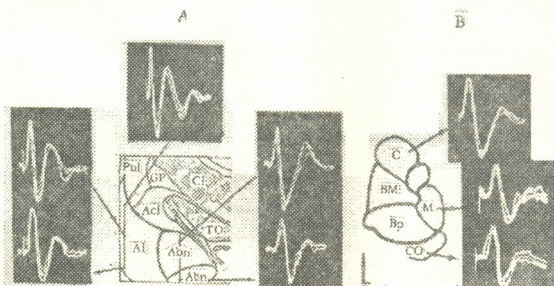


Fig. 1. Evoked responses of the basolateral (A) and corticomedial (B) parts of amygdala during stimulation (6V, 0.5 ms) of the posterior sylvian gyrus. Time and amplitude calibration: 20 ms, $100\mu\text{V}$

in these nuclei had latencies over 24 ms.

Stimulation of the anterior sylvian gyrus evoked responses in both amygdala. In lateral nucleus the response was triphasic with 7-16 ms latency (Fig. 2, A). In lateral nucleus evoked responses with minimal latency of 7-10 ms were recorded from stereotaxic coordinates: *A* 12, *L* 0.5-1.0, *H* 3-4.5. Responses were not obtained from electrodes implanted caudal to *A* 10.



In basal nucleus responses with relatively high amplitude were obtained on recordings in the dorsal part. Minimal latency time was 15 ms. Amplitudes of these responses ranged from 240 to 260 μV . In parvicellular part only small inconstant potentials were obtainable.

Central nucleus displays responses with intermediate latency 15-18 ms. Amplitudes

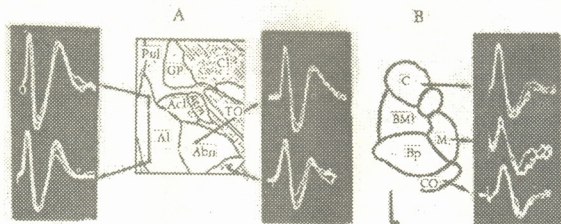


Fig. 2. Evoked responses of the basolateral (A) and corticomедial (B) parts of amygdala during stimulation (6-9 V, 0.5ms) of the anterior sylvian gyrus. Time and amplitude calibration: 20ms, 100 μV

of these responses were 220-240 μV . Evoked potentials in cortical and medial nuclei were registered at stronger stimulation. The responses were of long latency (20-26 ms). The amplitude was less than 200 μV (Fig. 2, B).

Data obtained point to a differential projection of the posterior and anterior sylvian gyri to the amygdaloid nuclei. These neocortical areas mainly are projected into the phylogenetically younger division of limbic system. Our experiments confirm the intimate connection of posterior and anterior sylvian gyri with lateral nucleus. Our results are in accordance with the findings of Druga [6] which describes direct fiber connection from these areas to the dorsal part of lateral nucleus.

Our results indicate that two pathways connect these structures. The short latency component is probably transmitted by a direct pathway. Medium and long latencies indicate that at least one and probably even more synaptic stations have to be passed in the way. The connections between the temporal neocortical areas and amygdaloid complex are the basis of the amygdaloid participation in the higher integrative function of the brain.

I. Beritashvili Institute of Physiology
Georgian Academy of Sciences

REFERENCES

1. E. Fonberg. *Acta Neurobiol. Exp.* **34**, 2, 1974, 435-466.
2. P. Gloor. In: *Handbook of Physiology. Sect. I. Neurophysiology.* 2. H. W. Field (Ed.). Baltimore, 1960, 1395-1420.
3. G. V. Goddard, *J. Compar. Physiol. Psychol.*, **58**, 1, 1964, 23-30.
4. J. S. Richardson. *Acta Neurobiol. Exp.* **33**, 3, 1963, 623-648.
5. H. H. Jasper, A. Ajmon-Marsan. *Stereotaxic atlas of the cat.* Ottawa, 1954.
6. R. Druga. *J. Hirnforschung*, **11**, 6, 1969, 467-476.



N. Archvadze

Active Avoidance Reactions (AAR) Dynamics in Rats with Dorsal Hippocampus Bilateral Coagulation

Presented by Academician V. Okudjava, June 17, 1997

ABSTRACT. Dorsal hippocampus bilateral coagulation deteriorates reactions on the painful irritant and conditional warning. Coagulation causes decrease of fear and inquisitive reactions. It is supposed that operated rats' specific state with lower emotional-motivational conditions in "open field" - self relieve ability by grooming and fear decrease depending on low motor activity - causes deterioration of learning processes.

Key words: HIPPOCAMPUS, ACTIVE AVOIDANCE, "OPEN FIELD", FEAR, INQUISITIVE.

The data about effects of the coagulation of the dorsal hippocampus on the formation of active avoidance reactions are different [1,2]. Most of explorers consider, that coagulation improves double-sided avoidance reactions [3,4], but in some cases hippocampectomy causes deterioration of the AAR [5]. The suggestions about effects of hippocampal coagulation on the emotional reactions

are contradictory as well [6,7].

The aim of our experiments was to investigate the influence of dorsal hippocampus bilateral coagulation on formation of the one-side AAR in white rats and their emotional-motivation behavior in "open field".

Before the formation of the AAR the intact and operated animals were tested in "open field" during 6 days. All fixed behavioral parameters were systematized into fear and inquisitive reactions.

Formation of AAR started on the 7th day. After reaching criterial level on the painful irritant, animals were given conditional irritant (light) during 10 sec. If a rat was not jumping on the shelf, during the following 10 sec electric

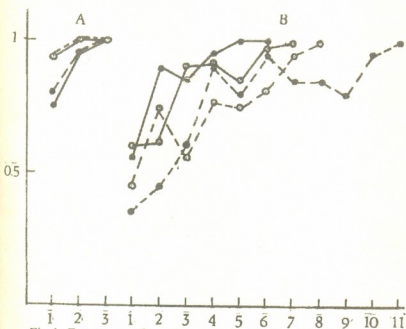


Fig.1. Frequency of reactions on electrical and light stimulus.

OX - Experimental days; OY - Reaction's frequency;
 A - Reactions on electric stimulus; B - Reactions on light stimulus;

- — - Rapidly learning intact rats;
- - - - Slowly learning intact rats;
- — - Rapidly learning operated rats.
- - - - Slowly learning operated rats;

stimulus on the background of light was given to it.

Animals were grouped by learning ability after reaching the criterial level. Intertrials spontaneous activity and latent periods of reactions were fixed. Intertrial intervals were varying according to the special selected timer programme for avoidance of time reflex formation and study of each subject in the similar conditions. During the experiments the rats have been placed in "open field" before and after each test.

Bilateral coagulation of the dorsal hippocampus causes deterioration of the reactions on the painful irritant and conditional warning as well. There is a possibility to differentiate intact and operated animals in 2 groups: rapid learner rats with high motor activity and slow learner rats with low motor activity. Rapid learner operated animals reach criterial level earlier than intact rats. Spontaneous activity of the intact rats significantly exceeds the same in the operated rats. And what is more, spontaneous activity of the rapid learner intact animals prevails over the one of the slow learner intact animals.

Rats testing in the "open field" before formation of AAR gives possibility to evaluate their emotional-motivational conditions. Fear and inquisitive reactions of the operated rats are lower than the same in the animals, but in both cases inquisition never prevails fear. Fear and inquisitive reactions of the rapidly learning rats exceed the same in the slowly learning animals. While AAR formation free behavior of animals in the "open field" was changed. The fear and inquisition of intact animals prevail over the emotional reactions in operated ones. After each trial fear and inquisition increase as well, but significantly rises fear reaction in rapid learning intact animals, while inquisition considerably increases in the slow learner rats. Emotional-motivational reactions of the rapid learner operated animals are weaker than the same ones in slow learners, and what is more, after the test the above mentioned parameters change slightly (Figs.2,3).

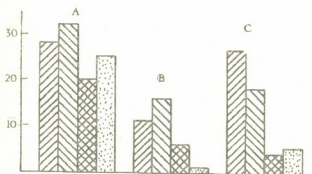






Fig. 2. Inquisitive reactions in "open field" test.

OY - Reaction's frequency; A - 6-days testing; B - before experiment; C - After experiment;

-  - Slowly learning intact rats
-  - Rapidly learning intact rats
-  - Slowly learning operated rats
-  - Rapidly learning operated rats

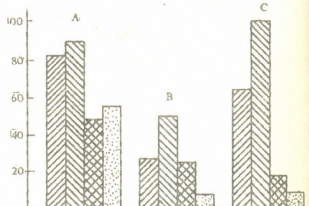






Fig. 3. Fear reactions in "open field" test

OY - Reaction's frequency; A - 6-days testing; B - before experiment; C - After experiment;

-  - Slowly learning intact rats
-  - Rapidly learning intact rats
-  - Slowly learning operated rats
-  - Rapidly learning operated rats

Slowly learning rats with dorsal hippocampus bilateral coagulation can't manage AAR realization. The difference is observed at first experimental day. If such difference between intact and operated animals is caused by coagulation of hippocampus as an information selector and comparator [8], such difference is unexpected as rats are not yet



informed about experimental situation on first day, at first trial. Difference is observed in the reactions on light stimulation as well. AAR's deterioration reason can not be intensification of oriental activity [1], as general activity of the operated rats in "open field" and their intertrial spontaneous activity are less than the same of intact animals. It is supposed that the reason of such AAR deterioration in slow learner rats is caused by decreasing of the emotional reactions on the painful irritant [9], and the latest is the result of fear reactions decline.

At the end of the experiment operated and intact rats are receiving less el. stimulation, but slow learner operated rats' lower emotional-motivational reactions are not able to provide formation of AAR simultaneously with the intact animals.

Dorsal hippocampus bilateral coagulation causes decrease of fear and inquisition as well. Differentiation of the rats by groups of learning ability indicates that such grouping coincides with the grouping of animals by general motor activity in "open field". Emotional-motivational conditions considerably define learning ability.

It is supposed, that general activity in "open field" is caused by prevailing of fear reactions over the inquisition, since curve of fear reactions rises upon the curve of inquisition. Intact animals give considerably more groomings and grooming durations are longer as well. It seems, that groomings against the background emotional stress represent the way out from the discomfortable situation and it seems to be of importance in self-relieved processes.

Experimental cabin depresses intact and operated rats. "Open field" parameters show decline of emotional-motivational conditions in comparison with six-day "open field" series. After each trial the fear and inquisitive reactions are increasing, but these parameters are more growing in rapid learner intact animals. Insignificant increase of the emotional-motivational reactions in operated animals points to their specific state. Lower emotional-motivational conditions, self-relief disability by groomings, fear decrease dependent low motor activity of slow learner operated rats cause deterioration of the learning processes.

Tbilisi I. Javakishvili State University

REFERENCES

1. E. Grashian, G. Karmosh, L. Andian. In: Gagrskié Besedy. Moskva. 5, 1968, 150 (Russian).
2. P. Milner. Physiological Psychology. M., 1973 (Russian).
3. R. Alvares-Pelaez. Physiol. Behav., 11, 1973, 603.
4. R. H. Green, W. W. Beatty, C. S. Schwartzbaum. J. Com. Physiol. Psychol., 56, 1963, 284-289.
5. H. Hunt, I. T. Diamond. Proc. 15th Intern. Congress of Psychology. 1957, 203-304.
6. A. G. Koreli. Hippocampus and emotions. Tbilisi. 1989 (Russian).
7. T. N. Oniani. Integrative Function of Lymbic System. Tbilisi, 1989 (Russian).
8. O. C. Vinogradova. Hippocampus and memory. M., 1975 (Russian).
9. A. A. Garibian. Role of deep structure in behavioral mechanisms. M., 1984 (Russian).

E.Chikvaidze, I.Kirikashvili, A.Lebanidze.

Electron Spin Resonance (ESR) of Copper Proteins and Some Model Systems

Presented by Academician M.Zaalishvili, February 12, 1998

ABSTRACT. Spectrum analysis of electronic spin resonances (ESR) has been carried out in order to find the correlation between the structure of Cu(II)-complexes of copper proteins and ferments and fermentative activity. The structure of Cu(II)-complexes and ligating atoms were examined in copper proteins and in some model systems. It was shown that in contrast to copper proteins and ferments the parameters of ESR typical for blue copper ions were not observed. The correlation between the chemical nature and coordinating number of ligating atoms with Cu(II) and spectrum parameters ESR was noted also.

Key words: COPPER PROTEINS, ESR SPECTRUM, LIGAND FIELD, CU(II)-COMPLEX.

Basically copper proteins contain three complex types Cu(II)-ions, for the first type the absorption spectrum with large coefficient extinctions and maximum absorption at 600 nm and correspondingly blue colour are typical. This spectrum (ESR) has unusual small value of hyperfine splitting $|A_{||}| < 0.01 \text{ cm}^{-1}$. They are called the blue complex coppers of the first type. For the second type the absorption spectrum and spectrum of ESR complexes Cu(II) with amino acids and peptids are typical. For the third type the close-disposed antiferromagnetic conjugated ions Cu(II) are typical, subsequently they have no spectrum of ESR. It was found that copper proteins and ferments contain all three types of Cu(II) -complexes [1].

Small value of constant hyperfine splitting in spectrum of ESR of "blue" complexes of copper was explained with great degree delocalization of uncoupled electrons by Malmstrom and Vanngard [2]. Brill [3] explained it by means of unsquared ligating ligands and mixing 4S and 4P orbits in ground state.

On the basis of ligands field theory by Kivelson and Neiman for tetragonal complexes density of uncoupled electrons on copper atoms was calculated [4].

$$\alpha^2 = A_{||} / 0.036 + (g_{||}-2) + 3/7 (g_{\perp}-2) + 0.04 \quad (1)$$

where $g_{||}$, g_{\perp} -principal values of g-factors; $A_{||}$ -hyperfine splitting quantity; α^2 - covalency degree; in case of pure ionic coupling $\alpha^2=1.0$ and of covalent - $\alpha^2=0.5$.

On the basis of crystalline field theory, Neiman and Zarizki [5] have calculated energy of structure CuO_6 for ligands with various symmetries for comparison with experimental results. They have introduced parameter $\gamma=(g_{||}-g_3)/(g_{\perp}-g_3)$, for calculation of which it is not required to know constant spin-orbital interaction λ and cube splitting

Table 1

Model systems	Coordinating atoms	g_{\perp}	g_{\parallel}	$A_{\parallel} \text{ cm}^{-1}$	α^2	γ	A_{\parallel} / γ ($\times 10^4$)
2,2-Dipyridyl	4 N	2.082	2.27	0.017	0.61	3.36	50.6
Histidine	4N	2.063	2.23	0.018	0.54	3.75	48.0
1,10 - Phenanthroline	4N	2.088	2.28	0.015	0.72	3.2	46.8
Imidazole	4N	2.06	2.267	0.018	0.68	4.36	41.3
Oxalate	4O	2.078	2.316	0.017	0.73	4.15	41.0
Bis-salicylaldehydeimine	2O,2N	2.045	2.20	0.0185	0.49	4.6	40.2
EDTA	4O,2N	2.09	2.337	0.015	0.71	3.8	39.5
Citrate	2O	2.074	2.349	0.016	0.72	4.8	31.25
Bis-acetylacetonate	4O	2.053	2.266	0.015	0.6	5.2	30.8

Table 2

Complexes Cu(II) ions with Proteins and Macromolecules	g_{\perp}	g_{\parallel}	$A_{\parallel} \text{ cm}^{-1}$	α^2	γ	A_{\parallel} / γ ($\times 10^4$)
DNA - I pH=5.15	2.08	2.23	0.0135	0.68	2.93	46.1
Bovine serum albumin pH=8.9	2.07	2.27	0.0170	0.81	3.95	43.0
Collagen pH=4.9	2.07	2.23	0.0136	0.68	3.36	40.5
Bovine serum albumin pH=4.3	2.06	2.26	0.0158	0.77	4.1	38.5
Human serum albumin pH=4.3	2.065	2.279	0.0158	0.79	4.4	36.0
Bovine serum albumin pH=6.55	2.07	2.304	0.0161	0.82	4.46	36.1
DNA-II pH=10.3	2.065	2.304	0.0150	0.79	4.8	31.25
Egg albumin pH=4.3	2.07	2.314	0.0143	0.78	4.6	31.1
Lisozime pH=4.3	2.07	2.327	0.0134	0.77	4.8	27.9

Table 3

Proteins with changing Cu(II) ions	g_{\perp}	g_{\parallel}	$A_{\parallel} \text{ cm}^{-1}$	α^2	γ	A_{\parallel} / γ ($\times 10^4$)
Methemoglobine	2.054	2.208	0.0201	0.86	4.0	50.25
Ferrinyoglobin pH=10.4	2.046	2.186	0.0190	0.78	4.2	45.2
Cytochrome C	2.05	2.216	0.0183	0.79	4.5	40.8
Human Carbonic Anhydrase	2.071	2.255	0.0163	0.81	4.26	38.3
Myoglobin	2.069	2.328	0.0162	0.85	4.9	33.06
Transferrin	2.053	2.231	0.0145	0.69	4.5	32.2
Ferrinyoglobin pH=6.4	2.054	2.273	0.0165	0.80	5.2	31.7
Phosphatase (Alkaline)	2.05	2.27	0.0165	0.79	5.6	29.5
Carboxypeptidase-A	2.057	2.327	0.0124	0.73	5.9	21.0

Copper Proteins (nonblue copper) Type-II	g_{\perp}	g_{\parallel}	$A_{\parallel} \text{ cm}^{-1}$	α^2	γ	A_{\parallel}/γ ($\times 10^4$)
Phthalocyanine	2.045	2.165	0.022	0.83	3.8	57.9
Laccase (<i>Polyporus versicolor</i>)	2.063	2.243	0.0194	0.85	4.17	46.5
Ceruloplasmin II	2.06	2.247	0.0189	0.84	4.24	44.6
Laccase II (<i>Rhus vernicifera</i>)	2.053	2.237	0.020	0.85	4.63	43.2
L-triptophan-2,2'-dioxigenase	2.065	2.265	0.017	0.81	4.20	40.0
Superoxide dismutase II pH=7.0	2.056	2.235	0.0175	0.79	4.33	40.0
Neurocuprein pH=7.1	2.06	2.27	0.0175	0.72	4.64	37.7
Dopamine- β -hydroxylase	2.056	2.282	0.017	0.82	5.05	33.6
Diamine oxidase	2.06	2.29	0.016	0.80	4.89	32.7
Superoxide dismutase I pH=12.0	2.062	2.263	0.014	0.72	4.37	32.0
Neurocuprein I pH=3.5	2.07	2.36	0.014	0.82	5.28	26.5

Table 5

Copper Proteins (blue copper) Type-I	g_{\perp}	g_{\parallel}	$A_{\parallel} \text{ cm}^{-1}$	α^2	γ	A_{\parallel}/γ ($\times 10^4$)
Ceruloplasmin	2.05	2.206	0.0074	0.47	4.27	17.38
Plastocyanines	2.05	2.23	0.0060	0.46	4.77	13.42
Asurins	2.06	2.26	0.0060	0.50	4.47	13.42
Laccase I (<i>Polyporus versicolor</i>)	2.03	2.19	0.0090	0.49	6.78	13.27
Laccase II (<i>Rhus vernicifera</i>)	2.047	2.298	0.0043	0.48	6.2	6.94
Umecyanin	2.05	2.317	0.0035	0.48	6.6	5.3

quantity Δ . It was found that while ligating number decreases, γ -increases from $\gamma \approx 4$ (for weak tetragonal distortions of octahedron) until $\gamma \approx 6.6$ (for square planar arrangements of ligands). We have obtained values for α^2 , γ and A_{\parallel}/γ . The results are shown in Tables. For model systems, when ligating with copper atoms are N-atoms γ -value is less than γ -value for oxygen. So that A_{\parallel}/γ value is inverse. Nitrogen atoms in comparison with oxygen atoms have great striving to create covalents coupling. This accounts for small value α^2 for N-complexes, in comparison with O-complexes, this also accounts for small value γ for nitrogen ligands [2].

In Tables copper complexes only with axial symmetry of ligands field were presented though it should be noted that in case of variation of pH solutions all three parameters will

be changed. It seems to be connected with charge redistributions and with such conformational variations of macromolecule when internal crystalline field is still axial.

In the case of protein models and macromolecules, also with Cu(II) substituted proteins α^2 -values changes within (0.86-0.68), and γ within (2.93-5.9). In the case of copper proteins region variation of these parameters is large, in our opinion it should be connected with great degree delocalizations of uncoupled electrons, also tetragonal distortions of symmetry.

Recent investigations showed, that in "blue" proteins small value of hyperfine splitting and large value of anisotropy γ -factors were connected with coordinating atoms of sulphur with copper ions [6].

It should be noted that in contrast to copper proteins and ferments, the parameters of ESR spectrum "blue copper" are not observed in any model systems. This indicates that the ligand atoms create rigid matrix, in which copper ion involves "unusual" state, it might define the functional loading of ion. It could be assumed that inclusion of "blue" coppers into the structure of copper proteins and ferments occurs immediately in process of forming their secondary or third structures. It leads to the unusual state of ion. As regards to "nonblue" coppers, it could be included into proteins structure later. It is confirmed by availability of ESR of model systems identical spectra of ESR of this copper.

Tbilisi I. Javakhishvili State University

REFERENCES

1. I. F. Boas, I.R. Pilbrow, and T.D. Smith. ESR of copper in Biological Systems: in-Biological Magnetic Resonance (ed. L.I.Berlin and I. Reuben.) 1,1978, 277.
2. G. Malmstrom, T. Vanngard. *Molecul.Biol.*2, 1960, 118-124.
3. A. S. Brill, G.F. Bryce. *Chem. Phys.* 48, 1968, 4398.
4. D. Kivelson, R.Neiman. *Chem. Phys.* 35, 1961, 149.
5. E. I. Neiman, I.M.Zarizki. *Sverkhprovodimost. Fizika, khimia, tekhnika.* 2, 4, 1989, 63-66.
6. A. P. Kalverda A.P.,Salgado I., Dennison C. and Canters G. *Biochemistry* 35, 1996, 3085.

M. Melikishvili, G. Mikadze, L. Visochev, Academician M. Zaalishvili

Thermal Denaturation of Rabbit Gastric Muscle Tropomyosin

Presented July 31, 1997

ABSTRACT. By the microcalorimetry method the structural stability of rabbit gastric muscle tropomyosin has been studied. It has been established that while the physiological values of ionic strength the molecule of tropomyosin is on the verge of melting and that the unfolding of molecule is a multisteped process with three pronounced peaks, which indicates that there are at least three structural areas in the molecule of rabbit gastric muscle tropomyosin which differ from each other by thermostability and hence they are characterized by the different molecular structural particularities.

Key words: TROPOMYOSIN, GASTRIC MUSCLE, SKELETAL MUSCLE.

Tropomyosin consists of two α -helical subunits which are interlaced with each other and form "coiled-coil" (bihelical) structure [1]. Privalov and Potekhin basing on structural particularities of tropomyosin molecule obtained by investigation of its thermal denaturation offered the blocking structure model for α -chains of skeletal muscles [2]. This model is represented by seven co-operated blocks in which the neighbouring blocks cause destabilization of each other. The three central blocks including the 127-190 residues are less stable than the others. The conformation of this part of tropomyosin molecule is determined by the condition of Cys-190 residue [2].

The conformational particularities of rabbit gastric muscle tropomyosin molecule and the stability of its structure while its thermal denaturation has been studied using the microcalorimetric method. Tropomyosin was obtained according to Drabikowsky et al. [3]. The reduction of tropomyosin and then 1) the blocking of its SH-groups by iodacetamide or 2) the forming of disulphide cross-links by 5,5'-dithiobis(2-nitrobenzoat)-(NbS)₂ has been carried out according to Lehrer [4].

Calorimetric measurements were done on the adiabatic scanning microcalorimeter DASM-I which was constructed by Privalov [2]. The heating rate was 0.25 or 1 degree in a minute, the concentration of proteins in different experiments was 0.25 or 1 degree in a minute, the concentration of proteins in different experiments varied in the range of 2-3 mg/ml. The error in the definition of transition of enthalpy doesn't exceed 10%.

While the melting of rabbit gastric muscle tropomyosin at neutral values of pH the curves of heat capacity have three peaks with characteristic temperature T_{m1} , T_{m2} and T_{m3} at 0.6 M KCl as well as at 0.15 M KCl (Fig. 1). These transitions indicate that in the rabbit gastric muscles tropomyosin there are at least three structural areas (three cooperative blocks) which differ from each other by their thermostability and hence they are characterized by the different molecular structural particularities. The

electrostatic forces between the charges on the surface of protein molecule obviously play significant role in the structure of tropomyosin. As the comparison of protein

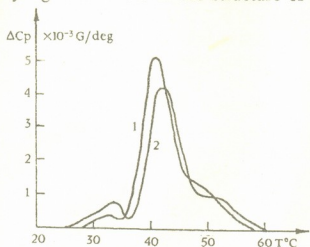


Fig. 1. The change of relative heat capacity of rabbit gastric muscle tropomyosin in 0.15M KCl (I curve) and 0.6M KCl (II curve). Buffer: 10mM tris -HCl, pH 7.5; the concentrations of both samples were 3 mg/ml; heating rate $-0.25^{\circ}\text{C}/\text{min}$

melting thermogrames in solutions of different ionic strength shows that the increasing of ionic strength as well as in the case of skeletal muscle tropomyosin [5] helps to separate structure areas mentioned above. We can suppose that the structure "loosens" (Fig. 1). In this case the thermal interval increases (in our case it was 4°C) and maximums part from each other (Table). The increasing of ionic strength in protein solution causes the more stability of molecule ($2-3^{\circ}\text{C}$). Thus K^{+} -ions effect not only on the ability of polymerization of molecule [6] but also on the condition of each molecule.

Table

Thermodynamic parameters of thermal denaturation of rabbit gastric muscle tropomyosin

Subject	$T_{m1}(^{\circ}\text{C})$	$T_{m2}(^{\circ}\text{C})$	$T_{m3}(^{\circ}\text{C})$	$T_{m4}(^{\circ}\text{C})$	$\Delta T(^{\circ}\text{C})$	$\Delta H_{\text{cal}}(\text{G/g})$
tropomyosin in 0.15 M KCl	33.0 ± 0.5	41.6 ± 0.5	49.0 ± 0.5		30.0 ± 0.5	15.0 ± 1.2
tropomyosin in 0.6 M KCl	33.6 ± 0.5	42.3 ± 0.5	52.3 ± 0.5		34.0 ± 0.5	12.0 ± 1.0
tropomyosin blocked by iodacetamide	38.6 ± 0.5	46.6 ± 0.5	53.7 ± 0.5		30.5 ± 0.5	17.0 ± 0.8
tropomyosin bounded by S-S links	35.8 ± 0.5	47.6 ± 0.5	55.6 ± 0.5	63.0 ± 0.5	35.4 ± 0.5	11.0 ± 0.5

From Fig. 1 we can see that rabbit gastric muscle tropomyosin shows low temperature transition in the range of $20-40^{\circ}\text{C}$ as well as rabbit skeletal and heart muscle tropomyosins [5, 7] and thus differs from chicken gastric muscle tropomyosin which doesn't exhibit the low temperature transition up to the main helix unfolding transition. In the ranges of experimental error it is impossible to find the region in the chicken gastric muscle tropomyosin which locally melts earlier than its main "helix-coil" transition [8]. It is considered that the molecule of chicken gastric muscle tropomyosin is more rigid than striated and heart muscle tropomyosin molecule [8]. As we have already seen the rabbit gastric muscle tropomyosin molecule melts in the range of three temperatural intervals. It is possible that these transitions are not just the transitions between two conditions but they indicate the unfolding of some structural regions, that have similar transitive temperatures. The existence of region with different stability like the skeletal muscle gives the significant flexibility to the rabbit gastric muscle tropomyosin molecule.

The skeletal muscle tropomyosin contains two types of α -helical polypeptide chains α and β . β -chain includes two Cys at 36 and 190 positions and one α -chain at 190



position [1]. In molecule both chains exist in helical register as the disulphide crosslinks between the cystein residues of these subunits are formed by $(\text{NbS})_2$ (the formation of links by $(\text{NbS})_2$ needs close proximity of two SH-groups) [4]. The chicken gastric muscle tropomyosin contains these two chains too but it doesn't form crosslinks [8] because the β -chain of this tropomyosin includes only one cystein residue in 36 position, and in α -chain cystein is localized in 190 position.

Fig. 2 represents the curves of thermal denaturation which are characteristic for rabbit gastric muscle tropomyosins blocked with iodacetamide and bounded by disulphide crosslinks of $(\text{NbS})_2$. The unfolding of tropomyosin blocked by iodacetamide shows three transitions while in the same conditions for the tropomyosin crosslinked by $(\text{NbS})_2$ the four transitions with corresponding T_{m-s} are observed (see the Table). The forming of crosslinks in tropomyosin molecule causes its stabilization (Fig. 2, Table) that coincides with literature data [2,5].

As Fig. 2 and the Table show the bounding by crosslinks increases not only the value of T_{m2} (which mainly corresponds to the unfolding of C-half of molecule [5] but also the value of T_{m3} (the unfolding of N-half) unlike to skeletal muscle tropomyosin in which the value of T_{m3} doesn't change [2,5]. It indicates that in the rabbit as well as in the N-half unlike the skeletal muscle tropomyosin where S-S links are formed only in C-half of molecule (at Cys-190) [4,5].

Analysis of thermal denaturation data of rabbit gastric muscle tropomyosin allows the supposition that while the physiological values of ionic strength the molecule of tropomyosin is on the verge melting and that the unfolding of rabbit gastric muscle tropomyosin is multisteped process with pronounced peaks. We can suppose that those definite

transmissions also reflect the subunit consistence of tropomyosin. These transmissions must be significant for the localization of interaction places with other components of contractile system on the tropomyosin molecule:

Institute of Molecular Biology and Biological
Physics, Georgian Academy of Sciences

REFERENCES

1. F. H. C. Crick. *Acta Crystallogr.*, 5, 1953, 689-697.
2. S. A. Potekhin, P. L. Privalov. *J. Mol. Biol.*, 159, 1982, 519-535.
3. W. Drabikowski, S. Dabrowska, B. Barylko. *Acta Biochem. Polonica*, 20, 1973, 1281-199.
4. S. S. Lehrer. *Proc. Nat. Acad. Sci. USA*, 72, 1975, 3377-3381.
5. D. L. Williams, Ch. A. Swenson. *Biochemistry*, 20, 1981, 3856-3864.
6. P. Johnson, L. B. Smillie. *Biochemistry*, 16, 1977, 2264-2269.
7. D. R. Betteridge, L. B. Lehrer. *J. Mol. Biol.*, 167, 1983, 481-496.
8. S. S. Lehrer, D.R. Betteridge, P. Graceffa, S. Wong, J. C. Seidel. *Biochemistry*, 23, 1984, 1591-1595.

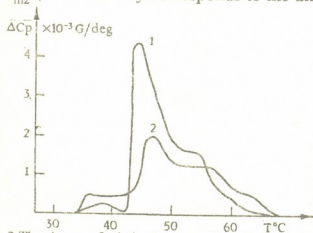


Fig. 2. The change of relative heat capacity of rabbit gastric muscle tropomyosin: 1 - tropomyosin blocked with iodacetamide; 2 - tropomyosin bounded by disulphide cross-links

Buffer: 1.0M NaCl, 1 mM EDTA; 0.05M Ná-phosphate, pH-7.4; the concentrations of samples were 2.3 mg/ml (I curve) and 1.9 mg/ml (II curve); heating rate-10°C/min

J.Gogorishvili, R.Sujashvili, Academician M.Zaalishvili

Some of the Physico-Chemical Properties of Proteins Extracted from the Kidney by 0.5M KCl Solution

Presented July 24, 1997

ABSTRACT. pH 5.5 fraction of proteins extracted from the rabbit kidney by 0.5M KCl solution has been studied by using superprecipitation, enzyme and viscometry methods. The fraction has not proved properties typical of myosin and actomyosin either in the presence or in the absence of skeletal muscle F-actin. The facts would be caused by the absence of calmodulin dependent light chain kinase in the fraction. The kinase is necessary for activation of thymus, platelet and some kinds of vertebrate smooth muscle myosin.

Key words: SUPERPRECIPITATION, MYOSIN, ACTOMYOSIN.

In regard to Nakayama [1] actomyosin like protein "Renosin" participates in osmotic functioning of kidney. Relying on [2] myosin-like and actomyosin-like proteins are in liver and thyroid gland and myosin-like protein is in pancreas. According to all available data Poglasov has made suggestion, that myosin-like proteins are responsible to support the tone of every cell, as well as to regulate permeability of cells [2]. Relying on investigations in [3] regulation of liver mitochondrial osmotic processes is not conditioned by actomyosin, but it is conditioned by inositolphosphatide and non-myosin ATP-ase. Relying on this and proper data [4] we have a doubt if it is actomyosin participating in the regulation of osmotic activity of kidney.

Myosin-like protein has been isolated from rabbit kidney by 0.5M KCl solution [2], with the difference that duration of extraction is 24 h instead of 20 min with the object of increasing protein yield. Superprecipitation ability of pH 5.5 fraction is obtained at 550 nm wave length by increasing of the optical density at different meanings of pH and in the presence or in the absence of Mg^{2+} , Ca^{2+} ions and rabbit skeletal muscle F-actin. ATP-ase activity is calculated from the released terminal phosphate according to [5] under the above mentioned conditions. The rabbit skeletal muscle actin was prepared according to [6] and it was transferred to F-actin by adding KCl up to the final concentration 0.1M. Viscometry tests were carried out by Ostwald viscometer, protein concentration was measured by using Biuret reagent.

The main property of myosin and actomyosin is precipitation under conditions of low ionic strength without adding of ATP. This effect is caused by kinetic lability of myosin and actomyosin particles. Kidney pH 5.5 fraction proteins have the same property, but with the difference that the suspended fractions are very small from the beginning and it makes impression of solution. Optical density of the colloidal system decreases within 5 min (Fig. 1) and it is accompanied with the formation of coarse aggregations. At any

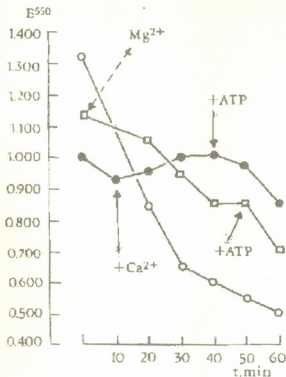


Fig. 1. Precipitation of pH 5.5 fraction dissolved in 0.05M KCl solution with falling optical density. Reaction area: 0.05M KCl, 0.01M tris - HCl (pH 7.0), CaCl_2 and MgCl_2 - 1mM, ATP - 1mM. $t = 20^\circ\text{C}$.

meaning of pH (6.0; 7.0; 8.0; 9.0) we have used, the above mentioned effect takes place (Fig. 1 shows the results obtained at pH 7.0 as typical instances). The dependence of optical density on fraction size has been formulated [7]:

$$E = KCl \frac{d^3}{d^4 + \alpha \lambda^4}, \quad (1)$$

where: E is optical density; K and α are constants, depended on suspension properties; C particles concentration; l thickness of suspension (cuvette width); d particles sizes; λ wave length.

For the first time, the formula has been used by us for description of volumetric changes of mitochondria [8], as long as relying on electron-microscopy studies [9] the dependence of volume of mitochondria on optical density has been established. According to the (1) formula (as to mitochondria) decrease of optical density is in accordance with swelling of mitochondria. Just as for the kidney pH 5.5 fraction, with the difference that particles of this fraction form aggregates gradually up to some critical range and after all they fall out. The particles dissolve again after stirring and initial optical density is restored. This effect is not observed in suspension of mitochondria.

Above mentioned relationship has not been changed by adding of ATP at any meaning of pH and there have not been observed any changes of optical density caused by particles striction and subsequent aggregation with overlapping of light fleet pathway.

It is certainly interesting that Ca^{2+} and pH 5.5 fraction interaction in the absence of ATP at each meaning of pH (6.0-9.0) leads to increase from the outset and then decrease

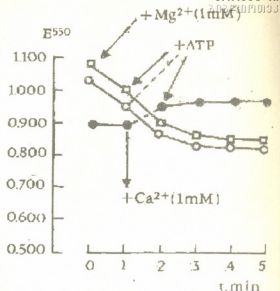


Fig. 2. Change of optical density of pH 5.5 fraction - F-actin mixture in 0.05 M KCl - solution. Reaction area: 0.05M KCl, 0.01M Tris - HCl (pH 7.0), ATP - 1mM; protein concentration: 1.6 mg/ml (ratio of pH 5.5 fraction: F-actin 4:1). $t = 20^\circ\text{C}$.

Table 1

Kidney pH 5.5 fraction ATP-ase activity at pH 6.0 and pH 7.0 in different conditions.Reaction area: 0.05M KCl, 0.01M tris - HCl or 0.1M succinate (pH 6.0) $t = 20^{\circ}\text{C}$

Protein concentration: 1.6 mg/ml or 2.1 mg/ml (together with F-actin) ATP - 5 mM

Protein	pH	added bivalent ions	ATP-ase activity $\mu\text{M Pi/mg.min.}$
1. pH 5.5 fraction	6.0	-	0.0014
2. pH 5.5 fraction + F-actin	6.0	-	0.0013
3. pH 5.5 fraction	6.0	2.5mM Mg^{2+}	0.0020
4. pH 5.5 fraction + F-actin	6.0	2.5mM Mg^{2+}	0.0010
5. pH 5.5 fraction	6.0	2.5mM Ca^{2+}	0.0023
6. pH 5.5 fraction + F-actin	6.0	2.5mM Ca^{2+}	0.0018
7. pH 5.5 fraction	7.0	-	0.0014
8. pH 5.5 fraction + F-actin	7.0	-	0.0014
9. pH 5.5 fraction	7.0	2.5mM Mg^{2+}	0.0020
10. pH 5.5 fraction + F-actin	7.0	2.5mM Mg^{2+}	0.0016
11. pH 5.5 fraction	7.0	2.5mM Ca^{2+}	0.0023
12. pH 5.5 fraction + F-actin	7.0	2.5mM Ca^{2+}	0.0018

Table 2

Kidney pH 5.5 fraction ATP-ase activity at pH 8.0 and pH 9.0 in different conditions.

Reaction area: 0.05M KCl; 0.01M tris - HCl. ATP - 5 mM

Protein concentration (see Table 1). $t = 20^{\circ}\text{C}$.

Protein	pH	added bivalent ions	ATP-ase activity $\mu\text{M Pi/mg.min.}$
1. pH 5.5 fraction	8.0	-	0.0005
2. pH 5.5 fraction + F-actin	8.0	-	0.0006
3. pH 5.5 fraction	8.0	2.5mM Mg^{2+}	0.0029
4. pH 5.5 fraction + F-actin	8.0	2.5mM Mg^{2+}	0.0029
5. pH 5.5 fraction	8.0	2.5mM Ca^{2+}	0.0009
6. pH 5.5 fraction + F-actin	8.0	2.5mM Ca^{2+}	0.0009
7. pH 5.5 fraction	9.0	-	0.0009
8. pH 5.5 fraction + F-actin	9.0	-	0.0009
9. pH 5.5 fraction	9.0	2.5mM Mg^{2+}	0.0044
10. pH 5.5 fraction + F-actin	9.0	2.5mM Mg^{2+}	0.0030
11. pH 5.5 fraction	9.0	2.5mM Ca^{2+}	0.0104
12. pH 5.5 fraction + F-actin	9.0	2.5mM Ca^{2+}	0.0050

Table 3

Study of kidney pH 5.5 fraction and pH 5.5 fraction - F-actin mixture viscometricallyReaction area: 0.6M KCl; 0.01M tris - HCl (pH 7.0) $t = 20^{\circ}\text{C}$

Protein and added components	Protein concentration mg/ml	η/η_0
1. Kidney pH 5.5 fraction	10.0	1.2
2. pH 5.5 fraction + + 2.5 mM Mg^{2+} + 1mM ATP	10.0	1.2
3. pH 5.5 fraction + F-actin + + 2.5 Mg^{2+}	12.5	2.9
4. pH 5.5 fraction + F-actin + + 2.5mM Mg^{2+} + 1mM ATP	12.5	2.9



of the optical density (Fig. 1). The fact agrees with above mentioned data. As to optical density - character of the phenomena is not clear yet.

Proceeding from Scholey et al. [10] studies of thymus soluble myosin, we may suppose that Ca^{2+} ions lead to aggregation of kidney pH 5.5 fraction soluble myosin without adding of calmodulin-dependent light chain kinase. pH 5.5 fraction optical density decreases after adding of ATP in the presence of Mg^{2+} and Ca^{2+} ions within the pH 6.0-9.0 range (Fig. 1). These studies confirm the absence of actomyosin in the fraction. Therefore it became necessary to study influence of F-actin. Above mentioned relationships have not been changed after adding of rabbit skeletal muscle F-actin, i.e. there is no myosin-like protein in the pH 5.5 fraction (Fig. 2).

Myosin has two maxima of fermentation activity - at pH 6.2 and at pH 9.0. But the special activity it shows at pH 9.0 [2]. ATP-ase as a component of actomyosin has optimum of activity in neutral medium [2].

We have investigated pH 5.5 fraction ATP-ase activity in the presence and in the absence of skeletal muscle F-actin and have established that the fraction has optimality of ATP-ase activity at pH 9.0 in the presence of Mg^{2+} ions as well as Ca^{2+} ions (see Tables 1,2). But this fact nevertheless does not verify the presence of myosin-like protein in the fraction, because firstly it does not prove maximal activity at pH 6.0 and secondly, Mg^{2+} ions have not been able to suppress fermentation activity which is low anyway (in comparison with muscle myosin). pH 5.5 fraction ATP-ase activity has not been increased by F-actin and typical of actomyosin optimum at pH 7.0 has not been mentioned either.

We have investigated kidney pH 5.5 fraction viscometrically to get supplementary information. It turns out the fraction has not revealed relationships typical to actomyosin in the presence of rabbit skeletal muscle F-actin (see Table 3). Hence, the presence of myosin- and actomyosin-like proteins in the kidney has not been corroborated by methods Poglasov [2] used and it is not confirmed by method of superprecipitation either. It is necessary to investigate influence of calmodulin dependent myosin light chain kinase in order to clear out whether myosin soluble form is available in liver and in kidney.

Institute of Molecular Biology & Biological Physics
Georgian Academy of Sciences

REFERENCES

1. O.Nakayama. The Japanese Circulation J., **22**, 1958, 641
2. B.F.Poglasov. J. Biochemistry, **271**, 1962, 161-166 (Russian)
3. P.M.Vignais, P.V.Vignais, A.L.Lehninger. Biochem. Biophys. Res. Commun., **11**, 1963, 313.
4. J.A.Gogorishvili, M.M.Zaalishvili. Bull.Acad.Sci.Georg. SSR, **50**, N 3, 1968, 649-654. (Russian)
5. J.C.Turakulov, L.J.Curgulceva, A.J.Gagelanz. J. Biochemistry, **32**, 1967, 106-110 (Russian)
6. F.B.Straub. Stud.Inst.Med.Chem.Univ.Szeged, **2**, 1, 1942.
7. D.C.Jou. Nefelometriya. M.-L. 1936 (Russian)
8. J.A.Gogorishvili. Candidate thesis, Tbilisi, 1968 (Russian)
9. H.Tedeshi, D.L.Harris. Archives of Biochemistry and Biophysics, **58**, 1, 1955, 52-67.
10. J.M.Scholey, K.A.Taylor, J.Kednick-Jones. Nature, **287**, 1980, 233-235.



L.Shanshiashvili, Ch.Todadze, I.Chogovadze, N.Natsvlishvili, G.Lezhava, D.Mikeladze

The Influence of Toluene and Ethyl Alcohol on Opiate and Dopamine Receptor Activity in Rat Brain.

Presented by the Corr.Member of the Academy V.Mosidze, September 25,1997

ABSTRACT. It has been shown that chronic ethanol and toluene treatment of rats gave similar results on the activity of dopamine and opioid receptors. It was found that both substances reduce the density of D_2 -dopamine receptors in *Nucleus accumbens* and *Globus pallidus*. In addition, it was shown that both treatments upregulated α and μ opioid receptors and downregulated δ opioid receptors in hippocampus. These results suggested that toluene-like ethanol has addictive properties and may be used by abusers.

Key words: ETHANOL, TOLUENE, D_2 -RECEPTOR, OPIOID RECEPTORS, ADDICTION.

Nucleus accumbens is the basic structure participating in drug addiction [1-3]. Since it is a structure taking part in emotional, motivational and memory processes, as well as drug dependency and the reinforcement behavior connected with them are mainly supposed to be the result of *Nucleus accumbens* hyperactivation [4].

The increase of dopaminergic activity in mesolimbic system has been known to determine opiate receptor changes in the structure of cerebral cortex and limbic system [5]. Besides, opiate antagonists like dopamine antagonists have been detected to suppress the euphoria caused by drugs with different activities [6], which is suggestive of the stable interaction between central dopaminergic and opiate structures in the formation of drug addiction phenomenon. Thus, the aim of our work was first to define if toluene belongs to the substances which cause dependency, second, if it influenced other dopaminergic structures, namely psychogenic ones and third, what kind of relationship dopaminergic and opiate structures had in the process of the formation of toluene and alcohol addiction.

Receptors of rat brain which show genetical attraction to alcohol have been studied. Simultaneously, there have been carried out tests on rats, whose alcohol-dependency is conditioned by influence of biological and "social" factors. Comparative study of alcohol and toluene was resulted by the fact that both substances belong to the organic solvents, though they have different strength. At the same time in definite conditions alcohol cause such mental changes which are like mental changes caused by toluene.

Wistar male rats with weights varying from 250 to 300gr were used in the experiments. The rats were put into separate cages and were given normal ration of food (NOR-rats). Later on, those individuals, that had genetical attraction to ethyl alcohol and basically drank only 15% alcohol, had been selected. After selection the animals were

receiving 15% ethyl alcohol with normal food ration during 30 days (ALC-rats). The second group of rats underwent toluene inhalation until they attain lateral posture during 30 days, three times a week, in all 12 periods (TOL-rats). After decapitation the brain was frozen at 30⁰ and hippocampus, *Globus pallidus* and *Nucleus accumbens* were separated.

The 10% homogenate in 0.3 mol/l sucrose solution was prepared from brain structures. After the centrifugation of homogenate 1000 x g the supernatant was centrifugated again during 2000 x g 30 min. The sediment, suspended in Tris-HCl buffer (50 mmol/l, pH 7.4), was used for the radioligand analysis.

D₂-receptor activity was defined in incubation medium 0.2 ml of which contained 100 mkg of membrane preparation, 3 mmol/l of MgCl₂, 50 mmol/l of Tris-HCl buffer, pH 7.4 and 1 nmol/l ³H-spiroperidol (20 ci/mmol, *Amersham*). Nonspecific binding was determined in the presence of 100 nmol/l sulpiride. For the determination of the opioid receptor 5 nmol/l ³H-naloxone (25 ci/mmol, *Amersham*) was added into incubation medium instead of spiroperidol. In order to determine μ , κ and δ -subtypes of opioid receptor 100 nmol/l levorphanol, 100 nmol/l ethylketocyclazocine and 100 nmol/l naloxone were correspondingly introduced into incubation medium. In the last case, the obtained number of binding sites was subtracted from the number of binding sites obtained with ethylketocyclazocine and levorphanol, which equaled to δ -subtype number. After 60 min incubation of membrane, the mixture was filtered through Whatman GF/C filters. After washing the filters radioactivity was counted on scintillation counter.

In order to define brain dopaminergic system activity *Nucleus accumbens* and *Globus pallidus* have been studied. The last one participates in the formation of psychotic phenomena [7].

The radioligand analysis of the above-mentioned structures revealed that ethyl alcohol and toluene provoke significant changes of dopaminergic activity.

Table 1

The quantitative changes of D₂-dopamine receptor in rat brain dopaminergic structures after treatment the animals with ethanol and toluene.

Animal groups	D-dopamine receptor quantity			
	Globus finol/mg	pallidus %	Nucleus fmol/mg	accumbens %
NOR-rats	147±7	100	82±5	100
ALC-rats	150±7	101	49±3*	61
TOL-rats	126±6*	85	44±3*	54

* p < 0.05

As it has been shown in Table 1, ethanol (ALC-rats) doesn't change D₂-receptor quantity in *Globus pallidus*, while it significantly decreases in rats (TOL-rats) after their inhalation with toluene (85%). Unlike *Globus pallidus*, under the influence of both dissolvents D₂-receptor activity sharply decreased (ALC-rats - 61%, TOL-rats - 54%).



Unlike ethanol, toluene causes the decrease of the number D_2 -dopamine binding sites in both experimental brain structures. This testifies that toluene influence provokes the hyperactivation of both dopaminergic structures thus causing D_2 -dopamine receptor desensitisation or "down regulation". This kind of desensitisation of dopamine receptors takes place after the chronic injection of rats with amphetamine [8], morphine [9], alcohol and cocaine [4], thus causing the degenerative changes of dopamine neurons for some definite time [10]. It has been ascertained, that initially dopaminergic hyperactivation, and later receptor desensitisation and dopamine depletion in *Nucleus accumbens* is the neurochemical basis of drug-dependency [3]. This effect of toluene in both structures indicates that its activity can be expressed in the formation of addictive reactions as well as in brain psychotomimetic activation and in the formation of hallucination.

Since brain dopaminergic neurons are closely related to opiate system, opiate receptor changes influenced by ethanol and toluene have been detected in further experiments. Obtained data show that alcohol drinking causes insignificant increase of μ -opioid receptors (108%), comparatively significant increase of κ -opioid receptors (118%) and sharp decrease of δ -opioid receptors (82%) (Table 2).

Table 2

Quantitative changes of opiate receptors of (μ , κ , δ)-subtypes in rat brain hippocampus after the chronic treatment with ethanol and toluene.

Animal groups	Opioid receptor subtypes					
	μ		κ		δ	
	fmol/mg	%	fmol/mg	%	fmol/mg	%
NOR-RATS	45.4±3.4	100	48.9±3.5	100	9.3±0.2	100
ALC-RATS	48.9±3.8	108**	57.1±4.2	**118	7.1±0.2	*82
TOL-RATS	54.1±4.1	120*	52.5±4.1	*109	8.4±0.3	**91

$M \pm m$ (n=6) *p < 0.05 **p < 0.1

After the inhalation with toluene the picture of receptor activity was the same with one distinction that μ -receptors sharply increased (120%).

Obtained data indicate that the substances provoking the changes of brain dopaminergic systems, also affect opiate receptors. It should also be noted, that unlike other opiate receptors, but like D_2 -dopamine receptor, δ -opioid receptor undergoes desensitisation under the influence of organic solvents. Since above-mentioned receptors are often localized on one structure, their distribution in brain is similar, they are closely related to each other [1] and that is why the increase of dopamine as well as enkephalin quantity in definite regions is assumed to be the basis of addictive phenomenon.

Thus according to the obtained data, D_2 -dopamine receptor, that perceives ventrosegmental projection motivated strengthening reactions in *Nucleus accumbens*, simultaneously activates with δ -opioid receptor in hippocampus. The last one partici-

pates in the formation of the behavioral reactions [11] and that is why their coordinated desensitisation may be the basis of the behavioral disorders connected with drug addiction.

This work was supported by research Grant N15-3 from the Georgian Academy of Sciences.

I. Beritashvili Institute of Physiology
Georgian Academy of Sciences
Institute of Addiction
Georgian Ministry of Health

REFERENCES

1. R.R. Goodman, S.H. Snyder et al. Proc. Natl. Acad. Sci. USA. 77, 1980, 6239-6243.
2. F.E. Pontieri, G. Tanda et al. Nature, 382, 1996, 255-257.
3. B. Everitt. MRC News, 71, 1996, 11-15.
4. Z.L. Risetti, F. Melis et al. Ann. N.Y. Acad. Sci. 654, 1992, 513-516.
5. M.E. Unterwald, J.M. Rubinfeld, M.J. Kreek. Neuroreport, 5, 1994, 1613-1616.
6. A.A. Houdi, M.R. Bardo, G.R. Van Loon. Brain Res., 497, 1989, 195-198.
7. L. Mrzijak, C. Bergson et al. Nature, 381, 1996, 245-248.
8. E.B. Nielsen, M. Nielsen, C. Breastrup. Psychopharmacol. 81, 1983, 81-85.
9. E. Acquas, E. Carboni, G. Di Chara. Eur. J. Pharm. 193, 1991, 133-134.
10. L.R. Steranka, E. Sanders-Bush. Eur. J. Pharmacol., 65, 1980, 439-443.
11. W.D. Blaker, G. Peruzzi, E. Costa. Proc. Natl. Acad. Sci. USA. 81, 1984, 1880-1882.

G. Gigolashvili, T. Dalalishvili, Corr.Member of the Academy D. Jokhadze

Comparative Study of Some Varieties of Mulberry Trees (*Genera Morus*) by the Method of Isoelectric Focusing

Presented September 15, 1997

ABSTRACT. Interspecific difference between *M. alba* and *M. nigra* and between *M. alba* var. GrusNIISH-4 and *M. nigra* var. Hybrid-2 have been shown by the isoelectric focusing of mulberry bud proteins. However difference at least of three kinds of protein is same in both species. At least one variety-specific protein for each varieties of *M.alba* have been observed.

Key words: MULBERRY, BUD PROTEIN ISOELECTRIC FOCUSING, VARIETY SPECIFIC PROTEINS.

The study of nature of the genetical origin in living organisms has great theoretical and practical importance. On one hand it makes possible to state their origin, their evolutionary congenerity among individuals and on the other hand it promotes us to foresee effective means and way to transform them for the benefit of man, that is the only way to success. The methods of molecular biology and molecular genetics outlined new possibilities and some important results have been received.

At molecular biological characterization of genetical origin of the organisms the main attention is paid to the hereditary material substrate-nucleic acids and to the end product of genome functioning - proteins. Hence the morphological conjugation of genome action and protein biosynthesis according to any protein peculiarities we can judge about corresponding genes as well as about the gene groups or finally about the whole chromosome.

Recently cultivated plants have been successfully studied by the method of comparative genome analysis. The data we received concern annual plants [1-3]. Perennial plants have been less studied.

The goal of the paper is to study a very important for Georgia, cultivated plant - mulberry tree (*genera Morus*). The leaves of this plant are the only food for bombyx and whole silkworm breeding is based on it. Five species of *genera Morus* are used in sericulture - *M. alba* L., *M. nigra* L., *M. multicaulis* Perr., *M.bombycis* Koidz. and *M. kagajamae* Koidz. [4].

At present we tried to study two varieties of *M.alba* -GruzNIISH-4 and Hydroid-2 and one variety of *M.nigra* - Khartuta. Mainly we studied their protein content by the method of isoelectric focusing and analyzed the results in order to study the state, the peculiarities of forms and the level of the relation.

The mulberry buds were collected in winter and freezed to -15°C and homogenized with the cool acetone [5]. Homogenate was filtered and washed twice with cool acetone. The proteins were extracted from 50mg powdered samples by adding $400\ \mu\text{l}$ 0.01 M

phosphate buffer solution (pH 7.4), containing 0.1 M Na_2SO_3 , as a protease inhibitor. Extraction was carried out with gentle shaking at $+4^\circ\text{C}$. After extraction the samples were centrifuged at $10000 \times g$ for 5 min. The low molecular weight contaminants were removed from supernatant by the chromatography on the Sephadex G-25 column. Protein concentration was measured by Bradford [6]. Isoelectric focusing was carried out PhastGel

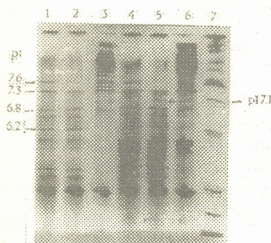


Fig.1 Isoelectric focusing of the mulberry shoot protein
M.alba-GruzNIISh-4 (N1-1 $\mu\text{g}/\text{per}$ sample; N4-2 $\mu\text{g}/\text{per}$ sample)
M.alba-Hybrid-2 (N2-1 $\mu\text{g}/\text{per}$ sample; N5-2 $\mu\text{g}/\text{per}$ sample)
M.nigra-Khartuta (N3-1 $\mu\text{g}/\text{per}$ sample; N6-2 $\mu\text{g}/\text{per}$ sample)
 N7-pI Marker protein

pI 3-9 (Pharmacia, Sweden) at 2000 V, during 500 volt hour. Silver staining of gels was carried out by Heikenshoven and Dernik [7].

Primarily it must be noted, that evident difference was stated between two species of mulberry trees – in both varieties of *M.alba* proteins of neutral and acidic nature predominate, while in *M.nigra* most of the proteins are of alkaline nature (Fig.1).

According to the electroforegrams three kinds of protein with isoionic pI 7.3, pI 6.8, pI 6.2 are found in all studied forms nearly in equal quantities. These proteins seem to be specific for the whole genera *Morus*.

The difference is observed in two studied *M.alba* varieties: protein pI 7.6 is found in GruzNIISh-4 and is not stated in Hybrid-2. At the same time Hybrid-2 obtains protein pI 7.1 which is not observed in the variety GruzNIISh-4. The rest of the proteins as it can be judged by electrophoregrams, are equal in the studied varieties, though some of them differ in quantity.

The above said two varieties of *M.alba* were received by interspecific hybridization [8], where female component was the variety *M.alba* -Cedrona for both varieties and male component for hybridization was *M.alba* -Cataneo for GrusNIISh-4 and *M.alba* -Tatarica for Hybrid-2. Issuing from studied varieties of mulberry trees must belong to *M.alba* - Cedrona (female component for both varieties) and specific proteins found in bud protein spectra of GruzNIISh-4 and Hybrid-2, corresponding to pI 7.6 and pI 7.1 - must be initiated respectively from *M.alba* - Catameo and *M.alba* - Tatarica.

Thus, on the ground of the bud protein electrophoretic spectra of the studied mulberry trees can be supposed that in this way it is possible to exhibit protein peculiarities, specific for genera, species and varieties. These data make possible not only to establish genetical transformation of the given object, but to plan effective selective work with the species as well.

REFERENCES

1. *V.G. Konarev*. Trudy po pryklad. botanike, genetike i selectsii, **52**, 1, 1973, 5-28 (Russian).
2. *V.L. Kretovich* (Red.) Rastitelnye belki I ikh biosintez. M., 1975 (Russian).
3. *A. Kh. Berulava*. Avtoref. cand. diss. Tbilisi, 1990 (Russian).
4. *G. Zviadadze*. Siakhleni tutis gvaris -*Morus L.* sistematikashi. Tbilisi, 1987 (Georgian).
5. *I. P. Gavriluk et al.* Trudy po priklad. botanike, genetike i selektsii, **52**, 1, 1973, 249-281 (Russian).
6. *R. Bradford*. Analytical Biochem. **72**, 2, 1976, 248-254.
7. *J. Heikenshoven, R. Dernik*. Electrophoresis, **6**, 1985, 103-112.
8. *G. Zviadadze, M. Shablovskaya, G. Japharidze*. Tutis selekcia. Tbilisi, 1964 (Georgian).



M. Jincharadze, G. Pruidze, N. Omiadze, N. Mchedlishvili.

Effect of Tea-Leaf Peptides on the Monophenol Monooxygenase and Catechol Oxidase Activities.

Presented by Corr. Member of the Academy D. Ugrekhelidze, August 25, 1997

ABSTRACT. The influence of tea-leaf peptides on the monophenol monooxygenase and catechol oxidase activities has been studied. It has been shown that the peptides have a regulatory effect on the leaf monophenol monooxygenase and catechol oxidase activities and at the same time affect the monophenol monooxygenase and catechol oxidase activities differently.

Key words: TEA-LEAF, MONOPHENOL MONOOXYGENASE, CATECHOL OXIDASE, PEPTIDE, MOLECULAR WEIGHT.

Monophenol monooxygenase (EC 1. 14. 18. 1.) and catechol oxidase (EC 1.10. 3. 2.) are enzymes widely distributed in the plant kingdom. They catalyse oxidative transformations of phenolic compounds. Previously these two enzymes were classified under one and the same code and considered to be a double function of enzyme catechol oxidase. According to the present-day nomenclature the two types of oxidative-reductive enzymes are strictly differentiated and classified separately: monophenol monooxygenases catalyze the hydroxylation of monophenols and dehydrogenation of o-diphenols, while catechol oxidases catalyze only the dehydrogenation of o-diphenols.

Tea-leaf monophenol monooxygenase and catechol oxidase activities were separated and their substrate specificity and properties were studied [1].

The intracellular localization and changes in tea leaf monophenol monooxygenase and catechol oxidase activities during plant vegetation period were studied [2,3]. Various factors regulating their activity were established. Low concentrations of gibberellic and ascorbic acids stimulated, while high concentrations of them inhibited the monophenol monooxygenase activity.

A regulator of phenolic nature increased monophenol monooxygenase activity; while oxidase is completely inhibited by its action. Amino acids and metal ions had different reaction [4].

The aim of the present work was to study the influence of peptides of different molecular weight (Mr) isolated from tea-leaves on the monophenol monooxygenase and catechol oxidase activities. From fresh tea-leaves the crude preparation of peptides was obtained and then fractionated by gelfiltration on sephadex G-15 column [5]. Peptides eluted from the column in amount of 0.1mg were added to the reaction mixture containing 0.1M citratephosphate buffer, 50 g enzyme and substrate. In the case of monophenol monooxygenase (substrate p-cresol) pH of the reaction mixture was 7.1, while pH for catechol oxidase (substrate catechol) was 5.3. The concentration of p-cresol was 2mM and catechol - 17mM [2,3]. Isolation of monophenol monooxygenase and catechol oxidase

from fresh tea leaves was carried out by the preliminary elaborated method [3].

The results are given in the Table. As it is seen from Table peptides are characterized by certain regulatory effects on tea-leaf monophenol monooxygenase and catechol oxidase. High molecular peptides (M_r 1000-5000) inhibit monophenol monooxygenase and catechol oxidase activities. The peptide with M_r 5000 has high inhibitory effect on these enzymes. It decreases monophenol monooxygenase and catechol oxidase activities by 41 and 51% respectively. The peptide with M_r 3700 strongly inhibits monophenol monooxygenase activity (by 50%) and comparatively weakly catechol oxidase activity (by 15%). The peptides with M_r s 1500 and 1200 inhibit only catechol oxidase and do not affect monophenol monooxygenase. Low molecular peptides (M_r 470-1000) act as activators, they affect mainly the monophenol monooxygenase activity. For example: the peptide with M_r s 840, increases the monophenol monooxygenase activity almost 2.5-fold, while catechol oxidase is slightly activated by its action. The peptides with M_r s 940, 700, 670 and 470 activate only monophenol monooxygenase and do not affect the catechol oxidase activity.

Table

Effect of tea-leaf peptides on the monophenol monooxygenase and catechol oxidase activities

Variant	Monophenol monooxygenase			Catechol oxidase		
	Specific activity $\Delta E/mg$ protein /min	Changes in the activity		Specific activity $\Delta E/mg$ protein /min	Changes in the activity	
		activation	inhibition		activation	inhibition
additive-free	0.14	-	-	7.80	-	-
the same "plus"						
peptide with M_r						
5000	0.08	-	41	3.59	-	54
3700	0.07	-	50	6.63	-	15
1500	0.14	-	-	7.80	-	-
1200	0.14	-	-	6.39	-	18
1000	0.14	-	-	6.79	-	13
940	0.20	45	-	7.80	-	-
840	0.33	136	-	9.59	23	-
700	0.22	57	-	7.80	-	-
670	0.21	50	-	7.80	-	-
560	0.19	36	-	7.80	-	-
470	0.22	57	-	7.80	-	-

Thus, it can be concluded that peptides have regulatory effect on tea-leaf monophenol monooxygenase and catechol oxidase. At the same time they affect the monophenol monooxygenase and catechol oxidase activities differently.

S. Durmishidze Institute of Plant Biochemistry
Georgian Academy of Sciences

REFERENCES

1. G. Pruidze, N. Omiadze, N. Mchedlishvili. Prik. biokh. i mikrobiol., **32**, 4, 1996, 315-319. (Russian).
2. G. Pruidze. Okislitelno-vosstanovitelnye fermenty chainogo rasteniya i ikh rol v biotekhnologii. Tbilisi, 1987, 186 s. (Russian).
3. N. T. Omiadze. Avtofef. kand. diss., Tbilisi, 1990, 24. (Russian).
4. N. T. Omiadze, G. N. Pruidze, N. I. Mchedlishvili. In: Chai: nauka proizvodstva, kommertsia. Tbilisi, 1992, **1(100)**, 22-27 (Russian).
5. G. Pruidze, M. Jincharadze, T. Varazashvili, N. Omiadze. Bull. Georg. Acad. Sci. **154**, 3, 1996, 448-449.

M. Gomarteli, T. Janelidze

Usage of Thermostable Xylanase Preparation Obtained from *Allescheria terrestris* for Plant Waste Hydrolysis

Presented by Academician G. Kvesitadze, May 27, 1997

ABSTRACT. In order to obtain sugar by nontraditional method, hydrolysis of vine cuttings has been carried out by means of enzyme preparation from microscopic fungi *Allescheria terrestris*. Maximum hydrolysis is reached after 24 hours. Deepness of hydrolysis was 18% of cellulose and 12% of hemicellulose. The obtained sugar mixture is used as alternative sugar source for preparing of sparkling wine by the process of secondary fermentation.

Key words: THERMOSTABLE ENZYMES; ENZYMATIC HYDROLYSIS; XYLANASES.

The aim of our work was to carry out the hydrolysis of plant wastes in semi-industrial conditions by enzyme preparations and searching possible use of hydrolysis products.

The experiments were carried out on the following microorganisms: microscopic fungi culture *Allescheria terrestris* and yeasts *Saccharomyces vini-39*. As substrates were used: preliminary ground vine cutting washed by water; Chapek medium. The enzymatic hydrolyses of vine cutting was carried out in flasks with 0.05m acetate buffer (pH 4.6) and different amount of substrate (0.1; 0.2; 0.4; 0.6; 1.0g), which were incubated in water bath shaker. Temperature of reaction medium was 65-70° C and incubation periods were 5, 24, 48 hours.

Amount of reducing sugar in the samples were examined by dinitrosalicylic acid reagent [1] and the amount of penthose by Maibaum method [2]. Their difference is considered as hexose amount.

The secondary fermentation analyses were carried out in the bottles with the following composition of the mixture: wine material – 742.2 ml; yeast suspension – 24.0 ml; monosaccharides – (xylose, glucose) – 2.2%. The incubation period was 3 weeks and the temperature – 12-14°C. Special aprometre was used for determining of liberated CO₂. The amount of CO₂ was determined according to BaCO₃ weight obtained by CO₂ binding.

Thermostable xylanase preparation was obtained from thermophilic fungi *Allescheria terrestris*, the xylanase activity of which consisted of 1500 U/g and cellulase 300 U/g.

Results of hydrolysis are given in Table 1. As it is shown from the results the deepness of hydrolysis after 24 hours is 18% in case of cellulose and 12% of hemicellulose. As the results show the prolongation of hydrolyses after 24 hours is not effective since the increase of monosaccharides in the reaction medium is negligible.

In order to increase the deepness of hydrolysis the low molecular sugars, performing enzyme inhibition, must be eliminated from the reaction medium.

Dynamics of reducing sugars accumulation of vine cuttings while enzymatic hydrolysis from *Allescheria terrestris*

Substrate mg	Time of hydrolysis					
	5 h		24 h		48 h	
	Pentoses	Glucose	Pentoses	Glucose	Pentoses	Glucose
100	0.65 mg	1.9 mg	1.2 mg	3.75 mg	1.35 mg	4.0 mg
	5.4%	9.5%	10.0%	18.7%	11.2%	20.0%
200	1.6 mg	3.8 mg	3.0 mg	7.2 mg	3.2 mg	7.45 mg
	6.6%	9.5%	12.5%	18.0%	13.3%	18.6%
400	3.2 mg	7.0 mg	7.0 mg	14.8 mg	7.1 mg	15.2 mg
	6.7%	8.7%	14.6%	18.5%	14.8%	19.0%
600	4.8 mg	9.6 mg	9.8 mg	20.7 mg	10.4 mg	17.6 mg
	6.7%	8.0%	13.6%	17.3%	14.4%	14.6%
1000	7.6 mg	17.6 mg	14.2 mg	37.0 mg	14.7 mg	37.6 mg
	6.3%	8.8%	11.9%	18.5%	12.3%	18.8%

Table 2

 Utilization of sugars and their mixtures while the secondary fermentation performed by *Saccharomyces vini-39*

Sample	Pressure in bottle, atm	BaCO ₂ g	Reaction on ethyl alcohol
Chapek's medium +2.2% xylose	2.0	12.2	+
Wine +2.2% xylose	1.8	10.9	+
Chapek's medium +1.1% xylose +1.1% glucose	3.1	18.8	+
Wine +1.1% xylose +1.1% glucose	2.7	16.4	+
Chapek's medium +2.2% glucose	4.5	27.4	+
Wine +2.2% glucose	4.2	25.6	+
Wine +2.2% enzymatic hydrolyzate	2.4	14.6	+
Control	5.1	30.5	+

The same is proved by the following: 24 hours later repeat addition of enzyme preparation in the medium increased the amount of reduced sugars by only 5-7% at the beginning stage (1-3 hours), which proved that enzyme was not inactivated.

Thus, the usage of technical preparation of *All. terrestris* allows to obtain hexose and pentose mixtures more than 80% of which were monosaccharides – xylose and glucose

with fermentation ability as an alternative sugar source.

It was confirmed that yeast *Saccharomyces vini-39* has the ability to assimilate and partly oxidize xylose up to CO_2 in case of artificial medium as well as in conditions of secondary alcohol fermentation. The same is confirmed by the value of pressure in hermetically closed bottles which are one of the main characteristics for sparkling process (Table 2).

At the same time it was noticed that while using artificial medium separately in xylose case and xylose with glucose as well, the pressure indicators were considerably higher compared with those experiments where wine material was used as fermentation medium.

S. Durmishidze Institute of Plant Biochemistry
Georgian Academy of Sciences

REFERENCES

1. J. Bailey Michael. "Xylanase assay" (DNS - stopping). 1990
2. Malii praktikum po biokhimii, Moskva, 1979, (Russian).



N. Manvelidze, E. Adeishvili, E. Kvesitadze

Selection of Antibiotic-Producing Basidiomycetes

Presented by Academician G. Kvesitadze, December 20, 1997

ABSTRACT. Basidiomycetes constitute a major class of higher fungi and have been used for medical purposes and as food since ancient times. Over 30 000 species of this group of fungi have been described. In order to get the maximum biosynthesis of antibiotics of basidiomycetes: *Oudemansiella species*, *Oudemansiella mucida*, *Agaricus species*, *Pterula* - 1 and 2 and *Xerula chrysopepla* - 1,2 and 3 the optimum conditions for their deep cultivation have been chosen.

Key words: BASIDIOMYCETES, ANTIBIOTICS, ANTIFUNGAL.

While cultivating basidiomycetes *Oudemansiella species*, *Oudemansiella mucida*, *Agaricus species*, *Pterula* - 1 and 2, and *Xerula chrysopepla* - 1, 2 and 3, natural conditions of their distribution were taken into consideration [1]. Cultivation of fungi was carried out at 27°C, different wood materials (leaves, cones...) were used as a source of carbon. The following mediums [3] were also examined as substrates:

		g/l
Medium 1:	yeast extract	4
	malt extract	10
	glucose	4
Medium 2:	yeast extract	4
	malt extract	10
	glucose	4
	agar	15-20
Medium 3:	yeast extract	4
	malt extract	10
	glucose	10
Medium 4:	potato powder	4
	glucose	20
Medium 5 :	yeast extract	1
	maltose	20
	glucose	10
	peptone	2
	KH ₂ PO ₄	0.5
	MgSO ₄ X 7H ₂ O	1
	FeCl ₃	10
ZnSO ₄ X 7H ₂ O	1.78	
CaCl ₂ X 2H ₂ O	73.5	

Antibiotic activity of investigated fungi

Strain	Volum, l.	Medium (activity is maximum)	Day (activity is maximum)	Prob on paper disk, mkg.	AGAR DIFFUSION ASSAY, mm.							
					<i>B. brevis</i>	<i>B. subtilis</i>	<i>M. uteus</i>	<i>E. dissolvens</i>	<i>M. michei</i>	<i>N. coryli</i>	<i>P. variotii</i>	<i>P. notatum</i>
<i>O. species</i>	5	1	10	100	+	+	+	+	38	20/45	12	25
<i>O. mucida</i>	5	1	9	50	+	+	7	+	30	+	12	10/30
<i>Agaricus sp.</i>	5	1	8	100	+	+	8	+	40	9	28	12/30
<i>Pterula 1</i>	2	1	28	1000	+	+	7	+	+	+	+	+
<i>Pterula 2</i>	20	1	9	100	15	13	11	+	23	+	+	15
<i>Xerula 1</i>	20	1	12	100	+	+	+	+	30	18	22	23
<i>Xerula 2</i>	0,5	3	4	1000	+	+	10	+	+	+	+	+
<i>Xerula 3</i>	0,5	5	22	100	9	9	+	+	+	+	+	+

The pH of mediums was adjusted to 5.5 by 1N HCl. The sterilization was carried out at 121°C, for 25 min. Sandy agar (15 g/l) was used to harden the mediums.

The first experiments were carried out in small volumes, in particular in 0.5 l., 1 l. and 2 l. flasks. In the case of hard-mediums 1 l. flasks of Fernbach were used. After choosing the optimum medium the cultivation was carried out in 20 l. fermenter. The fermenter was incubated at 27°C, with aeration 3 l/min and agitation 120 rpm.

It should be mentioned, that some of strains grew better and showed higher antibiotic activities in flasks than in fermenter. During cultivation in liquid medium the probes were taken, from flasks every 2-3 days, from fermenter - every day; and medium pH, concentration of glucose (% by special indicator) and amount of dry biomass were examined. Later the antibiotic activities of mycelia and cultural fluid have been analyzed. In the case of hard medium, after the complete spreading of fungi, they were incubated for some more days, to produce the secondary metabolites and after that only antibiotic activity was determined. The antibiotic activity was measured by the agar diffusion assay [2] on eight different test organisms:

bacteria:	<i>Bacillus brevis</i>	/gram-positive/
	<i>Bacillus subtilis</i>	/gram- positive/
	<i>Micrococcus luteus</i>	/gram- positive/
	<i>Enterobacter dissolvens</i>	/gram-negative/
fungi:	<i>Mucor miehei</i>	
	<i>Nematospora coryli</i>	
	<i>Paecilomyces variotii</i>	
	<i>Penicillium notatum</i>	

According to the antibiotic producing abilities, the tested strains can be conditionally divided into three groups:

- the antibiotic activity depends on conditions of cultivation;
 - activity determined in trace amounts;
 - activity is not stated.
- (see Table).

Eight basidiomycetes as producers of antibiotics have been studied. Due to the experimental data, only five of them: *Oudemansiella species*, *Oudemansiella mucida*, *Agaricales species*, *Pterula* - 2 and *Xerula chrisopepla* - 1 showed desirable antibiotic producing activity. The optimum conditions of cultivation, based on the following criteria: composition of nutrient medium, volume (aeration) and duration of growth have been selected.

S. Durmishidze Institute of Plant Biochemistry
 Georgian Academy of Sciences

REFERENCES

1. T. Anke. Canadian Journal of Botany. 73, 1995, 940-945.
2. G. Schneider: Dissertation vom Fachbereich Biologie der Universitaet Kaiserslautern, 1996.
3. H. Zahner, W.K. Maas. Biology of antibiotics, Springer Verlag, Berlin, 1972, 26-28.

E. Tavdshvili, P. Chelidze, D. Dzidziguri, E. Cherkezia,
 Academician G. Tumanishvili

The Study of Interdependency between the Changes of RNA Synthesis Intensity and the Morphological Transformation of White Rat Hepatocyte Nucleoli in Postnatal Period of Development

Presented September 15, 1997

ABSTRACT. In the postnatal period of development of white rats there is a direct interdependency between the ultrastructural transformation of nucleoli and their transcriptional activity.

Key words: NUCLEOLUS, TRANSCRIPTION, POSTNATAL DEVELOPMENT, NUCLEOLONEMA.

It is well known, that one of the main morphological criterion of ribosomal genes expression is the structural organization of nucleoli, which is strongly dependent on the amount and activity of r-genes. The intensity of r-genes transcription and also the processing of pre-ribosomal RNA is directly reflected in the structure of nucleoli. The changes in these processes arouse the development of particular types of nucleoli.

In our previous studies we have shown the strict correlation between the changes of ultrastructural organization of nuclei of different tissues and the changes of RNA synthesis intensity. In particular, such correlation between the structure of nuclei and the changes of their transcriptional activity was shown in intact and stimulated white rat hepatocytes [1]. The studies were taken also to show the analogous correlation in proliferated hepatocytes at the initial stages of postnatal development. The experiments were carried out on white rats at the age from first to 30th day from birth. The RNA synthesis intensity was defined according to the level of ^{14}C -UTP incorporation with non-soluble fraction. Simultaneously the samples were taken for electromicroscopic studies [2].

It was shown, that within the first 30 days from birth the daily

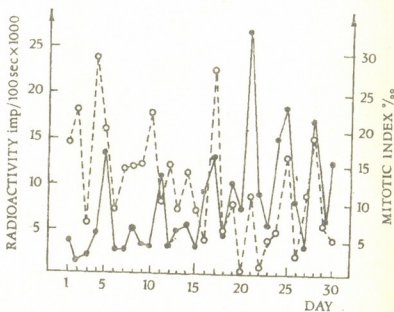


Fig.1. The changes of transcriptional (—) and mitotic (---) activity of rat hepatocytes in the postnatal period of development.

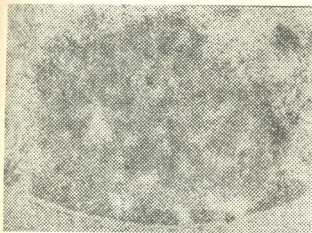


Fig.2. The ultrastructure of rat hepatocyte nuclei on the 1st day from birth.

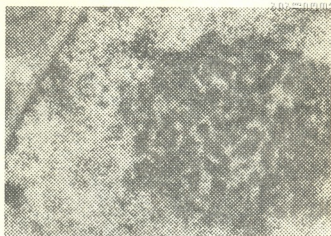


Fig.3. The ultrastructure of rat hepatocyte nuclei on the 21st day from birth.

changes of RNA synthesis takes place in white rat nuclei (Fig.1).

For revealing the interdependency between the ultrastructural and transcriptional changes of nuclei the electromicroscopic studies were carried out at periods that corresponded with the minimal (1st, 29th day from birth) and maximal (21st, 30th day from birth) level of transcription.

On the 1st day from birth rat hepatocytes have oval smooth-contoured nuclei (Fig.2). The premembrane and chromocentral chromatin condensation degree is rather high. The nucleoli are characterized with weakly developed nucleolonema and corresponding decrease of vacuoli amount. All these morphological features show that such nucleoli are of very low activity. Therefore, the electromicroscopic analysis revealed that at the first day from birth the nucleoplasmic and ribosomal activity in white rat hepatocytes is very low. Analogously the analysis of *in vitro* transcription activity curve (Fig.1) shows, that the 1st day rat nuclei are characterized with low RNA-synthesis level that corresponds precisely with the results of experiments *in situ*.

The electromicroscopic analysis of ultrathin sections of rat liver on the 21st day from birth (Fig.3) revealed the type of nucleoli that strongly differs from the described above. Circular smooth-contoured nuclei include oval increased in size nucleoli of 3 μm in diameter. The nucleolonemal strings as well as dense fibrillar component are strongly developed. In the nucleoplasm nuclear bodies are presented. Such morphological features of nucleolar structure show that the RNA synthesis is very active. This type of functionally active nucleoli known as the pseudonucleolonemal type was revealed also in the proliferated rat hepatocyte liver during the initial stages of regeneration on the 6th hour after the operation [1]. According to the results of our experiments the maximal level of transcription activity takes place on the 21st day from birth. Therefore, we can conclude that also in this case the intensity of RNA synthesis directly corresponds with the changes in nuclear ultrastructure.

To confirm the natural character of interdependency between the biochemical and morphological data we have carried out the analogous studies on animals of different age and with different transcriptional activity of nuclei.

The electromicroscopic studies of rat liver nuclei on the 29th day from birth showed the similarity of nuclei ultrastructure with the morphological indices of nuclei of rats on

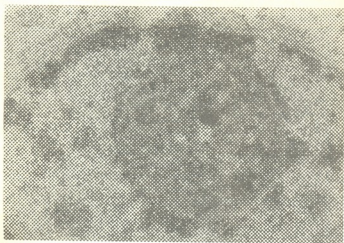


Fig.4. The ultrastructure of rat hepatocyte nuclei on the 29th day from birth.

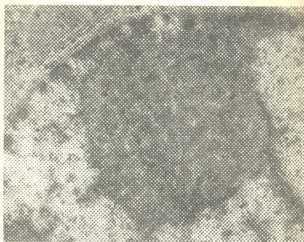


Fig.5. The ultrastructure of rat hepatocyte nuclei on the 30th day from birth.

the 1st day from birth. Weakly developed nucleolonema, small amount of fibrillar centers and decrease of vacuolar component indicate that the RNA synthesis is inactive. At the same time the biochemical studies *in vitro* revealed that on the 29th day from birth the transcriptional activity of isolated nuclei was minimal. Again, we have the example of well defined correlation between the data of biochemical and morphological analysis.

On the 30th day from birth (the period which according to results obtained in *in vitro* biochemical experiments is characterized with high transcriptional activity) (Fig.5) the ultrastructure of rat hepatocyte nuclei and especially the increasing size of nuclei and hypertrophy of nucleoli points at the strong growth of synthetic processes. The low degree of chromatin condensation also indicates the activation of nuclei (one of the main criterion of activation of genome of differentiated cells is the decompactization of chromatin [3]). The increasing amount of granular component indicates the activation of processing. Such hypertrophied compact nucleoli were described first in stimulated proliferated hepatocytes at the initial stages of liver regeneration (on the 22nd hour after the partial hepatectomy). Therefore, in this case also the correlation between the results of biochemical and morphological studies is very clear.

The obtained data makes it possible to conclude, that in the postnatal period of development there is a direct connection between the ultrastructural transformation of white rat nucleoli and their transcriptional activity and such interdependency between the morphological and biochemical parameters is natural phenomenon.

Tbilisi I. Javakhishvili State University

REFERENCES

1. D.Dzidziguri, P.Chelidze, M.Zarandia, E.Cherkezia, G.Tumanishvili. J.Epith. Cell Biol., **3**, 1994.
2. Idem. Proceedings Georg. Acad. Sci., Biological series, **18**, 5, 1992, 330-335. (Russian).
3. P. Chelidze. Ultrastructura i funktsiya yadryshka interfaznoi kletki. Tbilisi, 1985, 119p. (Russian).



M. Zimmermann, T. Ebanoidze

The Treatment of the Postextraction Syndrome with Taurolin®

Presented by Corr. Member of the Academy T. Dekanosidze, September 1, 1997

ABSTRACT. In a controlled clinical study with a total of 200 patients the broad spectrum agent and antitoxin taurolidine (Taurolin®) was clearly superior to conventional medication with the broad spectrum antibiotic chlortetracycline (Aureomycin) when applied topically to treat the postextraction syndrome (PS). Compared with the conventionally treated patient group, the clinical control parameters such as pain, swelling, secretion, tenderness to pressure and remission (secondary target criteria) in the Taurolin® group exhibited not only a markedly more rapid normalization of the score-data during the initial phase, but also an appreciably shorter interval until the patients were symptom-free. Age, gender, localization of the lesion or facultative systemic antibiotic or analgetic administration had no demonstrable effect in the course of the treatment, although the patients in the reference group required concomitant medication with antibiotics ($p=0.007$) and analgetics ($p=0.01$) considerably more often than those in the Taurolin group.

Key words: POSTEXTRACTION SYNDROME, TAUROLIDIN.

The postextraction syndrome (*Alveolitis sicca dolorosa*, *Dolor post extractionem*, dry socket) by Birn (1973) [1, 2] is an inflammation of an empty bone alveolus after an extraction and is considered as alveolus wall bordered osteomyelitis and concomitant neuritis. The frequency of this occurrence according to literature findings ranged from 0.9% [3] to 12.6% [4]. The causes of the non-formation of stable blood clot or its destroying with affected wound healing are: the local irritating factors [5], the strong tissue trauma [6], affected fibrinolysis [2], impairment of oral immunological balance [7], as well as particular bacterial infection's mechanisms [6]. Thus etiology of the postextraction syndrome is presented with the multifactorial causative complex.

The mouth cavity represents a mosaic of numerous microbiotopes of the various microbes, which are in close contact with the fresh extraction wound. The potential oralpathogenic microorganisms may penetrate into the alveolus from the root canal and from periapical ostitis, as well as from the sulcus of the gum, and from the plaque and saliva adhering to neighbouring teeth surfaces (secondary infection) [8]. Some authors [9, 10] have been able to prove that after a tooth extraction in case of disturbed wound healing aerobic-anaerobic mixed infections occur with dominant participation of gramnegative anaerobic microbes. Griffe and coworkers [11] and Nytzan and coworkers [12] postulate special leading microorganisms (*Bacteroides melanogenicus* or *Treponema denticola*) in etio-pathogenesis of the postextraction syndrome.

Alveolitis sicca dolorosa extremely seldom causes such complications as a sequestration of the large bone areas or a transition into secondary chronic osteomyelitis, and



despite this, we often encounter the clinical picture of illness during which a typical smell, bad taste and unbearable irradiating pain severely affect a patient physically and psychically. Together with the surgical revision and excochleation (scrape) of the alveolus the plan of the medical treatment includes antimicrobial chemical therapy with disinfectants and antibiotics. Biological, toxic, allergic side effects, as well as mechanisms of the natural or acquired bacterial resistance considerably limit the therapeutical spectrum [13].

Positive data about the active substance - Taurolidin as a broad spectrum antimicrobial chemical therapeutic remedy and antitoxin obtained from the field of fundamental research [14], of visceral surgery [15] and orthopedy [16] on the one side, and the first successful experiences in treatment of orofacial bone infections [17] on the other side encouraged us to apply this substance for medication of postextraction syndrome and to compare its effectiveness with the formerly applied remedies.

The investigation was performed at the jaw-surgery policlinic of Munich. The data were collected by means of a standardized documentary sheet. For a clinical study 200 patients with diagnosis of postextraction syndrome were observed. The investigation was performed according to the Helsinki Declaration.

The Taurolin and standard (control) groups were randomly chosen. Both testing substances were applied by the following form:

Group A (Taurolin - group)

Taurolin® - 3% irrigating liquid (Geistlich, Wolhusen, Switzerland)
(1g contains 30mg Taurolidine, 50mg polyvinylpyrrolidon)

Taurolin® - 3% dental emulsion (Geistlich, Wolhusen, Switzerland)
(1g contains 30mg Taurolidine, fatty acidtriglyceride, Lecithin)

B - group (standard group)

Isotonic NaCl 0,9% solution (Braun Melsungen, Melsungen, Germany)
(1ml contains 9mg NaCl).

Aureomycin® 3% ointment (Cyanamid Novalis, Wolfratshausen, Germany)
(1g contains 30mg chlortetracycline, vaseline, woolwax).

The individual duration of therapy, as well as interval between the checkups were determined by therapeutical necessity. The medical treatment was performed till complete remission. For the evaluation of both different therapeutic methods the following data were used: identification of patients; age, gender; results of clinical/radiological investigation; localization of the lesion; facultative systemic administration of antibiotic or analgetic.

Table 1

The influence of the facultative administration of antibiotics and/or analgetics on duration of the treatment of the groups

MEDICATION	TAUROLIN®		STANDARD	
	X	S	X	S
DURATION (days)	5.6	2.5	8.2	3.2
WITH ANTIBIOTIC	6.2	1.7	9.1	2.8
WITHOUT ANTIBIOTIC	5.5	2.9	7.7	3.4
WITH ANALGETIC	6.1	2.3	8.8	2.5
WITHOUT ANALGETIC	5.5	2.7	8.1	3.3

Parameters of clinical course; pain; swelling; secretion; tenderness to pressure; remission.

For relief of local pain we used the local anesthetic - Lidocain (Xylocain 2%®, Astrachemicals, Wedel, Germany), with Epinephrin 1:100 000. After this an excochleation of alveolus fundus was performed with simultaneous refreshing of alveolus bone tissue to remove rests of the destroyed clot of blood, remainders of the inflamed granulous tissue, tooth or bone fragments. The thus surgically prepared alveolus was cleaned with 3.0ml irrigating solution and was plugged with a gauze strip impregnated with 0.5-1g testing substance. Depending on the severity of the initial findings and the clinical course of the disease the treatment was repeated in intervals from 1 to 3 days till convalescence.

Taking into consideration the exploitative character of study the level of significance was determined by 5%. Suitable homogeneity tests were performed for the verification of the comparability of the groups. The duration of the treatment (primary target criterion) was analysed biostatistically deducing with the Wilcoxon-Mann-Whitney-U-test [18]. The course of clinical control parameters (secondary target criteria) were only descriptively recorded and shown in the form of a graph as arithmetical average values based on the level of the ordinal scale. The influence of a facultative administration of antibiotics and analgetics on the course of the treatment was examined.

The average age of both groups was 41.2 (± 16.5) year. The gender division was men/women proportion = 107/93, a fairly balanced proportion. In 90% of the cases the lesions were in the side of teeth area, the mandible being affected in 135 cases, the maxilla in 45 cases. The homogeneity tests did not show any statistical peculiarities ($\alpha=0.05$), so that the comparability of both groups was assured.

The average duration of the treatment during the medication of Taurolin was 5.6 (± 2.5) days, and in case of standard therapy - 8.2 (± 3.2) days. The difference remained highly significant (Wilcoxon-Mann-Whitney-U-test: $p < 0.0001$). The standard deviation established for group A was clearly below the corresponding value for group B. This is an indication that the application of Taurolin® allows to shorten the duration of the treatment.

The influence of facultative administration of antibiotics and analgetics on the duration of the treatment on the groups is shown on Table 1.

In 20.5% of the cases with standard therapy antibiotics were administered, which is a statistically significant higher share than in the group treated with Taurolin® (9.5%). As to facultative administration of analgetics, the lower frequency (5%) was observed than in the control group (8%). As can be seen from Table 1, the facultative administration of antibiotics and/or analgetics did not shorten the duration of the treatment.

Table 2.

The time intervals between the checkups and the number of the corresponding patients for the Taurolin and standard groups.

		V ₁	V ₂	V ₃	V ₄	V ₅	V ₆	V ₇	V ₈	V ₉	V ₁₀	V ₁₁	V ₁₂	V ₁₃
TAUROLIN	X	1.0	2.5	4.2	6.1	7.5	7.5	8.3	10.0	---	---	---	---	---
	n	100	100	92	47	21	4	3	2	1	0	0	0	0
STANDARD	X	1.0	2.6	4.4	6.2	7.2	8.9	10.0	10.7	12.0	12.0	13.7	---	---
	n	100	100	100	75	43	31	17	9	6	4	3	0	0



As the days of the treatment and investigation were not determined statistically, but by exclusively therapeutical indication, there were necessarily intra- and interindividual variations. The time intervals between the checkups and the number of corresponding patients for the Taurolin and the standard groups are shown in Table 2. During the treatment with Taurolin® the total number of the checkups was 370, which is significantly less than the total number of 488 checkups during the standard treatment.

The clinical application of Taurolin® allows lower doses of antibiotic and/or analgetics during the duration of the treatment, which is certainly of high clinical relevance as the patient can avoid part of the medication [13]. Taking into consideration the above-mentioned results Taurolin® seems to be a well-tolerated and effective therapeutically remedy, with a propitious benefit-risk ratio, that can have a valuable share in the chemotherapy of PS.

Munich University, Jaw Surgery Clinic and
Polyclinic.

REFERENCES

1. H. Birn. *Int J. Oral. Surg.*, **2**, 1973, 211-263.
2. H. Birn, O. Myhre-Jenses. *Int. J. Oral Surg.*, **1**, 1972, 121-125.
3. H. W. Archer. *J. Dent. Res.*, **18**, 1939, 256-257.
4. S. Walter. *Wundheilungsstörungen nach Zahnextraktionen*. Med Diplomarbeit, Greifswald, 1974.
5. H.G. Harang. *Oral Surg.*, **1**, 1948, 601-607.
6. A. J. MacGregor. *Br. J. Oral Surg.*, **6**, 1968, 49-58.
7. G. Kellner et al. *Stomatol.*, **72**, 1975, 302-316.
8. A. J. MacGregor. *J. Oral Surg.*, **28**, 1970, 885-887.
9. L. R. Brown et al. *J. Oral Surg.*, **28**, 1970, 89-95.
10. D. W. Kannangara et al. *Oral Surg. Med. Oral Pathol.*, **50**, 1980, 103-109.
11. M. B. Griffee et al. *Oral Surg. Oral Med. Oral Pathol.*, **54**, 1982, 486-489.
12. D. W. Nitzen. *Oral Maxillofac. Surg.*, **41**, 1983, 707-710.
13. E. Knoll-Köhler. *Zahnärzte. Welt*, **98**, 1989, 30-37.
14. J. I. Blenkarn. *Surg. Res. Commun.*, **2**, 1987, 149-155.
15. A. C. McCartney. et al. Liss Inc, New York, 1988, 361-371.
16. G. Lob. et al. Taurolin-Ein neues Konzept zur antimikrobiellen Chemotherapie chirurgischer Infektionen. Urban und Schwarzenberg, Munich /Wien /Baltimore, 1985, 158-163.
17. G. H. Nentwig, U. Knla. *Zahnärztl. Prax.*: **35**, 1984, 394-396.
18. G. A. Lienert. *Verteilungsfreie Verfahren in der Biostatistik*, Bd 1. Anton Hain: Meisenheim am Glam.



T.Shatilova, I.Oniani, M.Chikovani, Z. Zambakhidze

Organo-specific Stimulation as a Method of Treatment of the Pigmentary Dystrophy of the Retina

Presented by Academician T.Dekanosidze, October 20, 1997

ABSTRACT: 16 patients with retinitis pigmentosa underwent embryonal sclera transplantation. Positive results were received on the part of visual acuity and visual field. The authors explain it by the fact, that embryonal tissue causes stimulation of the regeneration process in recipient's eye. Functional improvement is connected with mitogenic radiation.

Key words: PIGMENTARY DYSTROPHY OF THE RETINA, EMBRYONAL SCLERA, TRANSPLANTATION, ORGANOSPECIFIC STIMULATION.

Etiology and pathogenesis of pigmentary dystrophy (PD) of the retina are not ascertained definitively. There exist acquired and hereditary, primary and secondary forms. Besides classic form of PD, without pigment and punctata-albescense PD in the presence of Laurence-Moon-Bardet-Bide's and Usher syndromes and also sector-like and one-side forms of PD are known. In this article we are able to refer to these points of pathogenesis of PD, which concern the problems of the therapy, that we are interested in.

First of all it is the theory, connected with the process of resorbition of disks pulled down by photoreceptors. It appeared that pulled down disks of photoreceptors of mutant rats which have PD type degeneration of the retina are not resorbed between the latters and the pigment epithelium and prevent metabolic processes [1]. It is known, that the atherosclerosis of posterior ciliary arteries causes annular and sector-like scotoma as during PD. But this however doesn't allow to equal these two diseases [2]. For treatment of PD there are remedies improving the trophic. Vessel-broaden medicines, intermedin, preparation of hypophysis, anticoagulants, nuclein preparations, taufon having effect on melanin enzyme are frequently used. In Helmholtz' Institute there was created the preparation ENKAD - complex of ribonucleins [3]. Injecting the 2% solution of salt through the mucous membrane of nose the substance directly gets into the spinal cord liquid passing the hemato-encephalitic barrier and has stimulative effect on the hypophysis [4].

There exist also surgical methods of treatment. V.A.Burnside made the straight eye muscle fibres grafting into suprachorioidean area [5]. There exist modifications of this operation [6]. But they are not wide spread because of possible complications on a state of intraocular haemorrhage.

An operation of bandaging of arteria *temporalis superficialis* is proposed. The operation was done while *dystrophy senilis*, *myopia magna* and PD. The operation turned out to be less effective while PD [7]. The principle of this operation is taken from surgeons who bandaged arteria *mammaria externa* in the hope that the bloodflow goes into coro-



nary artery, but the operation was not effective. The experiments with using the genetic therapeutics are carried out now. But transplantation of pigmental epithelium on human now is without results.

T.Shatilova [8] proposed an operation in transplanting the embryonic melitrised sclera during the diskhemie dystrophy of the retina and later also during the tapetoretinal degenerations.

For this article we dwelled upon the patients of the same ethnic group, all of them were from Calabria (Italy), being treated before in many Italian clinics and abroad (19 patients). As a material for transplantation served embryonic sclera melitrised. We described the methods of conservation [9].

The material for transplantation was taken according to accepted method in transplantology. Besides all generally accepted investigations, donors, as well as patients, have been observed on AIDS. Patients were consulted by physicians, cardiologists and neuropathologists.

17 patients out of 19 had typical PD, one had central dystrophy of the retina, others had punctate dystrophy. All the patients disease was double-sided. 9 patients had bad vision from their early childhood and 10 from the age 30-40. 5 patient's parents were close relatives, and 4 patient's relatives suffered from PD. Besides the main diseases the majority of patients had other eye pathology: 10 had cataract, 1 had glaucoma, 1 had subluxive lens, 6 patients had destruction of vitreal. 14 patients have been treated before conservatively, and 1 underwent surgery in Moscow. General condition of all the patients was satisfactory, 3 had moderately increased arterial pressure.

Operation was made to 16 patients, to 15 on both eyes and on one eye to 1. Eight patients underwent surgery under general anesthetic (droperidol, fentanil) and 8 under local anesthetic (2% novokain) with promedication. Operation period was without complications. Operation and after operation periods were taking a normal course, as to eyes, so to general condition.

On the 4-5 day after the operation all the patients noticed improvement in vision, orientation, and the patients having no regular vision before had more clear light perception.

Central visual acuity improved on 20 eyes: 10 - on the hundredths and 10 - on the tenths. No changes - 11 eyes. There was no any worsening in all the cases.

The least visual acuity before operation was 0.01 and after it 0.02.

The greatest visual acuity with correction before operation was 0.4 and after it 0.8.

The total field of vision of 10 patients out of 19 has broadened up to 100° , on 5 eyes up to 300° , on 4 eyes and more than 300° on 12 eyes. The least broadening - 51° and the biggest - 703° . Absence of changes and deterioration haven't been observed.

To sum up, we could ascertain obvious therapeutic effect. But what are the reasons of those positive shifts, which occur in the result of transplantation of embryonic tissue?

Our experimental investigation showed [8,9], that there exists veritable vegetation of tissue, but processes lasting in recipient tissue are more important for us: within the next few days after the grafting there is observed the increase in quantity of nuclei in recipient sclera, and then the formation of capillaries is also noticed. So there exists stimulation of cytogenesis processes.

As it is known academician V.P.Filatov [10] is considered to be the founder of

Visual acuity

N	Before surgery		After surgery	
	OD.	OS.	OD.	OS.
1	0.09-3.5D=0.3	0.09-1.5D=0.3	No changes	
2	0.03- correction=0.8	0.06- correction=0.2	No 0.03- =0.2	No 0.3- =0.4°
3	0.01	0.001	0.05	0.06
4	0.1-1.0D=0.4	0.2 (No correction)	0.2-1.0D=0.4	0.2 (No-correction)
5	0.001	0.001	0.02	0.02
6	I proection certa	I proection certa	No changes	
7	0.02 (No correction)	0.02 (No correction)	0.03-7.0D=0.05	0.03-7.0D=0.05
8	0.1 (No correction)	0.1 (No correction)	0.2 (No correction)	0.2 (No correction)
9	0.01(temporal.)	0.01-4.0D=0.02	No changes	
10	0.09-1.0D=0.4	0.06-1.5D=0.08	0.1-1.0D=0.5	0.07-1.5D=0.09
11	0.001(temporal.)	0.001(temporal.)	No changes	
12	0.001-4.0D=0.2	0.001-4.0D=0.2	correct=0.3°	
13	0	0.02-6.0D=0.06	0	0.02-6.0D=0.07
14	0.06-2.0D=0.1	0.09-2.0D=0.1	0.07-2.5D=0.3	0.09-2.0D=0.8°
15	0.03-correct=0.09	0.06-correct=0.2	0.06-correct=0.1	0.07-correct=0.3°
16	I proection certa	I proection certa	No changes	

bstimulation theory. From our point of view of the utmost interests is one of his primary observations, when after the transplantation of the cadaver cornea into the patients eye with leukoma he has observed enlightenment of turbid cornea on the border with transplantants. Hence occurred leukomas reclamation method. In this observation "organo-



specific stimulation" was obvious. V.P.Filatov himself hasn't applied this term, and the idea itself hasn't been expressed. His idea went in the direction of broadspectral biostimulation and he spread this idea to nonspecific tissue of human being and plants. This was discussed in different fields of medicine. Now we aren't talking about this. We are interested in "organo-specific stimulation". It is known that abundant reproducing in general is the source of mytogenetic radiation, which exists in our case as well; metabolic processes in adjoined and functionally connected tissues of sclera, chorioidea are stimulated and spread over pigmentary epithelium of the retina.

Complex anatomofunctional connections among sclera, chorioidea and the retina, originating from embryogenesis on the basis of these processes developed in sclera induced the retina. Modern ultrastructural investigations [11] have shown the existence of tight connection between Bruch's membrane, pigmentary epithelium of the retina and basil membrane of choriocapillary layer. L.S.Morse et al [11] ascertained stimulation of pigmentary epithelium growth by proliferative cell of endothelium. Further more there has been found the existence of mythogenetic activity.

So we see that sclera, chorioidea and the retina are so functionally connected that the state of the retina is reflected by the processes lasting in the sclera. It may be assumed that process of resorbtion of pulled down disks is stimulated.

We attach great importance to organospecific stimulation coming from embryonic tissue. Nowadays in treatment of such hard hereditary diseases as diabetes mellitus, pains of Parkinson, myostania, livercirosis specific embryonic cell transplantation is used.

As some authors mention influence of transplanted embryonic cell is in relation with genetic factor. Observation, carried out in National Institute of Health (NIH) in Batest, showed the possibility of practical use of genetic therapy.

The question rises: if there is the embryonic sclera transplantation in the presence of PD genetic therapy as well. This question requires special experimental observation.

For the present we can ascertain, that transplantation of embryonic sclera during the pigmentary dystrophy of the retina is an effective way of treatment of this desease.

Eye Disease Department of Tbilisi State Medical University

REFERENCES

1. O.Stroeva. Materials of Symposium "Actual question of Ophthalmology". M., 1982, 26-28.
2. G.Heine, W.Comberg. Jahrbuch unde Atlas der Augenheil Kunde. 1958, 5, 191.
3. L.Catsnelson, K.B.Trutneva, F.Bogovolsky. "Annals of Ophthalmology". 1982, 2, 28-31.
4. A.Novokhatsky, L.J.Chrakcha, G.E.Kalimnik. in: "Material of Conference Ophthalm." Odessa, 1968, 24-25.
5. R.Burnside. "Am. Jour. Ophthalmol." 1956, 7, 911-914.
6. T.Shlopak, D.Voloshinov, T.Bondareva. "J.Ophthalmol." 1970, 526-531.
7. C.Fedorov, G.Shikin. "Annals of Ophthalmol." 1982, 12, 28-31.
8. T.Shatilova, T.A.Aleksidze, M.A.Kvaliashvili, I.V.Oniani, Z.S.Zambakhidze. Works of Tbilisi Medical University, XXVI, 1976, 363-370.
9. T.Shatilova, Z.S.Zambakhidze. Material of 2nd Conference Ophthalmol. of Caucasus, 1971.
10. V.Filatov. "Annals of Ophthalm." 1937, 6, 35.
11. G.Morse, J.Terrel, J.Sidicato. "Arch. Ophthalmol." 1989, 107, 11, 1659.



L. Gogichaishvili, M. Chikhladze, N. Meskhishvili

Spring Palynospectra of Tbilisi and Dynamics of Allergic Diseases in Children in 1997

Presented by Academician T. Oniani, January 1, 1998

ABSTRACT. Content of pollen grains of allergenic plants in aerospectra was studied in various districts of Tbilisi. Material was obtained from 13 districts in the second and third decades of March and in April. In March the alder, willow, hazel nut and elm pollen grains were mostly observed. In April walnut, platan, maple, mulberry, vine, lilac, timothy-grass, nettle, milfoil pollen grains added to their number. Pollen amount greatly increased in April, in accordance with it the number of people with pollinosis increased as well.

Key words: POLLEN GRAINS, AEROPALYNOLOGICAL SPECTRA.

Palynological study of atmosphere is necessary for prophylaxis, diagnostics and treatment of pollinosis. According to the palynological spectra allergologist can properly find the disease provocative pollen, which help him to cure the patient.

Investigations carried out by us comprises 13 districts of Tbilisi unlike the previous investigations [1-3]. Pollen grains were collected in the atmosphere by special plates placed in different districts of the town at 3-5 m above the ground surface for 48 hours. No less than 8 plates were placed in each district. They were disposed in Didi Dighomi, Krtsanisi, Gldani, Didube, Chughureti, Nadzaladevi, Avlabari, Isani, Varketili districts. Pollen grains were treated by Erdthman's acetolysis method [4]. The number of pollen grains of alder, elm, willow, hazelnut, maple, walnut, mulberry, plane-tree, nettle, lilac and other plants were defined and recorded. Simultaneously the data on pollinosis were obtained from the children policlinics of the same districts and the policlinics of Saburtalo, Samgori, Mtatsminda, Isani, Vake, Chugureti districts. Great deal of data was obtained from the Allergogenic Service of the Children's First Hospital. As many as 85 children were investigated. Among them pollinosis was observed in different age: in one-year old children (8 cases), two-year old (4), three-year old (5); four-year old (9), five-year old (3), six-year old (1), seven-year old (6), eight-year old (7); nine-year old (13), 10 year old (4), 11-year old (3), 12-year old (6), 13-year old (9), 14-year old (1), 15-year old (3). Only one patient was of 10-month old. Results of the analysis are given in Figs. 1-2 and Table 1.

In the second decade of March, 1997 the total number of pollen grains in atmosphere was low. In the third decade their number 2.5 fold increased. In comparison with 1995-96 years pollen grain concentration in atmosphere was lower in 1997. It was expected as spring was late in 1997. It prevented plants from massive blooming. Then the heavy storm winds quickly dissipated pollen grains. So their number decreased greatly, but still alder, willow, hazelnut and elm pollen grains remained in atmosphere in such amount that they might cause pollinosis.

Pollen grain concentration in air and allergic diseases in Tbilisi, in March and April, 1997

District	Pollen amount in air, March, 1997	Diseases					Pollen amount in air, April 1997						
		Pollinosis	Allergic rhinitis	Allergic conjunctivitis	Dermal allergy	Bronchial asthma		Pollinosis	Allergic rhinitis	Allergic conjunctivitis	Dermal allergy	Bronchial asthma	
Didi Dighomi	20	-					877	1	5				1
Dighomi Massif	40	-			1		2142	3	3				2
Saburtalo	60	2	4			3	2084	3	3	2	2		1
Vake	85	2	2	9		3	2903	3	2	6	4		1
Mtatsminda	62	-					2990	1	-				1
Krtsanisi	59	1					2401	-					1
Gldani	65	-					2790	2	2	2	2		2
Didube	11	1					2163	-		1			1
Chughureti	-	1			1	6	1652	-		-			-
Nadzaladevi	92	-					1313	3	6	2			2
Avlabari	5						645	1					-
Isani	70				3		2900	4					3
Varketili	29						1132	2					-

In the second decade of March the number of pollen grains of hazel-nut increased greatly in Saburtalo and Nadzaladevi districts, but in Vake, Chughureti and Avlabari districts were lesser. In other districts (Didi Dighomi, Dighomi Massif, Mtatsminda, Gldani, Didube) only 3-4 pollen grains were found in 1cm^2 area but they couldn't cause allergy. In the third decade of March the number of pollen grains fivefold increased in Saburtalo district. In Mtatsminda, Krtsanisi, Isani districts their number increased moderately, in Varketili, Avlabari and Chughureti districts was still less and in Vake district was a bit increased.

The number of willow tree pollen grains was lesser in the second decade of March not mentioning the aerospectra indices of Vake district (10 grains/cm^2). Half of it was recorded in Didi Dighomi, Dighomi Massif, Gldani, Nadzaladevi and Isani districts. In Didube district the number of willow tree pollen grains was even lesser.

In the third decade of March the number of willow-tree pollen grains increased in Vake and Mtatsminda districts. It should be noted that the number of pollen grains of willow-tree doesn't exceed those of hazelnut in any district.

In the second and third decades the number of pollen grains of alder and elm was far lesser than that of willow-tree and hazelnut. Although in the third decade of March the

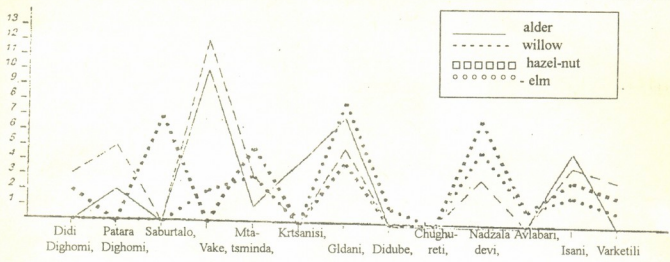


Fig.1 Tbilisi palynospectra in the second decade of March, 1997.

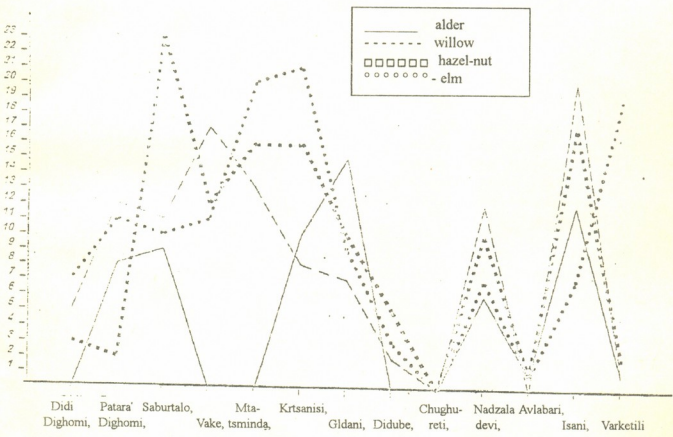


Fig.2. Tbilisi palynospectra in the third decade of March 1997

alder pollen grains made the only peak in Gldani district and another lower one in Isani district. The number of elm pollen grains increased in Mtatsminda and Krtsanisi districts. In March hazelnut pollen grains may cause allergy.

April is especially distinguished by an excessive number and variety of pollern grains. For example, if in Dighomi district in march 20 grains/cm² were recorded, their number was 877 in April.



Out of arboreous plants the number of oak, elm, mulberry, walnut, platan, willow-tree and out of herbaceous plants timothy, milfoil, nettle, etc. are especially great in the spectra.

As it was mentioned above, data on allergic diseases were collected systematically. In March the total number of allergic diseased people was found to be 39, in April it increased to 83. Pollinoses were mostly revealed in Vake, Saburtalo, Gldani, Nadzaladevi districts. As many as 85 patients were diagnosed to be diseased with pollinosis, 16 with allergic rhinitis, 16 with conjunctivitis, 14 with dermal allergy, 15 with bronchial asthma. We consider timothy, nettle, lilac, walnut and mulberry pollen grains to be the cause of acute allergy in April. Per case of the disease was revealed in Didi Dighomi, Mtatsminda, Krtsanisi, Avlabari and Varketili districts.

Thus, in March hazelnut and in April timothy, nettle, lilac, walnut and mulberry pollen grains are found to be causing allergy in Tbilisi. Mostly 1, 8, 9, 13-year old children are diseased with various forms of pollinosis. Vake, Saburtalo, Gldani and Nadzaladevi districts are distinguished with frequency of cases of pollinosis.

N. Ketskhoveli Institute of Botany
Georgian Academy of Sciences

REFERENCES

1. G. V. Gurgeniidze. Allergologia. Tbilisi, 1987, 161-170 (Russian).
2. R. M. Labadze. V In: Allergia v klinike i eksperimente. Tbilisi, 1979, 147-148 (Russian).
3. L. Gogichaishvili, M. Ramishvili, M. Sakvarelidze. Alergiul daavadebata gamomtsvevi zogierti mcenaris mtvis marcvis morfologia. Tbilisi, 1975, 5-30 (Georgian).
4. G. Erdmanth. Pollen morphology and plant taxonomy. Angiosperms (An introduction to palynology I). Stocholm-Waltham, Mass USA, 1952.



M.Badriashvili

The Metaphor of Torturer and Victim as the Basis of World Perception

Presented by Academician G.Tsitsishvili, December 31, 1997

ABSTRACT. The metaphor of torture and victim as a model of world new outlook reveals new properties, filling the knowledge and imagination with fresh meanings. By the united model of opposites those intentions of cultural values consciously or unconsciously born by the artistic image will be restored .

Key words: METAPHOR, TORTURE, VICTIM.

It is known that in the course of its existence the mankind has used numerous forms of governing, wore them off and threw away on the rubbish of the history. But the governing form of torture and victim is eternal as the world itself [1]. It is one of the basic forms of the mankind existence, peculiarities of which the mankind has experienced on itself, on its own flesh and blood, beginning from Cain and Abel's genus, followed by the Crucifixion up to now. Moreover, beginning from the insect being caught in spider's web and ended up by a weapon-carrying man. Shakespeare says: "Man is a king of animals!" This polysemantic phrase perfectly expresses man's inner substance, because it was just the man who created such weapons in the course of its civilization which may completely destroy both vital and nonvital worlds. Thus the man gave a verdict of victim to himself, and became the greatest torturer of the world.

The unity of torturer and victim is a mystic unity of life and death [2]; it is a sign of world's regulation and contains the whole spectrum of dependencies with moral, historical, social and cultural spheres. The artistic and functional image of torturer and victim at the cross-roads of epoches is one of the strongest structures stimulating historical development, which is destined to bring comprehension in the world, but not any finished thought [3]. The world from its sensitive side exists to notify a man about something new. An impulse to explain and solve the problems of being and consciousness constantly makes a man to seek new meanings and have knowledge of them.

In the metaphore of torture and victim as in a united model of opposites world's knowledge in respect to the universe is reflected where each man comes into this world to know ones destination and to realise it [4]. Those elements of the general world outlook which are original and individual in every culture are established in this artistic image. A metaphor as world outlook principle implies that the elements of the universe should be presented in constant process, current, dialectics of connections and relations formation. Ortega i Gaset states [5], that "the whole world rests on a very small body of a metaphor". It is an unusual, true knowledge about the universe which was taken out on the surface by intuition and placed in the visual field of the mind. That's why it is a vital impulse in which the epoch and eternal ideas of civilization are embodied.



The relationship of the creator to the original image and the essence which is put into it is similar to that of a man and the world. The knowledge of the world is a long time desire of a man. Every attempt and every motion in this direction is equivalent to the order singled out from chaos. The order in its turn is the expression of the highest legitimacy. The essence of being implies the act of understanding which is authentic creative impulse in penetration into problems and their solution, in which constant search of new meanings and functions is implied. The meaning found once is never dogmatized; it takes numerous realisation modifiers on the path of evolution increasing the amplitude of motion, correspondingly the number of meanings increase. The act of understanding i.e. the existence of man's being takes place.

The first man on the earth didn't dye of natural death; he became the victim of violence on the ground of envy. This was shepherded Abel being killed by his brother Cain whose sacrifice was not adopted by the Lord God. And he failed to rule over his sin, he lied before the God saying that he didn't know where his brother was. But Abel's blood was crying to the Lord God. Said the Lord God to Cain: "And now art thou cursed from the earth, which hath opened her mouth to receive thy brother's blood from thy hand" (Genesis, 4-11). The blood as an evidence, becomes Cain's torturer and the Supreme – the truthfull judge because it is the God of truth and law. Meanwhile tempted by the snake, Eve partook of the fruit from the tree of knowledge of good and evil and then gave it to Adam. Thus they neglected God's prohibition and became victims of God's fury, they lost Eden and involuntarily opposed the creator. The Lord God whose will was two creatures created from him didn't obey deprived them the happiness of eternal life for ever. Thus the great epoch of unity of opposites begins. The first man was confused and lost orientation. Sometimes he holds on the power, sometimes becomes defenceless and helpless like a child. He seeks the compensation of loss on the earth and in this search now he is a monster overcoming fear, now a simple flower plaited in a crown. Made of the earth he can't hold out against earthly temptations and rise over his earthen nature. He reveals his priority in interrelations with other human beings by suppressing them and ruling over them. It seems as if he throws the white glove before the Lord God to challenge. The Lord God inhabits in Heaven and the man lives on the earth trying to establish his power over the whole earth, suppresses every vital from smallest to the biggest and uses it for his benefit. He is the victim of temptation and in the search of the lost became rather rough and cruel as his attempts to return the lost was in vain; finally received the image of the torturer; his passions will die away when he turns into the earth and return to the first goal. And the current of life on the earth will go on. The man comes, lives, works and then again passes into the great nothingness which was the torturer of his doings. In the course of history there are numerous examples of power lovers in one or another sphere and everywhere man created like "God's image" being awared of one's own nothingness uses the power as compensation means.

It seems as if he makes protest and tries to restore the lost paradise on the earth, however this paradise is the shadow of shadow, besides it is upside down or may be it is a paradise created in one's own imagination? As there was passed too much time to remember exactly that harmony in one's distorted imagination! Once being the victim of temptation now he becomes a heartless torturer, who was deprived of joy in the Eden

garden, and he deprives the people to live happily in this world. Where was the soul inspired by God lost by which the mankind received a great charge of love and kindness and which should be returned to its primary reason as the spark to the fire!

The constant process of realisation the metaphor of torturer and victim in the global current of the world takes more and more load in a creative process where the artistic images work hard on the perfection of the utterance and polysemy of their functions. The united model of opposites and its realisation process represents a systematic principle conditioned by world outlook and transferred in artistic material. In the process of notions transformation the mixing of their functional and semantic rows takes place and, the widening of the meaning area by means of self-formation occurs. The artistic image goes beyond the basic semantic meaning, find out new and new meanings and starts the moving to the unity, by which it establishes a certain order, which is subordinated to the unconscious logic of symbolic thinking [6]. The artistic image has a demand for novelty, which determines the whole psycholinguistic process of logically inconsistent semantic fields.

The philological aspect of the problem is linked with the study of concrete contexts. From this side, of special interest is the analysis of separate creative works on the grounds of the so-called unity of opposites as on the form of symbolic comprehension of consciousness or on that peculiar expression of communication, which also symbolically expresses the interrelations of the torturer and victim in the essence of which the philosophy of mankind existence is unconsciously sedimented.

The work on the mentioned problem was carried out by scientific interest of setting correspondences and interrelations between social phenomena and artistic world of the writer. Otherwise those attitudes, outlooks and imaginations, aspirations and desires which in the course of centuries try to find outlet and which have been revealed by means of artistic language as a specific system of signs. The peculiarities of social models and structures strengthens the interest to the researched questions and make them actual both from historical and philosophical planes.

The metaphor of torturer and victim is a long time Odyssey of opposites in which the seeking mind looks for the beginning from the beginning, primary cause push between the light and dark. Accumulating intuitively this sensitive knowledge which is directed to selfstore, survival and renewal, it starts to subordinate the level of every day problem to the higher intention.

Shota Rustaveli Institute of Georgian Literature
 Georgian Academy of Sciences

REFERENCES

1. *M. Borodina, G. Gak. Aspekti semanticheskogo issledovania. M., 1980 (Russian).*
2. *D. Lakof, M. Jonson. Metafori s kotorymi my zhivjem. M., 1990 (Russian).*
3. *P. Riktor. Metaforicheskii protses kak poznanie, predstavlenie i oschuschenie. M., 1990 (Russian).*
4. *M. Foss. Metafora: simbol v opyte chelovechestva. (Translated from English), Tbilisi, 1989.*
5. *Ortega i Gaset. Filosofia metafory. M. 1964 (Russian).*
6. *E. Mak-Kormak. Teoria metafory. M., 1990 (Russian).*



M.Andriadze

Terminology of Old Georgian Professional Music According to Old Tropologion

Presented by Academician V.Beridze, February 11, 1988

ABSTRACT. Old Tropologion is the first independent hymnographic collection of Middle Ages for musical terminology. Earlier synonymic terms of chant and data on the forms of chanting performance have been analyzed.

Key words: OLD TROPOLOGION, CHANT.

Ancient traditions of the Georgian music as well as any Christian musical cultures are connected with spiritual music. In the course of centuries musical terminology was formed within the church music which according to hymnographic monuments could have been rather developed. As no special old manuscript about the development of Georgian music or any separate stages of it has not been found yet we must seek for it in inscriptions of liturgic and hymnographic monuments of Middle Ages.

Musical terminology of ancient period connected with Christian services is found in the very first independent hymnographic collection - Tropologion, which is famous for its terminology of IX-X centuries. We singled out and generalized only that terminology which is directly connected with the structure of chant and the way of its performance [1].

What was the meaning of the word *galoba* (chant) in old Georgian? The Dictionary of Old Georgian Language by I.Abuladze defines *galoba* as two independent lexical units. First meaning of the word *galoba* is psalmody, praise, singing, blessing, joy. The second meaning is blessing, praise, singing. Each meaning of the word is followed by the illustrations of old Georgian literary monuments. It should be noted that very often illustrations are given in two different editions which makes possible to compare synonymous meanings of one and the same word. It is obvious from the examples connected with the word *galoba*: e.g. "Icqes galobad psalmunita amit" in another edition is written as "Icqes psalmunebat psalmunsa amas." "Galobdes Debora da Barak" in another edition is written as "imakebla Debora da Barakman".

In the above examples the word *galoba* means psalm, praise, song. With the meaning of blessing the word *galoba* is given in the following passage: ugalobdit [bless] upalsa galobita [chanting] axlita"; "igaloba [sing] israilman galobai [blessing] ese žurymulsa zeda".

Thus, the notion of the word *galoba* in Georgian is filled both semantically and morphologically. It includes verb forms and nouns: which is illustrated in two examples above.

The whole repertoire of chanting up to VII-IX centuries in Georgia was collected in one collection - Tropologion. Besides dozens of hymnographic terms the Tropologion registered the instructions in the performance of chants. These are: *tkuan*, *itqodian*, *catkuan*, *mimogdebit*, *ukcion*, *gardamotkma*".

The word "tkuan" is used in the following context: "mçuxrisa z amsa tkuan cardgoma" [1, p.37].

"Zatikša romel kuirae daxvdes, mun stkune galobata xeltabanisa [1, p.73], "çina dyit mçuxrisa zamsa Ševidnen, qon kuereksi da locva, da tkuan ibaḳoi" [1, p.11].

The fact that *tkuan* corresponds to the word *galoba* first of all is proved by one of the references of Ochoechos. The simultaneous usage of the words *qon* and *tkuan* in previous example perfectly demonstrates the difference between these terms. The word *tkuan* (sing) has the meaning of chanting, whereas *qon* is the equivalent of *speech*, *action*.

The synonym of the word *tkma* must be the word "itḳodian" in Old Tropologion. For instance:

Šova yamidgan içqon sakitxavta kitxvad da amat dasadebelta itḳodian" [1,12]; "çqlis kurtxevad gavidodian, amas itḳodian" (p.40); "Šin-ḡa ševidodian, amas itḳodian" (1,41), which is again followed by the reference to *ηχος*. The musical meaning of *itḳodis* is proved earlier in the Books of the Bible: "itḳodis igi galobasa mas uplisasa knarita" [I Kings 16:16].

In I.Abuladze's Dictionary the lexical phrase "galobisa sitḡa" is defined as "keba" (praise), *simyera* (song) [2, p.39].

In Old Tropologion the opposite of *tkuan* and *itḳodian* is *ikitxon*, which is used in the lessons of the Bible. E.g.: "da iḳitxon saxarebai" [1, p.15, 190, 202];

"iḳitxon saḳitxavi da tkuan psalmuni" [1, p.204, 214], "iḳitxon saxarebai da ibaḳoi tkuan" [1, p.196].

Now let's see what *carstkua* or *çatkuan* mean.

The note "srulad çarstkua" follows the psalms text: "ḡmerto, ḡmerto çemo momxeden [1, p.196] and it can be understood in two ways: a) this stanza of the psalm should be performed with no omissions; b) this stanza of the psalm should be chanted completely from the beginning up to the end. The second note of the same content is met in Old Tropologion at the Saturday services on the Passion Week of the Easter: "aḳurtxon eklesiai, upalo ḡayatḡavi çatkuan da tavitgan ese ukcion". This note is followed by "dasadebeli upalo ḡayatḡavsas" [1, p.214].

If we take away the prefix *ca-* from the words we'll have the root "*tkuma*", which in Old Tropologion corresponds to chanting. In I.Abuladze's Dictionary "*tkuma*" and "*cartkuma*" are synonyms.

The word "*cartkuma*" is defined by the word "*tkuma*" and vice versa. [2, pp.185, 533]. Here are also corresponding extracts from the monuments of old Georgian writing. Even in this case to define the lexical unit better, one and the same text is given in different editions, which helps to make the definition more precise, E.g.: "galobai cartkues da ganvides" in the other editions is "galobit gamovides"

In contemporary translation of the New Testament the same extract is given as "igalobes da gasçies zetisxilis mtisaken".

Thus *çatkuan* or *cartkuan* should denote recitation. Maybe *cartkuma* or recitation and *galoba* or *tkuma* don't imply the similar way of performance.

In liturgic dictionary by K.Kekelidze *cartkma* or *gardamotkma* are defined as recitation. It should be mentioned that in old liturgic monuments the word *igalobon* is almost not met in this way. Instead of it there are used: *ayiḡon* ("oxitai ayiḡon", K.Kekelidze's Dictionary



p.335); *itqodian* ("paraskevsa šuadyitgan itqodian pirveli dasadebeli", Old Tropologion, p.198), *itqodi* ("odes ciškrisa qoveli ayaşrulo da saxarebis kičxvad gaxuidodi, amas itqodi [1. p.195]; *çartkues* "galobai çartkues da ganvides" [Mark, 14:16].

The word *gardamotkma* in Old Tropologion is met both in singular *gardamotkumai* [1, pp.396,455,489,506] and in plural forms *gardamotkumani* [1, pp.380, 415, 436, 473]. The word *gardamotkumai* is the name of a concrete chant, which is introduced in Easter cycle and is not met any more in Old Tropologion.

The word *gardamotkumai* is based on one and the same topic - the Resurrection taken from the New Testament. It is given sometimes by the form of monostrophe and sometimes by multistrophe which looks like stikhera. While analysing the Lektionaire hymnographic term *gardamotkma* Leeb [3] comes to the following conclusion: "*gardamotkma* is a musical term, which is used only in one place (during Palm Sunday) after reading the New Testament and from its etymology it means *Sprechgesang* and *recitation*. According to Leeb M. Tarkhnishvili translated this word as *tractus* which in Latin liturgy means continuity, continuous performance. To explain the word *gardamotkma* Tarkhnishvili choses such parallel term which explains the essence of this Georgian word. There are also two types of recitatives: on tune and certain melodic intonations (e.g. 'Good Lord, hear us'.) and *ostinato* i.e. continuous monotonous sound (*Ecteneia*). Thus *gardamotkumai* is the term transferred from Lektionaire into Old Tropologion, which indicates the performance of chanting by talking.

One more significant term found in Old Tropologion, is *mimogdebit*. The usage of such type chanting is met twice. [1, p.218]. Such chanting was introduced by St. Ignatius, and means two-sided chanting or antiphon chanting of two groups of choir, or by a group and the chanter.

Thus the oldest texts of Tropologion prove the existence of several terms synonymous to *galoba* (chanting) and terms meaning all forms of present day performance: *galoba* (chanting), *çartkma* (sing), antiphon.

I. Sarajishvili Tbilisi State Conservatory

REFERENCES

1. Old Tropologion. Prepared and edited by E. Metreveli, Ts. Chankievi, L. Khevsuriani. Tbilisi, 1980.
2. *I. Abuladze*. Dictionary of Old Georgian Language. Tbilisi, 1980 (Georgian).
3. *H. Leeb*. Die Gesänge im Gemeindegottesdienst von Jerusalem. Wien, 1970.
4. New Testament Stockholm. 1993.
5. *K. Kekelidze*. Georgian Liturgical Dictionary. Jerusalem Lectionary of the VII century (Georgian version) Tiphlis, 1912, 341 (Georgian).

Subscription Information

The "Bulletin of the Georgian Academy of Sciences"
is published bimonthly

Correspondence regarding subscriptions, back issues should be sent to:

Georgian Academy of Sciences,
52, Rustaveli Avenue, Tbilisi, 380008, Georgia
Phone : + 995-32 99-75-93;
Fax/Phone : + 995-32 99-88-23
E-mail : BULLETIN@PRESID.ACNET.GE

Annual subscription rate including postage for 1998 is US \$ 400

© საქართველოს მეცნიერებათა აკადემიის მოამბე, 1998
Bulletin of the Georgian Academy of Sciences, 1998

გადაეცა წარმოებას 20.05.1998. ხელმოწერილია დასაბეჭდად 20.07.1998.
ფორმატი 70x108^{1/16}, აწყობილია კომპიუტერზე. ოფსეტური ბეჭდვა.
პირობითი ნაბ. თ. 11. სააღრიცხვო-საგამომცემლო თაბახი 11.
ტირაჟი 300. შეკვ. № 311 ფასი სახელშეკრულებო.

რედაქციის მისამართი: 380008, თბილისი-8, რუსთაველის პრ. 52, ტელ. 99-75-93.
საქართველოს მეცნიერებათა აკადემიის საწარმოო-საგამომცემლო გაერთიანება "მეცნიერება",
380060, თბილისი, დ. გამრეკელის ქ. 19, ტელ. 37-22-97.